UNITED STATES
NAVAL POSTGRADUATE SCHOOL

THESIS

PERFORMANCE ANALYSIS AND INITIAL TESTS OF A TRANSONIC TURBINE TEST RIG

by

Richard Holvey Eckert

May 1966

PERFORMANCE ANALYSIS AND INITIAL TESTS OF A TRANSONIC TURBINE TEST RIG

by

Richard Holvey Eckert
Commander, United States Navy

Submitted in partial fulfillment
for the degree of

AERONAUTICAL ENGINEER

from the

UNITED STATES NAVAL POSTGRADUATE SCHOOL
May 1966

ABSTRACT

The primary purpose of the Transonic Turbine Test Rig of the United States Naval Postgraduate School, Monterey, California, is to permit investigation of turbine performance and flow conditions for transonic rotor inlet velocities. This turbine also has provisions for investigation of the effects on performance of widely varied axial and tip clearances. High turbine total-to-total pressure ratios are achievable, since an ejector-type exhauster assembly can maintain a partial vacuum in an airtight turbine discharge hood. This study is concerned primarily with initial turbine performance tests--of the nature of suitability tests--both with and without the rotor installed. The installation is described, and results of flow rate calibration and labyrinth seal leakage tests are included, along with turbine performance test results. Also presented are a simplified three-dimensional turbine performance prediction and a one-dimensional analysis of exhauster performance. The turbine performance prediction method uses the so-called equivalent enthalpy (and corresponding equivalent total thermodynamic properties) to permit analysis of the relative flow through the rotor in a manner analogous to that used for absolute flows.

TABLE OF CONTENTS

LIST OF TABLES

LIST OF ILLUSTRATIONS

TABLE OF SYMBOLS

Symbols

A	Cross-sectional area ($in.^2$)
A	Constant dependent on square-edged orifice geometry (dimensionless).
a	Exit opening of a cascade (in.).
B	Constant dependent on square-edged orifice geometry ($in.^{-1}$).
B	Subscripted, one through three; see Eqs. (122)-(124).
b.	Blade's departure from being straight-backed (in.).; see Fig. 53.
b	Between-teeth chamber heighth, labyrinth seals (in.).
C	Constant in square-edged orifice equation ($(^\circ R/in.Hg\text{-}in.H_2O)^{\frac{1}{2}}$ lbm/sec.)
C_1	Conversion factor, 2gJ (ft^2-lbm/sec^2-BTU).
C_2	Conversion factor, $2gJc_p$ ($ft^2/sec^2\text{-}^\circ R$).
c	Chord of blade (in.).
c_p	Specific heat, constant pressure (BTU/lbm-$^\circ$R).
D	Diameter (in.).
E	Kinetic energy (ft-lb).
e	Curvature of the back of a blade; see Eq. (288) and Fig. 53.
F	Force (lb).
f	Correction factor, see Eq. (200).
g	Universal gravitational constant (32.174 lbm-ft/lb-sec^2).
H	Total enthalpy (BTU/lbm).
H^{***}	Energy parameter, boundary layer (dimensionless); see App. I.
h	Static enthalpy (BTU/lbm).
h	Blade heighth (in.).
h_w	Differential pressure (in. H_2O).
HP	Horsepower.
I	Integrand.

Symbols

i	Incidence angle (deg. or radians).
i_s	Positive stalling incidence angle (deg. or radians).
$\mathbf{i}$	Unit vector.
J	Conversion factor (778.16 ft-lb/BTU).
j	Dimension for determining blade-back curvature (in.); see Fig. 53.
K	Discharge coefficient, flow metering or labyrinth seal (dimensionless).
k	Tip clearance (in.).
k_{is}	Head coefficient (dimensionless); see Eq. (81).
L	Distance between stations ahead of and after a rotor (in.).
M	Mach Number (dimensionless).
M	Moment (ft-lb or in-lb).
$\dot{m}$	Mass flow rate (slugs/sec).
m	Exponent used in boundary layer calculations (dimensionless); see p. 45 .
N	Rotational speed (RPM).
n	Number of throttlings, labyrinth seals (dimensionless).
n	Polytropic exponent (dimensionless); see pp. 79-80.
$\bar{n}$	Outward normal (unit)vector.
P	Pressure (in. Hg. abs).
p	Pressure (psia).
R	Gas constant for air (53.345 ft-lb/lbm- R).
R	Reaction force (lb).
Re	Reynolds Number (dimensionless).
r	Labyrinth seal overall (inlet total to exit static) pressure ratio (dimensionless).
r	Radius (in.).
r^*	Theoretical degree of reaction (dimensionless); see Eq. (80).

Symbols

s	Entropy (BTU/lbm-°R).
s^*	Non-dimensional entropy (s/c_p) or entropy increase ($\Delta s/c_p$).
s	Cascade blade pitch (in.).
s	Surface area ($in.^2$).
s	Labyrinth seal between-teeth spacing (in.).
T	Temperature (°R).
t	Temperature (°F).
t	Blade thickness (in.).
t	Labyrinth seal tooth thickness (in.).
t_e	Blade trailing edge thickness (in.).
t_{t_e}	Projection of Blade trailing edge thickness on the exit plane of the blade row (in.).
U	Peripheral velocity (ft/sec).
u	Velocity within a boundary layer (ft/sec).
V	Absolute velocity (ft/sec).
W	Relative velocity (ft/sec).
$\dot{W}$	Flow rate (lbm/hr).
$\dot{w}$	Flow rate (lbm/sec).
$\dot{w}_f$	Fraction of the total flow rate which passes between the hub streamline and any other streamline (dimensionless).
$\dot{w}_{rf}$	Reference flow rate parameter ($in.^2$); see Eq. (16).
X	Non-dimensional radius, r/r_m, where r_m is the mean streamline radius (dimensionless).
X	In square-edged orifice equations, $Re(10^{-6})$, (dimensionless).
X	In exhauster performance analysis, the axial distance downstream of the inlet to the diverging portion of the exhauster piping (in.).
X_e	See Eq. (268), (dimensionless).
Y	Non-dimensional axial velocity ratio, V_a/V_{a_m}, where V_{a_m} is the mean streamline axial velocity.

Symbols

Y_1 In flow measurement equations, expansion factor (dimensionless); see Eq. (159).

Y Pressure loss coefficient used in determining the loss coefficient.

Z Number of blades (dimensionless).

z' Absolute viscosity in centipoises.

z $= 100z'$ (centipoises).

z Axial distance in cylindrical coordinates (in.).

Greek Letters

α Discharge coefficient, labyrinth seals (dimensionless).

α Stator gas flow angle (deg. or radians)

α Coefficient of thermal expansion, flow metering (dimensionless).

β Rotor gas flow angle (deg. or radians).

β' Rotor geometric blade angle.

β Ratio of orifice or nozzle minimum diameter to upstream pipe diameter, in flow measurement (dimensionless).

γ Specific heat ratio, c_p/c_v (dimensionless).

γ^* Velocity carryover factor, labyrinth seals (dimensionless).

δ Labyrinth seal tooth radial clearance (in.).

δ Boundary layer thickness (in.).

δ Referred pressure p_{t_o}/p_{std}, $p_{std} = 14.7$psia (dimensionless).

δ^* Boundary layer displacement thickness (dimensionless).

δ^{***} Boundary layer energy thickness

ζ Less coefficient (dimensionless).

ζ Correction factor for Reynolds Number, square-edged orifices (dimensionless).

η Efficiency (dimensionless).

η Non-dimensional distance from the wall in a boundary layer (y/δ).

θ Referred temperature, T_{t_o}/T_{std}, $T_{std}=518.4$ R (dimensionless).

κ Curvature factor (dimensionless); see Eq. (258).

Greek Letters

λ Angle of flow in a meridional plane (deg. or radian).

λ Factor used in estimating blading secondary loss coefficients (dimensionless); see App. II.

λ_{mix} Pressure loss coefficient, blading leaving loss (dimensionless).

ξ Area restriction factor (dimensionless); see Eqs. (21) and (187).

ρ Density (slugs/ft^3).

Φ Non-dimensional flow function; see Eq. (10).

φ Labyrinth seal pressure ratio function (dimensionless); see Eq. (164).

φ_v Absolute flow velocity coefficient, V/V_{TH}, (dimensionless).

ψ Relative flow velocity coefficient, W/W_{TH}, (dimensionless).

ω Angular velocity (radians/sec).

Subscripts

a Ambient conditions.

a Axial.

ACT Actual (or computed) value.

b Refers to flow through stator blade row, exhauster performance analysis.

c Subsonic compression, in exhauster performance analysis.

c In turbine equations, refers to the flow director ring shrouding the rotor.

d In exhauster performance analysis, turbine hood conditions.

E Refers to so-called equivalent thermodynamic properties.

e In exhauster performance analysis, supersonic expansion.

e In turbine equations, entrance station of plenum.

eff Effective.

f Due to or corrected for friction.

H Hub.

Subscripts

I	In the vicinity of the cover plate (see Fig. 6).
i	Used with efficiency, η, to designate overall turbine (internal) efficiency.
i	Used with M to denote the moment about the turbine centerline acting on the stator-plenum assembly.
is	Value for isentropic expansion from inlet conditions.
ℓ	Refers to the turbine plenum labyrinth seal.
ℓ	In exhauster analysis, downstream of a shock.
m	Mean streamline.
N	In exhauster analysis, refers to ejector nozzle flow.
n	Refers to flow measurement nozzle.
o	Denotes inlet conditions.
o	Used with the coefficient of thermal expansion to denote the square-edged orifice value.
p	Used with force, F, to denote pressure forces.
p	Plenum condition.
p	Used with efficiency, η, to denote polytropic efficiency.
p	Used with loss coefficient, ζ, to denote profile loss coefficient.
R	Relative flow value.
R	Rotor value.
r	Radial.
ref	Referred value.
req	Required.
s	Stator.
s	In flow rate equations, refers to shaft labyrinth seal.
s	As second subscript denotes value for isentropic expansion from equivalent total conditions.
s	Used with loss coefficient to denote the secondary loss coefficient.

Subscripts

T	Tip.
T	In exhauster performance analysis, turbine.
TH	Theoretical value, i.e., for isentropic expansion.
u	Tangential.
u	In exhauster performance analysis, upstream of a shock.
z	Refers to the axial direction, cylindrical coordinates.
θ	Refers to angle coordinate in cylindrical coordinates
1	Station between the stator and the rotor.
1	Station at exhauster nozzle exit plane.
1	Streamline number one (hub).
2	Station at the rotor exit.
2	Station at the inlet to the diverging portion of the exhauster.
2	Streamline number two (between hub and mean streamlines).
3	Station at the exit of the exhauster piping.
3	Streamline number three (mean).
4	Streamline number four (between mean and tip streamlines).
5	Streamline number five (tip).

Superscripts

*	Denotes choked-flow.

1. Introduction.

Little qualitative information is available concerning turbine performance under conditions of transonic rotor entrance velocities and extreme total to static turbine pressure ratios. Additionally, axial and radial clearances in turbines for use in rocket applications and gas turbine plants are often subject to wide variations because of extreme temperature variation.

Information regarding radial clearance effects on efficiency available to designers indicates that tip clearances should be limited to about one percent of blade heighth. However, the smaller a turbine, the more expensive it becomes to achieve the close tolerances required to maintain this percent tip clearance. Also, temperature effects become more critical for smaller turbines, with respect to maintaining the desired radial clearance over a range of operating conditions.

Much less information is available to designers on the effects of axial clearances on performance. Methods of analysis of turbine performance generally used in turbine design assume axisymmetric, uniform flow conditions between blade rows, but do not consider the axial distance required to permit the flow to achieve such stabilized conditions. Consequently, axial clearances between blade rows are dictated primarily by space and weight considerations, rather than by knowledgeable considerations of axial clearance effects. It is even conceivable that optimum axial clearances, from a performance viewpoint, may be less than normally used for some types of blading.

The Transonic Turbine Test Rig installed at the Propulsion Laboratory of the Department of Aeronautics, U.S. Naval Postgraduate School, Monterey, California, was designed by Professor M. H. Vavra of that department to

permit investigation of the above-stated problems. This thesis is concerned with describing the installation and its capabilities, calibration tests, and initial performance tests of the turbine rig, with a stator consisting of converging nozzle type blading and an impulse type blading rotor.

Funds for designing and building the Transonic Turbine Test Rig, as well as operating funds, were furnished by the Bureau of Naval Weapons (RAPP-14). The generosity of that Bureau is greatly appreciated. The author is most appreciative, too, of the guidance and counsel provided by Professor Vavra, and of the assistance in performing experiments so willingly given by Mr. L. T. Clark of the Department of Aeronautics.

2. Installation.

The Transonic Turbine Test Rig (TTTR) installation is shown schematically in Fig. 1, whereas Fig. 2 is a photograph of the turbine hood and exhauster assembly (with the exhauster rotated 180° from its actual configuration in the TTTR installation). The turbine proper is a single-stage, impulse-type design. The salient components of the installation shown in Fig. 1 are the:

1. flow measurement nozzle;
2. removable standard orifice installation;
3. plenum labyrinth leak rate measurement standard orifice (two-inch pipe orifice, Fig. 1);
4. turbine plenum labyrinth seals;
5. shaft labyrinth seals;
6. turbine hood; and the
7. turbine proper and turbine plenum.

This turbine can be operated exhausting either to atmospheric pressure or, with the hood and exhauster installed, to a partial vacuum.

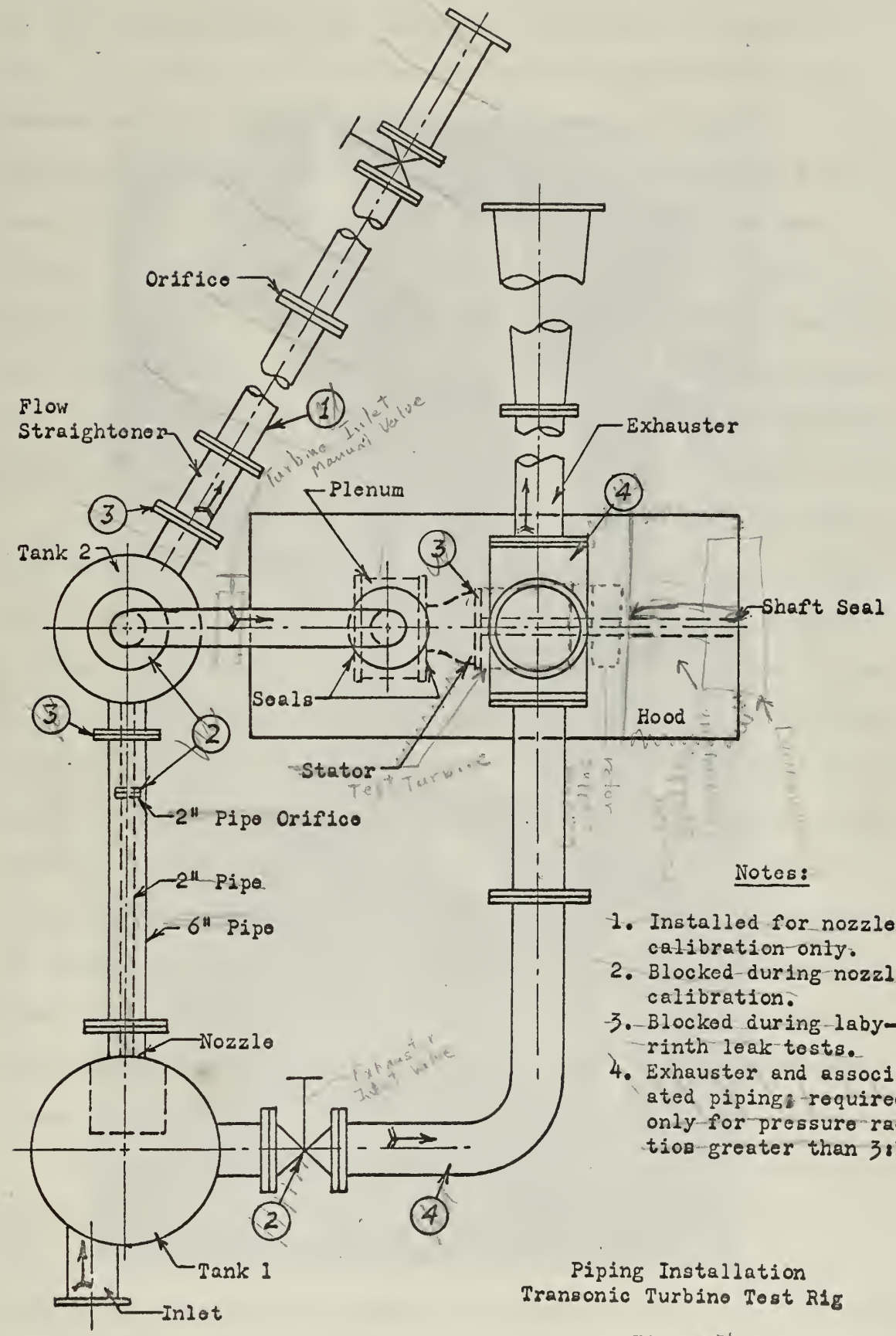

Notes:

1. Installed for nozzle calibration only.
2. Blocked during nozzle calibration.
3. Blocked during labyrinth leak tests.
4. Exhauster and associated piping; required only for pressure ratios greater than 3:1.

Piping Installation
Transonic Turbine Test Rig

Figure X

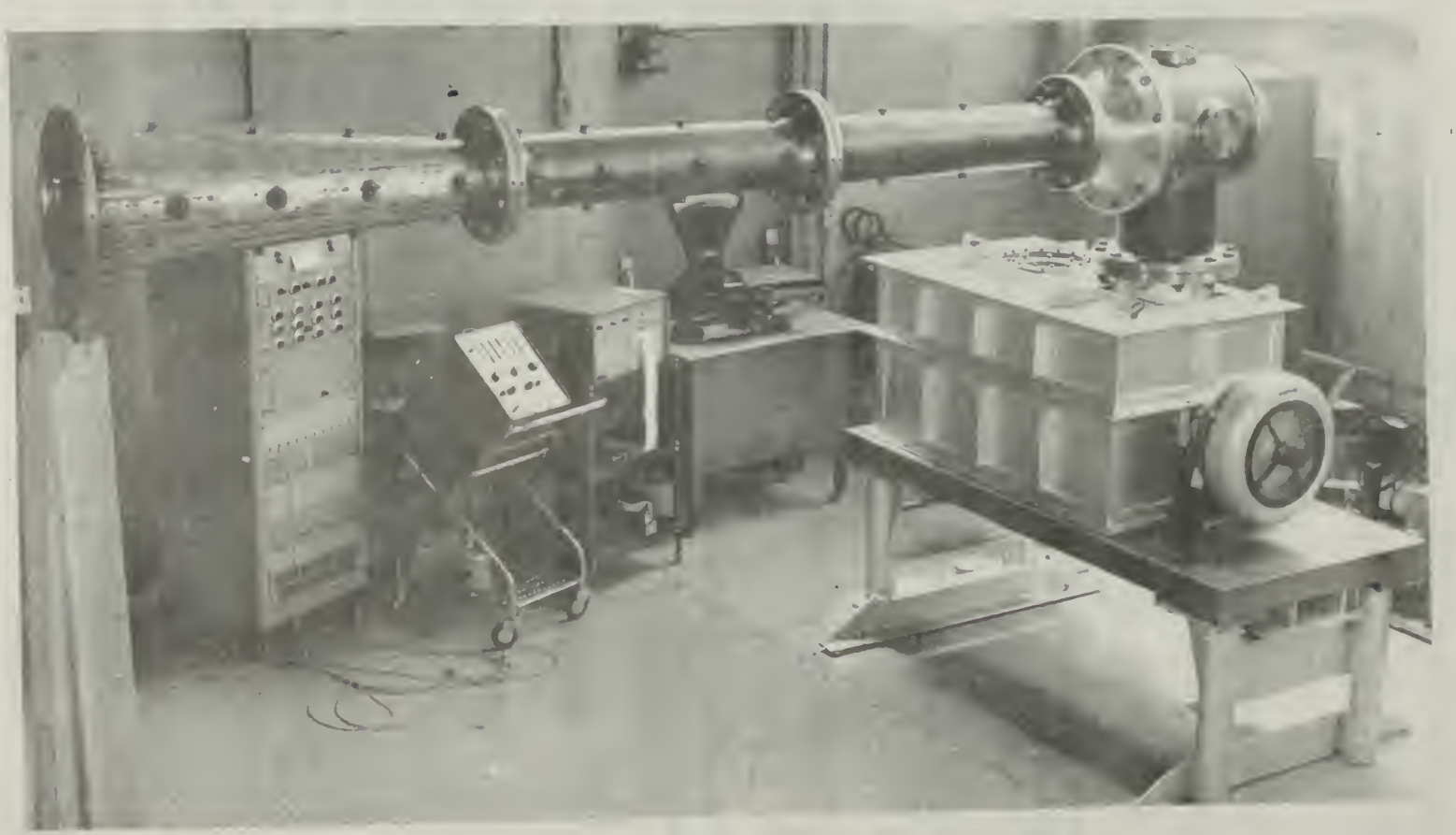

TURBINE HOOD AND EXHAUSTER ASSEMBLY
TRANSONIC TURBINE TEST RIG

FIGURE 2

Supply air is furnished by the Allis Chalmers, VA 312 compressor installed at the Propulsion Laboratory. Supply air temperature is regulated by means of an aftercooler installed downstream of the compressor. The maximum temperature of air supplied by the compressor is 300°F. However, since the turbine has aluminum blading, a limiting value of 200°F has been established for turbine inlet total temperature. The maximum turbine inlet total pressure attainable is about 43 psia. Exhausting to the atmosphere, the total to static pressure ratio possible is about 2.8, and a maximum total to total pressure ratio of about 5.6 is anticipated when exhausting to a partial vacuum (see Section 4, Exhauster Performance Analysis). Maximum turbine RPM is 20,000 and maximum horsepower is 200.

The flow rate through the turbine blading during operation is the flow measured by the flow nozzle less the plenum labyrinth seal leakage. The flow nozzle, with pressure and temperature tap locations indicated, is shown in Fig. 3, and the plenum labyrinth seal configuration is shown in Fig. 4. Since there is insufficient piping upstream of the flow nozzle to ensure undisturbed flow through the nozzle, calibration of the flow nozzle was required. The removable standard orifice assembly is provided for that purpose. Plenum labyrinth seal leak rate can not be measured during turbine operation; hence, the two-inch pipe orifice is provided for determining this flow rate in separate tests. During such tests, all flow to the plenum passes through the two-inch pipe and the only exit for the flow is through the plenum seals, since the stator exit is blocked by a special cover plate.

In analyzing exhauster performance, the flow rate to the exhauster ducting (see Fig. 5) consists of the flow from the turbine hood and the flow through the exhauster nozzle. The former consists of the flows through the turbine blades, through the plenum labyrinth seals, and through

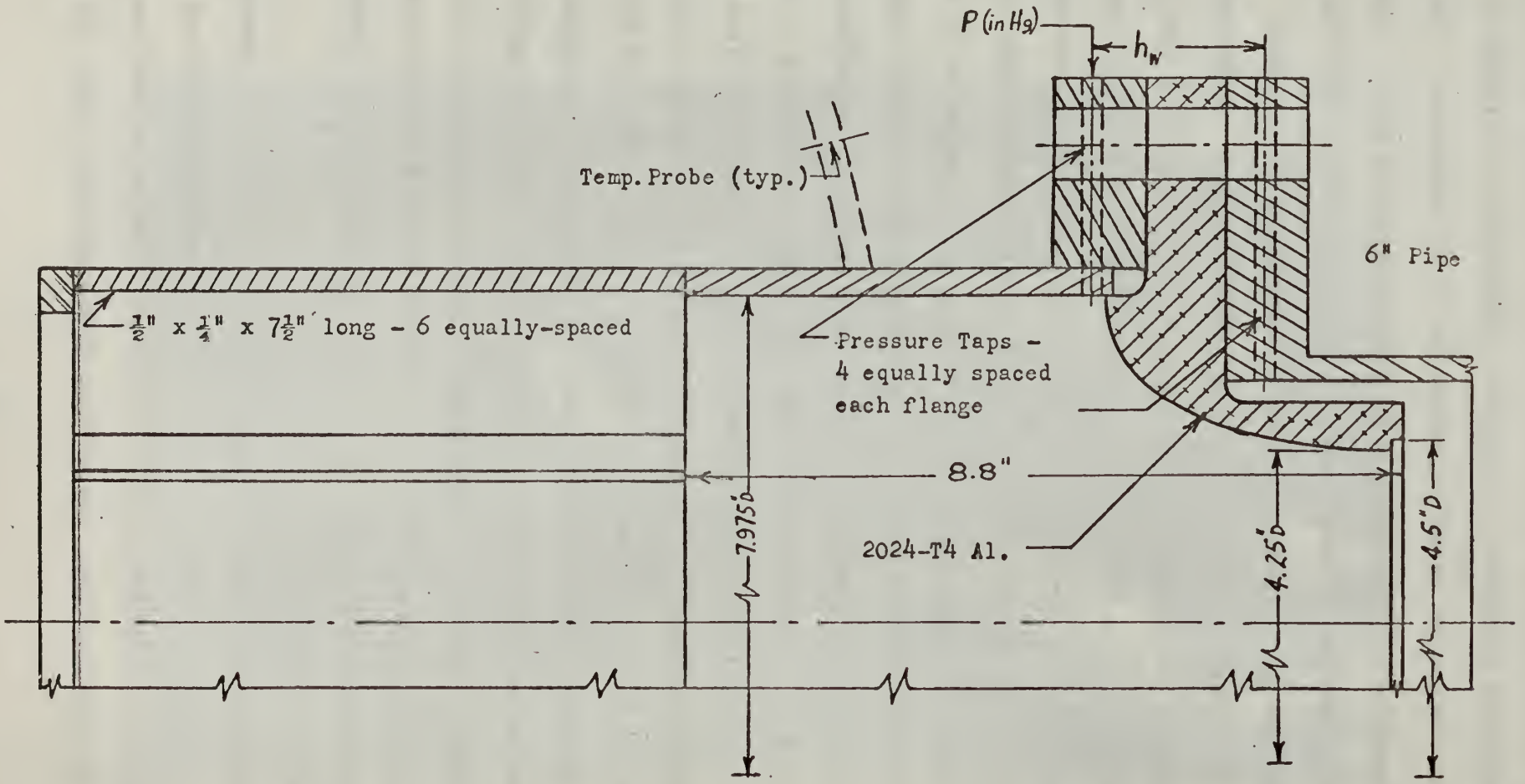

Flow Measurement Nozzle
Transonic Turbine Test Rig

Figure 3

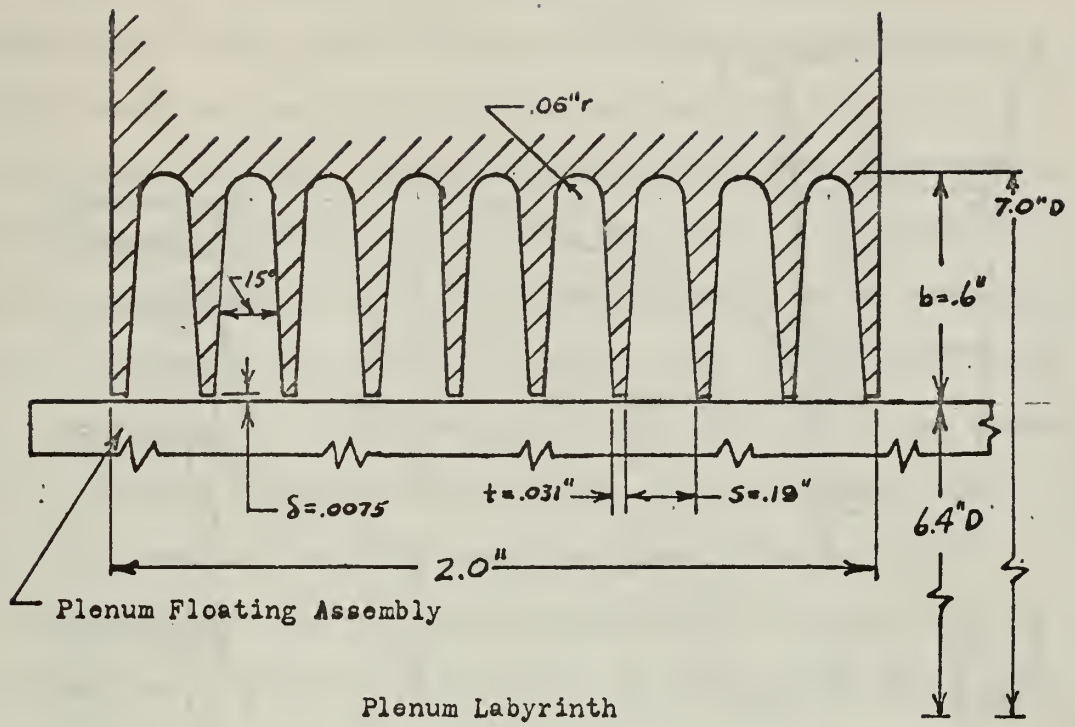

Plenum Labyrinth

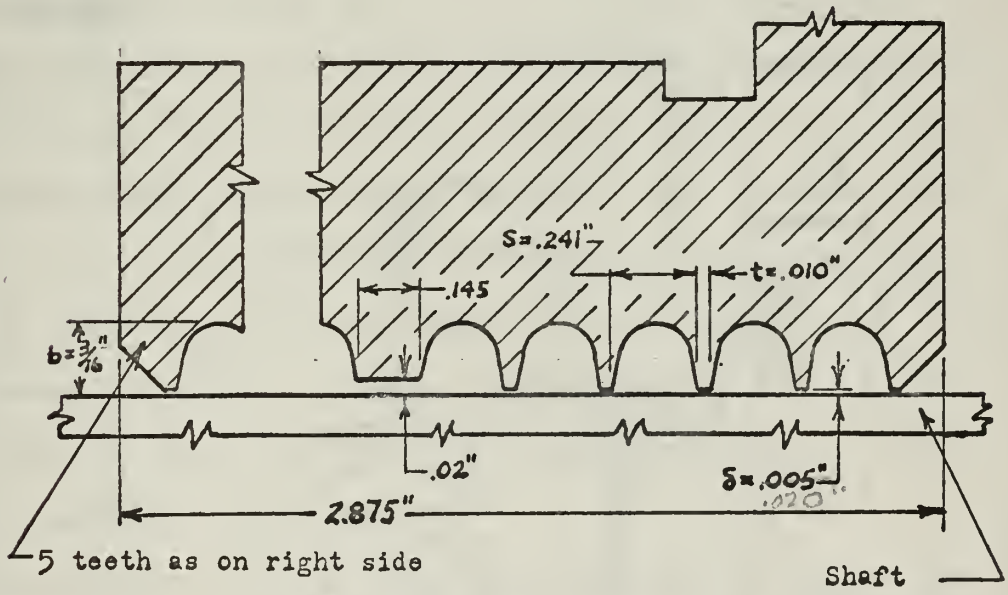

Shaft Labyrinth

Labyrinth Seal Configurations
Transonic Turbine Test Rig

Figure 4

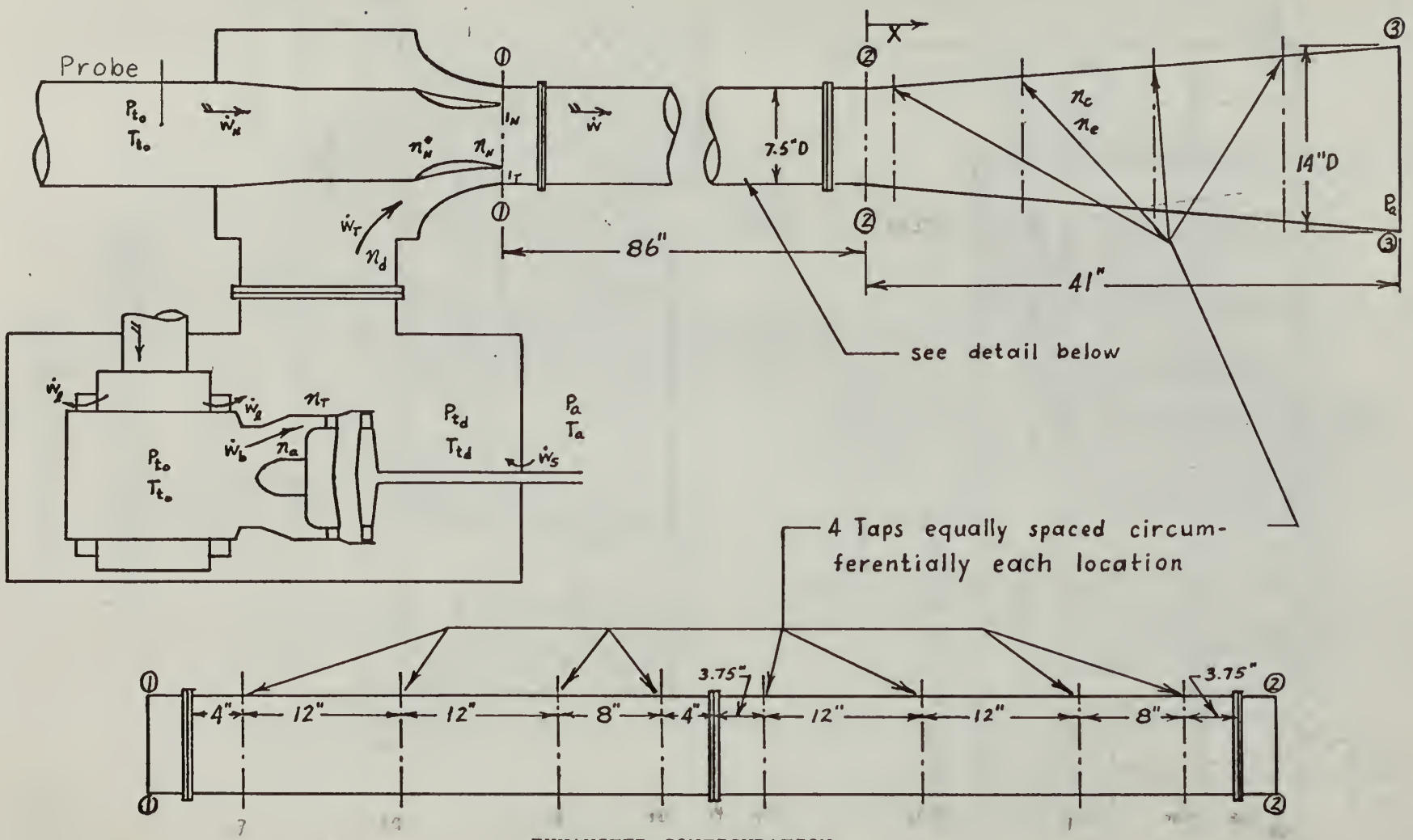

EXHAUSTER CONFIGURATION
TRANSONIC TURBINE TEST RIG

FIGURE 5

the shaft labyrinth seals (from the atmosphere to the partial vacuum in the turbine hood). There are no provisions for measuring the leakage through the shaft seal, and this flow rate must be estimated. Also, flow through the exhauster nozzle can not be measured directly. However, with the entire flow of the compressor routed to the turbine rig, the flow through the exhauster nozzle is the flow rate delivered by the compressor, determined as specified by Vavra, [9][1] minus the flow rate measured by the flow measurement nozzle. Additionally, since the flow through the exhauster nozzle will normally be choked, the flow rate can be determined quite accurately by measuring the total conditions ahead of the nozzle.

Both the removable and the two-inch pipe orifice assemblies conform to specifications for standard square-edged orifice installations as set forth by Stearnes, et. al. [2] Detailed information regarding specifications applicable to these assemblies, including pertinent dimensional information, is given by Eckert. [6]

The turbine proper and the turbine plenum are shown schematically in Fig. 6. The rear support and front hanger shown are attached in turn to a cradle flexure assembly affixed to the rig table. The set screw at the rear support is provided for setting axial clearances. Figs. 7 and 8 are photographs of the turbine with and without the rotor, respectively. Fig. 9 shows the manner in which the floating armature assembly fits into the plenum. As shown in Fig. 6, the following instrumentation is installed in the turbine and plenum assembly:

1. Static pressure (p_p) and static temperature (T_p) in the plenum;

2. Total pressure (p_{t_o}), static pressure (p_o) and total temperature (T_{t_o}) ahead of the stator;

[1]Figures in brackets refer to bibliography entries of Section 9.

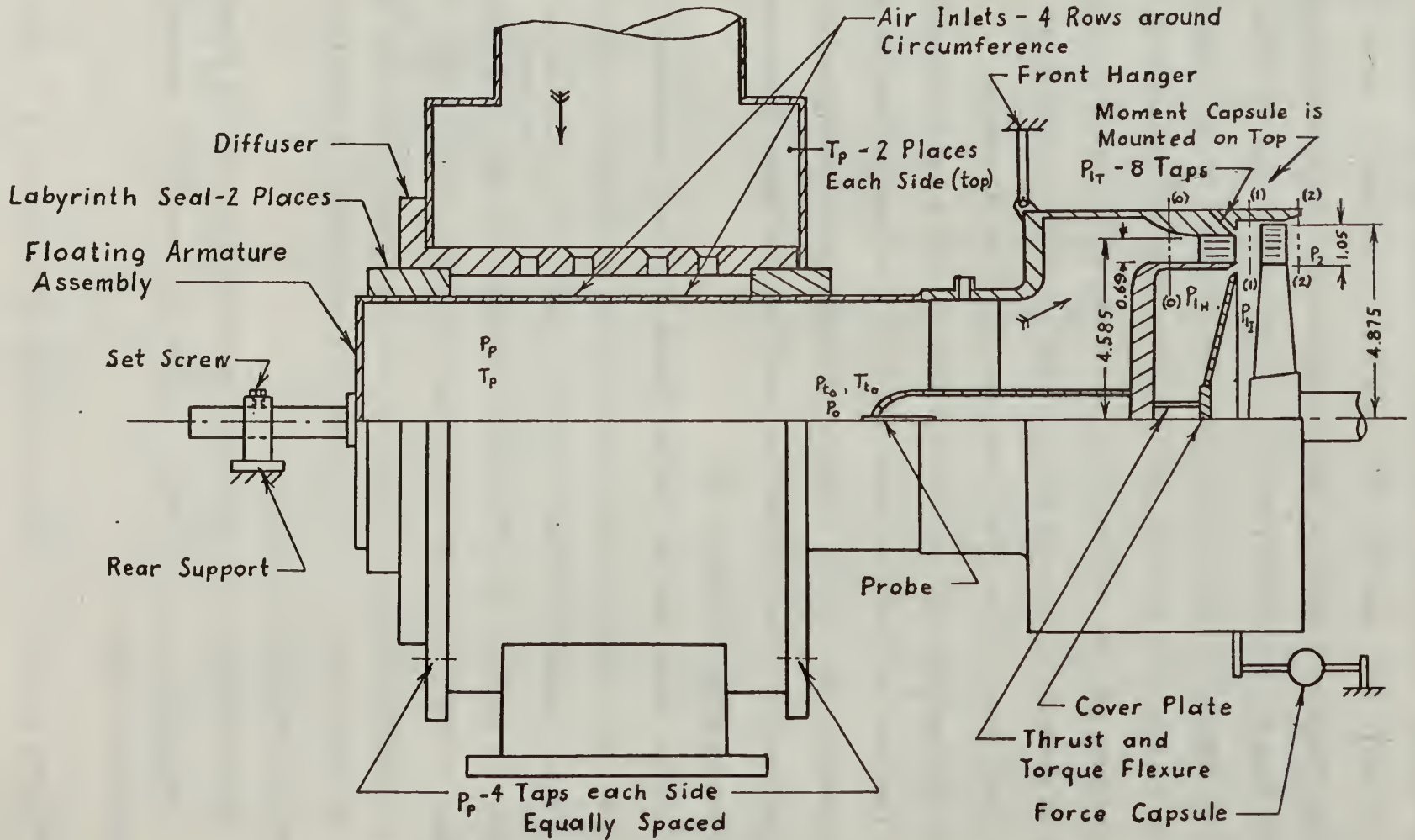

TURBINE AND PLENUM ASSEMBLY
TRANSONIC TURBINE TEST RIG

FIGURE 6

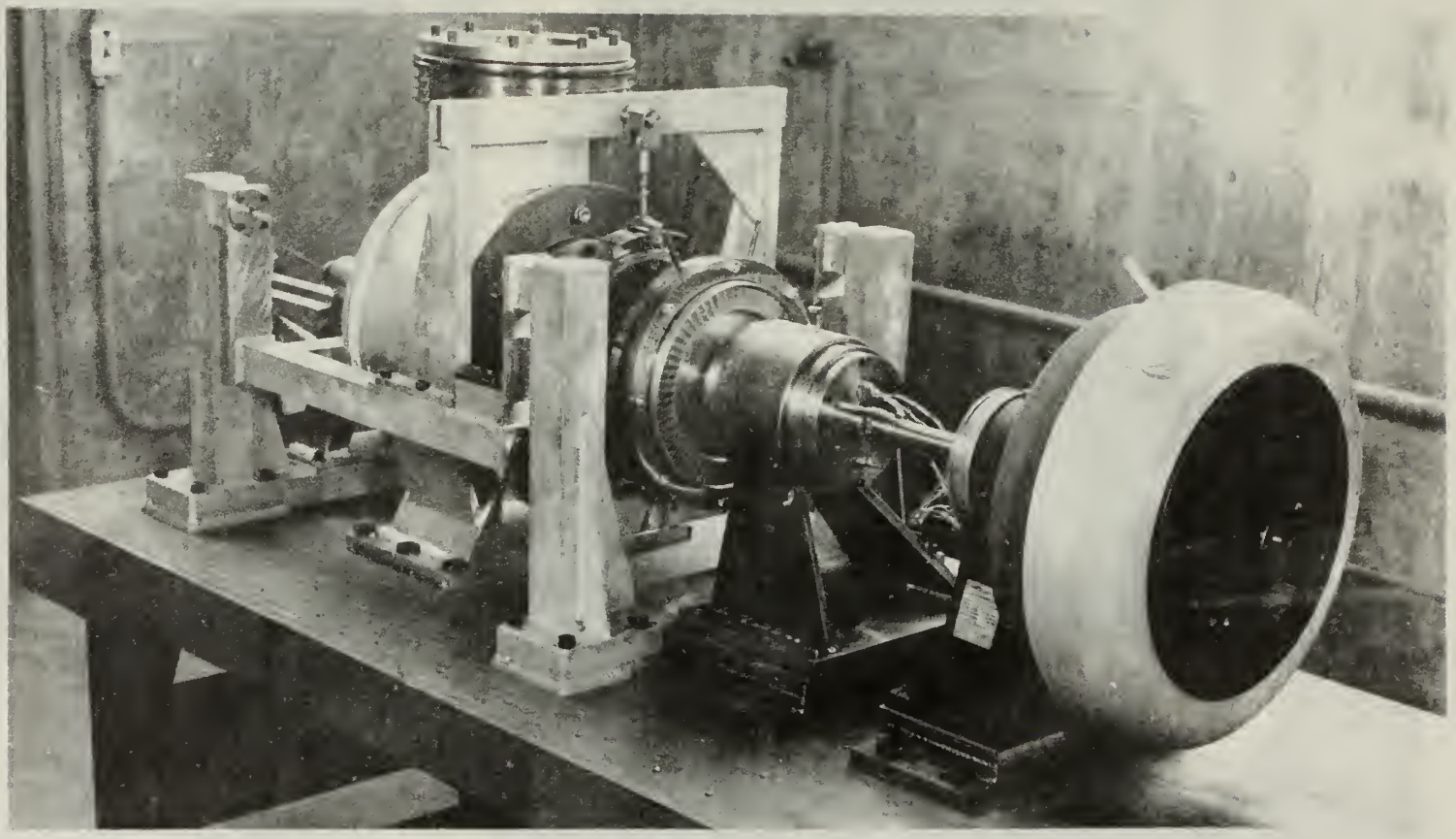

TURBINE, TRANSONIC TURBINE TEST RIG

FIGURE 7

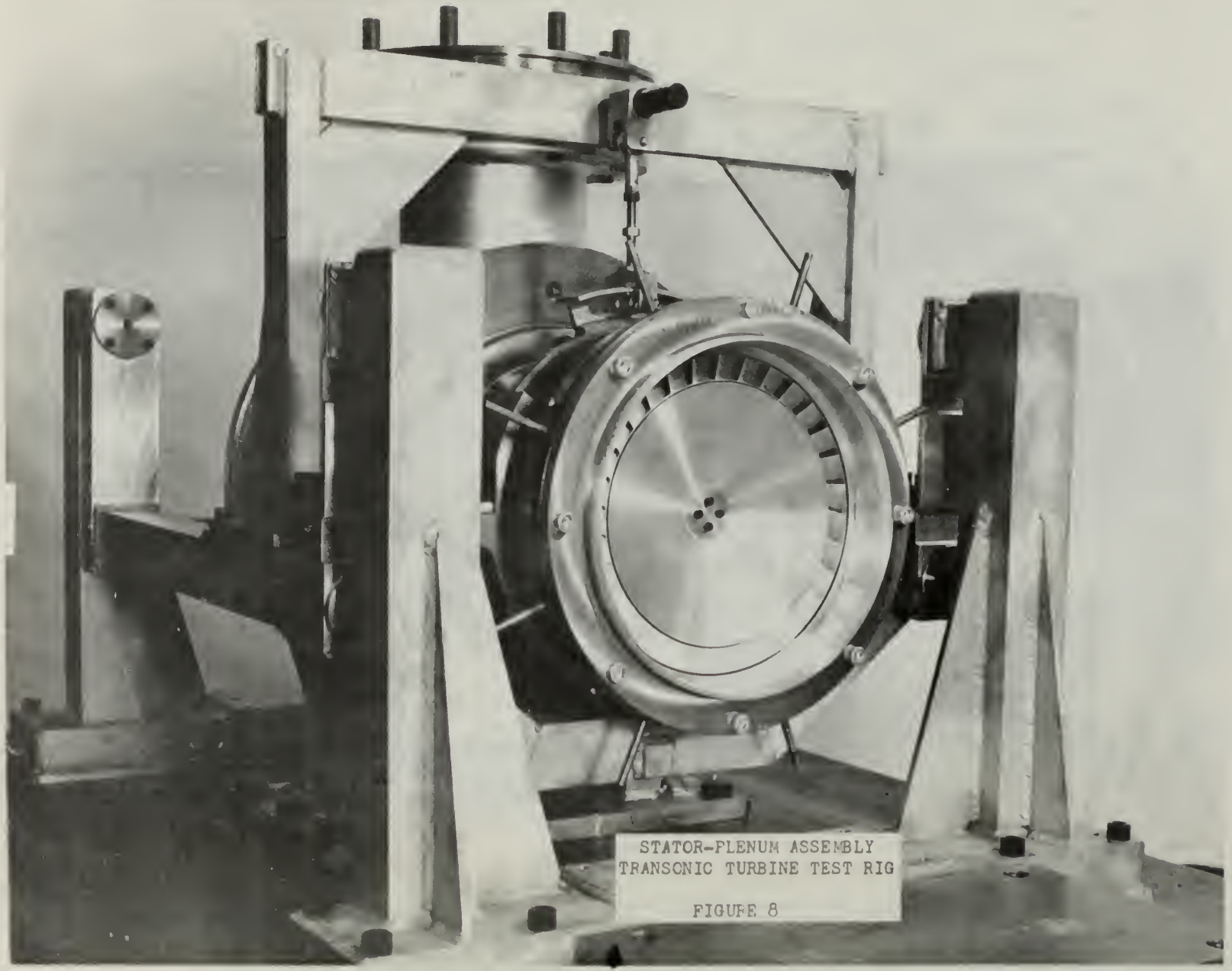

STATOR-PLENUM ASSEMBLY
TRANSONIC TURBINE TEST RIG

FIGURE 8

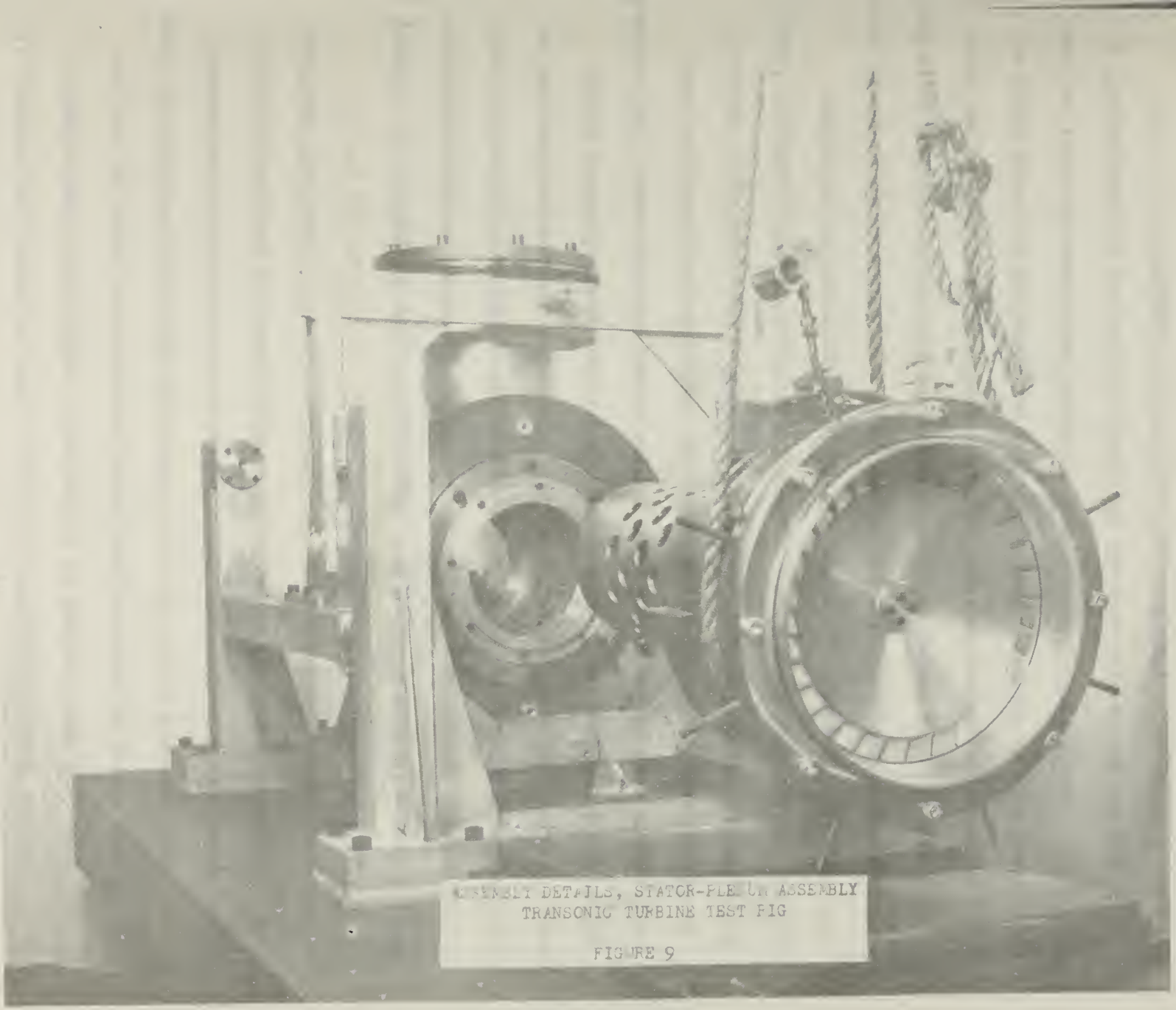

ASSEMBLY DETAILS, STATOR-PLENUM ASSEMBLY
TRANSONIC TURBINE TEST FIG

FIGURE 9

3. Static pressures at the hub (p_{l_H}) and at the tip (p_{l_T}) of the stator in the exit plane; and

4. Reluctance gages for measuring the axial force and the moment about the axis, acting on the stator-plenum assembly.

The air dynamometer used for measuring rotor torque is shown in Fig. 7.

Spoked-wheel type flexures are installed at both the front and rear bearings of the rotor bearing housing for measuring the axial force on the rotor. Strain gages are mounted on both sides of each of the three webs of these flexures. Pressure taps are installed around the sides and in the top of the turbine hood for measuring turbine total discharge pressure (p_{t_d}) during operation with the hood and exhauster installed.

The thrust and torque flexure shown in Fig. 6 was included to permit determination of the pressure (p_{l_I}) acting on the cover plate concentric with and inside the stator ring. The axial force acting on the cover plate will be determined by a flexure in the position shown. The pressure (p_{l_I}) can then be determined from this force and the pressure in the cavity behind the cover plate (p_{l_H}). However, the flexure shown has not been instrumented, since stator-only tests showed it to be too critical in wall thickness and axial groove size, with respect to desired sensitivity and adequate strength. In the future, this set-up will be replaced by a spoked-wheel type flexure.

The instrumentation of the stator and plenum assembly was designed to permit using the momentum and moment of momentum equations to determine stator performance. For accuracy in such performance measurement, the pressures at the hub and at the tip of the stator exit, and the pressure acting on the cover plate must be known, along with the reaction force and moment acting on the assembly. Additionally, the average of the hub and tip pressures is a better value for stator exit pressure (p_l)

than either value by itself. During stator tests without the rotor, the pressure acting on the cover plate was measured directly by using taps installed inside a specially fabricated cylinder placed over the rotor bearing housing. However, such pressure could not be determined for the turbine tests conducted to date.

The stator-plenum assembly can be moved axially a distance of 1.2 in. to achieve various stator to rotor axial clearances. Moreover, the rotor can be moved axially approximately 0.25 in. for increased range and flexibility in setting axial clearances.

Fig. 10 shows the turbine gas path and pertinent dimensions for maximum rotor blade heighth. The basic configuration shown is that for use with the converging nozzle stator guide vanes. The dashed lines indicate the gas path when the second set of guide vanes, of converging-diverging nozzle type, are installed. It is evident from Fig. 10 that a range of tip clearances from the minimum practicable to about 0.6 in. are attainable merely by reducing the rotor outer diameter. Additionally, through the use of inserts between the wheel outer diameter and the case, various gas path flare angles can be achieved, along with varied radial clearances and radial overlaps at the tip, obtainable by varying axial clearance.

The blading profiles of the two available stators are shown in Fig. 11, and the profiles of the two available rotors are shown in Fig. 12. The area ratio -- exit opening to throat -- of the converging-diverging blading is 1.25, corresponding to an isentropic Mach Number of 1.6. One rotor blading is double-circular-arc profile, while the other is a profile with gradually changing curvature.

The exhauster head (nozzle plus turbine hood flow inlet section) of the exhauster assembly shown in Fig. 5 is shown in Fig. 13. Axial locations of pressure taps in the ducting are indicated in Fig. 5. At

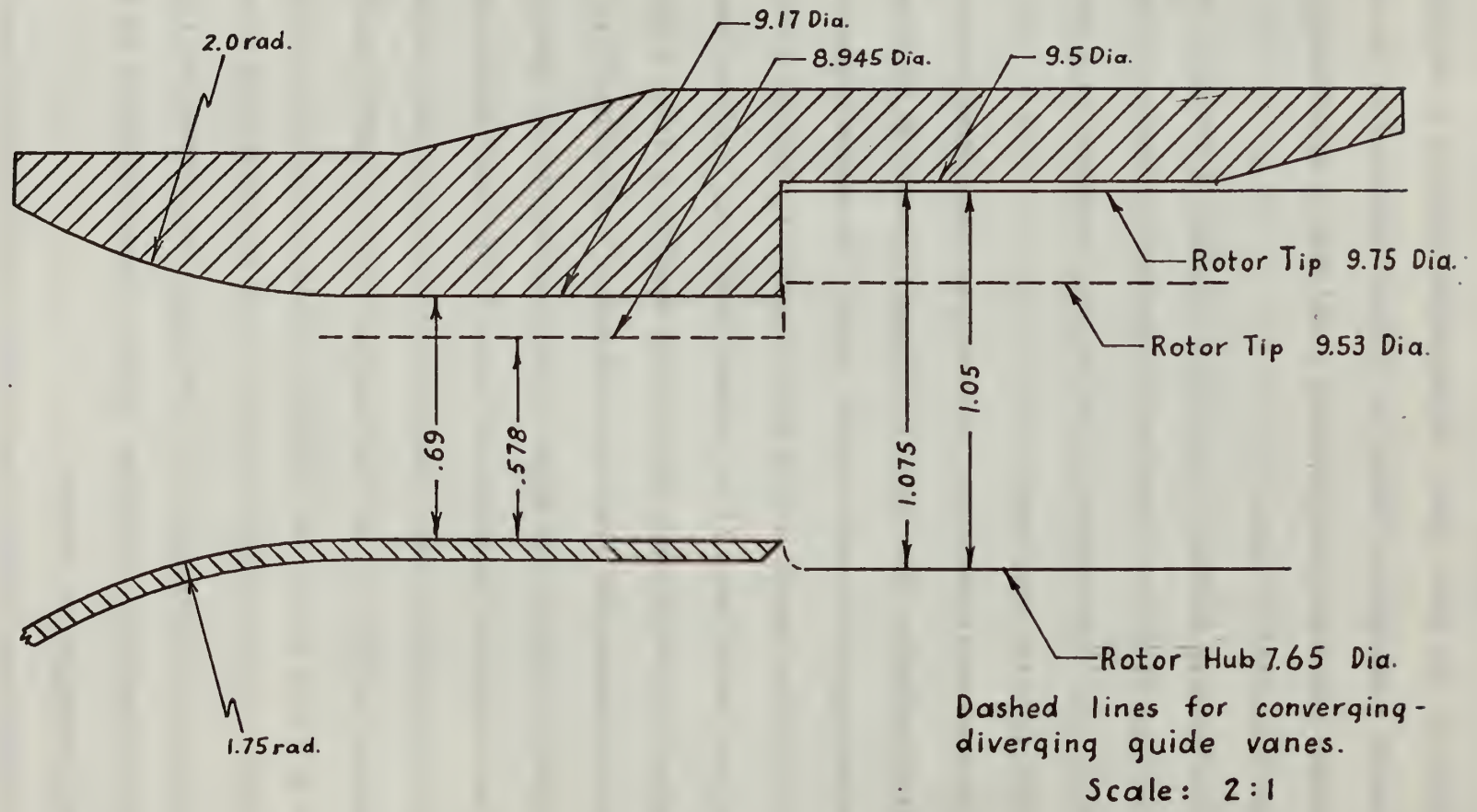

GAS PATH, TRANSONIC TURBINE

FIGURE 10

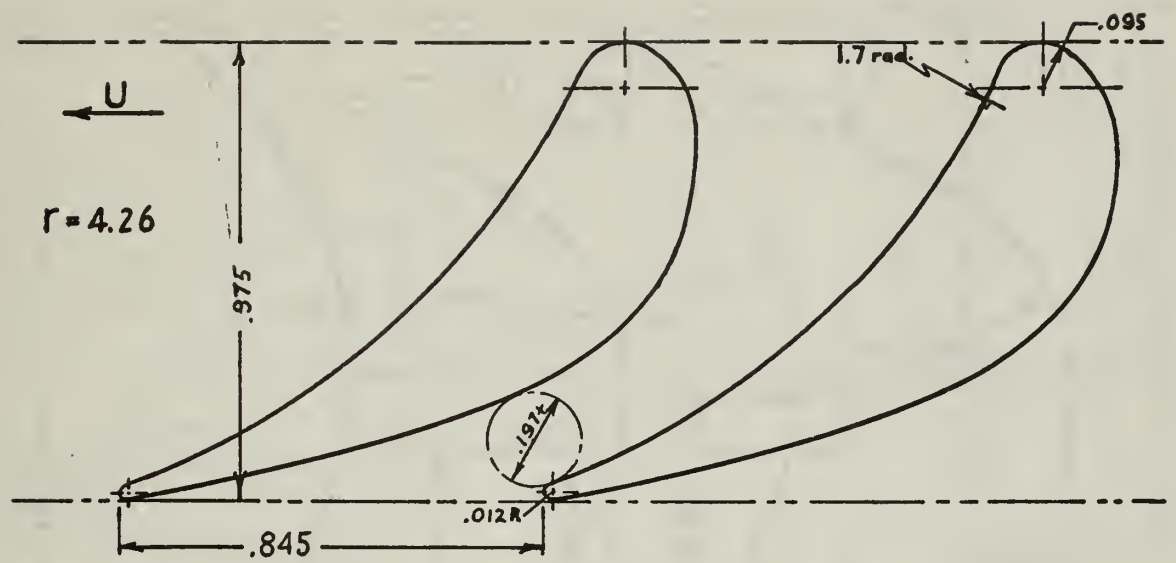

Converging Guide Vanes

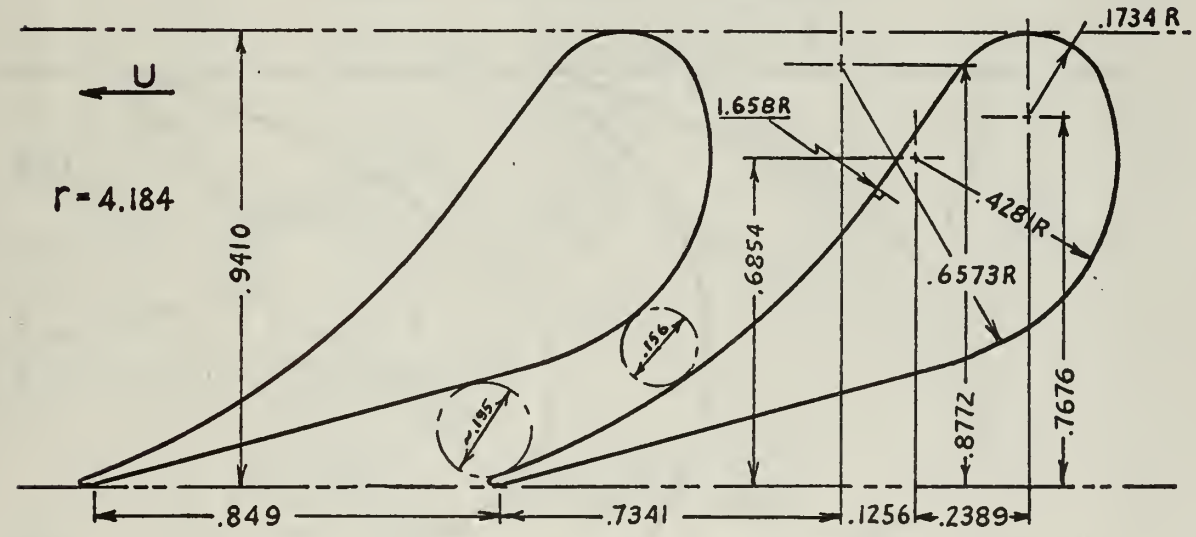

Converging-Diverging Guide Vanes

STATOR BLADE PROFILES
TRANSONIC TURBINE TEST RIG

FIGURE 11

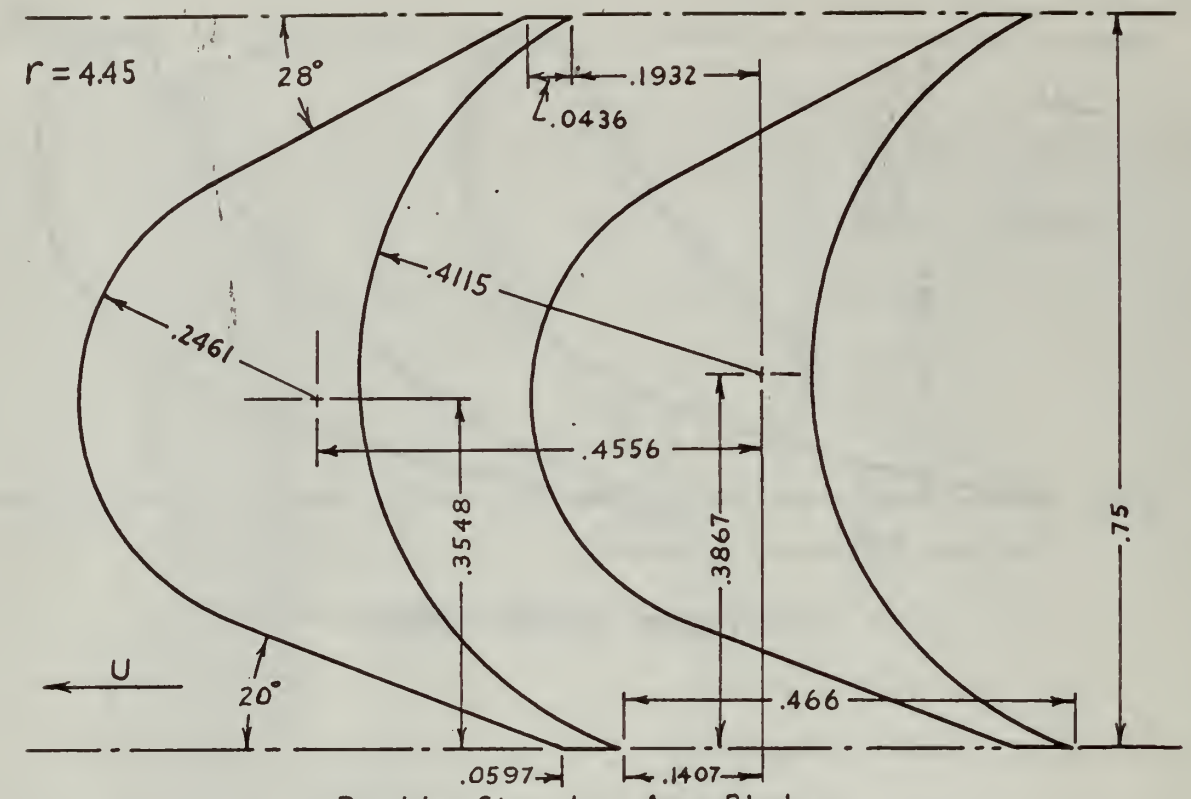

Double Circular Arc Blades

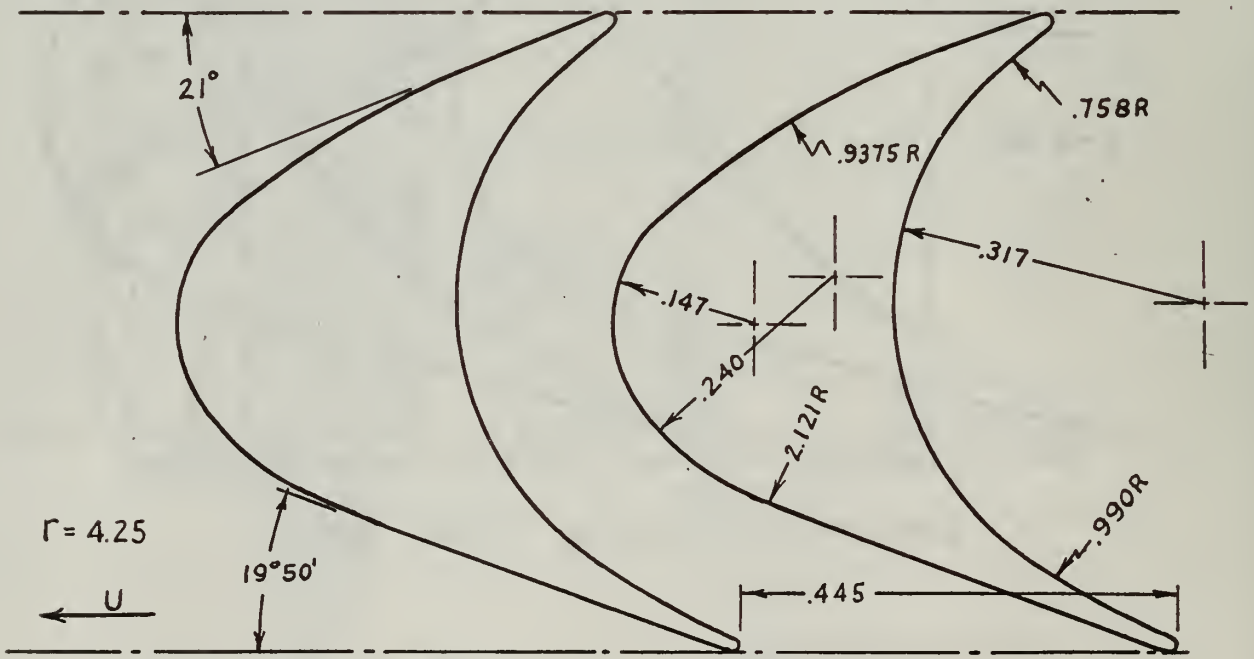

Multiple Arc Blades

ROTOR BLADE PROFILES
TRANSONIC TURBINE TEST RIG

FIGURE 12

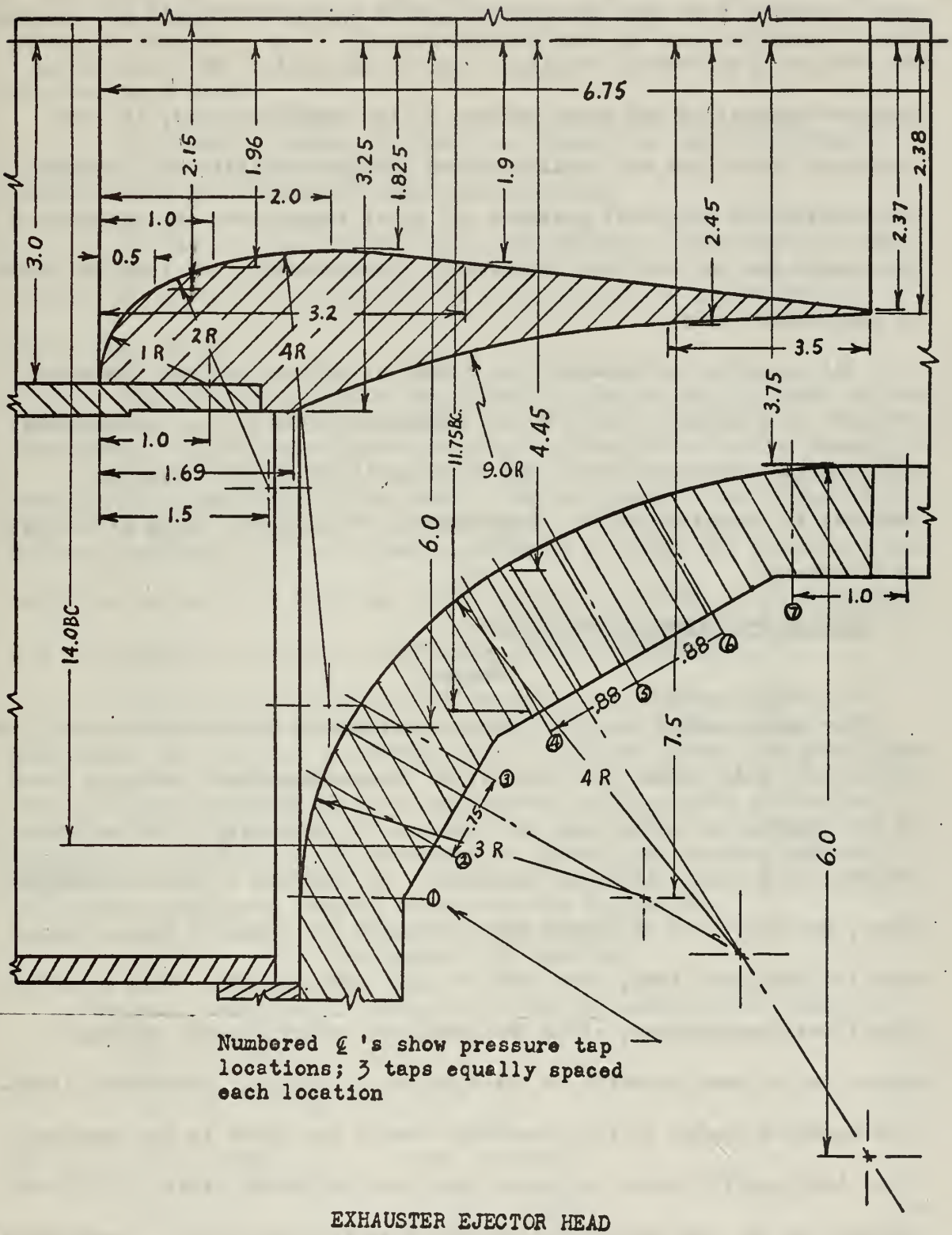

EXHAUSTER EJECTOR HEAD
TRANSONIC TURBINE TEST RIG

FIGURE 13

each location, four taps are equally spaced circumferentially and commoned for obtaining an average reading. Fig. 13 shows also the locations of pressure taps along the outer contour of the exhauster head; at each location, three taps are equally spaced circumferentially and commoned. The location of the total pressure and total temperature tap upstream of the nozzle has not yet been determined. Consequently, the location shown is approximate only.

All pressures are measured in inches of mercury against atmospheric pressure as reference, using 96 in. manometers with 0.1 in. graduations. Differential pressures across the flow nozzle and orifice taps are measured in inches of water. Temperatures are measured using an ice bath as reference.

3. Turbine Performance Prediction.

General

The basic method used for turbine performance prediction is that given by Vavra.[2] This method is a simplified three-dimensional analysis based on the equation of motion and the equation of continuity, with solutions obtained at between-blade-row locations. In contrast to the approach of Vavra, the equations of motion and continuity for relative flows, rather than for absolute flows, were used in rotor calculations. This procedure simplifies computations, since the predicted relative rotor gas exit angles can be used directly in the equation of motion. Therefore, iteration based on change in total enthalpy across the rotor is not required. Also, loss coefficients, estimated using the method of Ainley, [4,5] are obtained in the same manner for the rotor as for the stator. Consequently, their application must be in a manner analogous to that used for the stator.

[2]Vavra, M. H., Aero-Thermodynamics and Flow in Turbomachines (New York, London: John Wiley and Sons, Inc., 1960) Chap. 16.

Proper application is achieved by introduction of the so-called equivalent enthalpy (defined later). The assumptions made in the performance analysis are set forth below.

1. An infinite number of blades is assumed so that downstream conditions do not influence conditions upstream.

2. At the stations of interest, axisymmetric stream surfaces exist, so that all derivatives with respect to θ, i. e., in the peripheral direction, are zero.

3. The flow is adiabatic and steady so that along any given streamline there is no change of total enthalpy in the stator and no change in relative total enthalpy in the rotor. (Note, however, that since cylindrical coordinates are to be used, gradients of total and relative total enthalpy can exist in both the radial direction and the axial direction, due to streamline curvature, depending on inlet conditions.)

4. Since the equations are to be solved for between-blade-row locations, the increase in entropy due to friction within the blade rows can be determined using the loss coefficient and the inlet and outlet conditions. However, it is necessary to assume that entropy changes along the streamlines between blade rows are negligible.

Development of Formulas

The basic equations of motion for absolute and relative flows are:

$$\nabla H = \bar{V} \times (\nabla \times \bar{V}) + T \nabla s \tag{1}$$

$$\nabla H_R = \bar{W} \times (\nabla \times \bar{W} + 2\bar{\omega}) + T \nabla s \tag{2}$$

Total relative enthalpy, H_R, can be written:

$$H_R = h_1 + \frac{W_1^2}{2} - \frac{U_1^2}{2} = h_2 + \frac{W_2^2}{2} - \frac{U_2^2}{2} \qquad \vec{V} = \vec{W} + \vec{U} \tag{3a}$$

$$H_R = h_{2'} + \frac{W_{2TH}^2}{2} - \frac{U_2^2}{2} \tag{3b}$$

The subscripts indicate: 1 -- ahead of the rotor; 2 -- after the rotor; TH -- the theoretical value; and 2' -- the conditions after the rotor for isentropic expansion from $T_{tE} = H_e/c_p$ to p_2. For adiabatic flow, the total relative enthalpy remains constant along any given streamline. Hence, equivalent enthalpy, defined as:

$$H_E = h_{2'} + \frac{W_{2TH}^2}{2} = H_R + \frac{U_2^2}{2} \tag{4}$$

must also remain constant along each streamline. It follows from (3) and (4) that:

$$H_E = h_2 + \frac{W_2^2}{2} = h_1 + \frac{W_1^2}{2} - \frac{U_2^2 - U_1^2}{2} \tag{5}$$

It is evident that the use of equivalent enthalpy permits analysis of the relative flow through the rotor in a manner analogous to that used for absolute flows, including the use of normal thermodynamic relations.

Velocity coefficients are defined as:

$$\varphi_v = \frac{V}{V_{TH}} \qquad \text{for absolute flows} \tag{6}$$

$$\psi = \frac{W}{W_{TH}} \qquad \text{for relative flows} \tag{7}$$

Then, in terms of the loss coefficients:

$$\varphi_v = \sqrt{1 - \zeta} \qquad \text{for absolute flows} \tag{8}$$

$$\psi = \sqrt{1 - \zeta} \qquad \text{for relative flows} \tag{9}$$

Fig. 14 shows the relations between thermodynamic properties, velocities and loss coefficients in the form of a typical expansion through a turbine. The expansion process is shown for three different streamlines in order to emphasize the variation of properties which have to be considered in the analysis.

Figs. 15a - 15 c show the coordinate system and sign conventions used. Station subscripts, zero, one and two refer to ahead of the stator, between the stator and rotor, and after the rotor, respectively.

The equation of continuity is used in its non-dimensional flow function -- Φ -- form. Written in differential form:

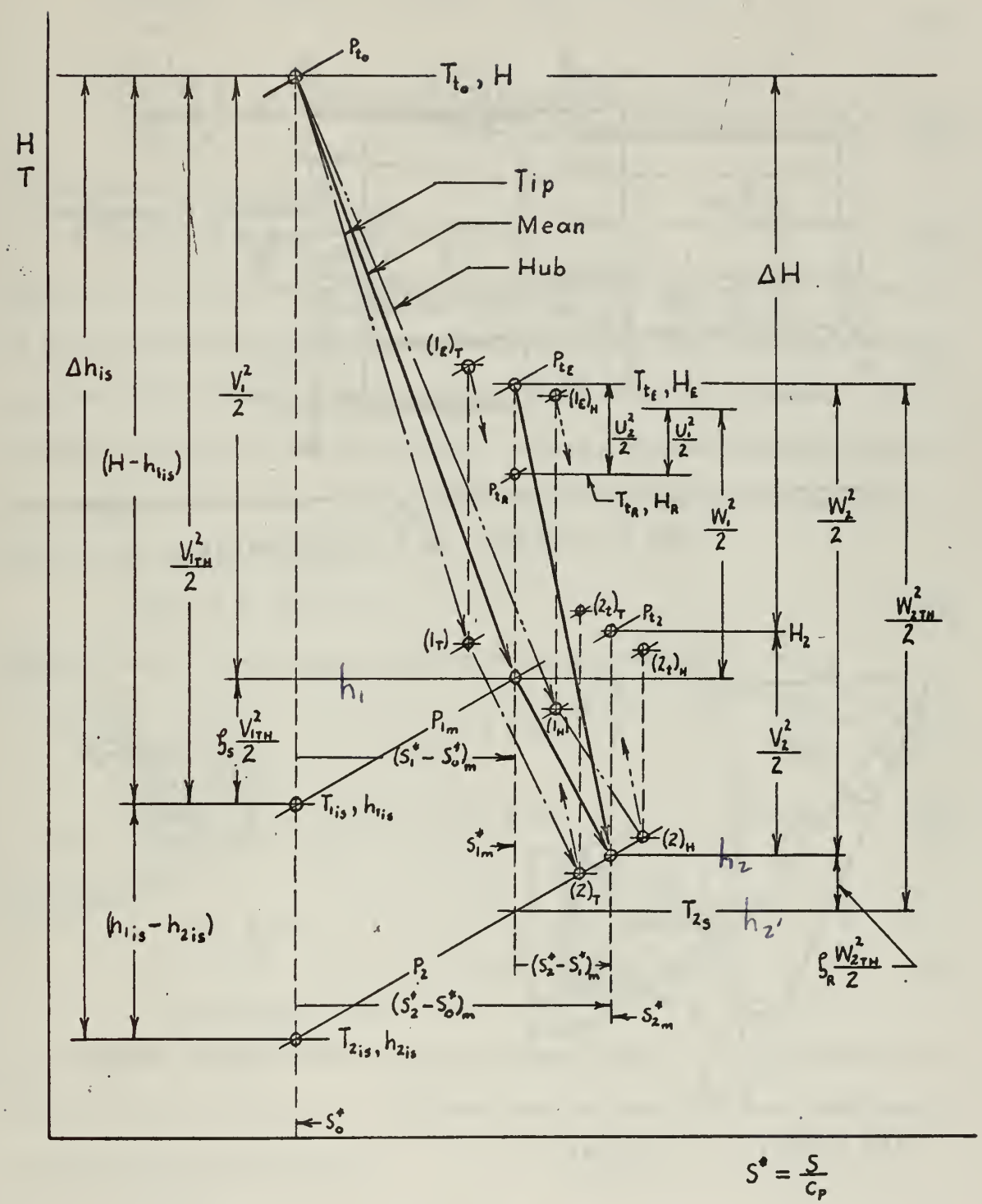

TURBINE EXPANSION PROCESS

FIGURE 14

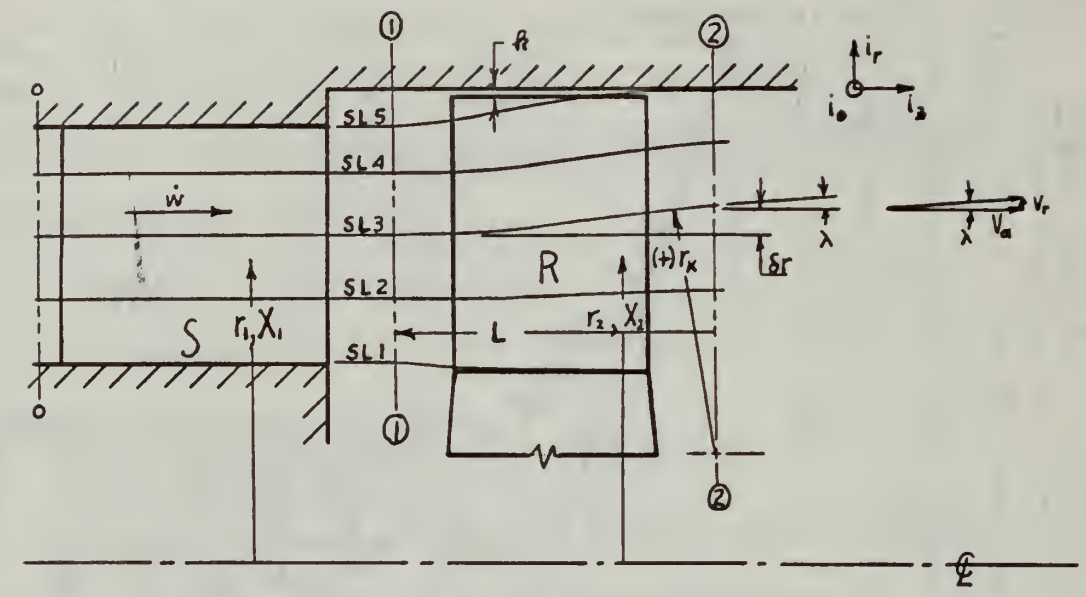

(a) Streamlines and Coordinates

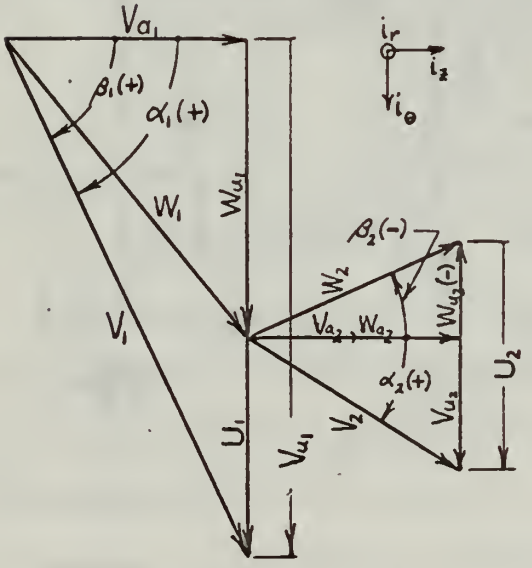

(b) Velocity Triangles

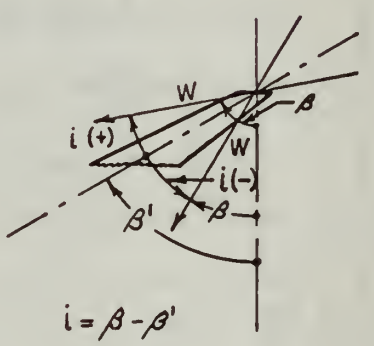

(c) Rotor Incidence Angles

COORDINATES, STREAMLINES, AND ANGLES
USED IN THE PERFORMANCE ANALYSIS

FIGURE 15

$$\frac{d\dot{w}\sqrt{T_{t_o}}}{P_{t_o}}\sqrt{\frac{R}{g}} = dA\,\Phi = dA\sqrt{\frac{2\gamma}{\gamma-1}\left[\left(\frac{p}{P_{t_o}}\right)^{\frac{2}{\gamma}} - \left(\frac{p}{P_{t_o}}\right)^{\frac{\gamma+1}{\gamma}}\right]} \tag{10}$$

$$\frac{d\dot{w}\sqrt{T_{t_E}}}{P_{t_E}}\sqrt{\frac{R}{g}} = dA\,\Phi = dA\sqrt{\frac{2\gamma}{\gamma-1}\left[\left(\frac{p}{P_{t_E}}\right)^{\frac{2}{\gamma}} - \left(\frac{p}{P_{t_E}}\right)^{\frac{\gamma+1}{\gamma}}\right]} \tag{11}$$

for relative flows. Then:

$$dA = \xi\, Z\, a\, dr \tag{12}$$

Here, 'a' is the blade exit opening (see Appendix II) and the factor, ξ, is an area restriction coefficient which accounts for loss of effective area due to the boundary layer on both sides of the flow channel. This factor is further defined below. Eq. (12) can be made non-dimensional by multiplying and dividing by $a_m r_m$, the product of mean streamline exit opening and radius. Hence:

$$dA = \xi\, Z\, \frac{a}{a_m}\, dX\, a_m r_m \tag{13}$$

Eqs. (10) and (11) in integral form become, respectively:

$$\frac{\dot{w}\sqrt{T_{t_o}}}{P_{t_o}}\sqrt{\frac{R}{g}} = a_m Z r_m \int_{X_H}^{X_T} \frac{a}{a_m}\,\xi\,\Phi\, dX \tag{14}$$

$$\frac{\dot{w}\sqrt{T_{t_E}}}{P_{t_E}}\sqrt{\frac{R}{g}} = a_m Z r_m \int_{X_H}^{X_T} \frac{a}{a_m}\,\xi\,\Phi\, dX \tag{15}$$

Defining:

$$\dot{w}_{rf} = \left[\frac{\dot{w}\sqrt{T_{t_o}}}{P_{t_o}}\sqrt{\frac{R}{g}}\right]_{Stator} = \left[a_m Z r_m \int_{X_H}^{X_T} \frac{a}{a_m}\,\xi\,\Phi\, dX\right]_{Stator} \tag{16}$$

For $\dot{w}_{rf}$, the reference flow rate, in square inches, 'a' and r_m must be in inches and p_{t_o} in psia.. It follows from (14) and (15) that continuity is satisfied, provided that:

$$\left[\int_{X_H}^{X_T} \frac{P_{t_E}/P_{t_o}}{\sqrt{T_{t_E}/T_{t_o}}}\,\frac{a}{a_m}\,\xi\,\Phi\, dX\right]_{Rotor} = \frac{\dot{w}_{rf}}{[a_m Z r_m]_{Rotor}} \tag{17}$$

Eq. (17) neglects the flow area available because of tip clearance. The differential area due to tip clearance is:

$$dA = 2\pi r\, dr \tag{18}$$

Letting r_c denote the inner radius of the flow direction ring around the rotor, the integral form of (15) becomes:

$$\left[\frac{\dot{w}\sqrt{T_{t_E}}}{P_{t_E}}\sqrt{\frac{R}{g}}\right]_{\substack{Tip\\ clnc}} = a_m Z r_m^2 \int_{X_T}^{X_c} \frac{2\pi X}{Z\, a_m}\, \xi\, \Phi\, dX \tag{19}$$

The Z in the denominator of the integrand is required because the entire annular area rather than a between-the-blade area results from integration of (19). For small tip clearances, sufficient accuracy should result from taking X of the integrand as a constant equal to X_T, X_c, or the average of the two. Considering tip clearance area, and assuming that the values of Φ, ξ, p_{te}, and T_{tE} in the clearance area are approximately the same as those for the rotor tip, (17) becomes:

$$\left[\int_{X_H}^{X_T} \frac{P_{t_E}/P_{t_o}}{\sqrt{T_{t_E}/T_{t_o}}}\frac{a}{a_m}\xi\,\Phi\, dX + 2\pi r_m \int_{X_T}^{X_c}\left(\frac{P_{t_E}/P_{t_o}}{\sqrt{T_{t_E}/T_{t_o}}}\xi\,\Phi\right)_T \frac{X}{Z\, a_m}\, dX\right]_{Rotor} = \frac{\dot{W}_{rf}}{[a_m Z r_m]_{Rotor}} \tag{20}$$

In addition to the requirement that overall continuity be satisfied by the stator and rotor flow, it is necessary that the flow rate between each two adjacent streamlines remains constant.

The term ξ in (12) is:[3]

$$\xi = 1 - \sum \frac{\delta^*}{a} = \frac{H^{***} - 1}{H^{***} - 1 + \zeta_p} \tag{21}$$

Here, ζ_p is the profile loss coefficient. For the stator, using ζ_p in (21) corresponds quite closely to the often-used practice of assuming that one-half the total loss occurs to the throat. However, for the rotor,

[3]Vavra, M. H., Problems of Fluid Mechanics in Radial Turbomachines (Rhode-Saint-Genese, Belgium: Von Karman Institute for Fluid Dynamics, 1965) VKI Course Note 55b, pp. G46-50.

there is no such direct correlation. In (21), H^{***} is the energy parameter defined as the energy thickness, δ^{***}, divided by the displacement thickness, δ^{*}. These thicknesses are given by:

$$\delta^{***} = \delta\left\{1-(1-X_e)\int_0^1 \frac{\eta^{3m}}{(1-X_e\eta^{2m})}\,d\eta\right\} \tag{22}$$

$$\delta^{*} = \delta\left\{1-(1-X_e)\int_0^1 \frac{\eta}{(1-X_e\eta^{2m})}\,d\eta\right\} \tag{23}$$

where:

$$X_e = 1-\left(\frac{p}{p_t}\right)^{\frac{\gamma-1}{\gamma}} \tag{24}$$

In (22) and (23), η , is the normally-used non-dimensional distance from the wall, y/δ ; also, m = 1/n, where n is the velocity profile exponent in: $(u/U) = (y/\delta)^{1/n}$.

The development of (1) and (2) into usable form is quite lengthy. Consequently, this development is included in Appendix I. It is evident that these two equations differ only by the term of (2), $(\bar{W}x2\bar{\omega})$, which represents the Coriolis acceleration. Consequently, the derivation given in App. I is for (2). The form of (1) used is obtained from the equation developed from (2) by substituting: H for H_E; α_1 for β_2 ; and U = 0. Also included in App. I are the derivations of (21) - (23), along with a plot of H^{***} for m = 0.15. The final form of (1) is:

$$\frac{d(\ln Y_1^2)}{dX_1} = -\cos^2\alpha_1\left[-\left(\pm k2r_m\frac{\delta r}{L^2}\right)-\left(\frac{4L^2+(\delta r)^2}{4L^2}\right)\frac{ds_1^*}{dX_1}\right]-2\tan\alpha_1\frac{d\alpha_1}{dX_1}$$

$$-\frac{2}{X_1}\sin^2\alpha_1+\frac{C_1\cos^2\alpha_1}{Y_1^2 V_{a_{1m}}^2}\frac{dH}{dX_1}-\left[\frac{C_1 H\cos^2\alpha_1}{Y_1^2 V_{a_{1m}}^2}-\sin^2\alpha_1\right]\frac{ds_1^*}{dX_1} \tag{25}$$

and that of (2) is:

$$\frac{d(\ln Y_2^2)}{dX_2} = -\cos^2\beta_2\left[-\left(\pm 2k r_m\frac{\delta r}{L^2}\right)-\left(\frac{4L^2+(\delta r)^2}{4L^2}\right)\frac{ds_2^*}{dX_2}\right]-2\tan\beta_2\frac{d\beta_2}{dX_2}-\frac{2}{X_2}\sin^2\beta_2$$

$$-\frac{4U_m\cos\beta_2\sin\beta_2}{W_{am}Y_2}-\frac{2U_m U_2\cos^2\beta_2}{W_{am}^2 Y_2^2}+\frac{C_1\cos^2\beta_2}{W_{am}^2 Y_2^2}\frac{dH_E}{dX_2}-\left[\frac{C_1 H_E\cos^2\beta_2}{W_{am}^2 Y_2^2}-\sin^2\beta_2\right]\frac{ds_2^*}{dX_2} \tag{26}$$

Here:

$Y = V_a/V_{a_m}$ (or W_a/W_{a_m})

$X = r/r_m$

k = 4 to 6, streamline curvature factor

δr = streamline displacement

L = length over which streamline displacement occurs

$s^* = s/c_p$, non-dimensional entropy

U = wheel speed, ft/sec.

$C_1 = 2gJ = (2)(32.174)(778.16)$ ft^2lbm/sec^2BTU, converts H to ft^2/sec^2 from BTU/lbm.

In the curvature term $(\pm k r_m \frac{r}{L^2})$, the plus sign is for curvature whose radius of curvature points in the positive radial direction (see Fig. 15a, p. 42).

Total temperature can be used in (25) and (26) by substituting C_2T_t for C_1H, where: $C_2 = 2gJc_p$. The entropy term in these equations is evaluated along the line of constant pressure for the blade exit. The required formula is:[4]

$$S^* = \frac{S_1 - S_0}{c_p} = \ln \left[\frac{H - \frac{V^2}{2gJ}}{H - \frac{V^2}{2gJ(1-\xi)}} \right] \tag{27}$$

Differentiating with respect to the non-dimensional radial coordinate:

$$\frac{ds^*}{dX} = \frac{d}{dX} \left\{ \ln \left| \frac{1 - \frac{Y^2 V_{a_m}^2}{C_1 H \cos^2\alpha}}{1 - \frac{Y^2 V_{a_m}^2}{C_1 H \cos^2\alpha (1-\xi)}} \right| \right\} \tag{28}$$

Since Y^2 appears in terms on the right side of (25) and (26), these equations must be solved by successive approximations. For a solution to be valid, it must satisfy both overall continuity and between-streamline continuity, as previously mentioned. Overall continuity is controlled

[4]Vavra, M. H., Aero-Thermodynamics and Flow in Turbomachines (New York, London: John Wiley and Sons, Inc., 1960) pp. 445-447.

primarily by the axial velocity, while between-streamline continuity is basically a function of the streamline positions assumed. In integral form, (25) and (26) are of the form:

$$\ln Y^2 = \int_{X_o}^{X} I\,dX + \ln C^2 \tag{29}$$

where X_o is arbitrary, and $\ln(C^2)$ is the constant of integration. With the boundary condition, Y = 1.0 at X = 1.0;

$$0 = \int_{X_o}^{1} I\,dX + \ln C^2$$

Then:

$$\ln C^2 = -\int_{X_o}^{1} I\,dX$$

and:

$$\ln Y^2 = \int_{X_o}^{X} I\,dX - \int_{X_o}^{1} I\,dX$$

Eq. (29) then becomes:

$$\ln Y^2 = \int_{1}^{X} I\,dX \tag{30}$$

In solving (25) and (26), the sign convention for the flow angles must be carefully observed (i.e., angles are positive in the direction of rotation). In addition, when integrating graphically or numerically according to (30), the direction of integration must be kept in mind. Integrating toward X < 1.0, the summation must be multiplied by -1.0. To facilitate solution, (30) can be expanded in an infinite series:

$$Y = e^{\frac{1}{2}\int_{1}^{X} I\,dX} = 1 + n + \frac{n^2}{2} + \frac{n^3}{6} + \frac{n^4}{24} + \frac{n^5}{120} + \ldots ; \quad n = \frac{1}{2}\int_{1}^{X} I\,dX \tag{31}$$

Method of Solution

Loss coefficients and gas flow angles were determined for both the stator and rotor using the method of Ainley. [4,5] In exception to that

method, however, a blockage factor due to trailing edge thickness was included in angle determinations. Also, leaving losses were computed using the procedure given by Vavra.[5] Computation of flow angles and loss coefficients is given in Appendix II. Loss coefficients were assumed to be independent of Mach Number and independent of radius, except for the influence of radial variation of incidence angle. Angles were determined for Mach Numbers of 0.5 and 1.0. Since only the mean streamline angles could be determined for M = 1, constant differences between values of flow angles for the mean streamline and those for the hub and tip streamlines were assumed for all Mach Numbers. Such differences were taken as those for M = 0.5. Smooth curves with inflection points at M = 0.75 were drawn between the values of angles at M = 0.5 and M = 1, following Ainley. [4,5] Only the converging guide vane, full rotor configuration has been analyzed.

Since the actual curvature of streamlines is quite uncertain at best, the curvature was assumed to be zero. The first terms of (25) and (26) then reduce to: $\cos^2(\ )\, ds^*/dX$. When this term is combined with the sine squared part of the final terms, (25) and (26) become:

$$\frac{d(\ln Y^2)}{dX_1} = -2\tan\alpha_1 \frac{d\alpha_1}{dX_1} - \frac{2}{X_1}\sin^2\alpha_1 + \frac{C_1 \cos^2\alpha_1}{Y_1^2 V_{a_{1m}}^2}\frac{dH}{dX_1} + \left(1 - \frac{C_1 H \cos^2\alpha_1}{Y_1^2 V_{a_{1m}}^2}\right)\frac{ds_1^*}{dX_1} \tag{32}$$

$$\frac{d(\ln Y_2^2)}{dX_2} = -2\tan\beta_2 \frac{d\beta_2}{dX_2} - \frac{2}{X_2}\sin^2\beta_2 - \frac{4 U_m \cos\beta_2 \sin\beta_2}{Y_2 W_{a_{2m}}} - \frac{2 U_m U_2 \cos^2\beta_2}{Y_2^2 W_{a_{2m}}^2} + \frac{C_1 \cos^2\beta_2}{Y_2^2 W_{a_{2m}}^2}\frac{dH_E}{dX_2} + \left(1 - \frac{C_1 H_E \cos^2\beta_2}{Y_2^2 W_{a_{2m}}^2}\right)\frac{ds_2^*}{dX_2} \tag{33}$$

These two equations, along with the continuity equation in the forms of

[5] Ibid., Eq. 5(63), p. 89.

(16) and (20), are the major equations to be solved in the analysis.

Conditions ahead of the stator were assumed as: constant total enthalpy; constant entropy; and uniform velocity with neither a tangential nor radial component. It follows from the adiabatic flow assumption that total enthalpy is constant at the stator exit also, and dH/dX at station one is then zero. Similarly, due to the assumption of constant entropy at the stator inlet, the only gradient of entropy existing after the stator is that due to friction through the blading, as given by (28). As a result of the assumed axial-component-only velocity ahead of the stator, the loss coefficient for the stator becomes constant at all radii and equal to the value for zero incidence angle.

The analysis was programmed for the CDC 1604 computer, using FORTRAN 60. The program is included as Appendix III. The procedural steps accomplished by the program, PERFORM, are set forth in succeeding paragraphs of this section.

Five streamline radial positions were used, including the hub and tip positions. Inputs for the program are listed below. Except as indicated, similar data is read into the computer for both the stator and rotor.

1. Radii of the five streamlines, in inches.

2. Values of gas efflux angles in radians for the mean streamline, and for Mach Numbers of: 0.5, 0.7, 0.75, 0.8 and 1.0.

3. Values of the differences in flow angles from the mean streamline value for the hub, mean (zero difference) and tip streamlines.

4. Rotor loss coefficients and rotor profile loss coefficients for five values of the ratio of incidence angle to stalling incidence angle (i/i_s): 0, 0.5, 1.0, -0.8, and -1.5.

5. Values of the throat opening dimension for the hub, mean and tip streamline radii.

6. The number of sets of values given in (7.) below for which computations are to be accomplished.

7. Conditions for which the analysis is to be done: Mach Number at the mean streamline at the stator exit (M_{1_m}); stator inlet total temperature (°R) and total pressure (psia.); Mach Number assumed for the mean streamline at the rotor exit; and turbine RPM.

Considerable use of parabolic equations is made to facilitate computation of values required in the analysis. Subroutine PARAB determines the required constants, a, b, and c, for the general equation:

$$y = a + bx + cx^2 \tag{34}$$

This subroutine solves three equations in three unknowns using appropriate determinants. Gas angles for the mean streamline at the stator and rotor exits are represented by (34) for two ranges of Mach Number: 0.5 to 0.75; and 0.75 to 1.0. For a given (input) Mach Number, the mean streamline angle can be determined. Using the angle differences between the mean streamline and the hub and tip values, the flow angles for the hub and the tip streamlines are computed. Then, the parabola for flow angle as a function of the non-dimensional radial coordinate, X, is found. Constants of Eq. (34) are also determined for: rotor total and rotor profile loss coefficients as functions of i/i_s, for i/i_s = 0 to 1 and i/i_s = 0 to -1.5; and the ratio of throat dimension, a, to the mean streamline value, a_m, as a function of X for both the stator and the rotor.

Subroutine STATOR solves (32), without the dH/dX term, by successive approximations. Since part of the input is the Mach Number of the flow for the mean streamline at the stator exit, and since the flow angle for this streamline is known, the axial velocity can be determined from:

$$T_{1m} = T_{t_o}\left[\frac{1}{1 + \frac{\gamma-1}{2} M_{1m}^2}\right] \tag{35}$$

$$V_{1m} = \sqrt{2 g J c_p (T_{t_o} - T_{1m})} \tag{36}$$

and:

$$V_{a_{1m}} = V_{1m} \cos \alpha_{1m} \tag{37}$$

(It should be noted that mass flow rate is yet to be determined.) In the iterative procedure, the first approximation is obtained with $ds^*/dX = 0$. In the second and succeeding approximations, the values of Y determined in the preceding iteration are used to find ds^*/dX. In determining values of Y, using (31), the series through the third power is used. When final values of Y are found, conditions at all streamlines are given by:

$$V_{a_1} = V_{a_{1m}} Y_1 \tag{38}$$

$$V_1 = \frac{V_{a_1}}{\cos \alpha_1} \tag{39}$$

$$T_1 = T_{t_o} - \frac{V_1^2}{2 g J c_p} \tag{40}$$

$$T_{1is} = T_{t_o} - \frac{T_{t_o} - T_1}{(1 - \zeta)} \tag{41}$$

$$P_1 = P_{t_o}\left(\frac{T_{1is}}{T_{t_o}}\right)^{\frac{\gamma}{\gamma-1}} \tag{42}$$

$$V_{u_1} = V_1 \tan \alpha_1 \tag{43}$$

Subroutine FLOWREF is called to solve (16) for the stator. This subroutine checks the pressure ratio, p/p_{t_o}, to determine whether or not the flow is choked for each streamline. For choked flow, the flow function, Φ, is set equal to Φ^*, where:

$$\Phi^* = \left(\frac{2}{\gamma+1}\right)^{\frac{1}{\gamma-1}} \sqrt{\frac{2\gamma}{\gamma+1}} \tag{44}$$

This equation is obtained from the expression for Φ in (10), with:

$$\frac{p}{P_{t_o}} = \left(\frac{2}{\gamma+1}\right)^{\frac{\gamma}{\gamma-1}} \tag{45}$$

Values of H^{***} are computed using the expression derived in App. I:

$$H^{***} = \frac{\left[\frac{1}{X_e-1} + \frac{1}{3m+1} + \frac{X_e}{5m+1} + \frac{X_e^2}{7m+1} + \frac{X_e^3}{9m+1} + \frac{X_e^4}{11m+1}\right]}{\left[\frac{1}{X_e-1} + \frac{1}{m+1} + \frac{X_e}{3m+1} + \frac{X_e^2}{5m+1} + \frac{X_e^3}{7m+1} + \frac{X_e^4}{9m+1}\right]} \tag{46}$$

The area reduction coefficient, ξ, is then found from (21). Integration is accomplished, and between-streamline flow fractions are determined. With $\dot{w}_f$ defined as the fraction of the total flow which passes between the hub and any other given streamline, there is:

$$\dot{w}_f = \frac{\int_{X_H}^{X} I_{\dot{w}}\, dX}{\int_{X_H}^{X_T} I_{\dot{w}}\, dX} \tag{47}$$

Here, $I_{\dot{w}}$ is the value of the integrand of (16). The actual flow rate in lbm/sec is given by:

$$\dot{w} = a_m Z r_m \frac{P_{t_o}}{\sqrt{T_{t_o}}} \sqrt{\frac{g}{R}} \int_{X_H}^{X_T} \frac{a}{a_m} \xi \Phi\, dX \tag{48}$$

It would be desirable to have one-quarter of the total flow pass between each pair of adjacent streamlines. However, this condition is not absolutely necessary, since for this analysis zero curvature was assumed and conditions ahead of the stator are completely uniform. As a result, the conditions at the stator exit can be used to establish both overall and between-streamline continuity requirements. Slight differences from multiples of one-quarter for the flow fractions given by (47) are

then tolerable. It remains mandatory, though, that the between-streamline flow be the same for the assumed streamlines at the rotor exit as for the corresponding streamlines at the stator exit.

Subroutine ROTOR1 is used to convert the absolute flow conditions ahead of the rotor to relative conditions. For angles and velocities:

$$U_1 = \frac{N\,2\pi\,r_1}{(60)(12)} \quad ; \quad r_1 \text{ in inches} \tag{49}$$

$$W_{u_1} = V_{u_1} - U_1 \tag{50}$$

$$\beta_1 = \tan^{-1}\left(\frac{W_{u_1}}{V_{a_1}}\right) \tag{51}$$

$$W_1 = \frac{V_{a_1}}{\cos\beta_1} \tag{52}$$

$$U_2 = U_1 \frac{r_2}{r_1} \tag{53}$$

In (53), r_2 is the radius of the given streamline at the rotor exit. Other necessary values are obtained from:

$$H_E = c_p T_1 + \frac{W_1^2}{2gJ} + \frac{U_2^2 - U_1^2}{2gJ} \tag{54}$$

$$T_{t_E} = \frac{H_E}{c_p} \tag{55}$$

and:

$$P_{t_E} = P_1 \left(\frac{T_{t_E}}{T_1}\right)^{\frac{\gamma}{\gamma-1}} \tag{56}$$

The values of H_E, T_{t_E}, and P_{t_E} are for the fluid entering the rotor along streamlines chosen for the stator and leaving the rotor along the same streamlines at radii assumed for the rotor. Similarly, the values of entropy, from which entropy increases through the rotor are determined for the several streamlines, are those for the matching streamlines at the stator exit. These entropy values are the increases in entropy through the stator blading, as measured from the constant (base) value of

entropy existent at the stator inlet. Hence, the rotor inlet value of entropy can be considered known for each streamline and the gradient of entropy with respect to X_2 at the rotor inlet can be found. Also, since H_E is constant along each streamline through the rotor, the gradient, dH_E/dX_2, is known. It is convenient to write:

$$s_2^* = \frac{S_2 - S_0}{C_p} = \frac{S_2 - S_1}{C_p} + \frac{S_1 - S_0}{C_p} = s_{21}^* + s_{10}^* \tag{57}$$

where s_{10}^* and ds_{10}^*/dX_2 are known. Then:

$$\frac{ds_2^*}{dX_2} = \frac{ds_{21}^*}{dX_2} + \frac{ds_{10}^*}{dX_2} \tag{58}$$

The unknown gradient in (58), ds_{21}^*/dx_2, is found using (28), written in terms of the relative flow properties.

The rotor loss coefficient required for the solution of (28) is determined in ROTOR1 by using the parabolic functions determined earlier in the program. The independent variable, i/i_s, is given by:

$$i = \beta_1 - \beta_1' \tag{59}$$

Here, β_1' is the blade angle. The resulting value of i is divided by the positive stalling incidence angle: $(13^\circ.4\ /57^\circ.3)$/radian. Loss coefficients, both total and profile, for the rotor are taken as constant and equal to the values for $i/i_s = 1$ and $i/i_s = -1.5$ should the value of i/i_s be greater than 1.0 or less than -1.5 respectively.

Subroutine ROTOR2 solves (33) by successive approximations using the values computed in ROTOR1 and assumed values of $W_{a_{2_m}}$ for the mean streamline and of Y_2 for the other streamlines. The assumed values of Y_2 for the first iteration are estimates. Then, for succeeding iterations, the preceding iteration's values of Y_2 are used. For convenience, the nonvariant part of ds_1^*/dX_2 is included with the invariant terms: $-2\tan\beta_2 \frac{d\beta_2}{dX_2} - \frac{2}{X_2}\sin^2\beta_2$. Since the gradient of Y_2 at the rotor exit is quite

severe, terms of (31) through the fifth power term are used.

When either satisfactory convergence of Y_2 values is obtained, or the prescribed number of iterations--13--have been completed, thermodynamic conditions at the rotor exit are determined using (38) - (43) written for equivalent properties. The absolute tangential velocity, V_{u2}, is obtained from (50), written for the values at station two. Satisfactory convergence of Y_2 values is defined as: no change greater than 0.005 in successive iteration values of Y_2 for any streamline.

Overall continuity is next checked using subroutine FLOWREF with the rotor exit properties. Eq. (19) as used in the computer program is written to include the flow through the tip clearance area as part of the flow between streamlines four and five. Written for the trapezoidal method of integration, the integral of (20) is:

$$\int_{X_H}^{X_T} \dot{I}_w \, dX = \sum_{i=1}^{4} \left[\left(\frac{P_{t\varepsilon}/P_{t_0}}{\sqrt{T_{t\varepsilon}/T_{t_0}}} \frac{a}{a_m} \rho \S \Phi \right)_{(i+1)} + \left(\frac{P_{t\varepsilon}/P_{t_0}}{\sqrt{T_{t\varepsilon}/T_{t_0}}} \frac{a}{a_m} \rho \S \Phi \right)_i \right] \left(\frac{X_{i+1} - X_i}{2} \right) \qquad (60)$$

When i = 4, the first term in the brackets becomes:

$$\left(\frac{P_{t\varepsilon}/P_{t_0}}{\sqrt{T_{t\varepsilon}/T_{t_0}}} \frac{a}{a_m} \rho \S \Phi \right)_{(i+1)} = \left(\frac{P_{t\varepsilon}/P_{t_0}}{\sqrt{T_{t\varepsilon}/T_{t_0}}} \rho \S \Phi \right)_5 \left(\frac{a_5}{a_m} + \frac{2\pi r_T (k/r_m)}{a_m Z (X_5 - X_4)} \right) \qquad (61)$$

Here, k is the tip clearance and, therefore, k/r_m is the ΔX_2 of the tip clearance. The term (X_5-X_4) in the denominator cancels in the solution of (60). Eq. (60) must yield the value of $\dot{w}_{rf}/(a_m Z r_m)_{Rotor}$ given by $\dot{w}_{rf}$ determined in the stator solution. If the rotor flow is less than required (i.e., the value from (60) is too small), the assumed value of axial velocity for the mean streamline is increased and, if greater, the mean streamline axial velocity is reduced. ROTOR2 and FLOWREF are then called successively until continuity is satisfied.

When overall continuity is satisfied, subroutine SLINE is called to

check between-streamline continuity. This subroutine checks the fractions of flow between streamlines one and two, one and three, and one and four at the rotor exit against the values of flow fractions between the same sets of streamlines at the stator exit. If the rotor and stator fractions for all three sets are equal within tolerance, the solution desired is known. If inequalities exist, the radial locations of streamlines two three and four at the rotor exit are adjusted and successive approximations continued. Also, all variables required in ROTOR2 and for the rotor equations in FLOWREF are adjusted, as required, to values appropriate for the new streamline locations. Then, ROTOR2, FLOWREF and SLINE are called as before until the equation of motion and both continuity requirements are satisfied.

It is appropriate at this point to discuss the methods used to determine required gradients, to correct radial locations of streamlines, and to correct gradients for new values of X_2. For variables for which parabolic equations were determined as f(X) initially, the gradients are given by:

$$\frac{d(\ )}{dX} = b + 2cX \tag{62}$$

The parabola itself and (62) need be corrected only for changes in the radius of the mean streamline, since the value of the variable at a given radius does not change. Then, since:

$$X = X' \frac{r_m'}{r_m} = \frac{r}{r_m'} \left(\frac{r_m'}{r_m} \right) \tag{63}$$

where the primes indicate the new values, the resulting correction factors required to permit using X' in the equations are:

$$F_{c_1} = \frac{r_m'}{r_m} \tag{64}$$

and:

$$F_{c_2} = F_{c_1}^2 \tag{65}$$

The constants, b and c, of the parabolic expressions of the type (34), and occurring in (62), are then: $b' = F_{c_1} b$; and $c' = F_{c_2} c$. The constant, a, is unchanged.

New values of streamline values of $X = X'$, in terms of the old value of r_m are obtained using flow fractions (see (47)) and:

$$X' = X \pm \left| \dot{w}_{f(REQ)} - \dot{w}_{f(ACT)} \right| \frac{dX}{d\dot{w}_f} \tag{66}$$

Here, the positive sign corresponds to a required increase in X due to too low a fraction of the total flow passing between the hub streamline and the streamline in question; the minus sign, then, corresponds to too great a flow fraction and a required decrease in X. The situation is illustrated in Fig. 16a. Note that the absolute value of flow fraction difference is used in (66) and that the gradient, $dX/d\dot{w}_f$, is always taken for increasing X. Then, in the nomenclature of Fig. 16a, there is:

$$\frac{dX}{d\dot{w}_f} = \frac{X(J) - X(I)}{\dot{w}_f(J) - \dot{w}_f(I)} \; ; \qquad J > I \tag{67}$$

The value, X', obtained yields the new radius to be used, with:

$$r = X' r_m \tag{68}$$

Since the hub streamline flow fraction is zero and the tip value is 1.0, only the radii for streamlines two, three and four need be corrected. New values of X are given by:

$$X_{new} = \frac{r}{r_{m(new)}} \tag{69}$$

New values of U_2 are obtained for the new values of r_2, using:

$$U_2 = U_{2(old)} \frac{r_{new}}{r_{old}} \tag{70}$$

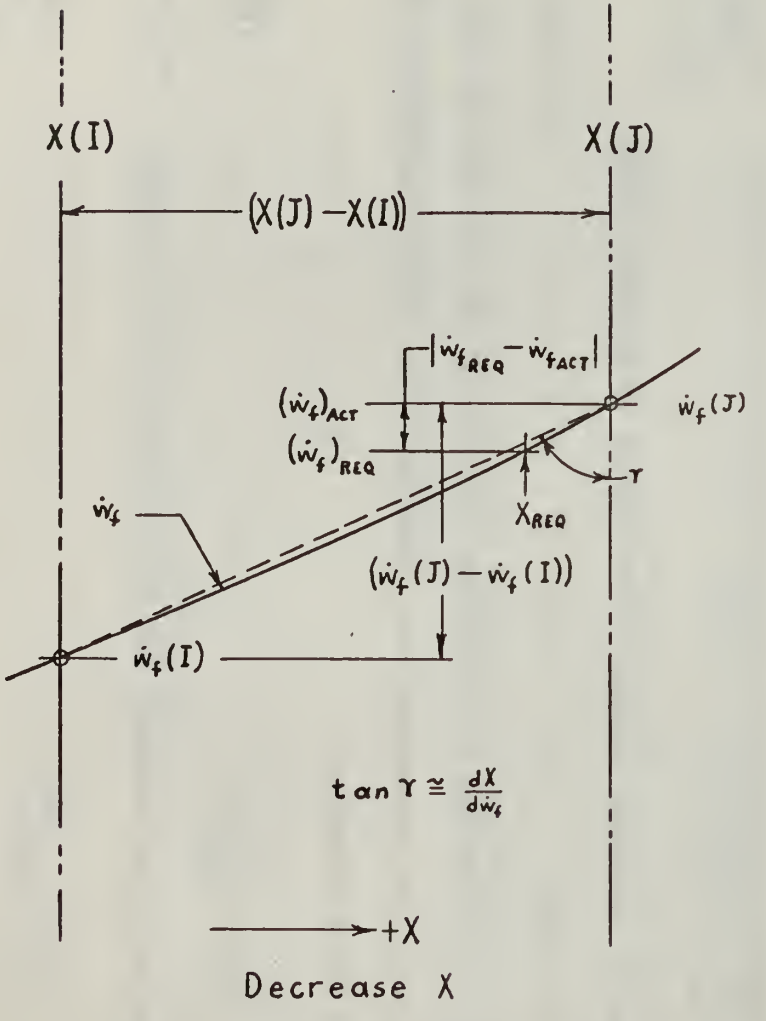

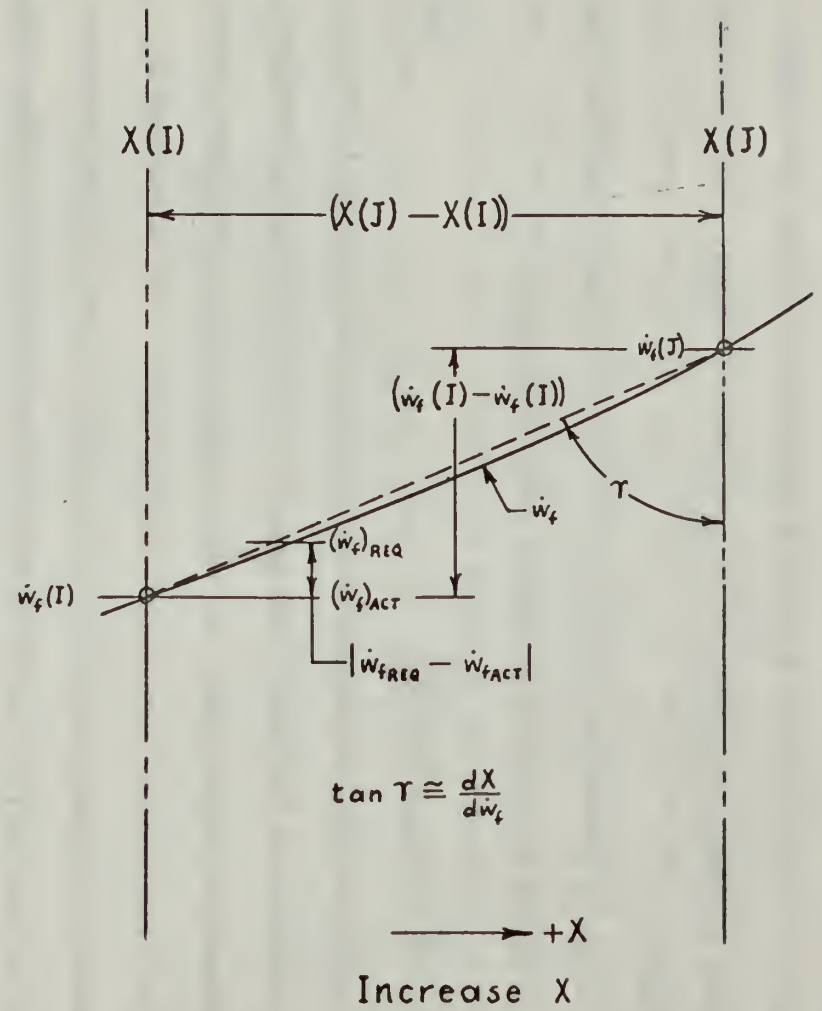

METHOD FOR CORRECTING STREAMLINE LOCATIONS
USED IN THE PERFORMANCE ANALYSIS

FIGURE 16a

The curve of Fig. 16b is supposed to represent some arbitrarily selected f(X) for illustration of the method used to determine gradients of entropy and equivalent enthalpy. Gradients at the hub and the tip are taken as the straight-line slopes between values of f(X) for streamlines one and two and streamlines four and five respectively. Gradients at intermediate streamlines (two, three and four) are taken as the average of the straight line slopes between values for these streamlines and the values for streamlines on either side. All slopes are computed for increasing X.

The manner in which values of s^*, H_E and the gradients of these two properties are determined for corrected streamlines is illustrated in Figs. 17a and 17b. The curves of Fig. 17a show the possible gradient variations for curves which might pass through the property value for the streamline of interest. Also shown are the straight line slopes to the property values for the streamlines to the left and to the right. Fig. 17b shows the increasing X portion of Fig. 17a with curve segments, straight line slopes and actual slopes at the streamline value of the property. To obtain the rate of change of the gradient, it is assumed that the straight line slope is the slope of the curve at the value of X one-half way to the adjacent streamline. The rate of change of slope is then the straight line slope minus the slope of the curve at the streamline point on the curve, divided by one-half the difference in X values between the two streamlines. Note that the positive case is used in obtaining the new value of X, whether this value is greater or smaller than the old value. If X must be decreased, the straight line slopes to the left of the streamline of interest are considered to extend to the right of the streamline point. Then, once the rate of change has been determined, the gradient for the new value of X for the streamline is the old gradient

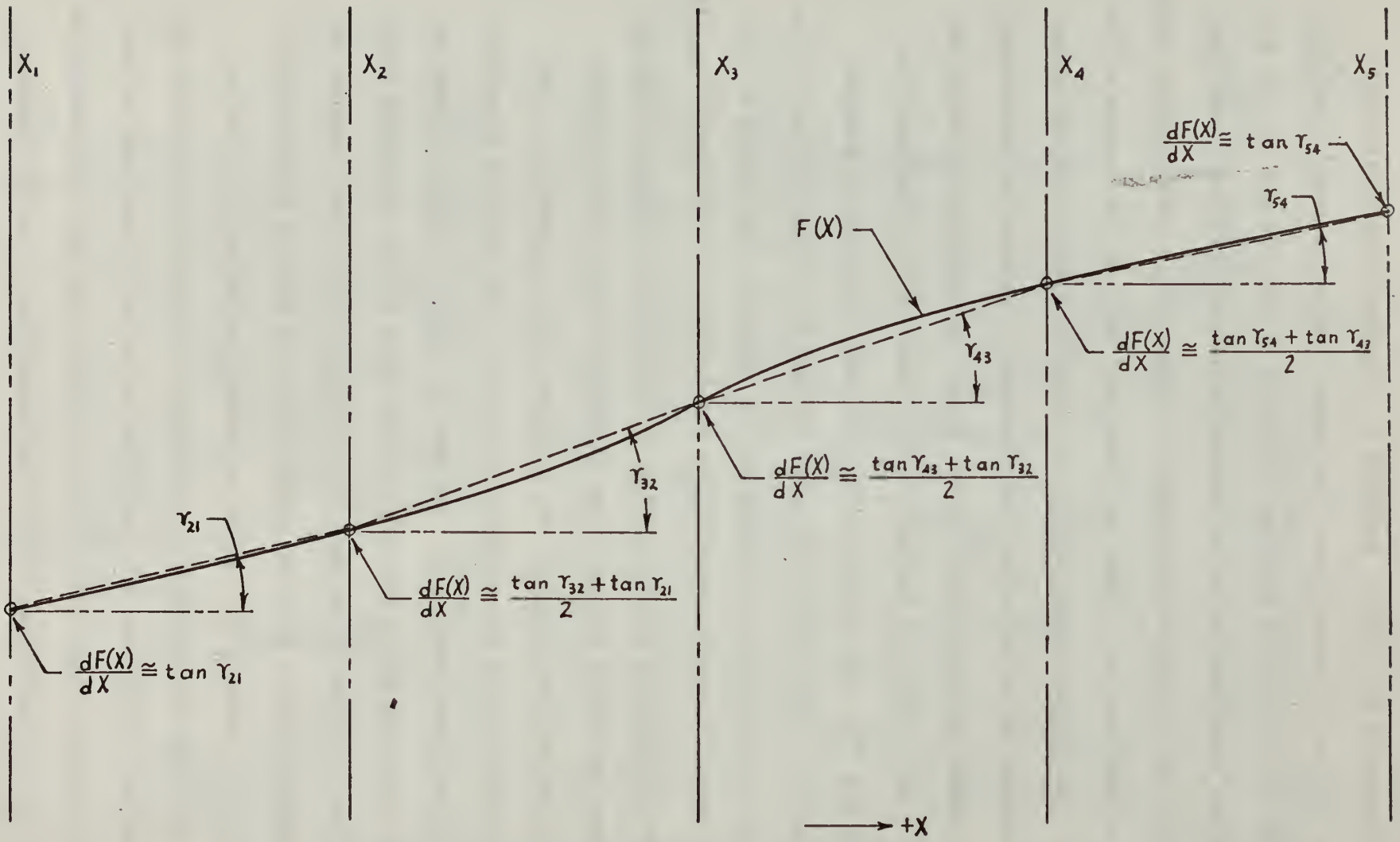

METHOD FOR APPROXIMATING SLOPES
USED IN THE PERFORMANCE ANALYSIS

FIGURE 16b

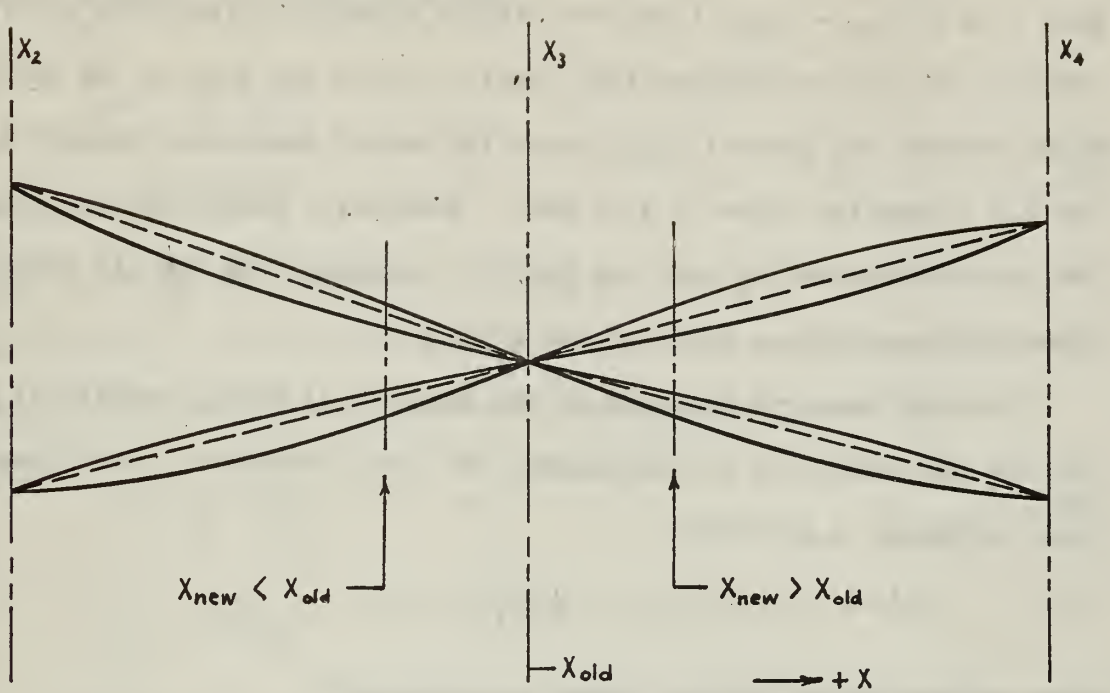

(a) Possible Curves F(X)

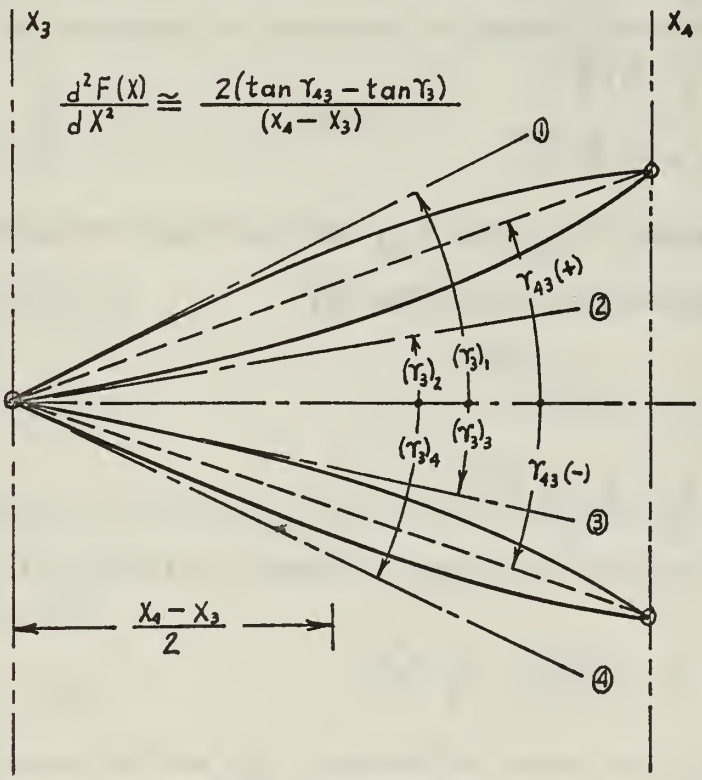

(b) $X_{new} > X_{old}$ Details

METHOD FOR DETERMINING RATE OF CHANGE OF GRADIENTS

FIGURE 17

plus ($\Delta X = X_{new} - X_{old}$) times the rate of change of slope with X. It is evident that the correct gradient results, since the sign of ΔX determines whether the plot of Fig. 17b or its mirror image, with respect to the old streamline value of X, is used. Similarly, using this new slope, the value of the variable at the new X is obtained from the old value plus ΔX times the new value of the gradient.

Once the required solution of the analysis is known, additional properties and quantities are determined for each streamline. The change in total enthalpy is given by:

$$\Delta H = H_1 - H_2 = (U_1 V_{u_1} - U_2 V_{u_2}) \frac{1}{gJ} \tag{71}$$

Then, sequentially, the following are determined:

$$T_{t_2} = T_{t_0} - \frac{\Delta H}{c_p} \tag{72}$$

$$P_{t_2} = P_2 \left(\frac{T_{t_2}}{T_2} \right)^{\frac{\gamma}{\gamma - 1}} \tag{73}$$

$$P_{t_1} = P_1 \left(\frac{T_{t_0}}{T_1} \right)^{\frac{\gamma}{\gamma - 1}} \tag{74}$$

The temperatures, $T_{2_{is}}$, and T_{2_s}, for isentropic expansion to p_2 from p_{t_0} and p_{t_E}, respectively, are given by:

$$T_{2_{is}} = T_{t_0} \left(\frac{P_2}{P_{t_0}} \right)^{\frac{\gamma - 1}{\gamma}} \tag{75}$$

$$T_{2_s} = T_{t_E} \left(\frac{P_2}{P_{t_E}} \right)^{\frac{\gamma - 1}{\gamma}} \tag{76}$$

The overall turbine efficiency (internal efficiency) is then:

$$\eta_i = \frac{\Delta H}{\Delta h_{is}} = \frac{T_{t_0} - T_{t_2}}{T_{t_0} - T_{2_{is}}} \tag{77}$$

Additionally, the stator efficiency, η_S, and the rotor efficiency, η_R, are computed using (78) and (79) below, even though they are related to the input loss coefficients by $(1 - \zeta)$. The values obtained in the output

provide a check on program operation.

$$\eta_S = \frac{T_{t_o} - T_1}{T_{t_o} - T_{1is}} \tag{78}$$

$$\eta_R = \frac{T_{t_\varepsilon} - T_2}{T_{t_\varepsilon} - T_{2s}} \tag{79}$$

Stator and rotor velocity coefficients, φ_v and ψ, are obtained as the square roots of (78) and (79), respectively. The theoretical degree of reaction, r^*, and the so-called head coefficient, k_{is}, are given by:

$$r^* = \frac{T_{1is} - T_{2is}}{T_{t_o} - T_{2is}} \tag{80}$$

$$k_{is} = \frac{\Delta h_{is}}{U_1^2/2gJ} = \frac{2\,c_p\,(T_{t_o} - T_{2is})\,gJ}{U_1^2} \tag{81}$$

In order to obtain mass-flow-weighted values of moment and horsepower, the following equations are used, where $\dot{w}_f$ is the flow fraction at the rotor exit, and the subscript $\dot{w}$ indicates the mass-flow-weighted value:

$$(\Delta H)_{\dot{w}} = \sum_{i=1}^{4} \left(\Delta H_{(i+1)} + \Delta H_i\right) \frac{\left(\dot{w}_{f(i+1)} - \dot{w}_{fi}\right)}{2} \tag{82}$$

Then:

$$HP_{\dot{w}} = \frac{(\Delta H)_{\dot{w}}\, J\, \dot{w}}{550} \tag{83}$$

$$M_{R\dot{w}} = \frac{HP_{\dot{w}}\,(550)}{\omega r} \tag{84}$$

Referred values are obtained, following NASA practice. For $\gamma = 1.4$:

$$HP_{ref} = \frac{HP_{\dot{w}}}{\sqrt{\theta}\,\delta} \tag{85}$$

$$M_{R_{ref}} = \frac{M_{R\dot{w}}}{\delta} \tag{86}$$

$$N_{ref} = \frac{N}{\sqrt{\theta}} \tag{87}$$

$$\dot{w}_{ref} = \frac{\dot{w}\sqrt{\theta}}{\delta} \tag{88}$$

Here:

$$\theta = \frac{T_{t_o}}{T_{STD}} = \frac{T_{t_o}}{518.4} \tag{89}$$

$$\delta = \frac{P_{t_o}}{P_{STD}} = \frac{P_{t_o}}{14.7} \tag{90}$$

Results and Discussion

The performance analysis was accomplished for assumed stator exit mean streamline Mach Numbers, M_{1_m}, between 0.9 and 1.4 in steps of 0.05. The general range of RPM used was 11,000 to 20,000. However, at assumed Mach Numbers of 1.1 and above at low RPM, the high values of rotor loss coefficients caused divergence in the iterations for Y_2 for the tip streamline. Also, for M_{1_m} = 1.4 and 18,000 RPM, and for M_{1_m} = 1.35 and 18,500 RPM, the pressure ratio across the rotor, p_{tE}/p_2, indicated choked flow in the rotor and overall continuity could not be satisfied. Since no provisions for this contingency are included in the program, 17,500 and 18,000 RPM were the upper limits for M_{1_m} = 1.4 and 1.35, respectively. Table I indicates the values of M_{1_m} and RPM for which the analysis was attempted without success.

TABLE I

PERFORMANCE ANALYSIS INPUT VALUES FOR WHICH RESULTS ARE NOT AVAILABLE

Mean Streamline Mach Number - Stator Exit (M_{1_m})	RPM (10^{-3})						
	11	12	13	14	18	19	20
1.1	X						
1.15	X						
1.2	X	X					
1.25	X	X					
1.3	X	X	X				
1.35	X	X	X		(18.5)	X	X
1.4	X	X	X	X	X	X	X

Stator inlet conditions--total temperature and total pressure--were chosen to give a static pressure of 14.7psia for the mean streamline at the stator exit, except that limiting values of 660°R and 43psia were used. At the higher Mach Numbers, M_{1_m} more than 1.25, stator exit plane pressure was a partial vacuum. Fig. 18 shows the schedule of input variables as functions of M_{1_m}.

Representative output from the program is included in Appendix III. Since most of the printout column headings are self explanatory, no general listing is given; however, App. III includes such description of print-outs as is required for clarity.

Table II summarizes the results of the performance analysis shown in Figs. 19 through 30 for ease of reference.

The analysis showed values of Y_1 to be essentially invariant with M_{1_m}. Consequently, a single curve of Y_1 versus X_1 is representative for all values of M_{1_m}. Moreover, since the flow discharge angle, α_1', was assumed to be constant for $M_{1_m} = 1$, and since α_1 values for $M_1 = 0.9$ differ from the $M_1 = 1$ values only by 0.05 , a single curve of V_{u_1} versus X_1 is well representative for all values of M_{1_m}.

Rotor exit conditions vary with each of the rotor inlet condition variables. Hence, the curves of Figs. 24 - 26 are included to represent the general nature of rotor exit conditions, as given by the analysis. However, the analysis showed that rotor exit plane pressure, p_2, is essentially constant with radius for each set of rotor inlet conditions. The maximum difference in values of p_2 for the several streamlines was approximately 0.5 psia for given rotor inlet conditions. It is evident from Figs. 24 and 25 that the method used for determining gradients of entropy and equivalent total enthalpy is satisfactory, since there are no marked inflections in the curves of s^* and H_E. It is interesting to note

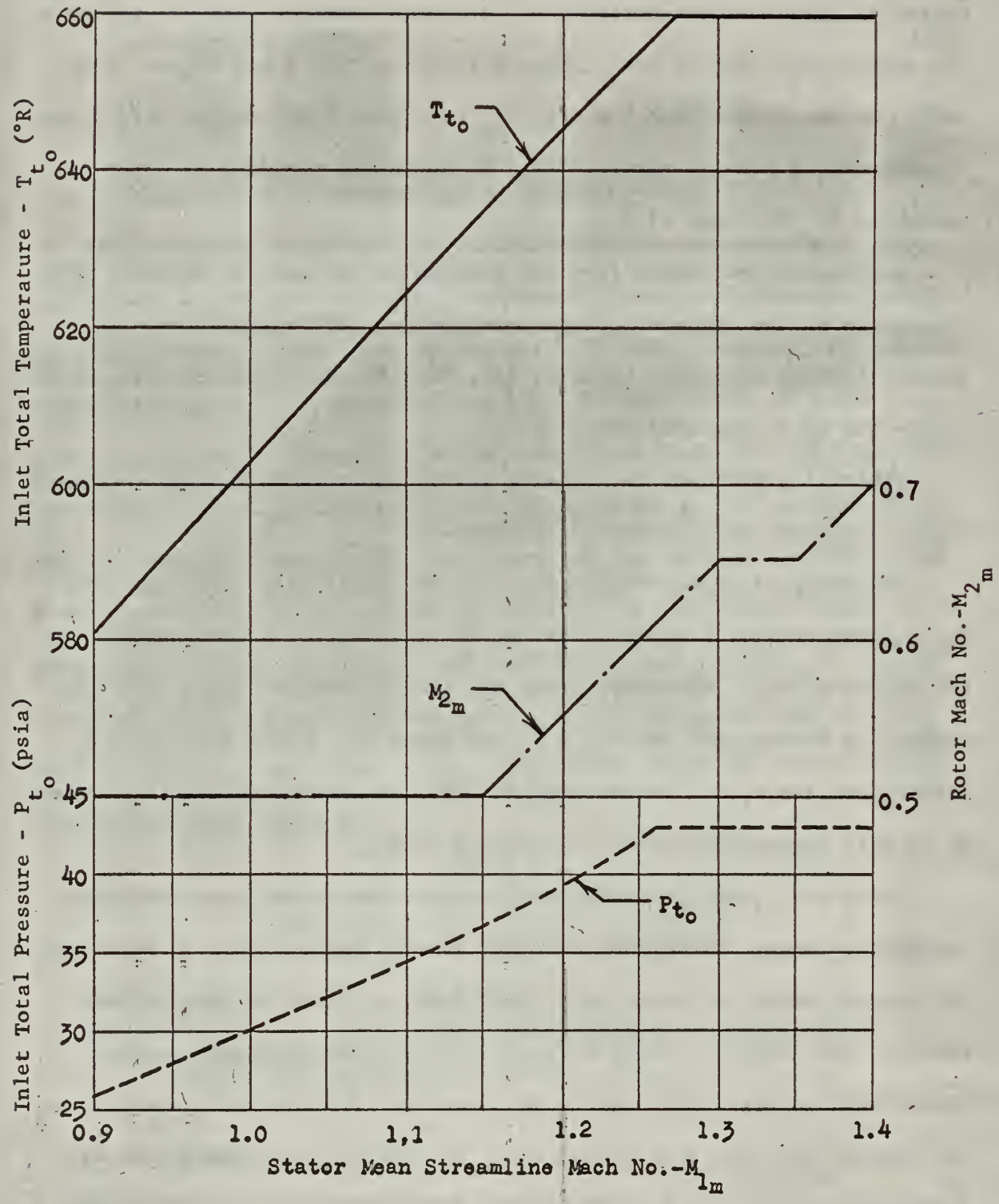

SCHEDULE OF VALUES OF INPUT VARIABLES
USED IN PERFORMANCE ANALYSIS

FIGURE 18

TABLE II

SUMMARY OF PERFORMANCE ANALYSIS
CONTENTS OF FIGS. 19-30

FIG.	SHOWS	VERSUS	REMARKS
19	Referred Flow Rate, $\dot{w}_{ref}$	p_{t_o}/p_1	
20	Stator Area Restriction factor, ξ	X_1	curves for p_{t_o}/p_1 = constant
21	$V_{a1}/\sqrt{\theta}$	p_{t_o}/p_1	
22	$V_{a1}/(V_{a1_m})$ & $V_{u1}/(V_{a1})_m$	X_1	curves essentially independent of M_{1_m}
23	p/p_{t_o}	X_1	curves for M_{1_m} = constant
24	s_1^*, s_2^*, & their sum	X_2	$M_{1_m} = 1$, N = 20,000
25	H_E	X_2	same as above
26	Y_2	X_2	$M_{1_m} = 1.0$
27	$(V_{a2})_m/\sqrt{\theta}$, M_{1_m}, & K_{is}	$N/\sqrt{\theta}$	
28	Internal Efficiency, η_i	k_{is}	for hub, mean and tip streamlines
29	Theoretical Degree of reaction, r^*	k_{is}	mean streamline
30	Referred Rotor Moment M_R/δ	$N/\sqrt{\theta}$	mean streamline

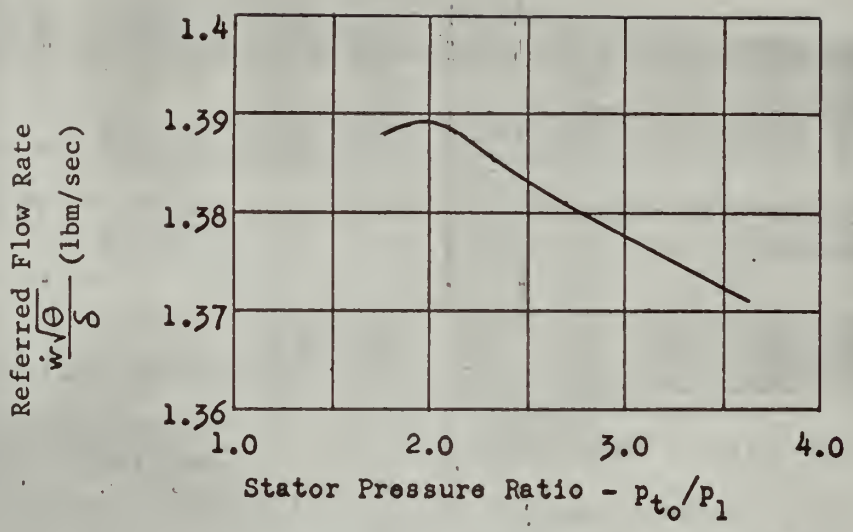

VARIATION OF REFERRED FLOW RATE
WITH STATOR PRESSURE RATIO-
PERFORMANCE ANALYSIS

FIGURE 19

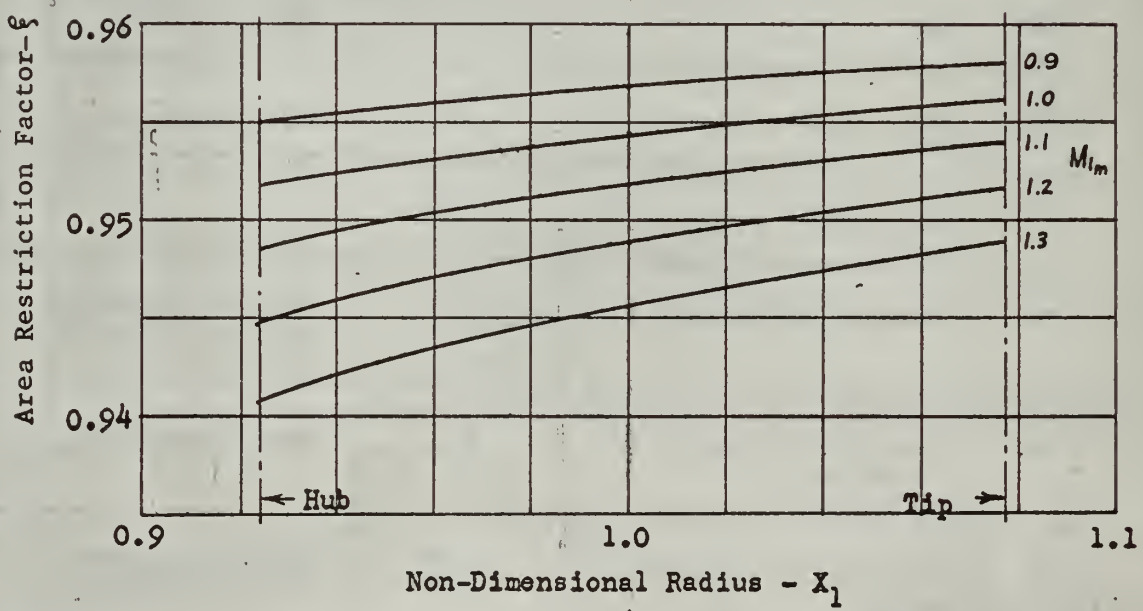

VARIATION OF STATOR AREA RESTRICTION FACTOR
WITH NON-DIMENSIONAL RADIUS
PERFORMANCE ANALYSIS

FIGURE 20

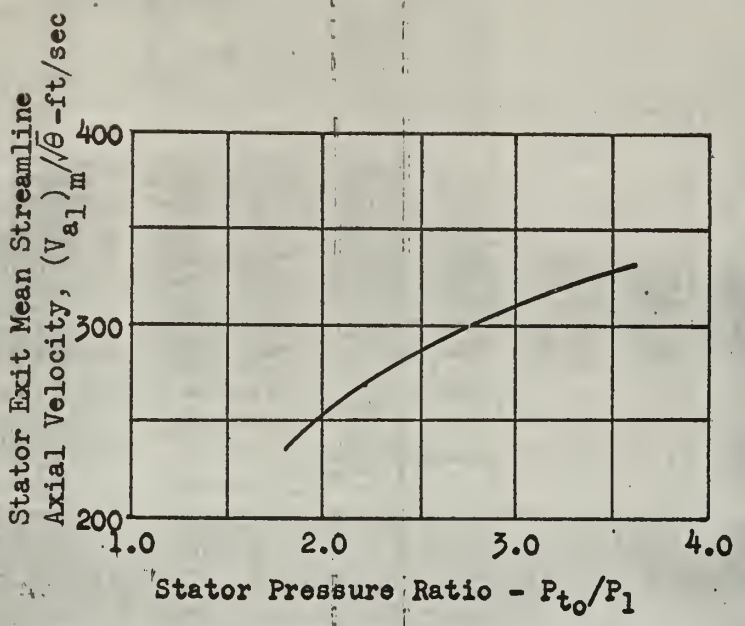

VARIATION OF STATOR EXIT MEAN STREAMLINE
AXIAL VELOCITY WITH PRESSURE RATIO
PERFORMANCE ANALYSIS

FIGURE 21

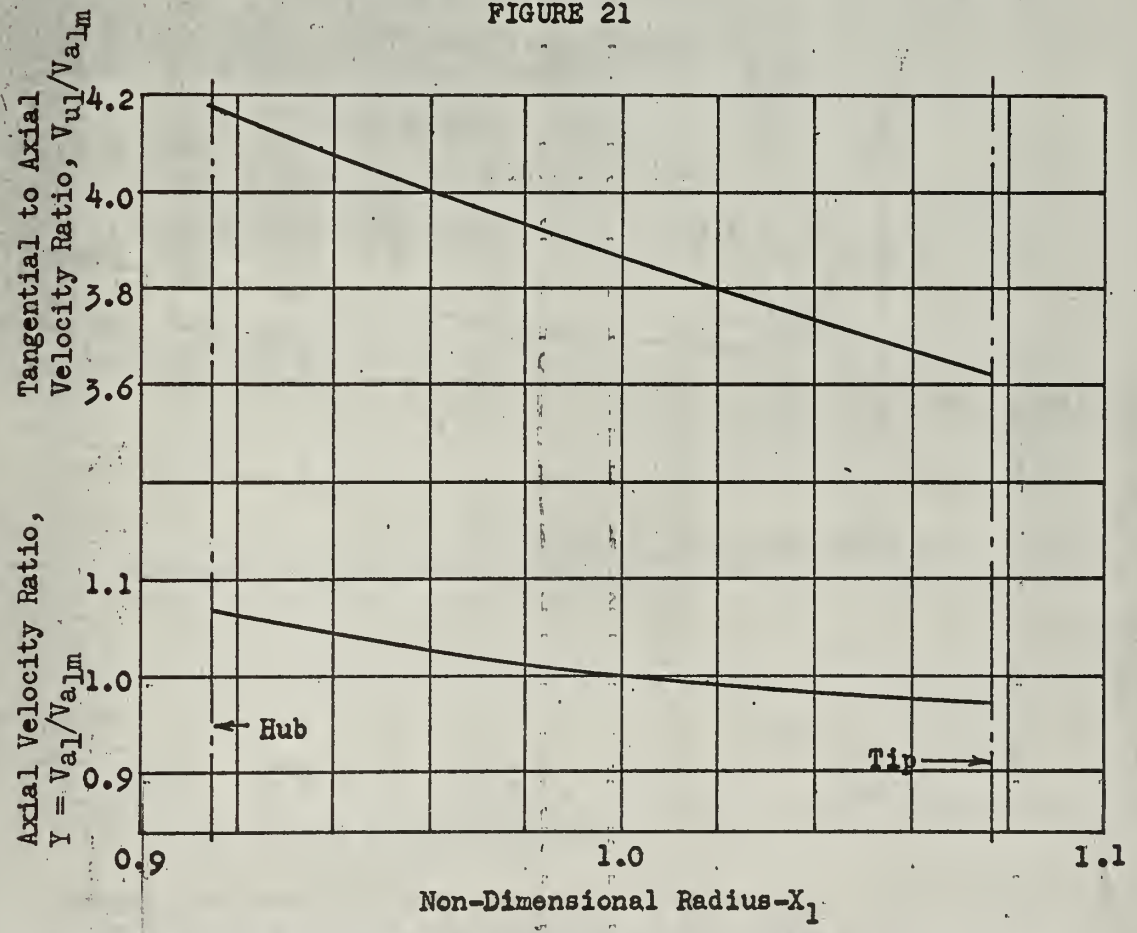

RADIAL DISTRIBUTION OF THE RATIOS OF STATOR EXIT AXIAL VELOCITY AND
TANGENTIAL VELOCITY TO MEAN STREAMLINE AXIAL VELOCITY-PERFORMANCE ANALYSIS

FIGURE 22

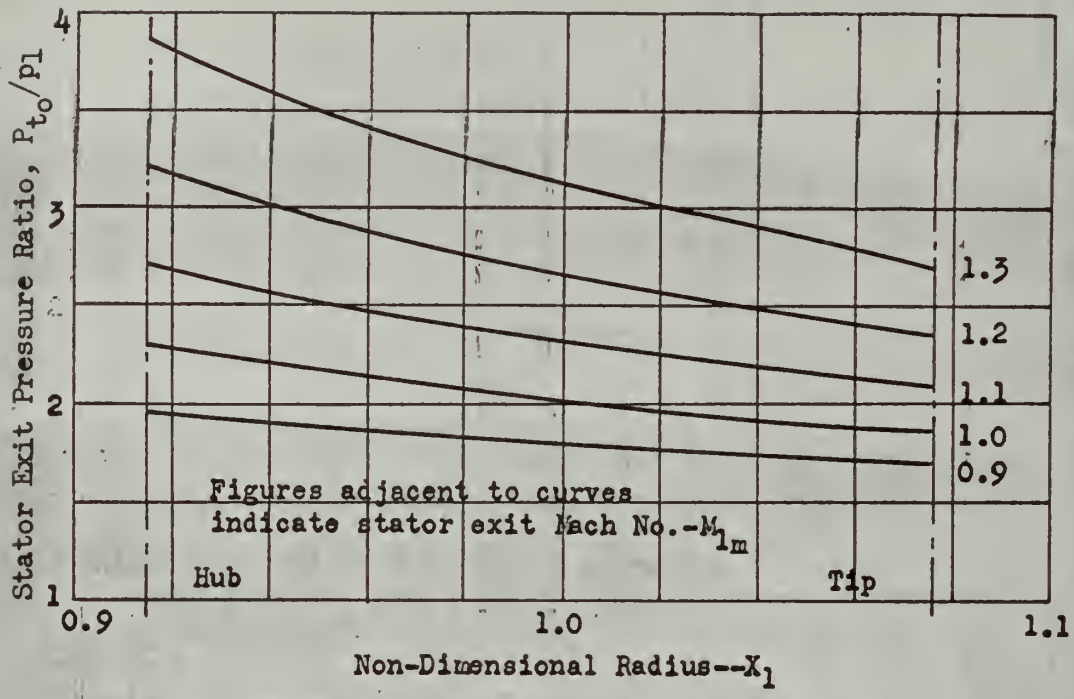

VARIATION OF STATOR EXIT PRESSURE RATIO
WITH NON-DIMENSIONAL RADIUS--PERFORMANCE ANALYSIS

FIGURE 23

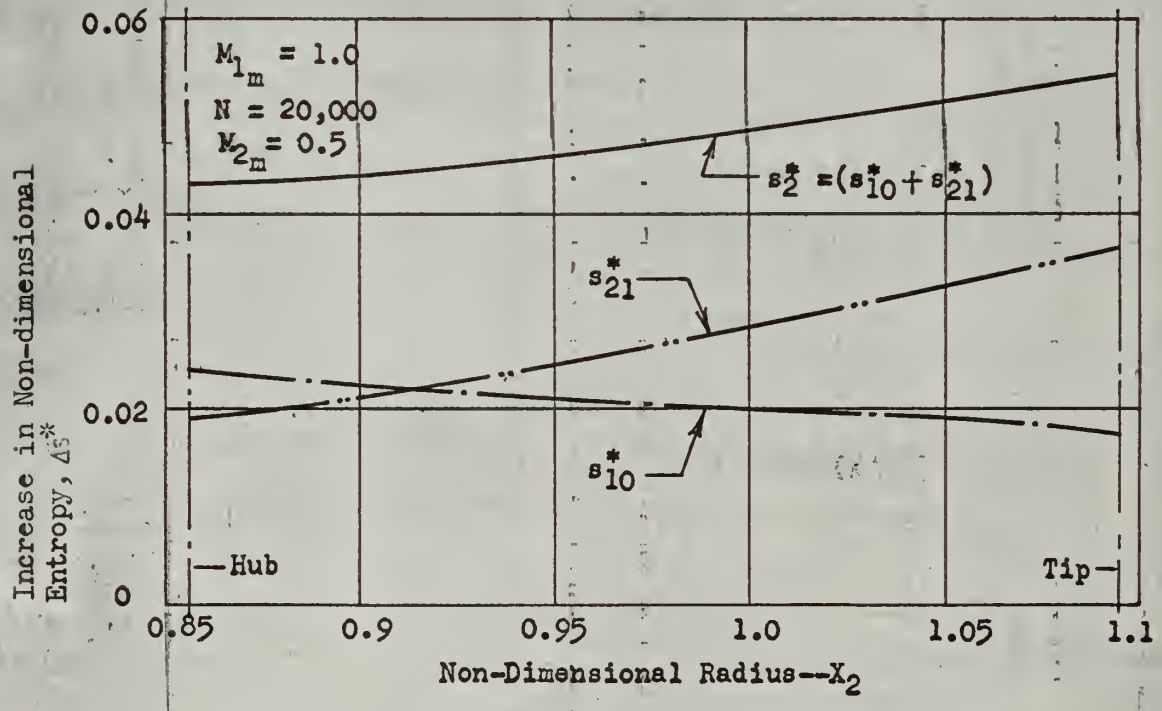

VARIATION OF INCREASES IN NON-DIMENSIONAL ENTROPY
WITH ROTOR EXIT NON-DIMENSIONAL RADIUS--PERFORMANCE ANALYSIS

FIGURE 24

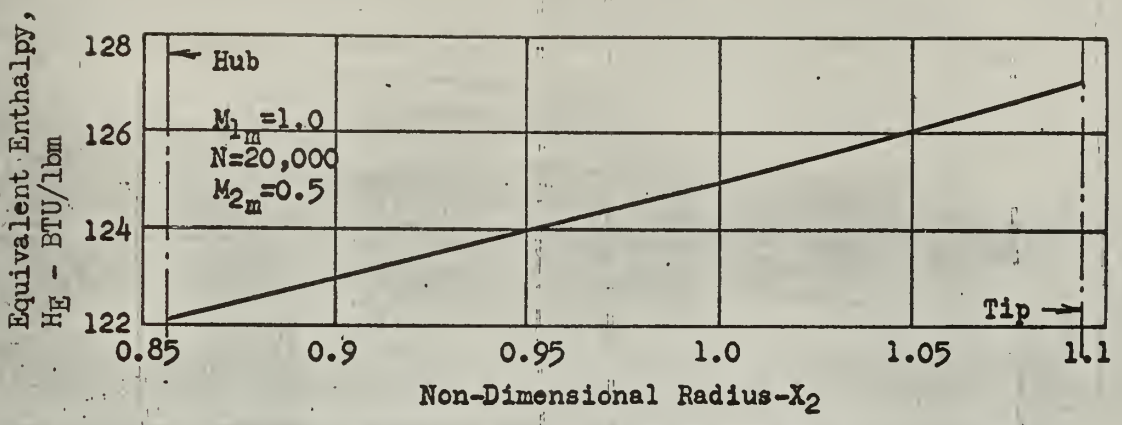

VARIATION OF EQUIVALENT ENTHALPY
WITH ROTOR EXIT NON-DIMENSIONAL RADIUS
PERFORMANCE ANALYSIS

FIGURE 25

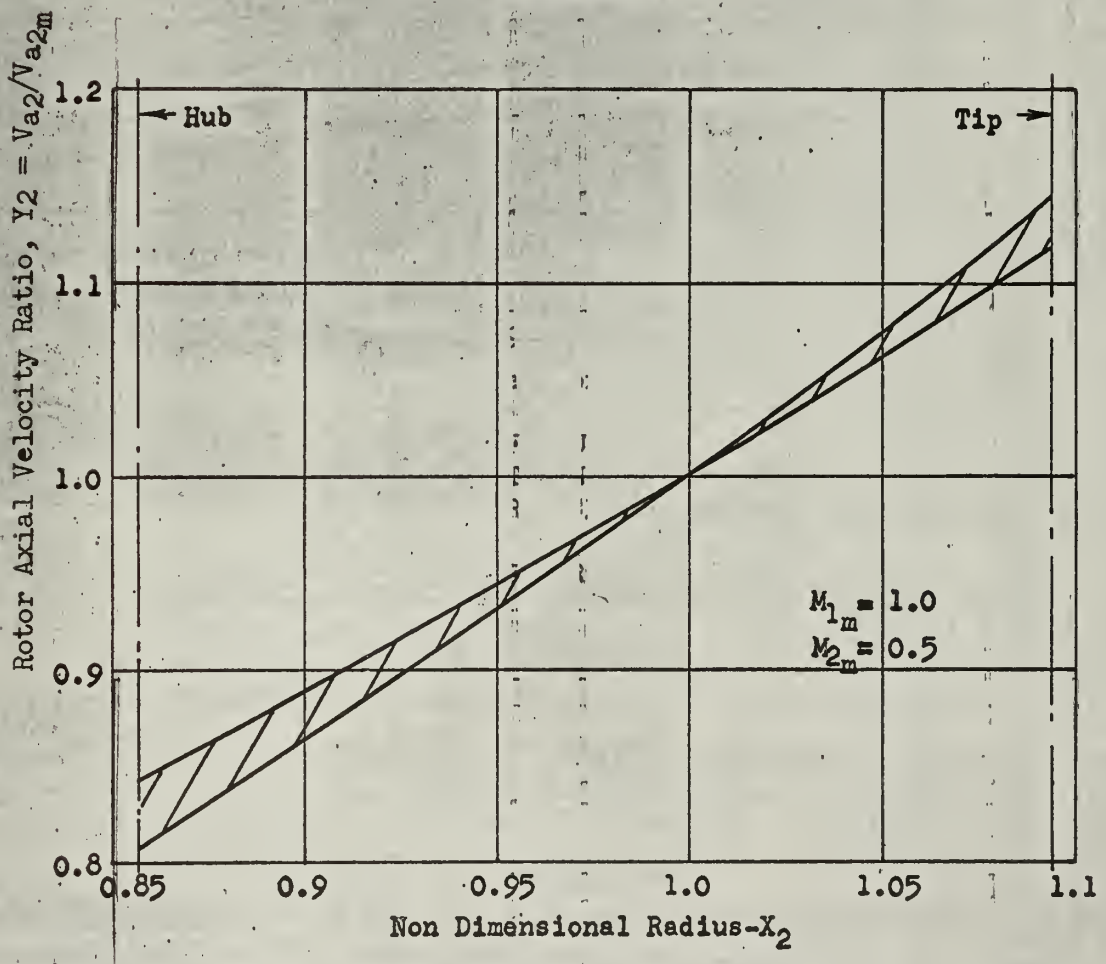

VARIATION OF ROTOR EXIT AXIAL VELOCITY WITH
NON-DIMENSIONAL RADIUS--PERFORMANCE ANALYSIS

FIGURE 26

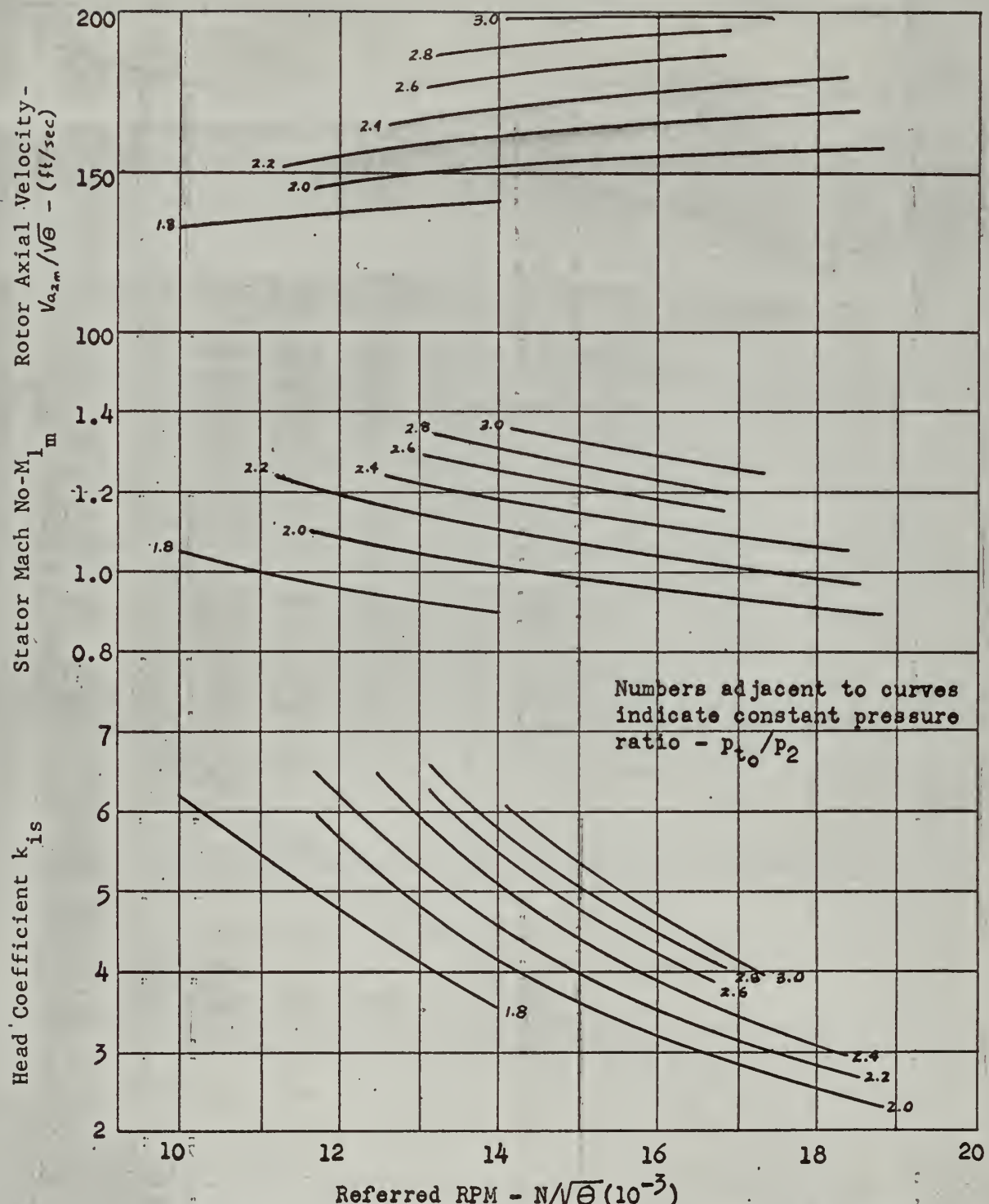

VARIATION OF ROTOR EXIT AXIAL VELOCITY, STATOR EXIT MEAN MACH NUMBER, AND HEAD COEFFICIENT WITH REFERRED RPM -- PERFORMANCE ANALYSIS

FIGURE 27

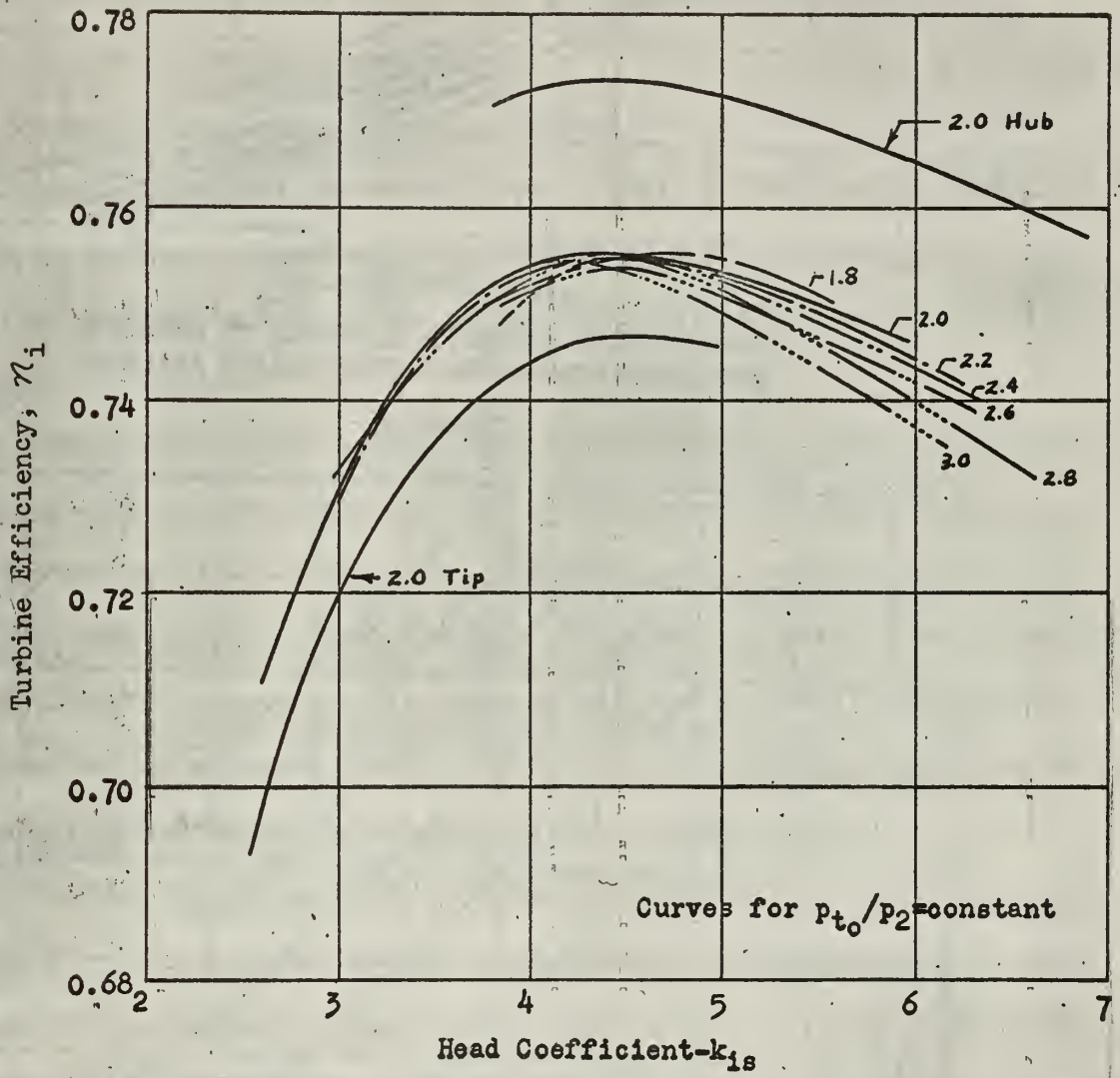

VARIATION OF TURBINE EFFICIENCY
WITH HEAD COEFFICIENT
PERFORMANCE ANALYSIS

FIGURE 28

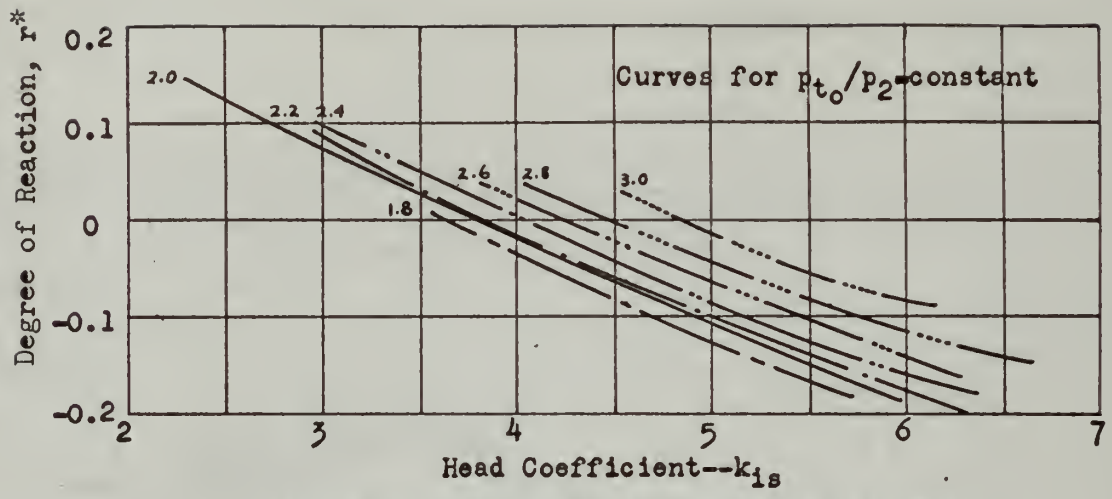

VARIATION OF THEORETICAL DEGREE OF REACTION WITH HEAD COEFFICIENT--PERFORMANCE ANALYSIS

FIGURE 29

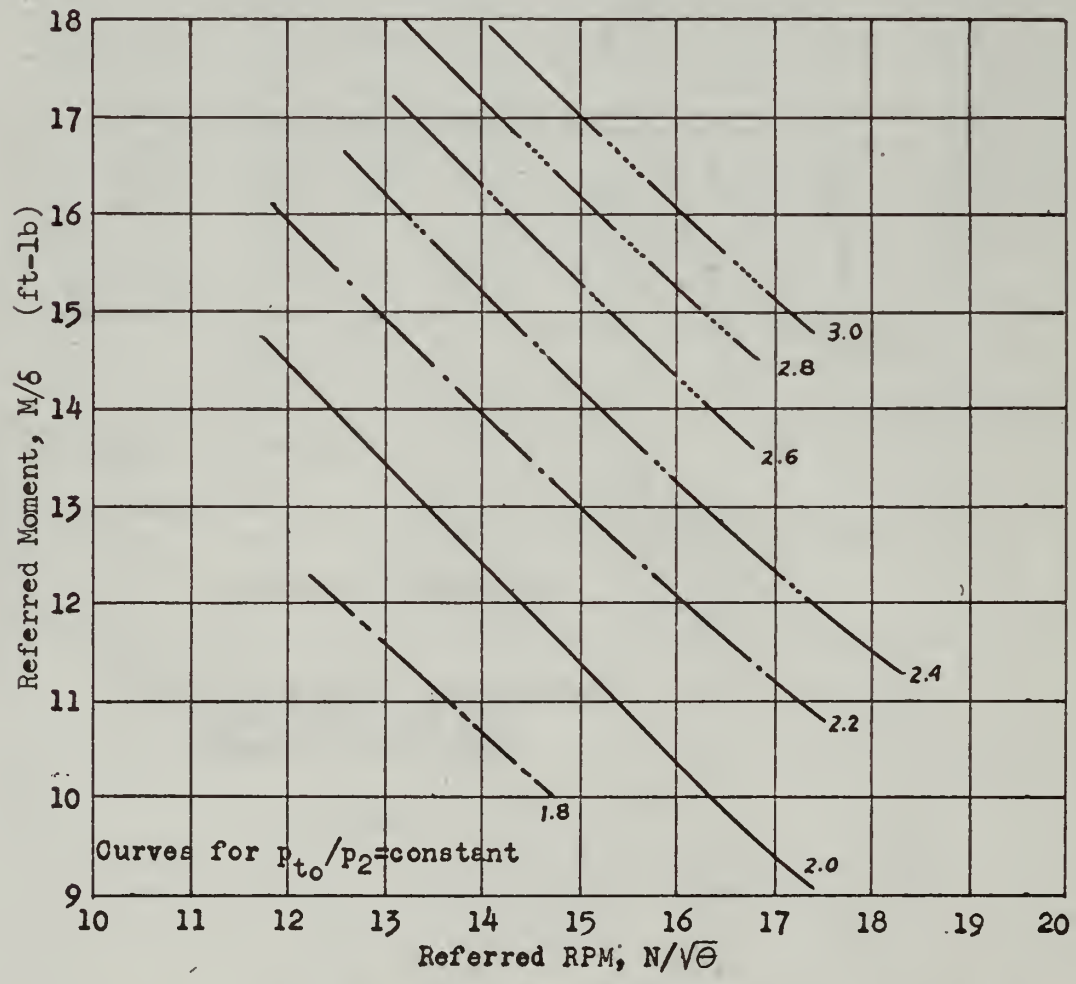

VARIATION OF REFERRED ROTOR MOMENT WITH REFERRED RPM -- PERFORMANCE ANALYSIS

FIGURE 30

that the band of variation of Y_2 with RPM for constant Mach Number, M_{1_m}, is relatively narrow. This observation, although valid in general, is offered with qualification, since, as stated previously, results could not be obtained for certain assumed inlet conditions for which the iteration for Y_2 became divergent.

Fig. 19 indicates that $\dot{w}_{ref}$ decreases with increasing pressure ratio, p_{t_o}/p_1, whereas for choked flow it could be anticipated that $\dot{w}_{ref}$ would be constant. However, it is evident from Fig. 20 that the reason for the decrease is that values of the area restriction factor decrease as p_{t_o}/p_1 increases.

Considering that normally the rotor exit plane pressure is known, selected performance parameters were plotted versus p_{t_o}/p_2, so that by cross-plotting, these performance parameters could be shown as functions of $N/\sqrt{\theta}$ and k_{is} for different values of p_{t_o}/p_2 = constant. The resulting curves, presented in Figs. 27 - 30, are designed to permit performance estimations for selected values of RPM, inlet total temperature, pressure ratio p_{t_o}/p_2 and either p_{t_o} or p_2. Figs. 27 - 30, in conjunction with the stator and rotor gas angle information included in App. II, and Figs. 19 and 21 - 23, provide sufficient information for determination of mean streamline performance. Recommended values of mean streamline radii for use in such a performance estimation are 4.26 in. for the stator and 4.45 in. for the rotor. Variation of conditions with radius in the stator exit plane can be found using Figs. 20 - 23. Moreover, since p_2 is essentially constant with radius, an approximation to variation of properties in the rotor exit plane can be obtained, by using p_2 = constant and estimated values of Y_2 taken from Fig. 26.

It might appear, on the basis of the curves of Fig. 28, that the mean streamline values of internal efficiency are not adequately representative

of turbine performance, since the mean streamline curve falls appreciably closer to the tip curve than to the hub curve. However, the average of the values of η_i for all streamlines is generally only 0.001 to 0.002 different from the mean streamline value. It is significant, too, that the values of ΔH for all streamlines vary little from the value for the mean streamline. Consequently, the mean streamline values of internal efficiency, as well as of the other performance parameters, can be considered excellent indicators of turbine performance as predicted by the performance analysis.

Unfortunately, time available did not permit thorough investigation of the circumstances leading to the indications of rotor choking. Outputs from the computer for indicated choked flow in the rotor show that the manner in which the area restriction factor and the flow function vary with pressure ratio might cause too-early indications of rotor choking. As the pressure ratio approaches the critical value, the rate of increase for Φ decreases while the rate of decrease of ξ is almost constant, so that their product increases only slightly. It appears that the rate of increase of this product becomes zero at the critical pressure ratio and then decreases with increased pressure ratio, p_{tE}/p_2 in this instance. It will be recognized that this decrease of the product, $\Phi\xi$, was shown to account for the non-constant referred flow rate. It is conceivable that, should rotor flow calculations show deficient flow rate at pressure ratios reasonably below the critical value, any increase in axial velocity yields increased pressure ratio with no increase in flow rate. Hence, large increases in axial velocity and pressure ratio result with succeeding iterations. The propriety of the effect of Φ in the foregoing is beyond question. However, whether the apparently overriding influence of the area restriction factor, ξ, is correct is considered problematical. It

is pertinent, though, that for assumed inlet conditions of $M_{1_m} = 1.35$ and 18,500 RPM, for which the analysis showed the rotor to be choked, if ξ were held constant after the first determination of rotor flow rate, the maximum rotor flow rate given by using Φ^* would not have increased the rotor flow rate to the value required. In this instance, then, the choking of the rotor was not caused by the decrease in values of ξ. The same observation holds also for the other choked-rotor result of the analysis.

The divergence in Y_2 values which prevented solutions at low RPM was probably caused in part by the higher loss coefficients for the rotor due to incidence angles approaching positive stall incidence. However, the loss coefficients by themselves should not have strong enough influence to generate the divergence. Rather, it is more probable that the initially assumed values of Y_2 were enough in error to start a divergence pattern after the first iteration, since either $Y_{2_{old}}/Y_{2_{new}}$ or that ratio squared is a multiplier of the several terms of the integrand for determining Y_2 (see (33), p. 48). Considering the effect of ζ in (28), p. 46, it is apparent that the higher the value of ζ, the greater is the subtractive term in the denominator. Still, once the value of ζ has been introduced into that term, later fluctuations or changes in the term are due to Y_2^2 (or to the ratio given above squared as a multiplier), for axial velocity considered as a constant. It is then apparent that high rotor loss coefficients can be said to establish a certain level of bias in the entropy terms which, when aggravated by relatively large fluctuations in Y_2 values, can ultimately drive the subtractive term of (28) to values greater than one. Of course, this latter event is the final manifestation of the divergence of Y_2 values, since the logarithm of a negative number is undefined. Obviously, the subtractive term of the numerator of (28) is affected by Y_2 value fluctuations, but only about one-half as much. In

the instant analysis, the large gas efflux angles aggravate the 'bias' produced by the loss coefficients, since the $\cos^2\beta$ in the denominator serves to increase the subtractive term.

The method used for this performance analysis appears sound and is deemed relatively easy to use. Convergence of iterations is quite rapid except as noted above. It was found that the rate of convergence was increased if initial input RPM, for otherwise constant input parameters, was the middle value of the expected RPM range, with subsequent RPM inputs increased or decreased from the initially assumed value. Obviously, this method, like all methods, can be considered no more accurate than the assumptions used in the solution. Undoubtedly, the most critical values assumed are those for the loss coefficients.

The program PERFORM used in this analysis, although apparently giving satisfactory results, can surely be improved. It was noted that values of a/a_m for the mean radius slipped somewhat from the desired value of 1 (to 0.9943 in one instance). Since this ratio is expressed as a parabolic function of X, and since slippage was due to the correction factors for the constants in the parabolic expression, the method for correcting rotor exit streamline radial locations should be reexamined with a view to decreasing the noted discrepancy. Also, it is considered that a more appropriate tolerance for flow fractions would be a percentage, say one percent, of the required flow fraction. This change would yield more uniform requirements for between-streamline flow rates, rather than the presently-used two, one, and three-fourths percent tolerances, used in order, for the one-fourth, one-half and three-fourths total flow points.

4. Exhauster Performance Analysis.

General

Analysis of the turbine during exhauster operation was undertaken to obtain preliminary estimates of total-to-total pressure ratios achievable across the turbine and to predict shock conditions which may occur in the exhauster piping. The analysis conducted was for one-dimensional flow, based on the momentum, continuity and energy equations. Extensive use was made of polytropic process relations and the non-dimensional flow function, Φ , which is obtained by combining the energy and continuity equations. The relations for expansion and compression processes are given below without proof.[6] For an expansion process:

$$\frac{\dot{w}\sqrt{T_{t_o}}}{A P_{t_o}}\sqrt{\frac{R}{g}} = \Phi = \sqrt{\frac{2\gamma}{\gamma-1}\left[\left(\frac{p}{P_{t_o}}\right)^{2/n} - \left(\frac{p}{P_{t_o}}\right)^{\frac{n+1}{n}}\right]} \tag{91}$$

where:

$$n = \frac{\gamma}{1-\eta_p(\gamma-1)} \tag{92}$$

η_p - polytropic efficiency

γ - specific heat ratio

$\dot{w}$ - flow rate (lbm/sec)

T_{t_o} - stagnation temperature at the inlet (^oR)

A - flow area at the station of interest (in^2)

p_{t_o} - stagnation pressure at the inlet (psia)

p - static pressure at the station of interest (psia)

R - gas constant for air (ft-lb/lbm-^oR)

g - universal gravitational constant (lbm-ft/lb-sec^2)

Similarly, for a compression process, there is:

[6]Vavra, M. H., Problems of Fluid Mechanics in Radial Turbomachines (Rhode-Saint-Genese, Belgium, Von Karman Institute for Fluid Dynamics, 1965) VKI Course Note 55a, pp. 22-35.

$$\frac{\dot{W}\sqrt{T_{t_1}}}{A P_{t_1}}\sqrt{\frac{R}{g}} = \Phi = \sqrt{\frac{2\gamma}{\gamma-1}\left[\frac{T_{t_2}}{T_1}\left(\frac{P_2}{P_1}\right)^{\frac{2}{n}} - \left(\frac{P_2}{P_1}\right)^{\frac{n+1}{n}}\right]} \tag{93}$$

Here, the subscripts one and two refer to inlet and station of interest respectively. The polytropic exponent is given by:

$$n = \frac{\gamma \eta_p}{1-\gamma(1-\eta_p)} \tag{94}$$

In (93), the quantity T is the static temperature and the other variables are as defined and have dimensions as specified for the expansion process.

Fig. 5, p. 26, shows the complete exhauster and its dimensions and Fig. 13, p. 37, shows the exhauster nozzle and the flow channel from the turbine hood. Fig. 5 also shows station designations and subscripts used in the analysis and the general locations where the several polytropic efficiencies apply.

Method of Solution

Choked flow is assumed for the flow through the stator blade row and the flow through the exhauster nozzle. For this condition, the pressure ratio in (91) is:

$$\frac{P}{P_{t_o}} = \left(\frac{2}{n+1}\right)^{\frac{n}{n-1}} \tag{95}$$

Then, (91) becomes:

$$\Phi^* = \left(\frac{2}{n+1}\right)^{\frac{1}{n-1}}\sqrt{\frac{2\gamma}{\gamma-1}\left(\frac{n-1}{n+1}\right)} \tag{96}$$

For choked conditions, flow rates must be determined using this value of $\Phi = \Phi^*$; however, (91) remains valid for determining pressure ratios lower than the critical value.

Fig. 31 shows the processes involved in the analysis as they might appear on a temperature-entropy diagram. Turbine and nozzle flow processes and the several solutions possible downstream of the nozzle exit plane are

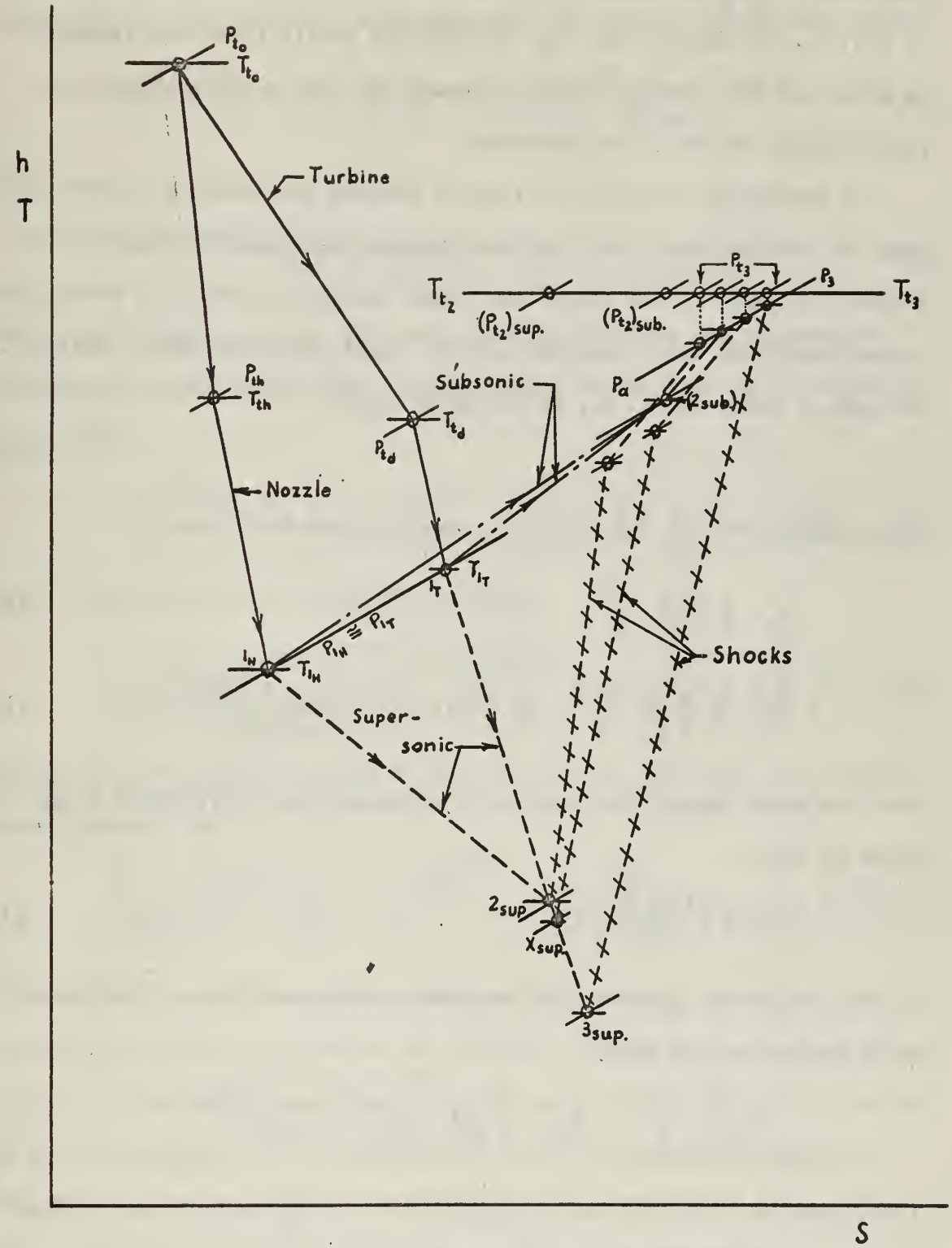

POSSIBLE EXHAUSTER FLOW PROCESSES

FIGURE 31

indicated. Station designations used in Fig. 31 correspond to those given in Fig. 5. At station two, the turbine and nozzle flows are assumed to be mixed and the combined flow is assumed to have uniform properties perpendicular to the flow direction.

As previously stated, the flow at station one consists of the flow from the turbine hood plus the flow through the exhauster nozzle. The former flow rate is the sum of the flows through the turbine, through the plenum labyrinth seals, and through the shaft labyrinth seal. Writing the sum of these flows, $\dot{w}_T$, in the order named:

$$\dot{w}_T = \dot{w}_b + \dot{w}_\ell + \dot{w}_s \tag{97}$$

The equations for $\dot{w}_\ell$ and $\dot{w}_S$, as derived in Section 5, are:

$$\dot{w}_\ell = \Phi_\ell \frac{A_\ell P_{t_o}}{\sqrt{T_{t_o}}} \sqrt{\frac{g}{R}} \; ; \quad \Phi_\ell = \sqrt{\frac{1 - P_{t_d}/P_{t_o}}{4.0791}} \tag{98}$$

$$\dot{w}_s = \Phi_s \frac{A_s P_a}{\sqrt{T_a}} \sqrt{\frac{g}{R}} \; ; \quad \Phi_s = 0.874 \left[\frac{1 - (P_{t_d}/P_a)^2}{10 + \frac{2}{\gamma} \ln (P_a/P_{t_d})} \right]^{1/2} \tag{99}$$

The flow rate through the turbine is obtained from (91), where $\Phi = \Phi^*$ is given by (96):

$$\dot{w}_b = \Phi^* \frac{A_b P_{t_o}}{\sqrt{T_{t_o}}} \sqrt{\frac{g}{R}} \tag{100}$$

For the expansion process from the hood to the exit plane of the nozzle, it is convenient to write:

$$\frac{\dot{w}_T \sqrt{T_{t_d}}}{P_{t_d} A_{l_T}} \sqrt{\frac{R}{g}} = \Phi_d = \sqrt{\frac{2\gamma}{\gamma - 1} \left[\left(\frac{P_{l_T}}{P_{t_d}} \right)^{\frac{2}{n_d}} - \left(\frac{P_{l_T}}{P_{t_d}} \right)^{\frac{n_d + 1}{n_d}} \right]} \tag{101}$$

Then, putting (98), (99) and (100) in terms of Φ's, there is, with (97):

$$\frac{\dot{w}_T \sqrt{T_{t_o}}}{P_{t_o}} \sqrt{\frac{R}{g}} = \Phi_b A_b + \Phi_\ell A_\ell + \Phi_S A_S \frac{P_a}{P_{t_o}} \sqrt{\frac{T_{t_o}}{T_a}} \tag{102}$$

Implicit in this relation is the assumption that the total conditions at

the inlet to the plenum labyrinth seals are the same as those ahead of the stator of the turbine. Combining the left side of (102) with (101):

$$\frac{\dot{w}_T\sqrt{T_{t_o}}}{P_{t_o}}\sqrt{\frac{R}{g}} = \Phi_d A_{l_T}\sqrt{\frac{T_{t_o}}{T_{t_d}}}\,\frac{P_{t_d}}{P_{t_o}} = \Phi_d A_{l_T}\left[\frac{P_{t_o}}{P_{t_d}}\right]^{\frac{n_T-1}{n_T}}\frac{1}{(P_{t_o}/P_{t_d})} \tag{103}$$

or:

$$\frac{\dot{w}_T\sqrt{T_{t_o}}}{P_{t_o}}\sqrt{\frac{R}{g}} = \Phi_d A_{l_T}\frac{1}{\left(P_{t_o}/P_{t_d}\right)^{\frac{n_T+1}{2n_T}}} = \Phi_d A_{l_T}\frac{1}{\left[\frac{P_{t_o}/P_{l_T}}{P_{t_d}/P_{l_T}}\right]^{\frac{n_T+1}{2n_T}}} \tag{104}$$

Here, the exponent, n_T, is the value corresponding to the polytropic efficiency assumed across the turbine. This expression can be written, with (102):

$$\frac{\dot{w}_T\sqrt{T_{t_o}}}{P_{t_o}}\sqrt{\frac{R}{g}} = \Phi_d A_{l_T}\frac{\left(P_{t_d}/P_{l_T}\right)^{\frac{n_T+1}{2n_T}}}{\left(P_{t_o}/P_{l_T}\right)^{\frac{n_T+1}{2n_T}}} = \Phi_b A_b + \Phi_\ell A_\ell + \Phi_s A_s\,\frac{P_a}{P_{t_o}}\sqrt{\frac{T_{t_o}}{T_a}} \tag{105}$$

Then, introducing the right side of (101):

$$\frac{A_{l_T}}{\left(P_{t_o}/P_{l_T}\right)^{\frac{n_T+1}{2n_T}}}\left(\frac{P_{t_d}}{P_{l_T}}\right)^{\frac{n_T+1}{2n_T}}\sqrt{\frac{2\gamma}{\gamma-1}\left[\left(\frac{P_{l_T}}{P_{t_d}}\right)^{2/n_d}-\left(\frac{P_{l_T}}{P_{t_d}}\right)^{\frac{n_d+1}{n_d}}\right]} = \Phi_b A_b + \Phi_\ell A_\ell + \Phi_s A_s\,\frac{P_a}{P_{t_o}}\sqrt{\frac{T_{t_o}}{T_a}} \tag{106}$$

The form of this equation used in the analysis is obtained, after some rearrangement, as:

$$\left\{\frac{2\gamma}{\gamma-1}\left(\frac{P_{t_d}}{P_{l_T}}\right)^{\frac{n_T+1}{n_T}}\left[\left(\frac{P_{l_T}}{P_{t_d}}\right)^{\frac{2}{n_d}}-\left(\frac{P_{l_T}}{P_{t_d}}\right)^{\frac{n_d+1}{n_d}}\right]\right\}^{1/2} = \frac{1}{A_{l_T}}\left(\frac{P_{t_o}}{P_{l_T}}\right)^{\frac{n_T+1}{2n_T}}\left[\Phi_b A_b + \Phi_\ell A_\ell + \Phi_s A_s\,\frac{P_a}{P_{t_o}}\sqrt{\frac{T_{t_o}}{T_a}}\right] \tag{107}$$

In (107), there remain two unknowns: p_{l_T} and p_{t_d}. Hence, it is necessary to solve the equation by iteration, using desired values of p_{t_o} and T_{t_o}. Although two solutions of (107) exist, the supersonic solution is not of interest in the analysis and only the subsonic solution is obtained. With an assumed value of p_{l_T}, p_{t_d} is determined from (107), the condition and velocity of the fluid flowing to the exhauster from the hood are established from the relations:

$$T_{t_d} = T_{t_o}\left(\frac{P_{t_d}}{P_{t_o}}\right)^{\frac{n_T-1}{n_T}} \tag{108}$$

$$T_{1_T} = T_{t_d}\left(\frac{P_{1_T}}{P_{t_d}}\right)^{\frac{n_d-1}{n_d}} \tag{109}$$

$$V_{1_T} = \sqrt{2\,g\,J c_p\left(T_{t_d} - T_{1_T}\right)} \tag{110}$$

Eq. (96) with (91) gives the flow rate through the nozzle; with the asterisk denoting M = 1.0 at the throat:

$$\dot{w}_N = \Phi^*_N \frac{A^*_N P_{t_o}}{\sqrt{T_{t_o}}}\sqrt{\frac{g}{R}} = \left(\frac{2}{n^*_N+1}\right)^{\frac{1}{n^*_N-1}}\sqrt{\frac{2\gamma}{\gamma-1}\,\frac{n^*_N-1}{n^*_N+1}}\left(\frac{P_{t_o}}{\sqrt{T_{t_o}}}\sqrt{\frac{g}{R}}\right)A^*_N \tag{111}$$

Since the flow rate at the nozzle exit is the same as at the throat, for the exit, station 1_N, there is:

$$\frac{\dot{w}_N\sqrt{T_{t_o}}}{A_{1_N}P_{t_o}}\sqrt{\frac{R}{g}} = \Phi^*_N\frac{A^*_N}{A_{1_N}} = \sqrt{\frac{2\gamma}{\gamma-1}\left[\left(\frac{P_{1_N}}{P_{t_o}}\right)^{\frac{2}{n_N}} - \left(\frac{P_{1_N}}{P_{t_o}}\right)^{\frac{n_N+1}{n_N}}\right]} \tag{112}$$

Here, the exponent n_N is used to indicate that different polytropic efficiencies are assumed for flow to the throat and from the throat to the exit. Eq. (112) can be solved by iteration to find p_{1_N}. Although both a supersonic and subsonic solution of (112) exist, the subsonic solution was not considered, since the back pressure required for a shock at the exit is about 27 psia for an isentropic nozzle. With p_{1_N} determined, (109) and (110), written for the nozzle variables are solved to determine the temperature and velocity at station 1_N.

The momentum equation, written between stations one and two, is:

$$\frac{\dot{w}_N+\dot{w}_T}{g}V_2 - \frac{\dot{w}_N}{g}V_{1_N} - \frac{\dot{w}_T}{g}V_{1_T} = A_2(P_1 - P_2) - F_f \tag{113}$$

The friction force, F_f, can be expressed as a pressure loss:

$$F_f = \frac{\pi}{4}D_2^2\,\Delta p = A_2\,\Delta p \tag{114}$$

This pressure drop, in turn, can be written as:

$$\Delta p = f \frac{L}{D_2} \frac{\bar{\rho}}{2} \bar{V}^2 \tag{115}$$

Here, L is the duct length between the two stations, D_2 is the duct diameter, $\bar{V}$ and $\bar{\rho}$ are the average of the values of velocity and density at stations 1_T and two, and f is the friction factor. Conditions for the flow through the outer annulus at station one are used, because the pressure loss is considered to be caused primarily by the friction along the duct walls. The factor, f, depends on Reynolds Number and pipe roughness. The approximate range of Reynolds Numbers obtained from preliminary calculations was 1.7 to 2.2 (10^5); and, for a surface roughness of 0.00015 ft. for commercial steel pipe, a surface roughness to diameter ratio of 0.00024 was obtained. With these values, f = 0.017 was determined from the Moody Diagram given by Eschbach. [1]

Letting $p_{1_f} = p_1 - \Delta p$, (115) becomes:

$$\left(\frac{\dot{w}_N + \dot{w}_T}{g}\right) V_2 - \left(\frac{\dot{w}_N}{g}\right) V_{1_N} - \left(\frac{\dot{w}_T}{g}\right) V_{1_T} = A_2 (P_{1_f} - P_2) \tag{116}$$

The total temperature of the fluid stream after mixing is given by:

$$T_{t_2} = \frac{\dot{w}_N T_{t_o} + \dot{w}_T T_{t_d}}{\dot{w}} \; ; \quad \dot{w} = \dot{w}_N + \dot{w}_T \tag{117}$$

Then, from continuity, there is:

$$V_2 = \frac{\dot{w} R T_2}{P_2 A_2} = \frac{\dot{w} R}{P_2 A_2} \left(T_{t_2} - \frac{V_2^2}{2 g J c_p}\right) \tag{118}$$

Solving (118) for p_2 and, with (117):

$$P_2 = \frac{\dot{w} R}{A_2 V_2} \left(\frac{\dot{w}_T T_{t_d} + \dot{w}_N T_{t_o}}{\dot{w}} - \frac{V_2^2}{2 g J c_p} \right) \tag{119}$$

Next, combining (119) and (116) to eliminate p_2:

$$\frac{\dot{w}_N + \dot{w}_T}{g} V_2 - \frac{\dot{w}_N}{g} V_{1_N} - \frac{\dot{w}_T}{g} V_{1_T} = A_2 P_{1_f} - \frac{\dot{w} R}{V_2} \left(\frac{\dot{w}_T T_{t_d} + \dot{w}_N T_{t_o}}{\dot{w}} - \frac{V_2^2}{2 g J c_p} \right) \tag{120}$$

Multiplying (120) by V_2, expanding the last term, combining like terms and transposing, the form used is obtained:

$$V_2^2\left[\frac{\dot{w}_N+\dot{w}_T}{g}-\frac{\dot{w}R}{2gJc_p}\right]-V_2\left[\frac{\dot{w}_N}{g}V_{1_N}+\frac{\dot{w}_T}{g}V_{1_T}+A_2P_{1_f}\right]+\dot{w}RT_{t_2}=0 \tag{121}$$

Let:

$$B_1=\frac{\dot{w}}{g}\left(1-\frac{R}{2Jc_p}\right) \tag{122}$$

$$B_2=-\left[\frac{\dot{w}_N}{g}V_{1_N}+\frac{\dot{w}_T}{g}V_{1_T}+P_{1_f}A_2\right] \tag{123}$$

and:

$$B_3=\dot{w}RT_{t_2} \tag{124}$$

The solution of (121) is then:

$$V_2=-\frac{B_2}{2B_1}\pm\sqrt{\left(\frac{B_2}{2B_1}\right)^2-\frac{B_3}{B_1}} \tag{125}$$

This equation will yield both a subsonic and a supersonic solution. With the velocity, V_2, known, the fluid properties at station two are obtained from (119) and:

$$T_2=T_{t_2}-\frac{V_2^2}{2gJc_p} \tag{126}$$

$$P_{t_2}=P_2\left(\frac{T_{t_2}}{T_2}\right)^{\frac{\gamma}{\gamma-1}} \tag{127}$$

For the subsonic solution of (125), the fluid is compressed in the diverging portion of the exhauster and (93) applies as:

$$\frac{\dot{w}\sqrt{T_2}}{A_3P_2}\sqrt{\frac{R}{g}}=\Phi_3=\sqrt{\frac{2\gamma}{\gamma-1}\left[\frac{T_{t_2}}{T_2}\left(\frac{P_3}{P_2}\right)^{\frac{2}{n_c}}-\left(\frac{P_3}{P_2}\right)^{\frac{n_c+1}{n_c}}\right]} \tag{128}$$

This equation is solved by iteration to determine p_3. Since the flow must adjust to atmospheric pressure at the exit plane of the diverging portion, if the value of p_3 obtained does not equal atmospheric pressure, the value assumed for p_{1_T} is in error. For $p_3 < p_a$, a higher value of p_{1_T} is assumed

and for $p_3 > p_a$, a lower value is taken. Iteration is then continued until the value of p_{1T} for which $p_3 = p_a$ is found. Values of fluid properties and the velocity at station three are then determined from:

$$T_3 = T_2 \left(\frac{P_3}{P_2}\right)^{\frac{n_c - 1}{n_c}} \tag{129}$$

$$V_3 = \sqrt{2 g J c_p (T_{t_2} - T_3)} \tag{130}$$

$$P_{t_3} = P_3 \left(\frac{T_{t_2}}{T_3}\right)^{\frac{\gamma}{\gamma - 1}} \tag{131}$$

The supersonic solution of (125) gives the velocity at station two. The temperature is obtained from (126), the pressure from (119), and the total pressure from (127). Knowing these properties, the location of a normal shock can be estimated. The possibilities which must be considered in the one-dimensional analysis are:

1. a normal shock at the inlet to the diverging portion, followed by subsonic compression;

2. supersonic expansion from the inlet to the diverging portion to some axial distance, X, downstream, with a normal shock at that point and subsequent subsonic compression; and

3. supersonic expansion to the exit plane of the diverging portion, followed by an oblique shock outside the exhauster.

Not listed in the above are supersonic expansion to an exit pressure either equal to or less than the full expansion pressure. In the analysis, this consideration is not of practical interest; however, consideration of these possibilities is included in the solution procedure for completeness.

Since the flow must adjust to ambient pressure, possibility (1.) is checked first, because it provides maximum pressure recovery. If the resulting value of p_3 is less than p_a, there can be no normal shock from

station two downstream. Then, any shock would have to be between stations one and two. Due to the assumption of uniform properties at station two -- necessary for application of the momentum equation between stations one and two, where mixing is assumed complete--no definitive information can be obtained regarding shock location upstream of station two. It is worth noting that should mixing be completed prior to the assumed station two, the pressure recovery would be less than that for the situation considered in the analysis. For the purposes of this analysis, then, the supersonic solution was considered non-existent if possibility (1.) did not provide sufficient pressure recovery.

The well-known normal shock relations, written for a shock at station two are:

$$\frac{P_\ell}{P_2} = \frac{2\gamma M_2^2 - (\gamma - 1)}{\gamma + 1} \tag{132}$$

$$\frac{T_\ell}{T_2} = \frac{\left(1 + \frac{\gamma-1}{2} M_2^2\right)\left(\frac{2\gamma}{\gamma-1} M_2^2 - 1\right)}{\left(\frac{\gamma+1}{2}\ \frac{\gamma+1}{\gamma-1} M_2^2\right)} \tag{133}$$

$$M_\ell^2 = \frac{M_2^2 + \frac{2}{\gamma-1}}{\frac{2\gamma}{\gamma-1} M_2^2 - 1} \tag{134}$$

$$\frac{P_{t_\ell}}{P_{t_2}} = \frac{\left(\frac{\gamma+1}{2} M_2^2\right)^{\frac{\gamma}{\gamma-1}}}{\left(\frac{\gamma-1}{2} M_2^2 + 1\right)^{\frac{\gamma}{\gamma-1}}} \left(\frac{2\gamma M_2^2 - (\gamma-1)}{\gamma+1}\right)^{-\frac{1}{\gamma-1}} \tag{135}$$

$$\frac{P_{t_\ell}}{P_2} = \left(\frac{\gamma+1}{2} M_2^2\right)^{\frac{\gamma}{\gamma-1}} \left(\frac{2\gamma M_2^2 - (\gamma-1)}{\gamma+1}\right)^{-\frac{1}{\gamma-1}} \tag{136}$$

Here, the subscripts, '2' and 'ℓ', refer to upstream and downstream of the shock respectively. For subsonic compression after the shock at two, there is:

$$\frac{\dot{w}\sqrt{T_\ell}}{A_3 P_\ell}\sqrt{\frac{R}{g}} = \Phi_3 = \sqrt{\frac{2\gamma}{\gamma-1}\left[\frac{T_{t_2}}{T_\ell}\left(\frac{P_3}{P_\ell}\right)^{\frac{2}{n_c}} - \left(\frac{P_3}{P_\ell}\right)^{\frac{n_c+1}{n_c}}\right]} \tag{137}$$

Again, this equation must be solved by iteration to yield p_3 and the value obtained is compared with atmospheric pressure. As noted above, the solution--no shock from station two downstream--is known if $p_3 < p_a$. If $p_3 = p_a$, the solution is known and the properties of the fluid at station three are determined from (129) - (131), with appropriate subscripts.

For $p_3 > p_a$ obtained from the shock-at-station-two-check, the next check made is for conditions in the exit plane with supersonic expansion to that station. The expansion equation is written as:

$$\frac{\dot{w}\sqrt{T_{t_2}}}{A_3 P_{t_2'}}\sqrt{\frac{R}{g}} = \Phi_3 = \sqrt{\frac{2\gamma}{\gamma-1}\left[\left(\frac{P_3}{P_{t_2'}}\right)^{\frac{2}{n_e}} - \left(\frac{P_3}{P_{t_2'}}\right)^{\frac{n_e+1}{n_e}}\right]} \tag{138}$$

Here, $p_{t_2'}$ is a fictitious stagnation pressure determined for stagnation conditions which would exist for a converging-diverging nozzle with a Mach Number, M_2, at the point where the area is A_2. Then:

$$P_{t_2'} = P_2\left(\frac{T_{t_2}}{T_2}\right)^{\frac{n_e}{n_e-1}} \tag{139}$$

With p_3 determined from iteration of (138), T_3 is obtained from (109), V_3 from (110), written with appropriate subscripts, and stagnation pressure from:

$$P_{t_3} = P_3\left(\frac{T_{t_2}}{T_3}\right)^{\frac{\gamma}{\gamma-1}} \tag{140}$$

Also, there is:

$$M_3 = \frac{V_3}{\sqrt{\gamma g R T_3}} \tag{141}$$

The value of p_3 obtained corresponds to the value for full expansion. If $p_3 = p_a$, the solution is known and the properties and velocity have been obtained. If $p_3 > p_a$, the flow is underexpanded and the flow adjustment required takes place outside the exit plane in the form of a Prandtl-Meyer expansion. In this instance also, the solution is known and the properties

at the exit are taken as those for full expansion, with comment that the noted expansion occurs. For $p_3 < p_a$, the practical consideration, two possibilities must be considered: an oblique shock at the exit; and a shock in the diverging portion. The highest pressure for occurrence of an oblique shock at the exit, p_{ℓ_3} is obtained from (132), with the upstream Mach Number equal to that for full expansion. If the pressure downstream of the shock is less than or equal to p_a, the solution is known as a shock at the exit. Exit conditions are then taken as those for full expansion, but with comment that an oblique shock occurs outside the exit plane.

If $p_{\ell_3} < p_a$, it is necessary to determine the location of the normal shock in the diverging portion. The process of solution is one of iteration, using supersonic expansion to an assumed distance X from station two, followed by a normal shock and subsequent compression. All equations required have been given previously, except the one used to determine the area at 'X'. From the geometry of the diverging portion there is:

$$A_u = \pi r_u^2 = \pi \left[r_2 + \frac{X}{L}(r_3 - r_2) \right]^2 \qquad (142)$$

The iteration, using (138), (132) - (136) and (137) in that order, and with appropriate subscripts, is continued until the distance X is found such that $p_3 = p_a$. Exit plane conditions are then determined using (129) - (131), with the subscript 'ℓ' substituted for two.

Computer Program

Program EJECTOR, included in Appendix IV, performs the analysis described in the foregoing paragraphs in the manner and in the order given. Inputs to the program are the values of polytropic efficiencies assumed, the number of different inlet conditions for which solution is desired, and the sets of values of inlet total temperature (°R) and total

pressure (psia). The program obtains the subsonic and supersonic solutions for both stator profiles (i.e., the converging and the converging-diverging nozzle types) for each set of inlet conditions. The several subroutines are listed below in the order called, and the function of each is given.

1. NOZZLE. This subroutine determines the conditions at the exit of the exhauster nozzle by iteration, using (111), (112), (109) and (110).

2. TURBINE. For an assumed value of pressure at station 1_T for the flow from the turbine hood, this subroutine solves (107) for p_{t_d} by iteration, using also (98), (99) and (100) to determine required flow rates (or, flow functions, Φ). Eq. (97) is used to find the total flow rate from the turbine hood to the exhauster piping.

3. MMENTUM. Eq. (125) is solved in this subroutine for the subsonic conditions at station two. In order to get values of velocity and density at this station, for use in determining average velocity and density required for calculation of the pressure loss, (125) is solved for zero friction. Pressure loss is then determined using (115), and (125) is again solved for the new value of p_{1_f}. Eqs. (117), (119), (126) and (127) then yield the additional properties at station two.

4. SUBCOMP. This subroutine solves (128) to determine exit pressure. The main program contains the required check for $p_3 = p_a$, assumes a new value of p_{1_T} as required, and again calls TURBINE, MMENTUM AND SUBCOMP. This sequence of events continues until the required condition is met. The subsonic conditions at station three are then determined from (129) - (131).

5. MMENTUM. After the subsonic solution is known, this subroutine is again called and the supersonic solution at station two is determined.

6. SHOCK. This subroutine solves the shock equations for the supersonic solution properties at station two--(132) - (136).

7. SUBCOMP. This subroutine is again called for the properties determined by SHOCK and the pressure, p_3, is determined. If $p_3 < p_a$, the solution is known as no shock at station two or in the diverging portion. If $p_3 = p_a$, the solution is known also and the conditions at station three are those given by (129) - (131). In the event that $p_3 > p_a$, the program proceeds through the subsequent steps.

8. SUPEXP. Using the MMENTUM solution conditions at station two, this subroutine determines conditions at station three for full expansion, using (139), (138), (109), (110), (140) and (141). The main program then checks for $p_3 = p_a$. If the equality is satisfied, or if $p_3 > p_a$, the solution is known as full expansion or under-expansion and the exit plane conditions are taken as those for full expansion. The output includes a Hollerith print of the condition found to identify the type solution obtained, i.e., either full or under-expansion. For $p_3 < p_a$, the subsequent steps are taken.

9. SHOCK. To determine the maximum back pressure for a shock at the exit plane, this subroutine is again called for the conditions found for full expansion to station three. The main program then checks post-shock pressure against ambient pressure. The solution is known as an oblique shock at the exit if this post-shock pressure is equal to or greater than ambient pressure. Such solution is specified by a Hollerith statement and the exit plane conditions are taken as those upstream of the shock. If the post-shock pressure is less than p_a, the program continues with the following calls.

10. SUPEXP. This subroutine is called for an assumed shock location, X, and with an area given by (142), to determine conditions for supersonic expansion to that location.

11. SHOCK. Conditions downstream, for a shock at X, are determined.

12. SUBCOMP. This subroutine is called next to find the exit plane pressure for the conditions downstream of the shock at X. Comparison of this pressure with ambient pressure is accomplished in the main program as before. If $p_3 = p_a$, the solution is known, the shock occurs at X, and conditions at station three are given by (129) - (131). If $p_3 > p_a$, the distance X is increased and if $p_3 < p_a$, the distance assumed is decreased. Iteration varying X continues until the required equality is obtained.

It must be noted that subroutine NOZZLE is called only once in the above series of steps. Hence, it is tacitly assumed that any slight expansion or shock at the exit plane of the nozzle is insignificant. Additionally, the pressure at station one is assumed constant and equal to the pressure for the flow from the turbine hood, since this pressure is used in the solution of the momentum equation.

Results and Discussion

Solutions of the exhauster analysis were obtained for inlet total pressures from 44 through 36 psia in two psia increments, and inlet total temperature was varied between 660 and 760°R in 25° steps for each value of inlet total pressure. The values of polytropic efficiencies assumed are: for the turbine, $\eta_T = 0.75$; from the turbine hood to station 1_T, $\eta_d = 0.925$; for flow to the nozzle throat, $\eta_N^* = 0.975$; from the nozzle throat to the nozzle exit, $\eta_N = 0.9$; for supersonic expansion in the diverging portion, $\eta_e = 0.8$; and for subsonic compression in the diverging portion, $\eta_c = 0.7$.

Results of the analysis showed process pressures to be essentially independent of inlet total temperature. Of primary interest is the variation of total to total pressure ratio across the turbine with inlet total pressure. Such variation for both the converging and the converging-diverging nozzle stator profiles is shown in Fig. 32.

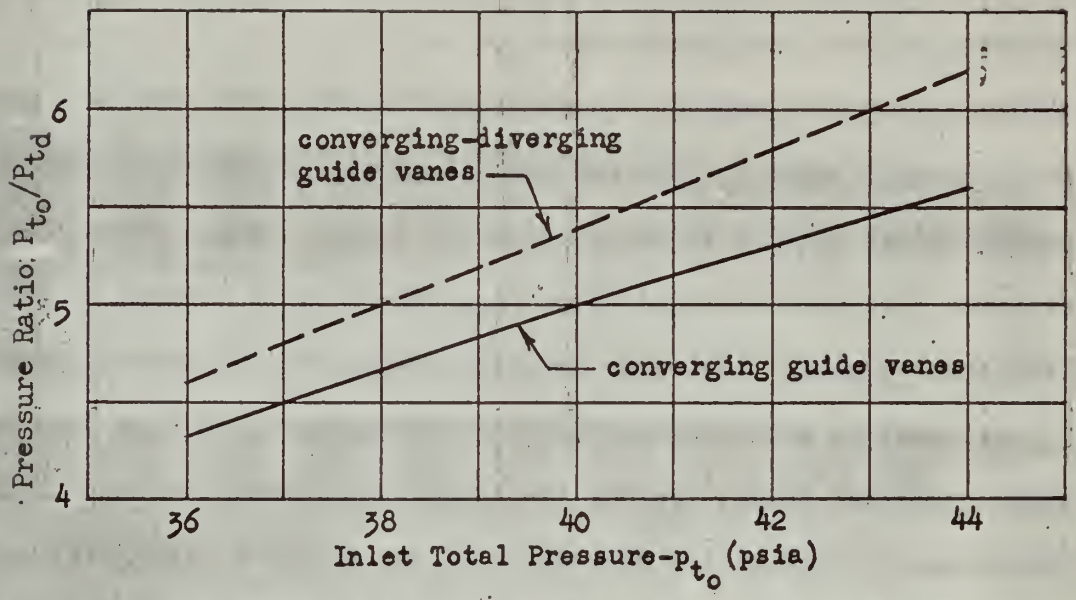

VARIATION OF TURBINE TOTAL TO TOTAL PRESSURE RATIO WITH INLET TOTAL PRESSURE-EXHAUSTER ANALYSIS

FIGURE 32

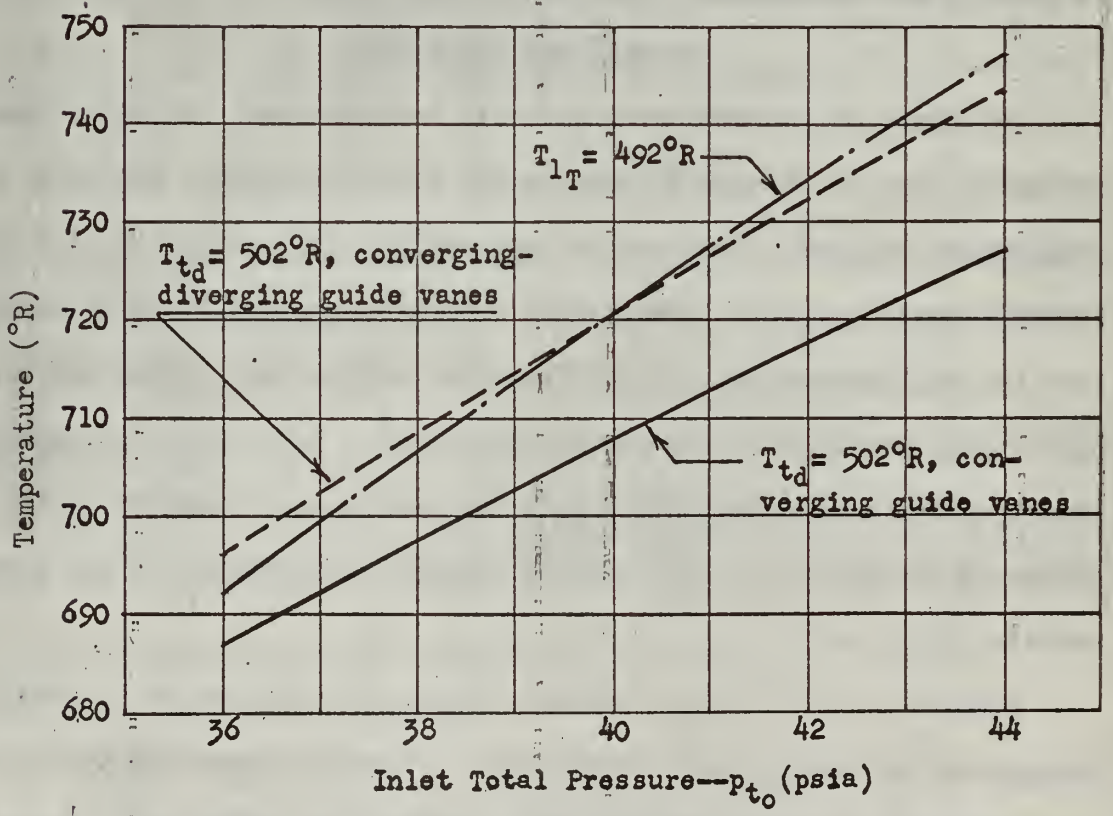

VARIATION OF TURBINE INLET TOTAL TEMPERATURE REQUIRED TO MAINTAIN SPECIFIED OUTLET TEMPERATURES WITH INLET TOTAL PRESSURE-EXHAUSTER ANALYSIS

FIGURE 33

Values of velocities and temperatures given by the analysis varied with both inlet total pressure and total temperature. However, values of supersonic Mach Numbers obtained for station two, the inlet to the diverging portion, were independent of inlet total temperature. Pressure in the exit plane for a shock at station two (maximum pressure recovery) was also independent of inlet total temperature. Maximum values of p_3 of 13.88 and 13.83 psia for the converging and converging-diverging guide vanes, respectively, were obtained for the maximum inlet total pressure of 44 psia . Hence, the analysis performed indicates that any shock adjustment will occur in the constant area duct upstream of station two. This result would seem to substantiate the expectations from general two-dimensional considerations that a series of oblique shocks followed by a normal shock will occur in the duct.

Values of referred flow rates, $\dot{w}\sqrt{\theta}/\delta$, obtained from the analysis were: 3.535 lbm/sec through the nozzle; 1.438 lbm/sec through the turbine for the converging guide vanes; and 1.022 lbm/sec through the turbine for the converging-diverging guide vanes. The totals for the two types of guide vanes, in the order given above, are 4.973 and 4.557 lbm/sec.

Although at present an upper limit of 660°R exists for turbine inlet total temperature, during future tests with the exhauster operating it may be found desirable to increase that limit to prevent undue condensation and/or freezing in the turbine discharge flow. Consequently, provided in Fig. 33 are curves of minimum inlet total temperatures required to maintain turbine hood temperature ten degrees above freezing and to maintain turbine hood flow temperature at the nozzle exit plane at 492°R. These values are plotted versus inlet total pressure. The curve for $T_{l_T} = 32°F$ is common to both sets of inlet guide vanes.

5. Determination of Flow Rates.

General

In Section 2, the several required flow rates were enumerated. In addition, the method for determining the flow rate through the exhauster nozzle was specified (see p. 21). To estimate this flow rate, (111) given in the preceding section can be used. In this section, the equations for use in determining the flow rates through the flow measurement nozzle, the plenum labyrinth seals and the shaft labyrinth seals are developed. Equations developed for the flow nozzle and plenum labyrinth leak rates are based on experiments, but the equation for shaft leakage provides flow rate estimation only.

Test Procedures

The configuration for flow nozzle calibration tests is indicated in Fig. 1, p. 21. The removable standard orifice assembly was installed, the outlet from tank number two to the turbine and the two-inch pipe were blocked, and the valve for controlling the flow to the exhauster nozzle was closed. The standard square-edged orifice of the removable assembly is fitted with both vena-contracta and flange taps. Upstream pressures were measured against atmospheric reference in inches of mercury, while differential pressures were measured in inches of water using a portable manometer with a range of 70 in., and with 0.1 in. graduations. Flow nozzle instrumentation is shown in Fig. 3, p. 24. The accuracy of pressures and differential pressures was taken as $\pm$ 0.03 in. and the accuracy of temperature measurements was assumed to be $\pm 1.0^{\circ}R$.

Flow nozzle calibration tests were made at essentially constant supply pressures of either 30 or 45 psia. Flow rate was controlled by using the valve at the exit of the removable standard orifice piping to set the differential pressure accross the vena-contracta taps. Supply

pressure was maintained by adjusting the main discharge valve of the compressor installation. Differential pressure was increased in increments of ten inches of water for increasing flow rates to the maximum differential pressure obtainable, then decreased by five inches of water, followed by incremental reductions of ten inches of water to minimum flow. Approximate ranges of flow rates of the tests were 1.44 to 3.67 lbm/sec at 30 psia, and 1.8 to 4.6 lbm/sec at 45 psia.

Instrumentation of the two-inch pipe orifice, which is used for determining plenum labyrinth seal leak rates, is basically the same as that of the removable standard orifice assembly. Plenum labyrinth leak rate tests were made by varying the supply pressure (approximately) from 24 to 44 psia. Pressures were set by observing the turbine plenum reading. Supply pressure was varied in increments of about five inches of mercury for increasing pressure; then, after an initial reduction of 2.5 in.Hg from the maximum supply pressure, incremental decreases of five inches of mercury were used. Tests were made without the exhauster and associated piping installed. Hence, the maximum ratio of seal inlet total to static discharge pressure was limited to approximately 3.

Formula Development

The basic flow equation for a square-edged orifice or flow nozzle, in lbm/hr, is:[7]

$$\dot{W} = 359.1\, D_2^2\, \alpha\, K\, Y_1 \sqrt{\rho_1 h_w} \qquad (143)$$

Here:

D_2 = orifice diameter or nozzle throat diameter (in.).

α = coefficient of thermal expansion based on D_2^2 (dimensionless).

[7]Stearnes, R. F., et. al., Flow Measurement with Orifice Meters (New York: Van Nostrand Co., Inc., 1951) p. 6.

K = discharge coefficient (dimensionless).

Y_1 = expansion coefficient (dimensionless).

ρ_1 = fluid density at upstream tap (lbm/ft^3).

h_w = differential pressure across taps (in. H_2O).

The equation of state for an ideal gas is:

$$\rho_1 = \frac{P_1 (144)}{R T_1} \tag{144}$$

Here, p_1 is in psia, R = 53.35 ft-lb/lbm-°R, and T_1 is in °R. For p_1 in inches of mercury, (144) becomes:

$$\rho_1 = \frac{P_1 (0.4912)(144)}{(53.35) T_1} = 1.328 \frac{P_1}{T_1} \tag{144a}$$

Inserting (144a) in (143) and converting to lbm/sec:

$$\dot{w} = 0.115 D_2^2 \alpha K Y_1 \sqrt{\frac{P_1 h_w}{T_1}} \tag{145}$$

The coefficient, α, is determined from the linear coefficient of thermal expansion, α_ℓ. For D_2' = orifice diameter at elevated temperature:

$$\left(\frac{D_2'}{D_2}\right)^2 = \left[1 + \alpha_\ell (\Delta t)\right]^2 = 1 + 2\alpha_\ell (\Delta t) + (\Delta t)^2 \alpha_\ell^2 \tag{146}$$

Neglecting the higher order final term and letting $(D_2')^2 = \alpha D_2^2$:

$$\alpha D_2^2 = \left[1 + 2\alpha_\ell (\Delta t)\right] D_2^2 \tag{147}$$

From (147) it is evident that:

$$\alpha = 1 + 2\alpha_\ell (\Delta t) \tag{148}$$

For both standard orifices, made of type 304 stainless steel,

$\alpha = (9.5)10^{-6}\ °F^{-1}$, giving:

$$\alpha_o = 1 + 0.0019\left(\frac{t - 68}{100}\right) \tag{149}$$

(The value, 0.00193 was used in calculations.)[8] For the flow nozzle, made

[8] Ibid., p. 257.

of 2024-T4 aluminum, $\alpha = (12.6)\ 10^{-6}\ {}^{\circ}F^{-1}$, and:

$$\alpha_n = 1 + 0.00252\left(\frac{t-68}{100}\right) \tag{150}$$

The discharge coefficient, K, is dependent on the ratio of orifice or nozzle diameter to upstream pipe diameter (i.e., $\beta = D_2/D_1$), Reynolds Number based on D_2, and the type measuring taps used. To simplify computations for square-edged orifices, the following relation may be used:[9]

$$\frac{K}{(1 + A/R_e)} = \frac{K^*}{(1 + A/R_e^*)} \tag{151}$$

where:[10]

$$A = D_2(830 - 5000\beta + 9000\beta^2 - 4200\beta^3 + B) \tag{152}$$

with:

$$B = \frac{530}{\sqrt{D_1}} \qquad \text{for flange taps} \tag{153a}$$

$$B = \frac{530}{\sqrt{D_1}} - 100 \qquad \text{for vena-cont. taps} \tag{153b}$$

The Reynolds Number expression can be written: [11]

$$R_e = \frac{6.316\,\dot{W}}{D_2\,z'} \tag{154}$$

where z' is absolute viscosity in centipoises at flow temperature and pressure. For z' independent of pressure and assuming linear variation of z' in the temperature range from 50 to 300°F, there is:[12]

$$z = 100z' = 1.9 + 0.24\left(\frac{t}{100} - 1\right) \tag{155}$$

Putting (155) in (154), with $\dot{W} = 3600\dot{w}$, and defining, $X = R_e(10^{-6})$:

$$X = \frac{2.275\,\dot{w}}{D_2\,z} \tag{156}$$

[9] Ibid., p. 65. [10] Ibid., p. 212. [11] Ibid., p. 64. [12] Ibid., p. 335.

Let $\beta = 1 + A/R_e$. Then:

$$\beta = 1 + \frac{A(10^{-6})}{X} \tag{157}$$

Eq. (151) then becomes:

$$\frac{K}{\beta} = \frac{K^*}{\beta^*} \tag{158}$$

For flange taps, values of $K^* = K_\infty$, corresponding to $Re^* = \infty$, are tabulated.[13] Eq. (158) for flange taps is then:

$$K = \beta K_\infty \tag{158a}$$

For vena-contracta taps, this shortcut method is not authorized and values of K_∞ are not tabulated. With K tabulated as a function of Reynolds Number,[14] an iterative procedure using these variables is normally required, with flow rate, $\dot{w}$, as a third variable. However, by judicious choice of Re^*, and hence K^*, (148) becomes for vena-contracta taps:

$$K = \frac{\beta K^*}{\beta^*} \tag{158b}$$

For the removable standard orifice assembly, Re^* was chosen as (10^6), giving $K^* = 0.698$. For a Reynolds Number of $2(10^5)$, the value of K determined from (158b) differs by 0.114 percent from the tabulated value, while the range of Reynolds Numbers for tests was approximately $3.9(10^5)$ to $1.3(10^6)$. Similarly for the two-inch pipe square-edged orifice, Re^* was selected as (10^5), giving $K^* = 0.6103$. At a Reynolds Number of $5(10^4)$, the computed value of K differs from the tabulated value by about 0.1 percent, and at $Re = 2(10^5)$ the difference is about 0.13 percent. The range of Reynolds Numbers in the tests conducted to date was approximately $5(10^4)$ to $1.2(10^5)$. Tests yet to be conducted with the exhauster installed will

[13] Ibid., Table 19. [14] Ibid., Table 20.

be at somewhat higher Reynolds Numbers than $1.2(10^5)$. However, since it is anticipated that the labyrinth seal flow will become choked at pressure ratios (plenum total to seal discharge static) only slightly higher than 3:1, Re = $2(10^5)$ is considered a realistic upper limit.

The expansion factor, Y_1, compensates for compressibility in the flow through the orifice or nozzle and is defined as:[15]

$$Y_1 = 1.0 - (0.41 + 0.35\beta^4)\frac{\Delta P}{\gamma P_1} \tag{159}$$

Here, Δp and p_1 must be in consistent units, and γ is the specific heat ratio. For $\gamma = 1.4$, $\Delta p = h_w$ (in. H_2O), and $p_1 = P_1$ (in. Hg), this equation becomes:

$$Y_1 = 1.0 - \frac{0.41 + 0.35\beta^4}{(1.4)(13.59)}\frac{h_w}{P_1} \tag{160}$$

Eq. (145) can be written in the form:

$$\dot{w} = C\alpha\xi Y_1\sqrt{\frac{P_1 h_w}{T_1}} \tag{161}$$

Here, the constant, C, includes D_2^2 and either K_∞ , for flange taps, or K^*/ξ^*, for vena contracta taps. Values of C, along with values for A of (152), and the several constants in the expressions for Y_1 and X, were determined by using the CDC 1604 computer. Table III lists the values to be used for each standard orifice. In solving (161), it is necessary to assume initially that $\xi = 1$. With the resulting value of $\dot{w}$, X is determined from (156), and the required value of ξ is obtained from (157). Eq. (161) is then solved using this new value of ξ.

Since the object of the flow nozzle calibration was the determination of the discharge coefficient, K_n, (145) is written:

$$K_n = \frac{\dot{w}\sqrt{T_1}}{0.115\, D_2^2\, \alpha_n Y_1 \sqrt{P_1 h_w}} \tag{162}$$

[15] Ibid., p. 71.

TABLE III

FLOW EQUATION CONSTANTS - SQUARE-EDGED ORIFICES
TRANSONIC TURBINE TEST RIG

Orifice Installation	$\beta = \frac{D_2}{D_1}$	Flange Taps		Vena Cont Taps		C_x	C_y
		C	A	C	A		
		EQ(161)	EQ(152)	EQ(161)	EQ(152)	EQ(156)	EQ(160
Removable	0.6995	1.4257	0.00218	1.4405	0.001756	0.5359	0.026
2" pipe	0.3991	0.0476	0.000305	0.04761	0.0002249	2.7561	0.022

EQUATIONS

(161) $$\dot{w} = C \alpha \xi Y_1 \sqrt{\frac{P_1 h_w}{T_1}}$$

(152) $$A = D_2(830 - 5000\beta + 9000\beta^2 - 4200\beta^3 + B)$$

(156) $$X = \frac{(6.316)(3600)\, 10^{-4}\, \dot{w}}{D_2 Z} = C_x \frac{\dot{w}}{Z}$$

(160) $$Y_1 = 1.0 - \left[\frac{0.41 + 0.35\beta^4}{(1.4)(13.59)}\right] \frac{h_w}{P_1} = 1.0 - C_y \frac{h_w}{P_1}$$

(155) $$Z = 1.9 + 0.24 \left[\frac{t}{100} - 1\right]$$

(149) $$\alpha = 1.0 + 0.00193 \left[\frac{t - 68}{100}\right]$$

(157) $$\xi = 1.0 + \frac{A\,(10^{-6})}{X}$$

Then, with the flow rate, $\dot{w}$, determined from (161), α_n given by (150), and Y_1 by (159a), K_n is found from (162).

The basic method used for estimating leak rates through labyrinth seals is that developed by Egli. [7] The equation of continuity combined with the energy equation for an ideal labyrinth seal (i.e., all kinetic energy is destroyed after each throttling) is:

$$\dot{w} = \alpha \varphi \frac{A P_{t_o}}{\sqrt{T_{t_o}}} \sqrt{\frac{g}{R}} \tag{163}$$

where:

$$\varphi = \left[\frac{1 - (P/P_{t_o})^2}{n + \frac{2}{\gamma} \ln (P_{t_o}/P)} \right]^{1/2} = \left[\frac{1 - r^2}{n + \frac{2}{\gamma} \ln (1/r)} \right]^{1/2} \tag{164}$$

α = discharge coefficient for a single throttling (dimensionless).

A = cross sectional area of seal passage (in^2).

p_{t_o} = total pressure at seal entrance (psia).

p = static pressure at seal discharge (psia).

T_{t_o} = total temperature at seal inlet (°R); T_{t_o} = constant across the seal for assumed adiabatic flow.

R = gas constant for air (ft-lb/lbm-°R)

n = number of throttlings.

r = overall seal pressure ratio (p/p_{t_o}).

To account for a non-ideal labyrinth seal, a velocity carryover factor, γ^*, is introduced to adjust for carryover of kinetic energy from one throttling to the next. Eq. (163) then becomes:

$$\dot{w} = \alpha \gamma^* \varphi \frac{A P_{t_o}}{\sqrt{T_{t_o}}} \sqrt{\frac{g}{R}} \tag{165}$$

For δ = tooth clearance, t = tooth width, and s = chamber width, (see Fig. 4, p. 25):

α = f(δ/t, n) = constant

f(δ/s, n) =

$\tau^* = f(\delta/s, n) = \text{constant}$

The dimensionless seal pressure ratio function, φ , was developed by series expansion with a lower limit of pressure ratio across any one throttling of 0.8. Since preliminary analysis of exhauster performance showed an overall pressure ratio across the shaft labyrinth seal of about 0.55, this assumption was considered valid for the ten throttlings of that seal. However, since plenum labyrinth seal leak rates were determined experimentally, use of (165) was limited in this instance to attempts to correlate experimental data with the method used and to determine whether test data for overall seal pressure ratios of 0.34 to 0.6 could be extrapolated to lower pressure ratios of 0.16 to 0.34. For the two identical labyrinths on either side of the plenum, (165) can be written, introducing the non-dimensional flow function, Φ :

$$\Phi_\ell = \frac{\dot{w}_\ell \sqrt{T_{t_o}}}{A_\ell P_{t_o}} \sqrt{\frac{R}{g}} = 2 K_\ell \varphi_\ell \qquad (166)$$

If α and τ^* are in fact constant, K = constant, and experimental data for higher values of r can be extrapolated to lower values of r. Since it is anticipated that the flow through the seal will be choked at $\varphi_{max} = 0.2798$ (r = 0.225), the range of extrapolation required would be relatively small.

The curves of α versus δ/t given by Egli [7] make determination of α for the geometry of the shaft seal somewhat uncertain. Consequently, the value of $\alpha = 0.76$ was taken from experimental data presented by Jerie, [8] where α is plotted as a function of δ/t and δ/b. Here, b = chamber heighth (see Fig. 4, p. 25). Plots of τ^* versus δ/s given by Egli are based on experimental data for $\delta > 0.01$ in. Egli's citation of Friedrich's tests of straight-through labyrinths with $\delta = 0.006$ to

0.01 in., and with two and three throttlings, indicates that somewhat smaller values of γ^* than those given by Egli would be proper for the geometry of the shaft seal of the TTTR. Considering also, ten rather than two or three throttlings, and data for multiple throttlings given by Jerie, Friedrich's value of 1.15 was selected for γ^* in preference to Egli's value of 1.25. With these values of α and γ^*, the final formula for estimating shaft seal leakage is, with $A = \pi\,(1.2)(0.005)$:

$$\dot{w}_s = 0.0128\,\frac{P_{t_o}}{\sqrt{T_{t_o}}}\,\varphi_s \tag{167}$$

Then, introducing the non-dimensional flow function, Φ :

$$\Phi_s = \frac{\dot{w}_s\sqrt{T_{t_o}}}{A_s\,P_{t_o}}\sqrt{\frac{R}{g}} = 0.874\,\varphi_s \;;\quad T_{t_o} = T_a\,,\quad P_{t_o} = P_a \tag{168}$$

Since $\varphi = f(r)$, the shaft seal leakage can be represented by a single plot of Φ versus overall seal pressure ratio, r. This plot is shown in Fig. 34.

Results

Since the tolerance for vena-contracta taps is less than that for flange taps, plotted and tabulated data included herein are vena-contracta values unless otherwise indicated.

Fig. 35 shows nozzle discharge coefficient, K_n, versus Reynolds Number as determined from tests of 8 September and 13 September 1965. It is evident from this plot that K_n can be taken as constant at Reynolds Numbers greater than about $6(10^5)$--($\dot{w} \cong 2$ lbm/sec). Values of K_n = constant were determined by the method of least squares for the following data groups: 8 September tests at 30 psia; 13 September tests at 30 psia; these two tests combined; 13 September tests at 45 psia; and all listed tests combined. Resulting minimum least-square-error values of K_n are tabulated in Table IV. In addition, values of K_n = constant for vena-

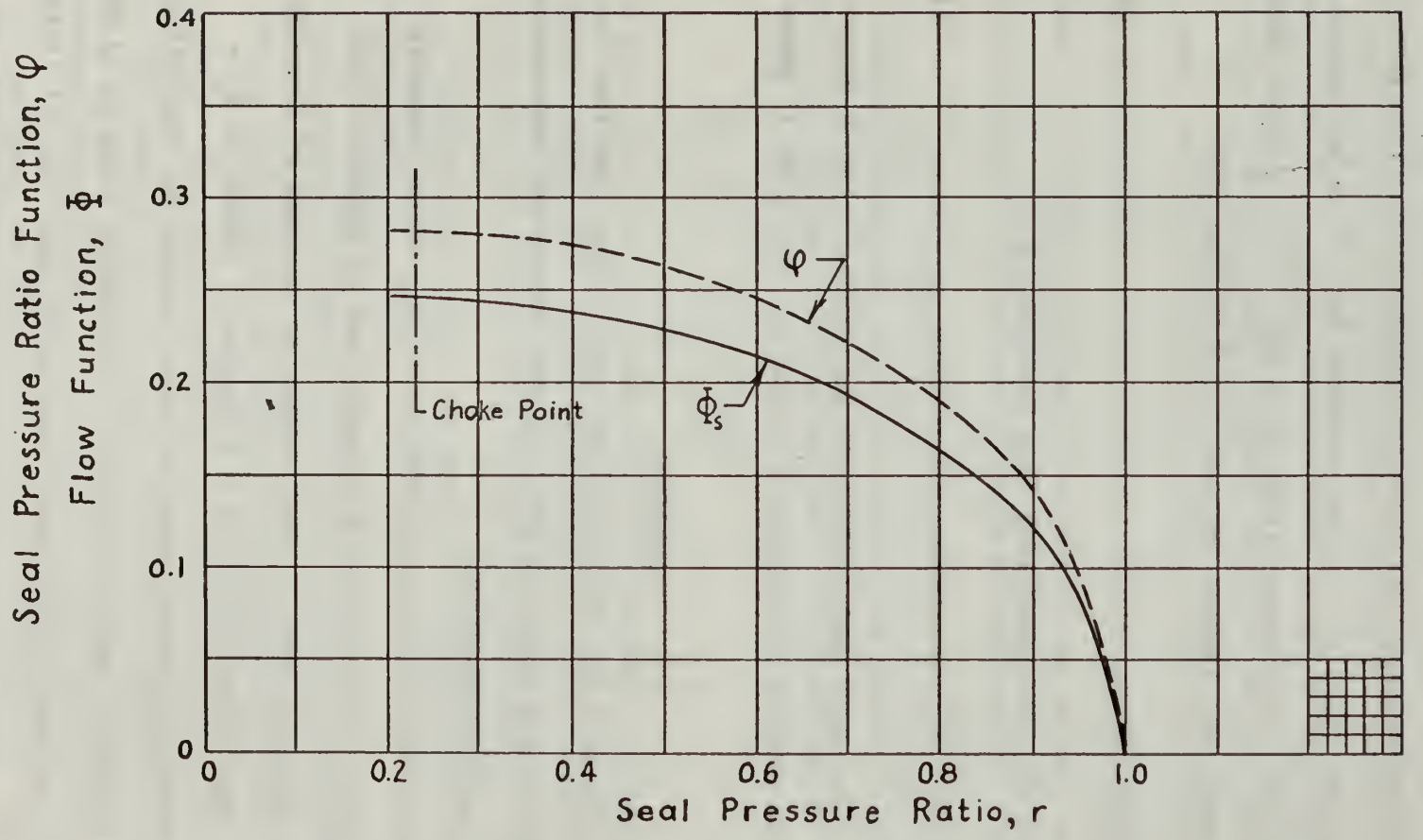

SHAFT SEAL FLOW FUNCTION

FIGURE 34

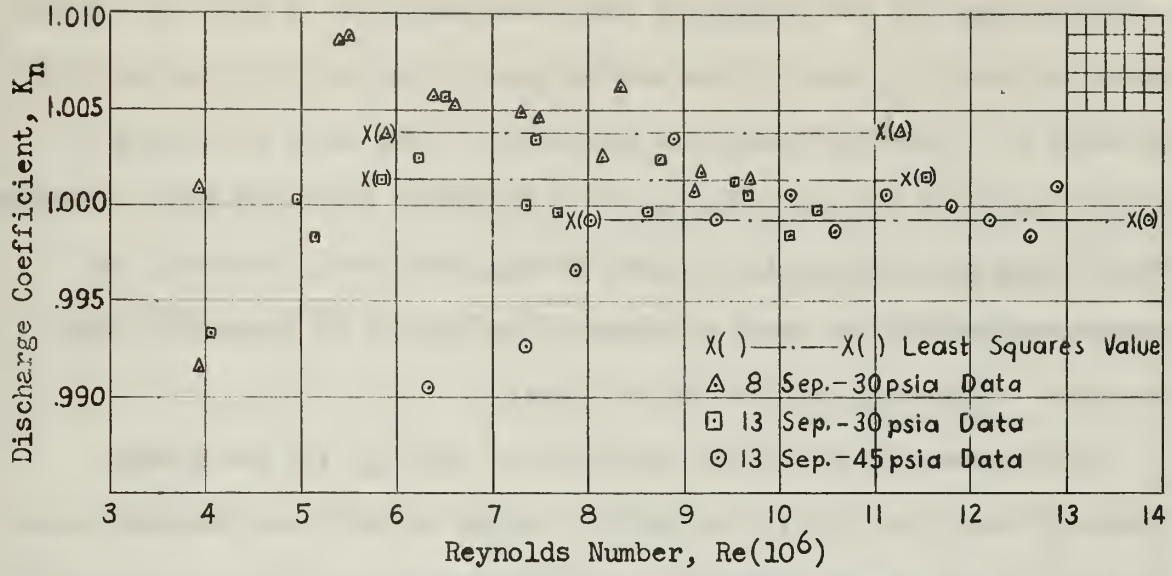

FLOW NOZZLE DISCHARGE COEFFICIENT

TRANSONIC TURBINE TEST RIG

FIGURE 35

TABLE IV

Flow Nozzle Discharge Coefficients

Transonic Turbine Test Rig

Test Date	Nominal Pressure	Data Points	Flange Taps		Vena Cont Taps	
			Error #	Kn	Error #	Kn
8 Sep	30 psia	9	.00828	.9994	.00599	1.0038
13 Sep	30 psia	12	.01055	1.0026	.00684	1.0012*
8/13 Sep	30 psia 30 psia	21 21	.01531	1.0012	.01071	1.0024
8/13 Sep	45 psia	12	.01614	1.0011	.01633	1.0012
13 Sep	45 psia	12	.00497	1.0008	.00864	.9992*

\# Error figures show least squares average difference of data points from Kn for minimum error

* Recommended values

contracta data for the individual tests are indicated in Fig. 35. Recommended values of K_n for 30 psia and 45 psia are indicated by an asterisk in Table IV. Some difficulty was encountered with water collecting in orifice pressure tap lines during the 8 September tests (30 psia). Although these lines were continually drained during such tests, the data are considered inferior to those obtained at 30 psia on 13 September, when the water collection problem did not exist.

Experimentally determined values of K_ℓ and $\bar{\Phi}_\ell$ for the plenum labyrinth seal (see (166)) are plotted versus overall seal pressure ratio in Figs. 36 and 37 respectively. It is apparent from Fig. 36 that extrapolation of K_ℓ to lower pressure ratios would be of questionable accuracy. Hence, subsequent tests with the exhauster operating will be required. To provide a mathematical expression for $\bar{\Phi}_\ell = f(r)$, the data plotted in Fig. 37 were fit with a parabola by the method of least squares. The general equation used in the curve fitting was:

$$r_\ell = a + b\bar{\Phi}_\ell + c\bar{\Phi}_\ell^2 \qquad (169)$$

In addition to experimental data, the known condition that at $r = 1.0$, $\bar{\Phi}_\ell = 0$, was introduced. Since all values of $\bar{\Phi}_\ell$ were of like sign (+), symmetry about the r axis was assumed by setting $b = 0$. The tests of 20 October 1965 showed considerable variation between values of K_ℓ and $\bar{\Phi}_\ell$ computed from data for increasing supply pressure and decreasing supply pressure. Consequently, especial care was taken to assure flow stabilization prior to recording data during the 26 October tests. Although the noted discrepancy was not eliminated, it was reduced materially. Hence, the 20 October, decreasing supply pressure values of $\bar{\Phi}_\ell$ (corresponding to K_ℓ points to the upper right in Fig. 36) were neglected in the curve fitting process. The resulting least-squares second order

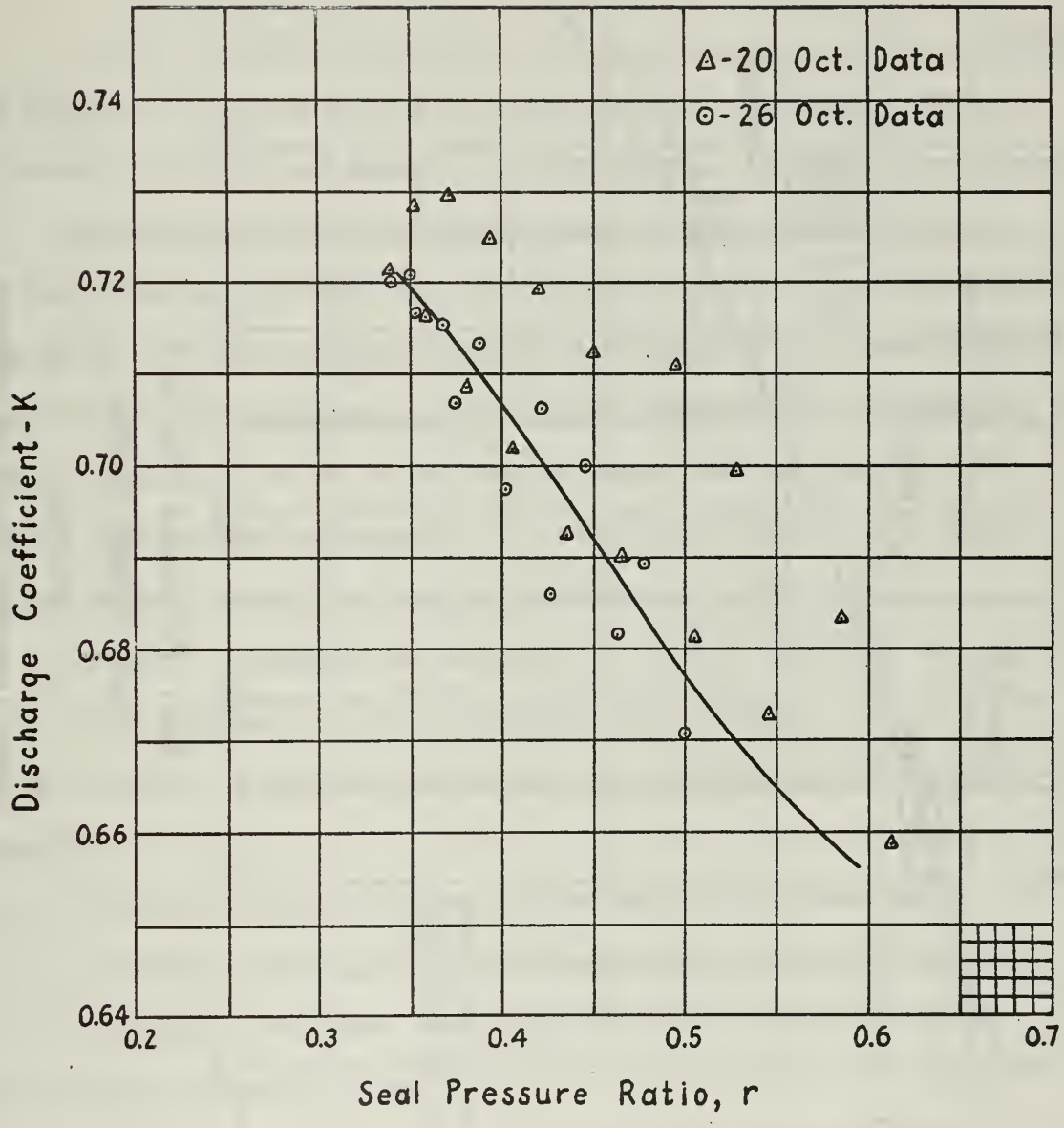

PLENUM LABYRINTH SEAL DISCHARGE COEFFICIENT

FIGURE 36

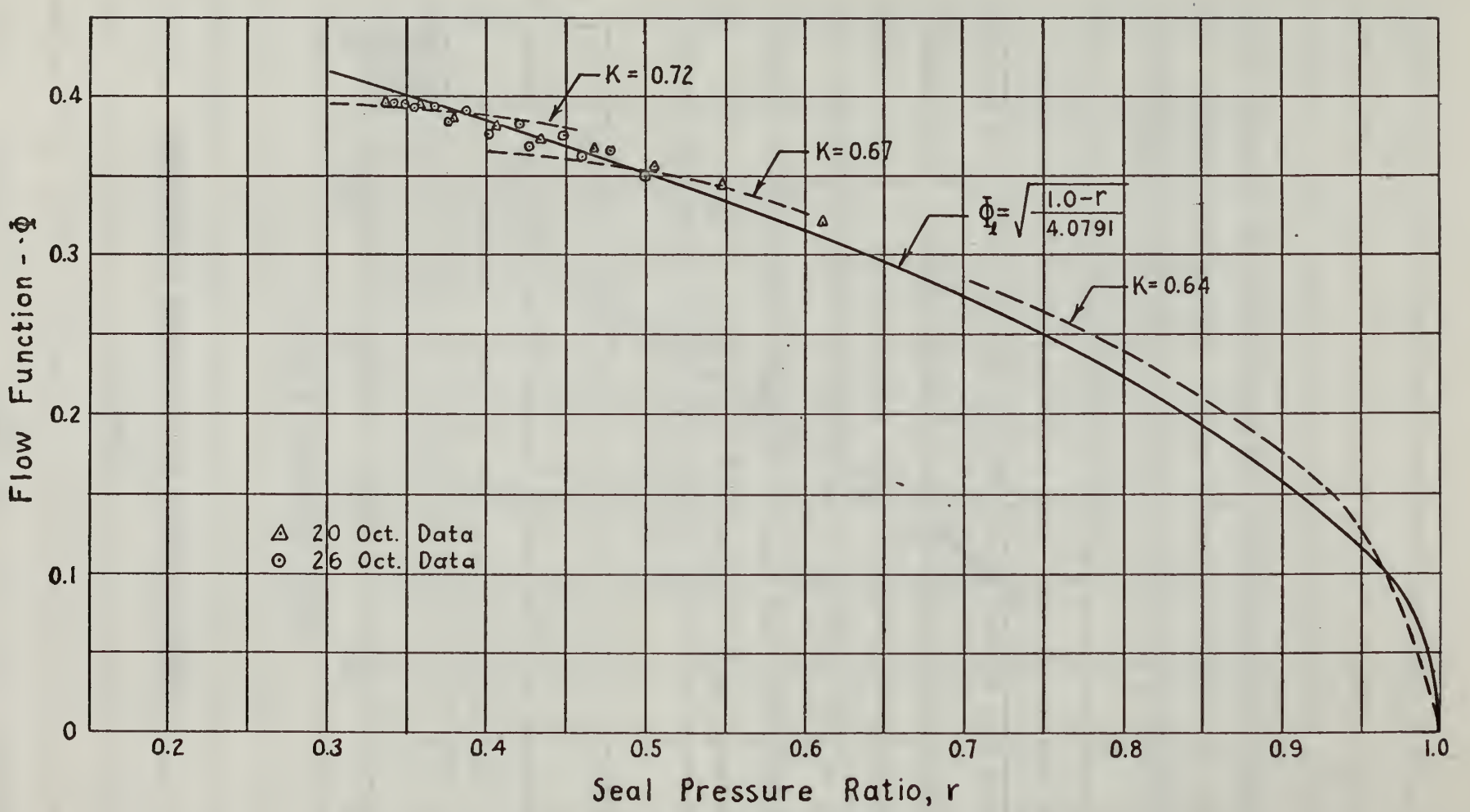

LEAST SQUARES PARABOLA

FOR THE

PLENUM LABRYINTH SEAL FLOW FUNCTION

FIGURE 37

polynomial obtained, for which the least squares error is 0.02079, is:

$$r_\ell = 1.0 - 4.0791\,\Phi_\ell^2 \tag{170}$$

Solved for the normally dependent variable, Φ_ℓ, (170) becomes:

$$\Phi_\ell = \sqrt{\frac{1.0 - r_\ell}{4.0791}} \tag{170a}$$

This equation is plotted in Fig. 37 along with the experimental data. Also shown in Fig. 37 are segments of three curves, $\Phi_\ell = 2K\varphi$, for values of K_ℓ appropriate to three different ranges of seal pressure ratio.

Data reduction required and the solution of (164) were accomplished by using the CDC 1604 computer. Listed below with their purposes described are the various programs used. The programs themselves are included in Appendix V, along with the description of inputs and outputs for each program. Since these programs use the equations of this section in a straight-forward manner, no detailed explanation is given.

1. ORIFICE. Computes the constant C of (161), the value of A of (152) and the constants in the expressions for Y_1 and X.

2. FLOCAL. Determines the values of K_n of (162), based on experimental data.

3. FLOCAL2. Finds the least squares value of K_n = constant.

4. LABRINT. Solves (164) for pressure ratios from 0.025 to 0.975.

5. LABLEAK. Determines flow rates and values of K_ℓ and Φ_ℓ of (166), using experimental data.

6. MINSQ2. Determines the least squares parabola for plenum labyrinth leakage (169).

Discussion and Recommendations

Based on the results of nozzle flow rate experiments conducted, it is recommended that a value of 0.9992 be used for the nozzle discharge coefficient in (145). However, for supply pressures of 30 psia or lower,

a value of 1.0012 would be more appropriate.

Eq. (170a) is recommended for determination of plenum labyrinth leak rates in the pressure ratio range: r = 0.03 to 1.0. Since plenum labyrinth leak rates (0.04 to 0.1 lbm/sec) are very much smaller than turbine flow rates (2.0 to 3.9 lbm/sec), the slight errors in leakage flow rates introduced by the use of this equation should have negligible effect on the accuracy of turbine flow rates. Furthermore, this equation should give satisfactory flow rates at pressure ratios, r, higher than those used in its generation.

For exhauster operation with a supply pressure of 45 psia to the exhauster nozzle and the turbine, the estimated shaft seal leak rate given by (167) is about 0.003 lbm/sec, while flow rates through the exhauster nozzle and the turbine are estimated as 9.38 and 3.87 lbm/sec, respectively. Using Egli's [7] values of discharge coefficient and carryover factor ($\alpha = 0.9$ and $\gamma^* = 1.25$), shaft seal leak rate estimates would be about 50 percent greater than estimates given by (167). However, plenum labyrinth leak rates predicted using values of α and γ^* determined from Egli are approximately 50 to 70 percent greater than the leak rates determine experimentally. Hence, (167) is recommended for predicting shaft seal leakage flow rates.

The recommended flow rate equations are given in Table V for ready reference.

Tolerance in Flow Measurement

The overall error tolerance in percent in flow measurements using square-edged orifices is given by the square root of the sum of the squares of "exponents times tolerances, in percent" ascribable to the individual items in the flow equation. Hence:[16]

[16] Ibid., p. 24.

TABLE V

SUMMARY OF FORMULAS FOR DETERMINING FLOW RATES
TRANSONIC TURBINE TEST RIG

Desired Flow Rate	Basic Formula	Auxiliary Formulas
Nozzle (lbm/sec)	$\dot{w} = 2.073 \alpha_n Y_1 \sqrt{\frac{P_1 h_w}{T_1}}$	$\alpha_n = 1.0 + 0.00252\left[\frac{t_1 - 68}{100}\right]$ $Y_1 = 1.0 - 0.023 \frac{h_w}{P_1}$
Plenum Labyrinth Seal Leak Rate (lbm/sec)	$\dot{w} = 0.116 \frac{\Phi_l P_{t_o}}{\sqrt{T_{t_o}}}$	$\Phi_l = \sqrt{\frac{1.0 - r}{4.0791}}$ $r = \frac{p}{p_{t_o}}$
Shaft Labyrinth Seal Leak Rate (lbm/sec)	$\dot{w} = 0.01466 \frac{\Phi_s P_{t_o}}{\sqrt{T_{t_o}}}$	$\Phi_s = 0.874\, \varphi$ $\varphi = \left[\frac{1.0 - r^2}{10 + \frac{2}{\gamma} \ln (1/r)}\right]^{1/2}$ $r = \frac{p}{p_{t_o}}$; $\gamma = \frac{c_p}{c_v}$

$$\Delta(\dot{w}) = \left\{ [2\Delta(D_2)]^2 + [\Delta(\alpha)]^2 + [\Delta(K)]^2 + [\Delta(Y_1)]^2 \right.$$
$$\left. + [\tfrac{1}{2}\Delta(h_w)]^2 + [\tfrac{1}{2}\Delta(P_1)]^2 + [\tfrac{1}{2}\Delta(T_1)]^2 \right\}^{1/2} \qquad (171)$$

Tolerances of the individual items for the Transonic Turbine Test Rig installation are given in Table VI.

The error in values of discharge coefficients of the flow nozzle and the square-edged orifice must be approximately the same. It follows that the tolerances in flow nozzle flow rate measurements must be the same as those for the square-edged orifice used in calibration. Hence, vena-contracta-based values are preferable, due to a lower error tolerance than that for flange taps.

Tolerances in measured labyrinth leakage rates also should be dependent on the tolerance of the calibration orifice. However, it is apparent from Fig. 35 that there is considerable scatter in the data. Hence a tolerance arbitrarily set at ± 10% would appear reasonable.

Error tolerances in estimated shaft seal leak rates are difficult to specify exactly. Here, a reasonable tolerance could be set at ± 20%, based on the qualifications set forth in the literature cited.

6. Calibration of the Force and Moment Measurement System

The axial force and moment about the turbine axis of the stator-plenum assembly are measured by Wiancko, two-arm, variable reluctance bridge force pickups using a phase shift frequency modulated oscillator. The linear range of the oscillator is from ten to 12kc. The permissible loadings of the two capsules are 50 lb. and 600 in-lb for the force and moment pickups, respectively.

Tests were conducted to establish the linearity conformance of the measurement systems and to determine whether or not cross-coupling exists between the two systems. In addition, readings of force and moment were

TABLE VI

PERCENT TOLERANCES OF FLOW EQUATION VARIABLES
AND PARAMETERS - SQUARE-EDGED ORIFICES
TRANSONIC TURBINE TEST RIG

a. Independent of the Orifice:

$\Delta(\alpha) = \pm 0.05$

$\Delta(Y_1) = 0 \text{ to } \pm 0.05$ for $0.0 < \frac{h_w}{P_1} < 0.015$

$= \pm 0.5 \text{ to } \pm 1.0$ for $0.015 < \frac{h_w}{P_1}$

$\Delta(h_w) = \frac{\pm 0.03}{h_w} (100)$

$\Delta(P_1) = \frac{\pm 0.03}{P_1} (100)$

$\Delta(T_1) = \frac{\pm 1.0}{T_1} (100)$

b. Removable Standard Orifice Assembly:

$\Delta(D_2) = \pm \frac{0.0005}{4.2425} (100) = \pm 0.0118$

$\Delta(K) = \pm 1.0$ for flange taps

$= \pm 0.4 \text{ to } \pm 0.6$ for vena contracta taps

c. Two-inch Pipe Orifice:

$\Delta(D_2) = \pm \frac{0.0005}{0.825} (100) = \pm 0.0606$

$\Delta(K) = \pm 1.0$ for flange taps

$= \pm 0.4 \text{ to } \pm 0.6$ for vena contracta taps

taken during plenum labyrinth leak tests to check for net force and/or moment due to the flow through the plenum labyrinth seals.

Fig. 38 shows schematically the configurations for the force and moment calibration tests. Standard weights were used to obtain known forces and moments. The following description of procedures applies to the force system; however, the same procedure is used for moment calibration, except that maximum load is 600 in-lb and increments of load are 100 in-lb rather than the corresponding values of 50 lb and 12.5 lb for force capsule calibration. The zero setting was obtained with no load as ten kc and, with the full load of 50 lb, the bandwidth was adjusted to set the reading at 12kc. Linearity was checked with one-half full load applied, with the desired reading as 11kc. If this reading was not obtained, the linearity was adjusted so that the new reading was different from 11kc by three times the original difference from 11kc, and in the same direction as that difference. The zero point, bandwidth and linearity were then adjusted in order repeatedly until the desired readings were obtained without further adjustment (i.e., ten, 12 and 11kc for zero, full and one-half loads, respectively). Starting with zero load, the force was increased in increments of 12.5 lb to the maximum load and then decreased by the same increments to zero load, with readings recorded for each load. The differences in readings for loading and unloading at each given force indicate the hysteresis (and non-linearity) of the system. The maximum departure observed for the force capsule was eight cycles per second (0.2 lb) at the one-half load point; maximum departure for the moment system was five cycles per second (1.5 in-lb).

Cross-coupling between the two systems was checked by applying a fixed load to one system and then applying various loads to the other, while watching for changes in reading of the former. Although it was

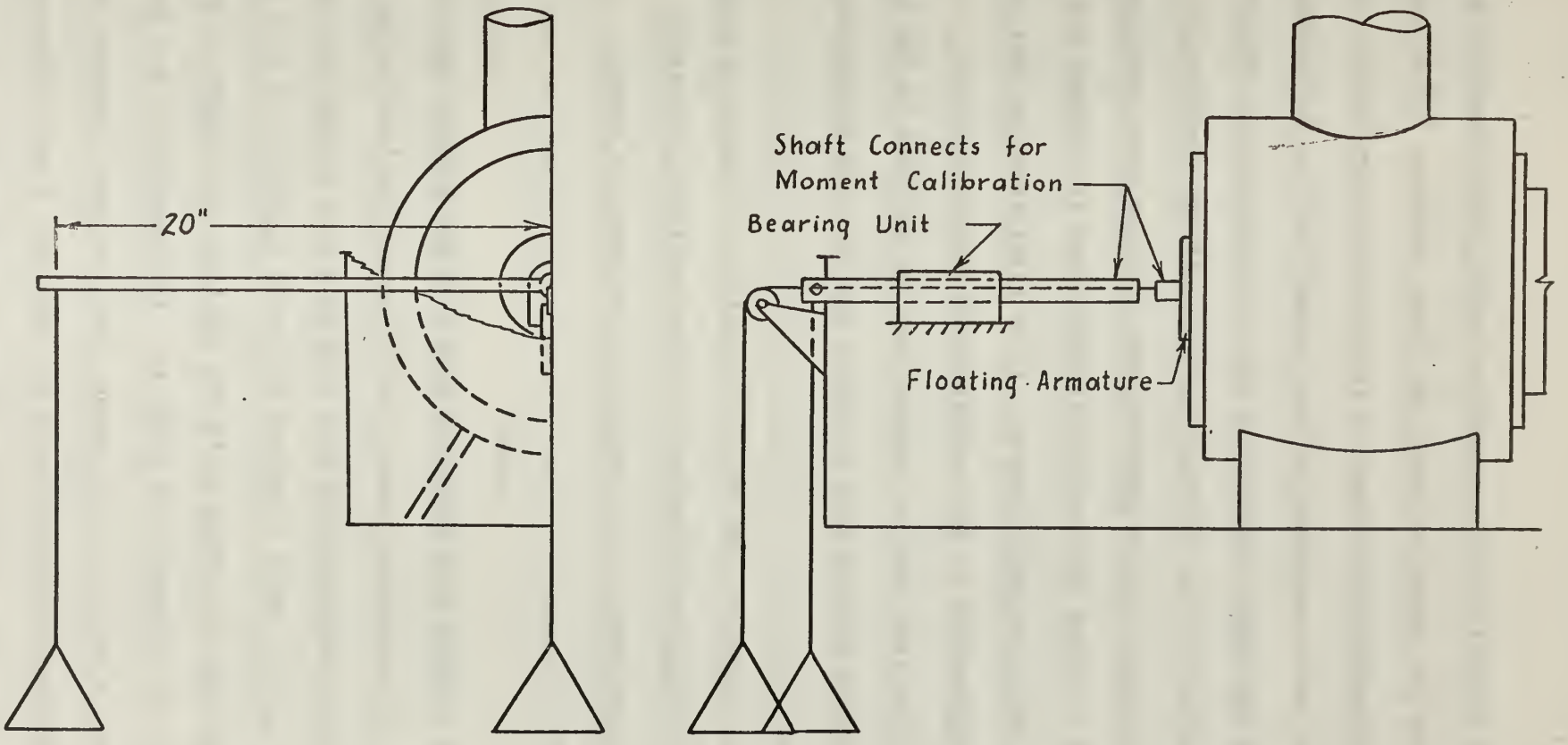

CONFIGURATION FOR CALIBRATION OF THE FORCE
AND MOMENT MEASUREMENT SYSTEMS

FIGURE 38

concluded that no significant cross-coupling exists, there remained some doubt as to whether the moment affected the force reading. The uncertainty arose because unpredictable changes in force reading were noted. These changes in reading were consistent neither in magnitude nor direction; also, by jiggling the moment calibration arm the reading could often be returned to the proper value. It was concluded that the variation of force readings was caused by the indeterminate friction force developed between the shaft to which the moment calibration arm is attached and the bearings through which the shaft passes. It is significant in this regard that full-load displacement of the capsules used is only 0.05 in. Pertinent also is the fact that no changes could be detected in the force reading while applying moments with a wrench, and with the aforementioned shaft disengaged.

During plenum labyrinth leak test, no significant changes in either force or moment readings were observed. It was concluded, therefore, that the flow through these seals produces no net force or moment.

6. Turbine Tests.

General

Tests of the turbine were conducted both with and without the rotor installed. Only the converging nozzle profile stator has been tested and tests with the rotor installed were done with this same stator and the full-size, uncut rotor. Axial clearance for tests conducted to date was 0.243 in. The gas path for these tests was the basic path shown in Fig. 10, p. 34. Rotor tip clearance was 0.025 in. Instrumentation for the tests was as shown in Fig. 6, p. 28, except that the total pressure probe line apparently became disengaged inside the machine. Hence, subsequent to the third rotational test, the total pressure upstream of the stator, p_{t_o}, was not measured. Values of p_{t_o} were determined by applying a

correction, based on previous runs, to the static pressure at the probe location, p_o. It bears repeating that the pressure on the downstream side of the cover plate inside the stator was measured during stator tests but not during tests with the rotor installed.

Prior to each test, the force and moment measurement systems were calibrated for proper readings at zero, full and one-half loads, as described in the preceding section. Also, prior to each test with the rotor installed, the rotor moment measuring system was calibrated for: minimum reading of zero at 50 in-lb; and maximum reading 100 at 700 in-lb. Then, the applied moment was increased from 50 to 700 and then decreased to 50 (in-lb). Readings obtained were plotted versus applied moment to yield the calibration curve. During all tests it was necessary to maintain a tare loading in the axial direction to keep force readings in the linear range.

During stator tests, inlet total pressure was varied from minimum values to the maximum achievable ahead of the stator, about 42.5 psia. Data were recorded at increments of supply pressure of about five inches of mercury.

Since it was planned to present turbine performance data in the form of curves for constant pressure ratio (total inlet to static discharge), for tests with the rotor installed the dynamometer was set initially for maximum power absorption. Supply pressure was increased until the value for the desired test pressure ratio was obtained. With desired pressure set, and with maximum power absorption, minimum RPM for the test pressure ratio resulted. Then, RPM was increased by reducing power absorption and data was obtained at desired values of RPM, while turbine inlet total pressure was maintained essentially constant. Inlet total temperatures were kept below 200°F, while the minimum inlet total temperature used--

computed in advance--was that value for a static temperature of 42°F at the rotor discharge.

Experience showed that supply air pressure and temperature and RPM each affected the others to a considerable extent. Hence, every effort was made to record RPM, rotor moment, stator force and moment, and the several pressures and temperatures as simultaneously as possible.

Data Reduction

The turbine flow rate is determined by subtracting the plenum labyrinth leak rate from the flow rate through the flow measurement nozzle. The former is obtained from (170a) and the latter from (145), with K_n, the nozzle discharge coefficient, equal to 0.9992.

As stated in Section 2, the instrumentation of the stator-plenum assembly was designed to permit use of the momentum and the moment of momentum equations to determine stator performance. In vector form, the general momentum equation, for the assumed steady flow, is:

$$\int_{s_1} d\dot{m}_1 \bar{V}_1 - \int_{s_e} d\dot{m}_e \bar{V}_e = \int_{s_1} -\bar{n}_1 p_1 ds_1 + \int_{s_e} -\bar{n}_e p_e ds_e + \bar{F} \qquad (172)$$

Similarly, the moment of momentum equation can be written:

$$\int_{s_1} \bar{r}_1 \times \bar{V}_1 \, d\dot{m}_1 - \int_{s_e} \bar{r}_e \times \bar{V}_e \, d\dot{m}_e = \int_{s_1} -\bar{r}_1 \times \bar{n}_1 p_1 ds_1 + \int_{s_e} -\bar{r}_e \times \bar{n}_e p_e ds_e + \bar{M} \qquad (173)$$

The integral term for shear forces between fluid particles in the exit plane of the stator has been omitted from each of these equations. Such forces act perpendicular to the turbine axis and would have no effect in the momentum equation for the axial direction. Also, their effects in the moment of momentum equation would be small, since the forces at either side of the between-blade flow channels oppose each other and should be nearly equal. In (172) and (173), the terms F and M represent the force and moment, respectively, exerted on the flow by the blades and walls, and

are due to pressure and shear forces.

The control volume used consists of the inner flow passages for the fluid, with openings at the inlet, station 'e', and at the stator exit, station one. Fig. 39 shows these stations, along with the several pressures, dimensions and forces pertinent to the reducing (172) and (173) to the forms used in data reduction. Fig. 6, p. 28, shows the stator-plenum assembly in more detail.

It is evident from Fig. 39 that integrals for the entrance station contribute no axial force, since the pressure acts perpendicular to the axial direction, and since the velocity of the fluid entering the control volume has no axial component; too, provided that the pressure and velocity at the inlet opening are symmetrical with respect to the turbine centerline, no net moment about the centerline acts on the flow at the inlet. Hence, the integrals containing pressure and velocity at the inlet reduce to zero in the equation for the moment of interest also. The expression for the axial force then becomes:

$$F_a = \dot{m} V_{a_1} + p_1 A_s \tag{174}$$

and that for the moment about the centerline reduces to:

$$M_a = \dot{m} r_{m_1} V_{u_1} \tag{175}$$

Here, V_{a_1} and V_{u_1} are the values at the mean radius, r_{1_m}.

The force and moment pickups, affixed as shown in Fig. 39, measure the reaction force and moment acting on the stator-plenum assembly. Hence, these pickups measure the negative of F_a and M_a. Letting R_i and M_i denote the reaction force and moment, (174) and (175) become:

$$R_i = -\dot{m} V_{a_1} - p_1 A_s \tag{176}$$

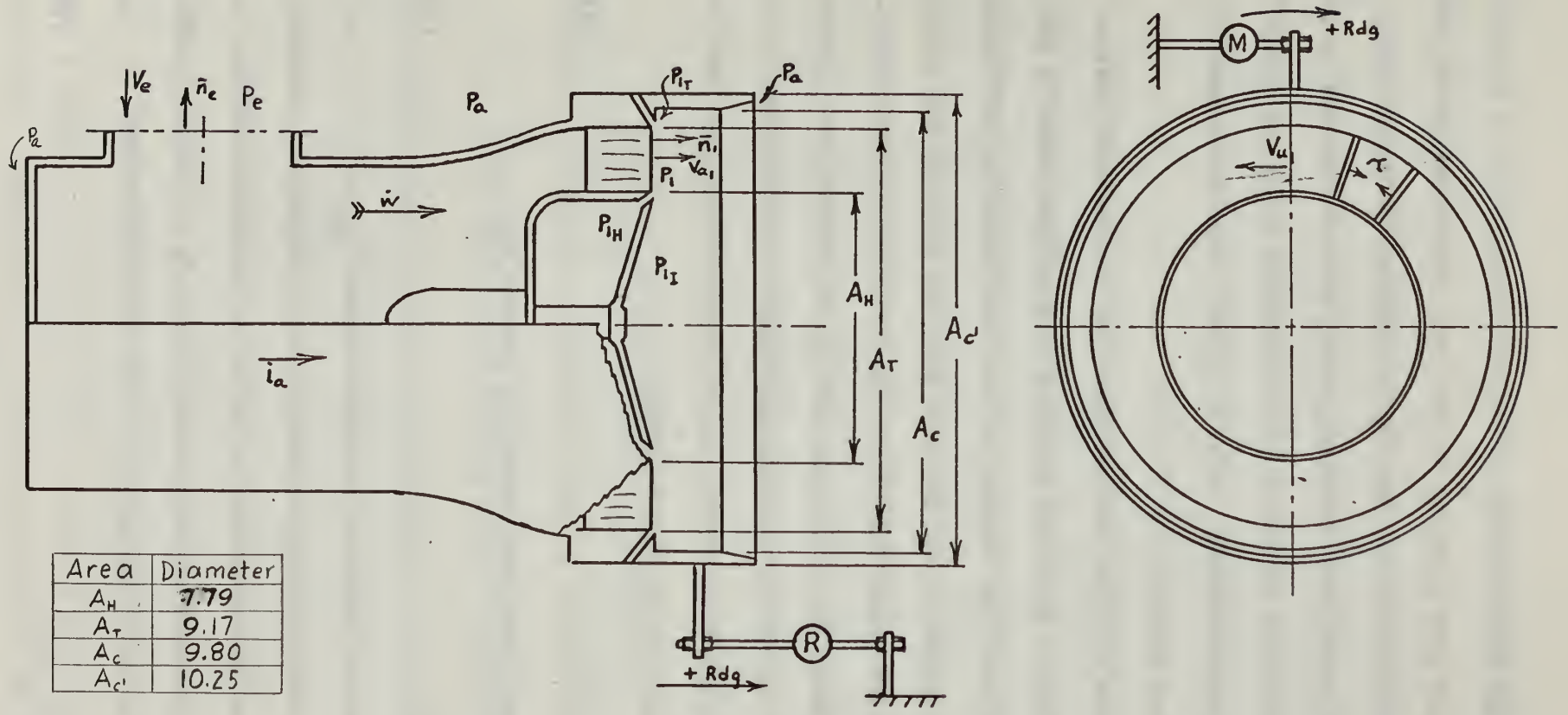

Area	Diameter
A_H	7.79
A_T	9.17
A_c	9.80
$A_{c'}$	10.25

ILLUSTRATION OF THE STATOR-PLENUM ASSEMBLY
FOR MOMENTUM CONSIDERATIONS

FIGURE 39

$$M_i = -\dot{m}\, r_{m_1} V_{u_1} \tag{177}$$

Included in the force measured by the axial force capsule is any differential force acting on the exterior of the assembly. As shown in Fig. 39, ambient pressure acts to the right over the entire case, while acting in the negative direction are the pressure on the cover plate, p_{1_I}; the pressure p_{1_T}, acting on the area $(A_C - A_T)$; and, presumably, ambient pressure acting on the annular area $(A_C' - A_C)$. Let R be the reaction force measured by the force pickup, taken as positive in the positive i_a direction. For R positive, the force reading given by the force measurement system will be positive (i.e., greater than ten kc). Then, since the sum of all forces in the axial direction is zero:

$$R + \dot{m} V_{a_1} - p_1 A_S + p_a A_C - p_{1_T}(A_C - A_T) - p_{1_I} A_H = 0 \tag{178}$$

Solved for the desired quantity, V_{a_1}, and substituting $\dot{w}/g$ for $\dot{m}$, there is:

$$V_{a_1} = \frac{g}{\dot{w}}\left[R + p_a A_C - p_1 A_S - p_{1_T}(A_C - A_T) - p_{1_I} A_H\right] \tag{179}$$

Considering that a positive moment acting on the stator-plenum assembly results in a negative reading from the moment measurement system (less than ten kc), for M_S defined as the measured moment for the stator:

$$M_S = m\, r_{m_1} V_{u_1} \tag{180}$$

Solved for V_{u_1}, and with $\dot{w}/g$ for $\dot{m}$:

$$V_{u_1} = \frac{g}{\dot{w}} \frac{M_S}{r_{m_1}} \tag{181}$$

With an imposed axial load (tare), R in (181) must be the force given by the reading minus the tare force.

With V_{a_1} and V_{u_1} known from the solutions of (179) and (181), the

momentum mean flow discharge angle at station one is obtained from:

$$\alpha_1 = \tan^{-1} \frac{V_{u_1}}{V_{a_1}} \tag{182}$$

Then, there are:

$$V_1 = \frac{V_{a_1}}{\cos \alpha_1} \tag{183}$$

$$T_1 = T_{t_o} - \frac{V_1^2}{2gJc_p} \tag{184}$$

$$T_{1is} = T_{t_o} \left(\frac{P_1}{P_{t_o}}\right)^{\frac{\gamma-1}{\gamma}} \tag{185}$$

and, stator efficiency is given by:

$$\eta_s = \frac{T_{t_o} - T_1}{T_{t_o} - T_{1is}} \tag{186}$$

For choked flow conditions through the stator, an area restriction factor, ξ, can be obtained using the non-dimensional flow function, Φ. This area restriction factor indicates the fraction of the throat area which would be required to pass the actual flow rate under isentropic conditions and is analogous to the factor, ξ, used in the turbine performance analysis (Section 3). This restriction factor is defined as:

$$\xi = \frac{\dot{w}}{\dot{w}^*} = \frac{\frac{\dot{w}\sqrt{T_{t_o}}}{A^* P_{t_o}}\sqrt{\frac{R}{g}}}{\frac{\dot{w}^*\sqrt{T_{t_o}}}{A^* P_{t_o}}\sqrt{\frac{R}{g}}} = \frac{\Phi}{\Phi^*} \tag{187}$$

Here, Φ^*, is the choked-flow isentropic value of Φ for the throat area, A^*, and $\dot{w}^*$ is the isentropic flow rate for choked flow. Then:

$$\Phi^* = \left(\frac{2}{\gamma+1}\right)^{\frac{1}{\gamma-1}} \sqrt{\frac{2\gamma}{\gamma+1}} \tag{188}$$

The non-availability of the throat pressure is the reason why the restriction factor can not be found for non-choked flow, since, for such condition, Φ_{is} must be found from:

$$\Phi_{is} = \sqrt{\frac{2\gamma}{\gamma-1}\left[\left(\frac{P_{th}}{P_{to}}\right)^{\frac{2}{\gamma}} - \left(\frac{P_{th}}{P_{to}}\right)^{\frac{\gamma+1}{\gamma}}\right]}\,; \qquad th-\text{throat} \tag{189}$$

In addition to the foregoing, an effective exit plane area was determined using the axial velocity given by (179) and continuity considerations. The continuity equation, solved for this area is:

$$A_{eff} = \frac{\dot{w} R T_1}{P_1 V_{a_1}} \tag{190}$$

When compared with the geometric area of the exit plane annulus, this area gives an approximation for the blockage of flow area due to both boundary layer effects and trailing edge thickness.

To be calculated for turbine tests are: the momentum mean values of absolute and relative velocities, angles and properties after the stator and rotor; turbine horsepower; and the efficiencies of the stator, rotor and the complete turbine.

Since the pressure, p_{1_I}, is not measured during tests with the rotor installed, use of the momentum equation (179) must be considered approximate only. For comparison purposes, however, p_{1_I} is estimated so that V_{a_1} can be obtained from (179) for use in (182). Due to viscosity, the fluid between the rotor and the cover plate will have some mean value of angular velocity, which can be expressed as a fraction, f, of the rotor angular velocity. Any value of f assumed is, of course, quite conjectural. However, it is known that the fluid adjacent to the rotor has an angular velocity equal to that of the wheel, while the fluid adjacent to the cover plate is at rest. Fig. 40 shows a fluid particle of unit depth into the paper. The forces acting on the particle are the centrifugal force due to the particles angular velocity, $\omega_f = f\omega$, and the pressure force. The pressure forces are:

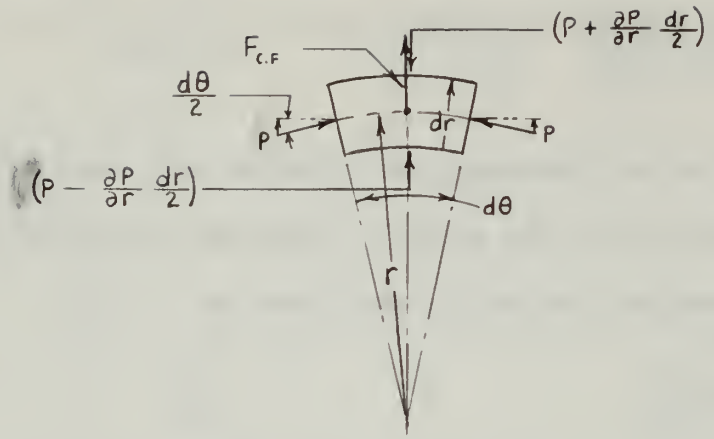

PARTICLE RADIAL EQUILIBRIUM

FIGURE 40

$$F_p = \left(p - \frac{\partial p}{\partial r}\frac{dr}{2}\right)\left(r - \frac{dr}{2}\right)d\theta - \left(p + \frac{\partial p}{\partial r}\frac{dr}{2}\right)\left(r + \frac{dr}{2}\right)d\theta + 2p\frac{d\theta}{2}dr \tag{191}$$

Since the centrifugal force per unit mass is $\omega_f^2 r$, the centrifugal force acting on the particle is:

$$F_{C.F} = \omega_f^2 r(\rho r\, d\theta\, dr) \tag{192}$$

For radial equilibrium of the particle, the pressure forces must equal the centrifugal force. Expanding (191), equating (191) and (192) and dividing by $r d\theta\, dr$:

$$\frac{dp}{dr} = \rho \omega_f^2 r \tag{193}$$

Integrating from $r = r_{1_H}$, where $p = p_{1_H}$, to r, where the pressure is p:

$$p - p_{1_H} = \frac{\rho \omega_f^2}{2}(r^2 - r_{1_H}^2) \tag{194}$$

or:

$$p = p_{1_H} - \frac{\rho \omega_f^2}{2}(r_{1_H}^2 - r^2) \tag{195}$$

The differential axial force acting on the cover plate is:

$$dF_a = p\,dA = \left[P_{1_H} - \frac{\rho\omega_f^2}{2}(r_{1_H}^2 - r^2)\right] 2\pi r\,dr \tag{196}$$

This equation, integrated from r = 0 to r = r_{1_H}, and divided by the area of the cover plate yields the expression for determining the average effective pressure to be used as p_{1_I}:

$$P_{1_I} = \frac{2\pi \int_0^{r_{1_H}} \left[P_{1_H} - \frac{\rho\omega_f^2}{2}(r_{1_H}^2 - r^2)\right] r\,dr}{2\pi \int_0^{r_{1_H}} r\,dr} \tag{197}$$

Integrated, (197) is:

$$P_{1_I} = \frac{\frac{P_{1_H} r_{1_H}^2}{2} - \frac{\rho\omega_f^2}{2}\frac{r_{1_H}^4}{2} + \frac{\rho\omega_f^2}{2}\frac{r_{1_H}^4}{4}}{\frac{r_{1_H}^2}{2}} \tag{198}$$

or:

$$P_{1_I} = P_{1_H} - \frac{\rho\omega_f^2}{4}\frac{r_{1_H}^2}{(144)^2} \tag{199}$$

For p_{1_H} in psia, ρ in lb-sec^2/ft^4, and r_{1_H} in inches, the factor, 144^2 in.^{4} converts the second term of (199) to psia. Expressing ω_f as a fraction of the rotor angular velocity, (199) becomes:

$$P_{1_I} = P_{1_H} - \frac{\rho(f\omega)^2 r_{1_H}^2}{4(144)^2} \tag{200}$$

Using assumed values of f = 0.5 and ρ = 0.002378, the pressure given by (200) is used in (179) to obtain an approximate value of the flow angle at the stator exit and the fluid properties at station one. However, the values obtained are not used in subsequent calculations. Rather, the conditions at one are obtained from continuity considerations and the value of V_{u_1} given by (181). The isentropic expansion temperature at station one is determined from (186). An iteration process is then used. The velocity at one is given by:

$$V_1 = \sqrt{2gJc_p(T_{t_o} - T_1)} \tag{201}$$

Values of T_1 are assumed by adding increments to $T_{1_{is}}$. The velocity is determined from (201), and the flow angle at one is given by:

$$\alpha_1 = \sin^{-1}\left(\frac{V_{u_1}}{V_1}\right) \tag{202}$$

Then, a value of T_1' is computed for comparison with the value assumed:

$$\rho_1 = \frac{\dot{w}}{A_1 V_1 \cos\alpha_1} \qquad (lbm/ft^3) \tag{203}$$

$$T_1' = \frac{p_1}{\rho_1 R} \tag{204}$$

When a match for $T_1' = T_1$ is obtained, the velocity and temperature are known, and V_{a_1} is found from:

$$V_{a_1} = V_1 \cos\alpha_1 \tag{205}$$

The solution for the relative flow velocities and angles ahead of the rotor is obtained using the velocity triangle relationships:

$$W_{u_1} = V_{u_1} - U_1 \; ; \quad U_1 = \omega r_{1_m}/12 \tag{206}$$

$$\beta_1 = \tan^{-1}\left(\frac{W_{u_1}}{V_{a_1}}\right) \tag{207}$$

$$W_1 = \frac{V_{a_1}}{\cos\beta_1} \tag{208}$$

Equivalent enthalpy is determined from:

$$H_E = c_p T_1 + \frac{W_1^2}{2gJ} + \frac{U_2^2 - U_1^2}{2gJ} \; ; \quad U_2 = \omega r_{2_m}/12 \tag{209}$$

With p_2 known as ambient pressure, conditions after the rotor are obtained by the iterative process, based on continuity, used for the stator, but with appropriate relative flow variables and equivalent enthalpy. The required relative peripheral velocity, W_{u_2}, is determined from the measured rotor moment, M_R. The change in total enthalpy across

the rotor is given by:

$$\Delta H = H_0 - H_2 = \frac{M_R \omega g}{\dot{W}} \tag{210}$$

Here, ΔH is in ft^2/sec^2. Then, from Euler's turbine equation, written for positive ΔH:

$$V_{u_2} = \frac{U_1}{U_2} V_{u_1} - \frac{\Delta H}{U_2} \tag{211}$$

The required value of W_{u_2} is then found from:

$$W_{u_2} = V_{u_2} - U_2 \tag{212}$$

The isentropic temperature used as a base for assuming values of T_2 is that value, T_{2_S}, for isentropic expansion from T_{t_E} and p_{t_E} to the pressure p_2. There is:

$$p_{t_E} = p_1 \left(\frac{T_{t_E}}{T_1}\right)^{\frac{\gamma}{\gamma-1}} \tag{213}$$

and:

$$T_{2S} = T_{t_E} \left(\frac{p_2}{p_{t_E}}\right)^{\frac{\gamma-1}{\gamma}} \tag{214}$$

When the assumed and computed values of T_2 agree within tolerance, the relative velocity, flow discharge angle, and temperature at station two are known. The following equations are used to complete the solution:

$$\alpha_2 = \tan^{-1}\left(\frac{V_{u_2}}{V_{a_2}}\right) \tag{215}$$

$$V_2 = \frac{V_{a_2}}{\cos \alpha_2} \tag{216}$$

$$p_{t_2} = p_2 \left(\frac{T_{t_2}}{T_2}\right)^{\frac{\gamma}{\gamma-1}} \tag{217}$$

Referred values are obtained, as is done in the performance analysis, using:

$$\theta = \frac{T_{t_o}}{518.4} \tag{218}$$

$$\delta = \frac{P_{t_o}}{14.7} \tag{219}$$

$$M_{R_{ref}} = \frac{M_R}{\delta} \tag{220}$$

$$N_{ref} = \frac{N}{\sqrt{\theta}} \tag{221}$$

$$\dot{w}_{ref} = \frac{\dot{w}\sqrt{\theta}}{\delta} \tag{222}$$

$$HP_{ref} = \frac{HP}{\sqrt{\theta}\,\delta} \tag{223}$$

$$k_{is} = \frac{\Delta h_{is}}{U_1^2/2} \; ; \qquad \Delta h_{is} \text{ in } ft^2/sec^2 \tag{224}$$

and:

$$r^* = \frac{h_1^* - h_2^*}{\Delta h_{is}} \tag{225}$$

The quantity, k_{is}, is defined as the head coefficient and is related to the often-used velocity ratio, U_1/C_o, where $C_o^2/2 = \Delta h_{is}$ by:

$$\frac{U_1}{C_o} = \sqrt{\frac{1}{k_{is}}} \tag{226}$$

The theoretical degree of reaction, r^*, is the ratio of isentropic enthalpy drop from p_1 to p_2 (determined along the line of constant entropy given by stator inlet conditions) to the isentropic enthalpy drop from p_{t_o} to p_2.

The several efficiencies desired from the rotor solution are found from:

$$\eta_R = \frac{T_{t_E} - T_2}{T_{t_E} - T_{2_S}} \tag{227}$$

for rotor efficiency; and:

$$\eta_i = \frac{\Delta H}{\Delta h_{is}} = \frac{T_{t_o} - T_{t_2}}{T_{t_o} - T_{2is}} \tag{228}$$

for internal efficiency. The velocity coefficients are:

$$\varphi_v = \frac{V_1}{V_{1TH}} = \sqrt{\eta_s} \tag{229}$$

$$\psi = \frac{W_2}{W_{2TH}} = \sqrt{\eta_R} \tag{230}$$

Computer Program

The data reduction computer program, TTTRPGS, included in Appendix VI, proceeds through the various computations required in the solution of the foregoing equations by using subroutines described below. Inputs to the program are: the number of test data sets to be reduced; the date of test (month and day); ambient pressure and temperature; the number of data points for each data set; a value for the variable, TYPE, which indicates whether the data is for stator-only (TYPE = 0) or full turbine (TYPE $\neq$ 0) tests; and all experimental data. All experimental data inputs are the values as recorded during the test, except that temperatures are in °F rather than in millivolts, and rotor moments are in in-lb rather than in percent of maximum moment.

Subroutines are called in the following order:

1. FLORATE. Determines the flow rate measured by the flow nozzle (145) and the plenum labyrinth leak rate (170a) and (166). The turbine flow rate is then found as the former flow rate minus the later.

2. STATOR. Solves the stator equations and determines the properties at the stator exit. Values based on the solution of the momentum equation are computed and printed, but values used in subsequent calculations are those obtained from iteration using continuity considerations. Also determined by this subroutine are the values for the area restriction factor, stator efficiency and stator velocity coefficient. Mean streamline radius is taken as 4.26 in.

3. ROTOR. This subroutine converts absolute flow conditions at

one to relative flow quantities, determines ΔH, and performs the iteration using continuity considerations to determine relative gas efflux angle and velocity, and temperature at the rotor exit. The other thermodynamic properties, flow angles, rotor efficiency and rotor velocity coefficient are computed also. A value of 4.45 in. is used for the mean streamline radius.

4. REFERD. This subroutine converts data to their referred and/or non-dimensional forms.

Outputs from TTTRPGS are the thermodynamic properties, velocities, flow angles for both the absolute and relative flows as appropriate, along with the non-dimensional values (k_{is}, efficiencies, r^*, etc.), and the actual and referred values of rotor moment, horsepower, RPM and flow rates.

Results

Three tests without the rotor installed were conducted on 27 December 1965 and on 5 and 6 January 1966. Large fluctuations in axial force readings were noted during the first test and the data obtained were unusable. The turbine hood was removed to eliminate the backflow caused by impingement of discharge air on the hood. All subsequent testing, including tests with the rotor installed, was done with the hood removed. Data from the second stator-only test were not considered valid, since an open turbine plenum drain line was found at the conclusion of the test. Consequently, only the data from the third test form the basis for results presented for tests without the rotor installed.

The turbine was rotated for the first time on 12 January 1966, and five additional tests were made between that date and 16 February. Rotor moments measured during the first two such test were obviously too high, since unbelievable turbine efficiencies resulted. Results of these two

tests were considered valid only for stator performance considerations. Turbine tests were discontinued during the fifth test run on 28 January, due to suspected bearing failure in the air dynamometer unit. Upon disassembly of that unit, the bearings were found to be satisfactory. However, the dynamometer rotor had been scraping against its housing. Moreover, the spline at the dynamometer end of the quill shaft connecting the rotor to the dynamometer unit was badly fretted, indicating possible misalignment. After reassembly and reinstallation of the dyanmometer, the turbine was realigned and testing was resumed. It was necessary to seat the dynamometer spline (male) as deeply as possible in the quill shaft to maintain adequate undamaged spline bearing and shear areas. Dynamometer bearing failure was again suspected on 18 February during preparations for the seventh test. At this time, the dynamometer was returned to the manufacturer for disassembly, inspection and necessary repair. Hence, testing was again interrupted pending return of the dynamometer and receipt of the new quill shaft which had been ordered. The turbine became operable again on 15 April. However, it was too late for further turbine performance tests for inclusion in this study. Consequently, zero speed and zero torque tests were made as the final tests for consideration herein.

It is pertinent to consideration of the test results that the total pressure probe pressure line parted inside the stator-plenum assembly at the conclusion of the third test. Values of p_{t_o} used in data reduction for subsequent tests were determined by applying a correction, deduced from previous tests, to the static pressure readings, p_o, obtained at the probe location.

Results of the stator-only and the turbine tests are shown in Figs.

41 through 49. For ease of reference, Table VII indicates the contents of these figures. Also shown in Figs. 41 through 49 are selected results of the performance analysis.

Discussion and Conclusions

As is evident from Fig. 41, stator-only tests yielded values for stator efficiency of 0.9, based on the continuity equation iteration, and 0.93, based on the momentum equation. The difference between values of the gas efflux angle (α_1) given by the two methods of solution (see Fig. 42) reflects the difference in efficiency values, since common values of tangential velocity were used in computations performed by the two methods. The values for α_1 used in the performance analysis are seen to definitely favor the continuity-based values, whereas the estimated stator efficiency used for the performance prediction was 0.9095. Any error in the continuity-based values can be due only to the stator exit area used in computations. This area was the stator exit annular area minus the product of blade heighth, number of blades, and the dimension for the projection of blade trailing edge thickness on the stator exit plane. Although accuracy of this exit plane area is dependent on manufacturing tolerances, the area must be considered quite accurate. The momentum-based values are very critical with respect to the pressure terms and also depend on the axial force. For a typical data point ($p_{t_o}/p_1 = 2.61$), the fluctuation in the latter quantity over a period of about ten seconds was $\pm$ 1.25 lbs from the average value of 24.65 lbs. With the flow rate of 3.44 lbm/sec, a variation of $\pm$ 9.4 ft/sec results. Considering that the values of axial velocity obtained for this test point were 404 ft/sec from the momentum equation and 334 ft/sec from continuity considerations, the fluctuation in axial force measurements appears to be relatively unimportant. It must be considered then that

TABLE VII

SUMMARY OF THE TURBINE TEST RESULTS
PRESENTED IN FIGURES 41 THROUGH 49

Figure	Shows	Versus	Remarks
41	Stator efficiency, η_s	p_{t_o}/p_1	
42	Gas efflux angle, α_1	p_{t_o}/p_1	
43	Turbine efficiency, η_i	k_{is}	curves for p_{t_o}/p_2= constant
44	Referred Flow Rate, $\dot{w}\sqrt{\theta}/\delta$	k_{is}	same as above
45	Theoretical degree of reaction, r*	k_{is}	same as above
46	Referred moment, M_R/δ	$N/\sqrt{\theta}$	same as above
47	Rotor efficiency, η_R	incidence angle, i	same as above
48	$V_{a_1}/\sqrt{\theta}$	p_{t_o}/p_1	
49	$V_{a_2}/\sqrt{\theta}$	$N/\sqrt{\theta}$	curves for p_{t_o}/p_2 = constant

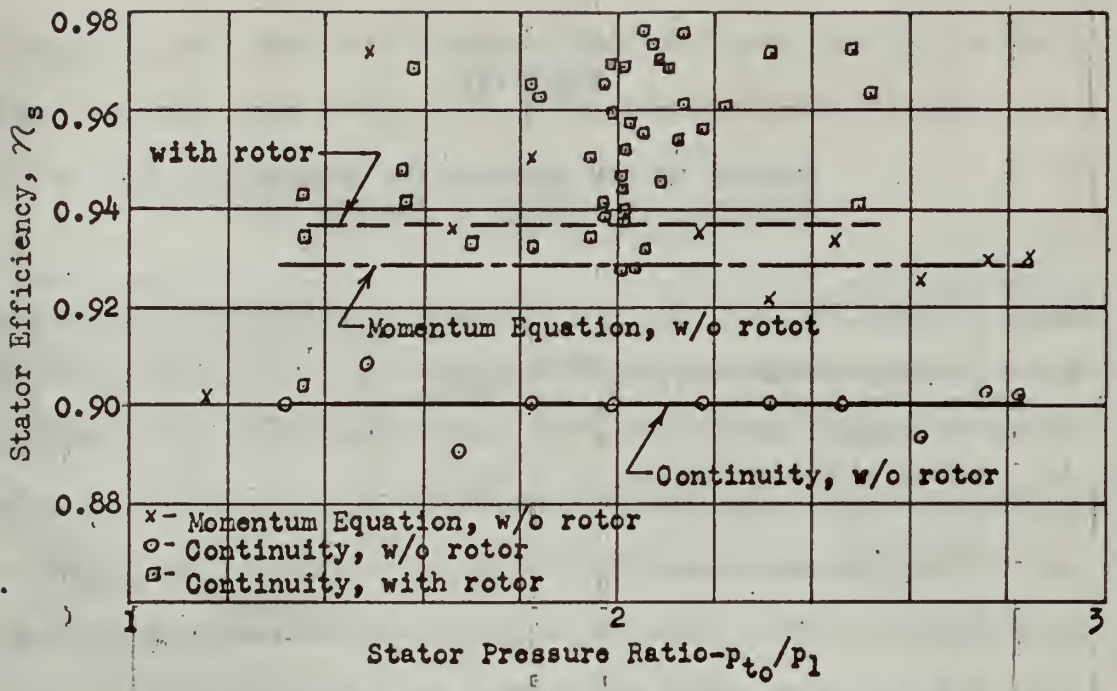

EXPERIMENTALLY DETERMINED VALUES OF STATOR EFFICIENCY-TTTR

FIGURE 41

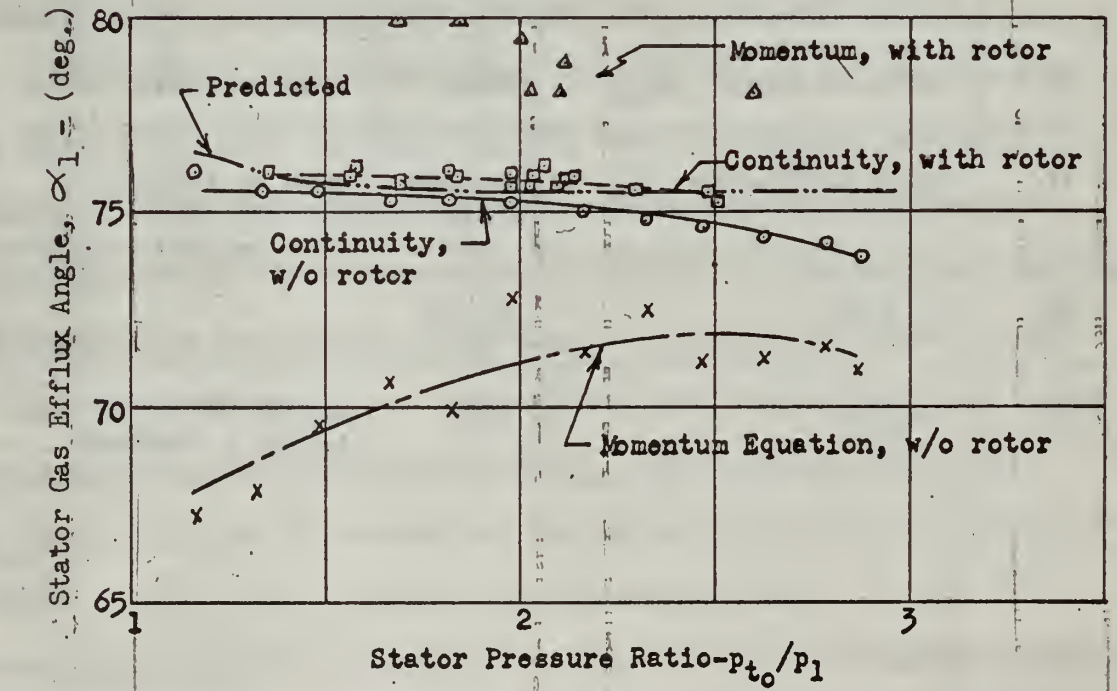

EXPERIMENTALLY DETERMINED VALUES OF STATOR GAS EFFLUX ANGLE-TTTR

FIGURE 42

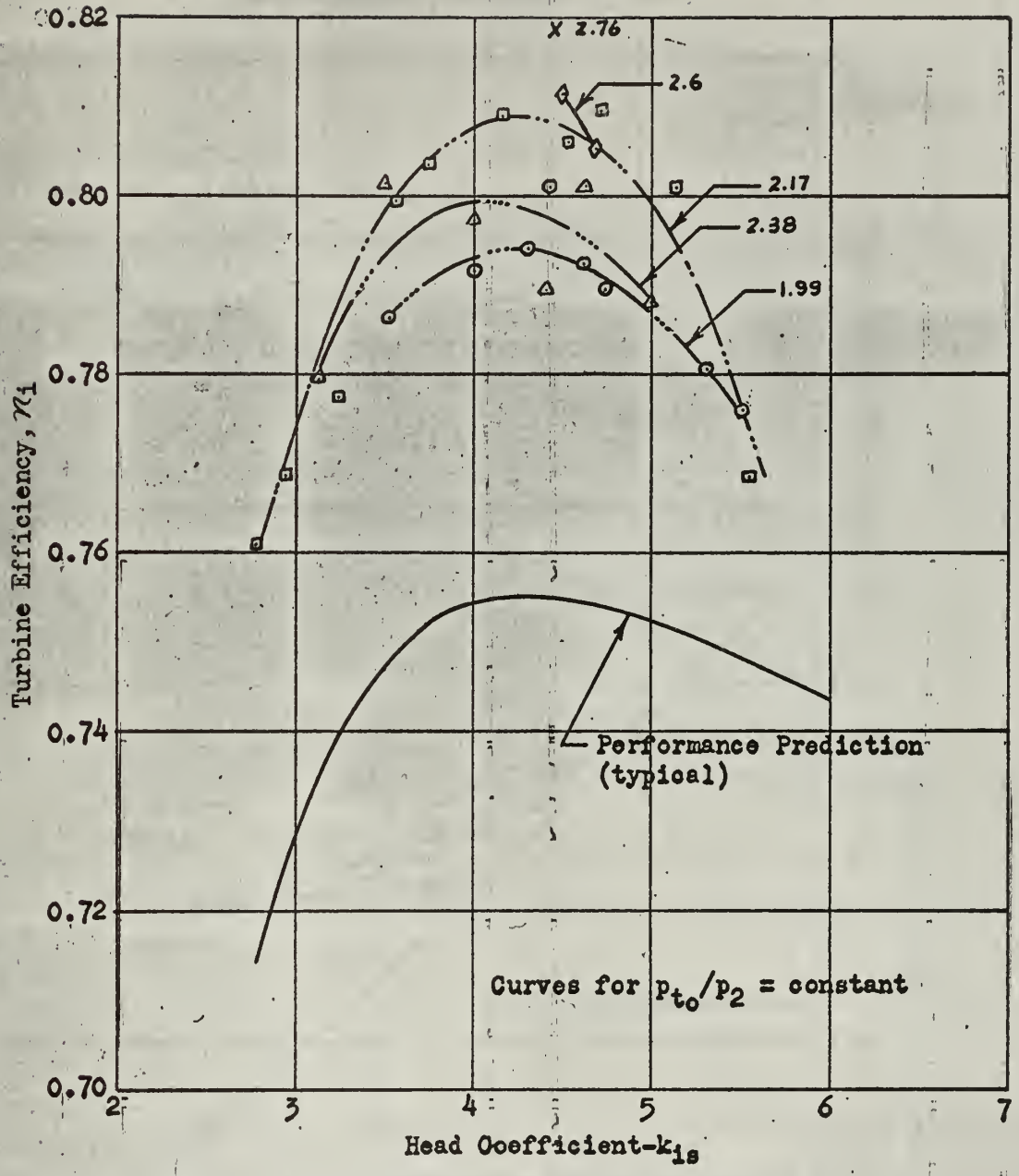

EXPERIMENTALLY DETERMINED VALUES OF
TURBINE EFFICIENCY-TTTR

FIGURE 43

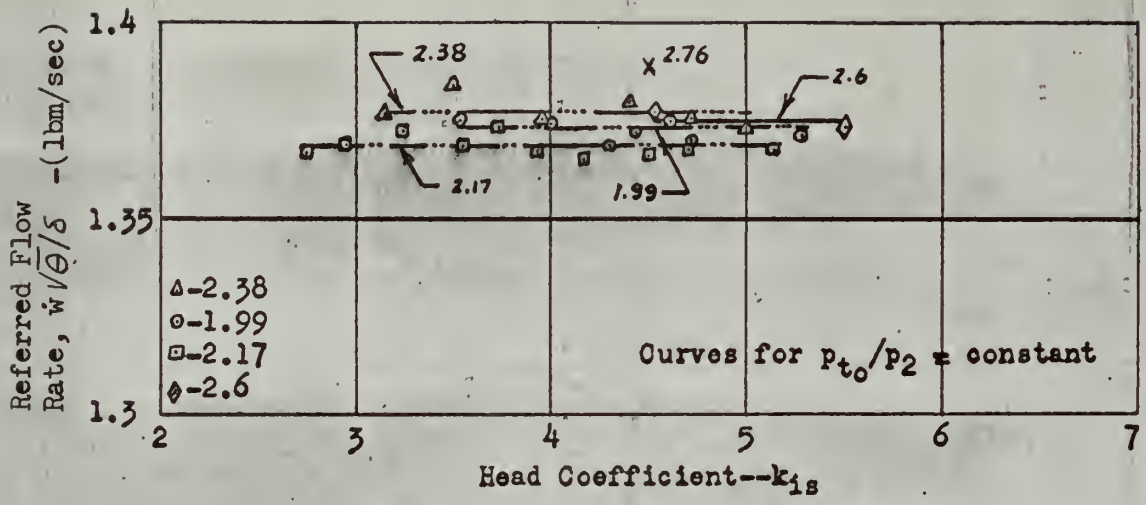

EXPERIMENTALLY DETERMINED VALUES OF REFERRED FLOW RATE--TTTR

FIGURE 44

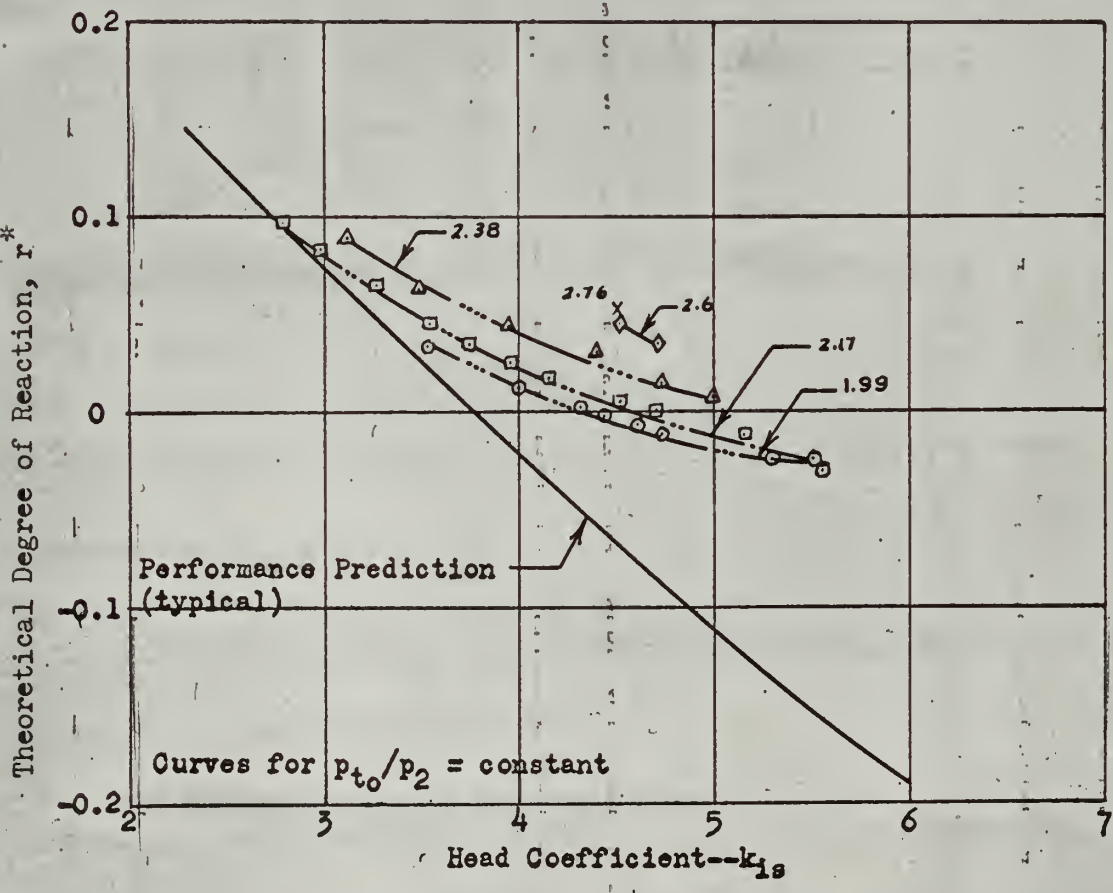

EXPERIMENTALLY DETERMINED VALUES OF THEORETICAL DEGREE OF REACTION-TTTR

FIGURE 45

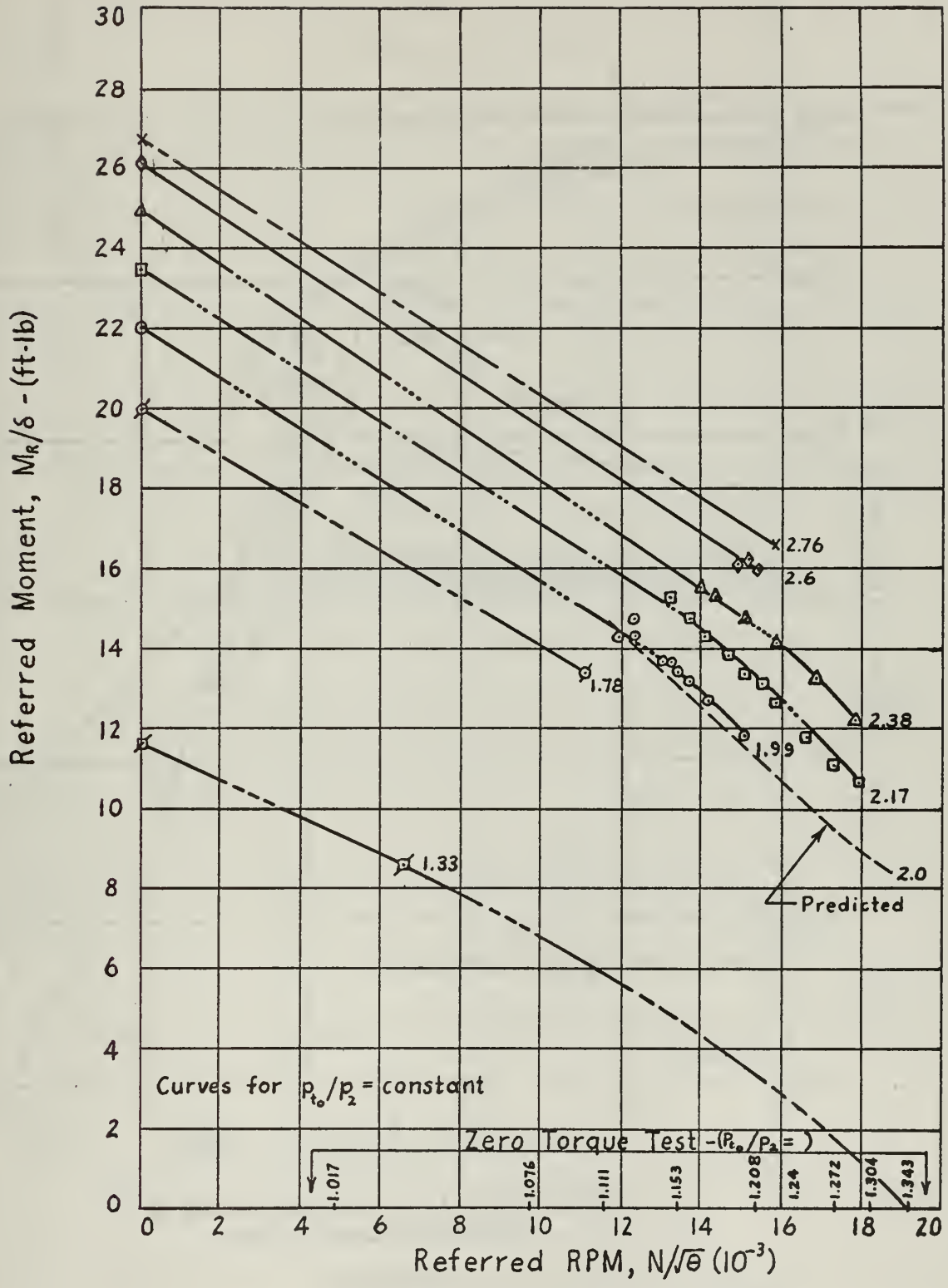

EXPERIMENTALLY DETERMINED VALUES OF REFERRED ROTOR MOMENT--TTTR

FIGURE 46

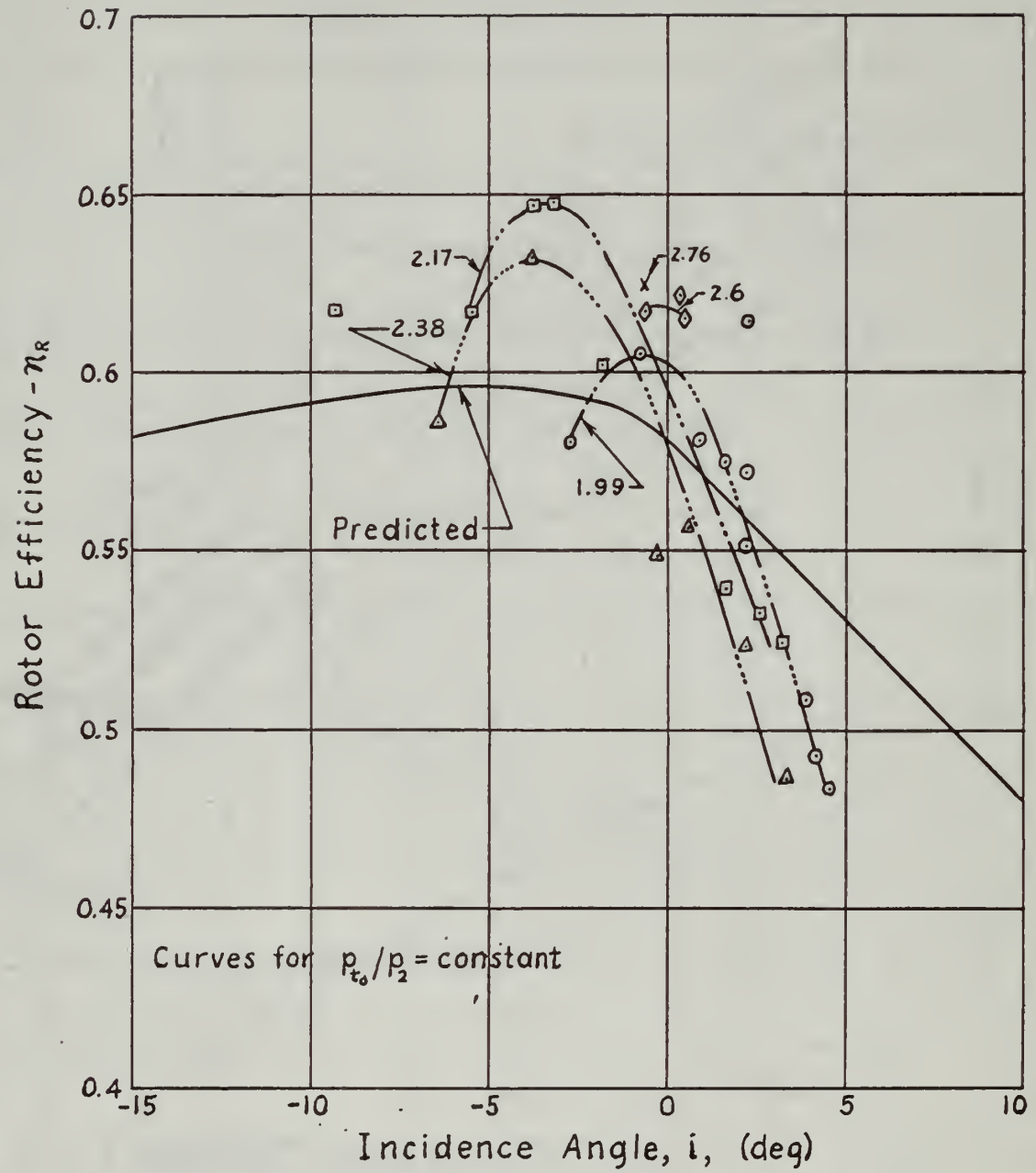

EXPERIMENTALLY DETERMINED VALUES OF ROTOR EFFICIENCY--TTTR

FIGURE 47

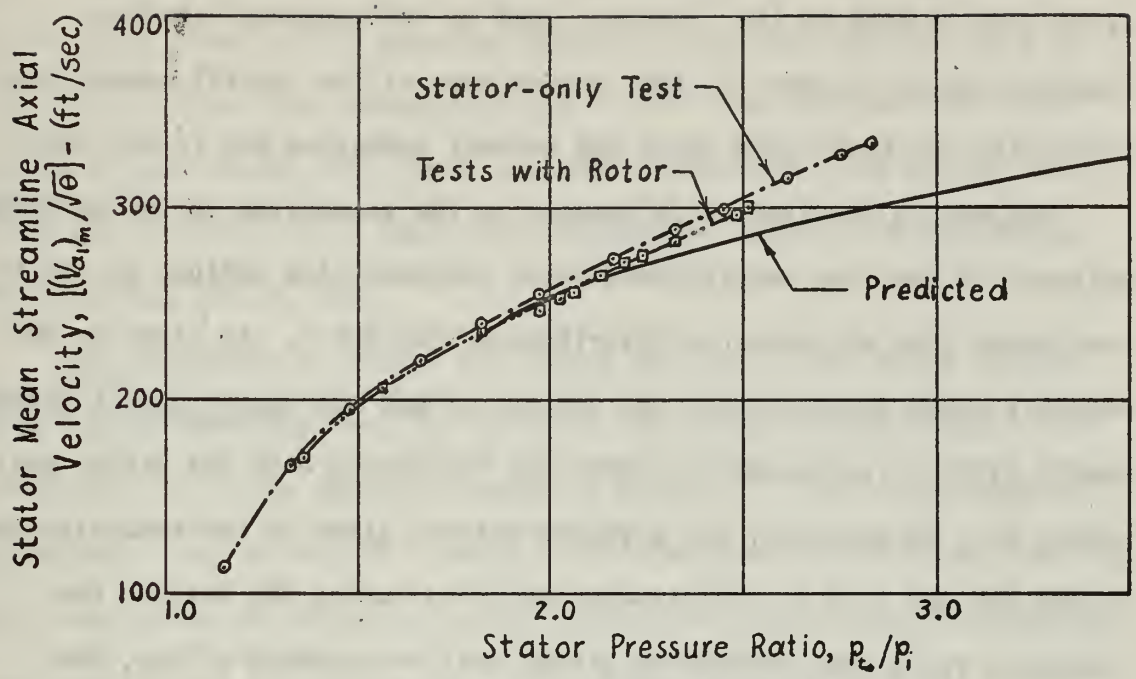

EXPERIMENTALLY DETERMINED VALUES OF
REFERRED STATOR AXIAL VELOCITY--TTTR

FIGURE 48

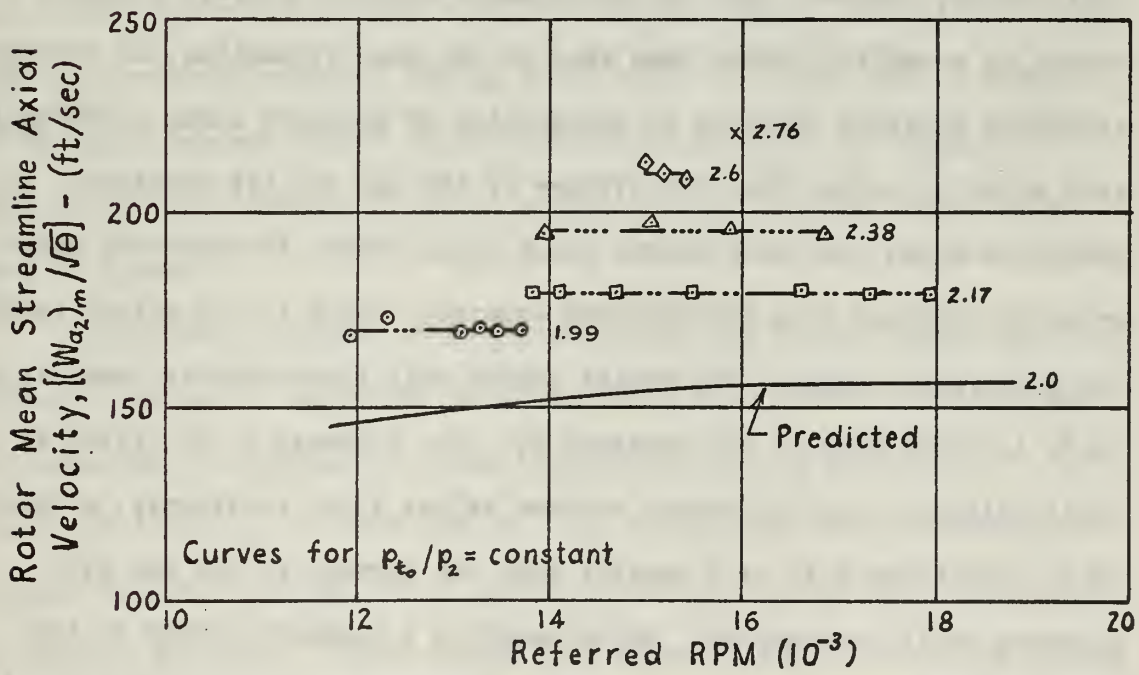

EXPERIMENTALLY DETERMINED VALUES OF
REFERRED ROTOR AXIAL VELOCITY--TTTR

FIGURE 49

either one or more of the pressures used in the momentum equation computations is in error or that one or more of the initial assumptions concerning the areas upon which the several pressures act is not valid.

Subject to the limitation imposed by the assumption in the performance analysis of the loss coefficients being constant with radius, it can be considered that the pressure distribution from hub to tip given by the analysis would indicate that the average of hub and tip values of pressure should yield a representative value for the pressure in the stator exit plane, p_1. In addition, the pressure pattern given by the analysis--low at the hub and high at the tip--was observed during the tests. For instance, for a mean streamline stator exit Mach number of one, the performance analysis gave values (in psia) of 13.03 and 16.21 at the hub and the tip, respectively, while matching test values are 13.97 and 15.84. Considering, however, that the performance analysis average pressure occurs at a smaller radius than that of the mean streamline, an average effective pressure obtained by integration of pressure times differential area would be higher than the average of the hub and tip pressure. It should be noted that such higher value would reduce the value of axial velocity obtained from the momentum equation, which is the effect required for stator-only tests. The entire stator exit plane annular area, 18.38 $in.^2$, is acted upon by the pressure p_1. For a change of 70 ft/sec in axial velocity, the difference between values given previously, a value of p_1 only about 0.42 psia greater than the average of hub and tip pressure would be required. Unfortunately, a pressure survey in the stator exit plane would be required to accurately determine the radial pressure gradient which would be needed for finding the force-average pressure. The performance analysis pressure distribution could be used

as an approximation, however. Further consideration of the pressure terms which occur in the momentum equation indicates that it would be desirable to know the pressure acting on the flow director ring downstream of the stator exit plane, on both the annular area at the sharp break at the stator exit plane and the annular area at the downstream end (see Fig. 39, p. 122).

Any comparison of stator efficiency and gas efflux angle values given by the momentum equation and from continuity considerations for tests with the rotor installed would be subject to the considerations given above for the rotor. However, it is evident from Fig. 42 that for the rotor tests the values of axial velocity obtained from the momentum equation are too low (i.e., α_1 too large). Of some interest is the fact that the radial gradient of pressure obtained with the rotor installed was somewhat more severe than that for stator-only tests. For the conditions considered in the preceding paragraph, the values of hub and tip pressures measured during tests with the rotor were 13.5 and 16.41 psia, respectively. These considerations serve to emphasize previously-made comments that the pressure acting on the cover plate must be known.

The parabolic nature of the equation for the radial distribution of pressure acting on the cover plate indicates that pressure taps should be installed at the center of the cover plate and at a radius of 0.707 times the cover plate outer radius. The redesigned thrust and torque flexure will, of course, yield the force acting on the cover plate, as previously discussed. Even though this flexure and pressure taps in the cover plate effectively give the same information, installation of both is considered desirable.

It should be noted that the spread of stator efficiency values for

tests with the rotor installed, Fig. 41, is not reflected in values of α_1, Fig. 42. This situation is considered to be caused by the difficulty noted previously of obtaining all readings rapidly enough to preclude effects of variation of test conditions. Since provisions for automatic data logging are nearing completion at the time of this writing, this problem should be alleviated in the near future.

Of considerable interest is the increased stator efficiency with the rotor installed, which can be estimated as 0.93 to 0.94, over that without the rotor. This result belies the assumption that conditions downstream do not affect upstream conditions. Since it seems unlikely that stator blade profile losses are reduced by the presence of the rotor, it is conjectured that the rotor acts to reduce the effects of secondary flow losses. Considering the sharp break in the gas path in the stator exit plane, it seems probable that the presence of the rotor may provide sufficient flow guidance in that area to reduce losses due to vortex formation as the flow spills over into this relatively large region. The increased severity of pressure gradient in the stator exit plane for tests with the rotor installed over that observed for stator-only tests indicates that the flow pattern in the area is altered by the presence of the rotor. Installation of pressure taps in the flow director ring at this break could, perhaps, give some insight into the nature of the flow alteration, as well as being desirable for application of the momentum equation.

The curves of Figs. 43-46 illustrate the performance of the turbine as measured in tests three through six with the rotor installed and with an axial clearance of 0.243 in. Some evidence of the effects of non-simultaneous readings exists in the scatter in values of internal efficiency, Fig. 43, whereas the moment curves of Fig. 46, which depend only

on flow rate and measured torque, do not exhibit undue scatter. Constancy of referred flow rate is indicated by Fig. 44, with $w_{ref} = 1.375$ lbm/sec. The variation of theoretical degree of reaction indicated in Fig. 45 is considered quite reasonable for an impulse-type turbine. Figs. 48 and 49 are included here for illustrative purposes and discussion in the next section, with respect to comparison of performance prediction and test results.

Both internal efficiency, Fig. 43, and rotor efficiency, Fig. 47, vary with incidence, angle in a manner characteristic of an impulse-type turbine, i.e., with a narrow range of incidence angles for high efficiencies. Except for the differences between maximum rotor efficiency values for the different pressure ratios, the curves of Fig. 47 could be replaced by a single curve.

The values of rotor gas efflux angle are not depicted graphically, since this angle varied over a small range: -67.1° to -67.8°, with the higher value applicable to higher pressure ratios, p_{t_0}/p_2. In addition, the stator area restriction factor, ξ, was essentially constant, varying from 0.944 to 0.952, and with the variations indicative of no dependence on stator pressure ratio.

7. Discussion and Recommendations.

Comparison of experimental and performance prediction results indicates that the most serious deficiency in the performance analysis is in the variation of the area restriction factor, Fig. 20, while experiment yielded an essentially constant value. The effect is indicated in the reduced referred mass flow rates after the flow is choked given by the performance analysis, Fig. 19. The effect is evident also in the agreement between the predicted curve of referred axial velocity and experimental values at lower pressure ratios, p_{t_0}/p_1, with subsequent

departure at higher pressure ratios, Fig. 48. Apparently ξ should be taken as constant after the flow is choked, so that $\dot{w}_{ref}$ will be constant.

Quite obviously, any performance prediction is no more accurate than the values used for stator and rotor efficiencies. The differences in magnitude between predicted and observed values of internal efficiency, rotor efficiency, and stator efficiency with the rotor installed serve to emphasize this fact. The high deflection through the rotor, 129°, makes estimation of η_R quite arbitrary, since very little is known about turbine losses for rotors with deflections of greater than about 110-115°. General practice in gas turbine design limits the turning angle to 105°. Predicting the positive stalling incidence angle is subject to the same difficulties attending the choice of rotor efficiency. From Fig. 47, the stalling incidence angle for the transonic turbine can be estimated as about five or six degrees, whereas the predicted value used was 13.4°. The effect of this difference is evident in Figs. 43, 47 and 45. The much greater low-loss ranges for the prediction curves of Figs. 43 and 47 are clear indications. However, the manner in which the theoretical degree of reaction is influenced (Fig. 45) requires further explanation. One must first imagine that the predicted curve of Fig. 45 is moved upward so that its position corresponds to the higher efficiency (over predicted) obtained from the tests. Then, assuming that the loss coefficient remains constant, when positive stalling incidence is reached, the smaller the value of this incidence angle, the higher will be the RPM at which the loss coefficient becomes constant. This consideration means that the negative reaction portions of the prediction curves of Figs. 29 and 47 would flatten out (towards zero reaction).

The gas efflux angles used in the performance analysis proved to

agree very well with those determined experimentally. Fig. 42 indicates almost exact agreement for the stator, while the predicted values for the rotor angle of 67.76° to 69° agree favorably with the values of 67.1° to 67.8° observed experimentally. Further, the exit Mach Number for which the value of 67.8° was obtained was about 0.6, and the corresponding value of β_2 used in the performance prediction was 67.85°.

The discrepancy between predicted and measured values of referred rotor exit axial velocity, Fig. 49, can be attributed largely to the differences noted previously between predicted and experimentally determined values of the stator area restriction factor.

It is considered that the addition of instrumentation recommended earlier in this paper is necessary prior to further testing. In addition, it is recommended that attempts to correlate the performance prediction program as given herein (or a similar program) be continued, by assuming different loss coefficients and different radial variation of such loss coefficients. It is pertinent in this regard that a thesis reporting on cascade tests of the converging guide vanes and the double circular arc rotor blades will be published shortly.

BIBLIOGRAPHY

1. Eschbach, O. W. (ed.) Handbook of Engineering Fundamentals, 2nd ed. New York, London, Sydney: John Wiley and Sons, Inc., 1952.

2. Stearnes, R. F., et. al. Flow Measurement with Orifice Meters. New York: Van Nostrand Co., Inc., 1951.

3. Vavra, M. H. Aero-Thermodynamics and Flow in Turbomachines. New York, London: John Wiley and Sons, Inc., 1960.

4. Ainley, D. G. and Mathieson, G. C. R. An Examination of the Flow and Pressure Losses in Blade Rows of Axial-Flow Turbines. Aeronautical Research Council, R & M No. 2891, 1955.

5. Ainley, D. G. and Mathieson, G. C. R. A Method of Performance Estimation for Axial-Flow Turbines. Aeronautical Research Council, R & M No. 2974, 1957.

6. Eckert, R. H. Determination of Flow Rates, Transonic Turbine Test Rig. USNPGS TN 66T-1. January 1966.

7. Egli, A. The Leakage of Steam through Labyrinth Seals. Transactions of the ASME, v. 57, 1935, 115-122.

8. Jerie, J. Flow through Straight-Through Labyrinth Seals. Proceedings of the Seventh International Congress of Applied Mechanics, 1948, v. 2, Pt. 1. 70-82.

9. Vavra, M. H. Determination of Flow Rates of Allis Chalmers Axial-Flow Compressor, VA-312 of Propulsion Laboratory by Means of Square-Edged Orifices. USNPGS TN 63T-2, August 1963.

10. Vavra, M. H. Problems of Fluid Mechanics in Radial Turbomachines, Pts. I and II. Von Karman Institute Course Note 55a. Rhode-Saint-Genese, Belgium: Von Karman Institute for Fluid Dynamics, March 1965.

11. Vavra, M. H. Problems of Fluid Mechanics in Radial Turbomachines, Pts. III and IV. Von Karman Institute Course Note 55b. Rhode-Saint-Genese, Belgium: Von Karman Institute for Fluid Dynamics, March 1965.

APPENDIX I

FORMULA DEVELOPMENT FOR TURBINE PERFORMANCE PREDICTION

A. Equation of Motion for Relative Flows.

The equation of motion for relative flow in vector form, (2), p. 39, is:

$$\nabla H_R = \overline{W} \times (\nabla \times \overline{W} + 2\overline{\omega}) + T \nabla s \tag{2}$$

Expanding the several terms of (2) gives:

$$\nabla H_R = \frac{i_\theta}{r}\frac{\partial H_R}{\partial \theta} + i_z \frac{\partial H_R}{\partial z} + i_r \frac{\partial H_R}{\partial r} \tag{231}$$

$$\nabla \times \overline{W} = \begin{vmatrix} i_\theta & \frac{i_z}{r} & \frac{i_r}{r} \\ \frac{\partial}{\partial \theta} & \frac{\partial}{\partial z} & \frac{\partial}{\partial r} \\ rW_u & W_a & W_r \end{vmatrix} = i_\theta \left(\frac{\partial W_r}{\partial z} - \frac{\partial W_a}{\partial r}\right) + \frac{i_z}{r}\left(\frac{\partial (rW_u)}{\partial r} - \frac{\partial W_r}{\partial \theta}\right) + \frac{i_r}{r}\left(\frac{\partial W_a}{\partial \theta} - \frac{\partial (rW_u)}{\partial z}\right) \tag{232}$$

$$W \times (\nabla \times W) = \begin{vmatrix} i_\theta & i_z & i_r \\ W_u & W_a & W_r \\ \left(\frac{\partial W_r}{\partial z} - \frac{\partial W_a}{\partial r}\right) & \frac{1}{r}\left(\frac{\partial (rW_u)}{\partial r} - \frac{\partial W_r}{\partial \theta}\right) & \frac{1}{r}\left(\frac{\partial W_a}{\partial \theta} - \frac{\partial (rW_u)}{\partial z}\right) \end{vmatrix}$$

$$= i_\theta \left\{ W_a \frac{1}{r}\left[\frac{\partial W_a}{\partial \theta} - \frac{\partial (rW_u)}{\partial z}\right] - W_r \frac{1}{r}\left[\frac{\partial (rW_u)}{\partial r} - \frac{\partial W_r}{\partial \theta}\right]\right\} +$$

$$i_z \left\{ W_r \left[\frac{\partial W_r}{\partial z} - \frac{\partial W_a}{\partial r}\right] - W_u \frac{1}{r}\left[\frac{\partial W_a}{\partial \theta} - \frac{\partial (rW_u)}{\partial z}\right]\right\} +$$

$$i_r \left\{ W_u \frac{1}{r}\left[\frac{\partial (rW_u)}{\partial r} - \frac{\partial W_r}{\partial \theta}\right] - W_a \left[\frac{\partial W_r}{\partial z} - \frac{\partial W_a}{\partial r}\right]\right\} \tag{233}$$

$$\overline{W} \times 2\overline{\omega} = (i_\theta W_u + i_z W_a + i_r W_r) \times (i_z\, 2\omega) = i_r (2\omega W_u) - i_\theta (2\omega W_r) \tag{234}$$

$$T \nabla s = T\left(i_\theta \frac{1}{r}\frac{\partial s}{\partial \theta} + i_z \frac{\partial s}{\partial z} + i_r \frac{\partial s}{\partial r}\right) \tag{235}$$

Combining (231) through (235) and writing the equations for each unit vector:

$$i_\theta: \frac{1}{r}\frac{\partial H_R}{\partial \theta} = \frac{W_a}{r}\left[\frac{\partial W_a}{\partial \theta} - \frac{\partial (rW_u)}{\partial z}\right] - \frac{W_r}{r}\left[\frac{\partial (rW_u)}{\partial r} - \frac{\partial W_r}{\partial \theta}\right] - 2\omega W_r + \frac{T}{r}\frac{\partial s}{\partial \theta} \qquad (236a)$$

$$i_z: \frac{\partial H_R}{\partial z} = W_r\left[\frac{\partial W_r}{\partial z} - \frac{\partial W_a}{\partial r}\right] - \frac{W_u}{r}\left[\frac{\partial W_a}{\partial \theta} - \frac{\partial (rW_u)}{\partial z}\right] + T\frac{\partial s}{\partial z} \qquad (236b)$$

$$i_r: \frac{\partial H_R}{\partial r} = \frac{W_u}{r}\left[\frac{\partial (rW_u)}{\partial r} - \frac{\partial W_r}{\partial \theta}\right] - W_a\left[\frac{\partial W_r}{\partial z} - \frac{\partial W_a}{\partial r}\right] + 2\omega W_u + T\frac{\partial s}{\partial r} \qquad (236c)$$

For assumed axisymmetric flow, all derivatives with respect to θ are zero. Then:

$$i_\theta: \quad 0 = -\frac{W_a}{r}\frac{\partial (rW_u)}{\partial z} - \frac{W_r}{r}\frac{\partial (rW_u)}{\partial r} - 2\omega W_r \qquad (237a)$$

$$i_z: \frac{\partial H_R}{\partial z} = W_r\frac{\partial W_r}{\partial z} - W_r\frac{\partial W_a}{\partial r} + \frac{W_u}{r}\frac{\partial (rW_u)}{\partial z} + T\frac{\partial s}{\partial z} \qquad (237b)$$

$$i_r: \frac{\partial H_R}{\partial r} = \frac{W_u}{r}\frac{\partial (rW_u)}{\partial r} - W_a\frac{\partial W_r}{\partial z} + W_a\frac{\partial W_a}{\partial r} + 2\omega W_u + T\frac{\partial s}{\partial r} \qquad (237c)$$

Eq. (237a) can be rewritten:

$$\frac{\partial (rW_u)}{\partial z} = -\frac{W_r}{W_a}\frac{\partial (rW_u)}{\partial r} - 2\omega r\frac{W_r}{W_a} \qquad (238)$$

Substituting this expression in (237b):

$$\frac{\partial H_R}{\partial z} = W_r\frac{\partial W_r}{\partial z} - W_r\frac{\partial W_a}{\partial r} + \frac{W_u}{r}\left(-\frac{W_r}{W_a}\frac{\partial (rW_u)}{\partial r}\right) - 2\omega\frac{W_u W_r}{W_a} + T\frac{\partial s}{\partial z}$$

or:

$$\frac{\partial H_R}{\partial z} = -\frac{W_u W_r}{rW_a}\frac{\partial (rW_u)}{\partial r} + W_r\frac{\partial W_r}{\partial z} - W_r\frac{\partial W_a}{\partial r} - 2\omega\frac{W_u W_r}{W_a} - T\frac{\partial s}{\partial z} \qquad (239)$$

Multiplying (237c) by W_r and (239) by W_a:

$$W_r\frac{\partial H_R}{\partial r} = \frac{W_u W_r}{r}\frac{\partial (rW_u)}{\partial r} - W_a W_r\frac{\partial W_r}{\partial z} + W_a W_r\frac{\partial W_a}{\partial r} + 2\omega W_u W_r + W_r T\frac{\partial s}{\partial r}$$

$$W_a\frac{\partial H_R}{\partial z} = -\frac{W_u W_r}{r}\frac{\partial (rW_u)}{\partial r} + W_a W_r\frac{\partial W_r}{\partial z} - W_a W_r\frac{\partial W_a}{\partial r} - 2\omega W_u W_r + W_a T\frac{\partial s}{\partial z}$$

Adding these two equations:

$$W_r \frac{\partial H_R}{\partial r} + W_a \frac{\partial H_R}{\partial z} = T\left(W_r \frac{\partial s}{\partial r} + W_a \frac{\partial s}{\partial z}\right) \tag{240}$$

For adiabatic flow, total relative enthalpy is constant along any given streamline. Hence, the stream derivative is zero. With $\partial/\partial\theta = 0$:

$$\bar{W} dt \cdot \nabla H_R = 0 = W_a \frac{\partial H_R}{\partial z} + W_r \frac{\partial H_R}{\partial r} \tag{241}$$

or:

$$\frac{\partial H_R}{\partial z} = -\frac{W_r}{W_a} \frac{\partial H_R}{\partial r} \tag{241a}$$

Then, with (241), (240) becomes:

$$\frac{\partial s}{\partial z} = -\frac{W_r}{W_a} \frac{\partial s}{\partial r} \tag{242}$$

Substituting (241a) and (242) in (239):

$$-\frac{W_r}{W_a} \frac{\partial H_R}{\partial r} = -\frac{W_u W_r}{r W_a} \frac{\partial (r W_u)}{\partial r} + W_r \frac{\partial W_r}{\partial z} - W_r \frac{\partial W_a}{\partial r} - 2\omega \frac{W_u W_r}{W_a} - \frac{W_r}{W_a} T \frac{\partial s}{\partial r}$$

Then, multiplying this expression by $(-W_a/W_r)$ gives:

$$\frac{\partial H_R}{\partial r} = \frac{W_u}{r} \frac{\partial (r W_u)}{\partial r} - W_a \frac{\partial W_r}{\partial z} + W_a \frac{\partial W_a}{\partial r} + 2\omega W_u + T \frac{\partial s}{\partial r} \tag{243}$$

Comparison of (243) and (237c) shows the expressions to be identical. Hence, this expression is the equation which must be solved. Rewriting (243) and with $\left(W_a \frac{\partial W_a}{\partial r} = \frac{1}{2} \frac{\partial (W_a^2)}{\partial r}\right)$ there is:

$$\frac{\partial (W_a^2)}{\partial r} - 2 W_a \frac{\partial W_r}{\partial z} + \frac{2 W_u}{r} \frac{\partial (r W_u)}{\partial r} + 4 \omega W_u - 2 \frac{\partial H_R}{\partial r} + 2T \frac{\partial s}{\partial r} = 0 \tag{244}$$

Eq. (4), p. 40, can be written:

$$H_R = H_E - \frac{U^2}{2} \tag{4}$$

Also, (5), p. 40, can be written:

$$T_2 = \frac{H_E}{c_p} - \frac{W_2^2}{2c_p} \qquad (5')$$

Eqs. (4) and (5') are now introduced into (244). The nature of the equations relating total relative and equivalent enthalpies dictates that (244) be applied to the rotor discharge with this substitution. Then:

$$\frac{\partial(W_{a_2}^2)}{\partial r_2} - 2W_{a_2}\frac{\partial W_{r_2}}{\partial z} + 2\frac{W_{u_2}}{r_2}\frac{\partial(r_2 W_{u_2})}{\partial r_2} + 4\omega W_{u_2} - 2\frac{\partial}{\partial r_2}\left(H_E - \frac{U_2^2}{2}\right) + 2\left(\frac{H_E}{c_p} - \frac{W_2^2}{2c_p}\right)\frac{\partial s_2}{\partial r_2} = 0 \qquad (245)$$

The multiplier of the final term can be expressed:

$$\frac{1}{c_p}\left[2H_E - \left(W_{a_2}^2 + W_{u_2}^2 + W_{r_2}^2\right)\right] = \frac{1}{c_p}\left[2H_E - W_{u_2}^2 - W_{a_2}^2\left(1 + \frac{W_{r_2}^2}{W_{a_2}^2}\right)\right] \qquad (246)$$

Eq. (246) becomes, with ($\tan^2\lambda = W_r^2/W_a^2$) and ($1+\tan^2\lambda = 1/\cos^2\lambda$):

$$\frac{1}{c_p}\left[2H_E - W_2^2\right] = \frac{1}{c_p}\left[2H_E - W_{u_2}^2\right] - \frac{W_{a_2}^2}{c_p \cos^2\lambda_2} \qquad (247)$$

Eq. (245), combined with (247), and with some rearrangement, gives:

$$\frac{\partial(W_{a_2}^2)}{\partial r_2} - 2W_{a_2}\frac{\partial W_{r_2}}{\partial z} - \frac{W_{a_2}^2}{c_p\cos^2\lambda_2}\frac{\partial s_2}{\partial r_2} + 2\frac{W_{u_2}}{r_2}\frac{\partial(r_2 W_{u_2})}{\partial r_2} + 4\omega W_{u_2} - 2\frac{\partial H_E}{\partial r_2} + \frac{\partial(U_2^2)}{\partial r_2} + \frac{1}{c_p}\left[2H_E - W_{u_2}^2\right]\frac{\partial s_2}{\partial r_2} = 0 \qquad (248)$$

There is also:

$$\frac{\partial(U_2^2)}{\partial r_2} = \frac{\partial(\omega^2 r_2^2)}{\partial r_2} = 2\omega^2 r_2 \frac{\partial r_2}{\partial r_2} = 2\omega^2 r_2 \qquad (249)$$

Eq. (248) and (249) combine to give:

$$\frac{\partial(W_{a_2}^2)}{\partial r_2} - 2W_{a_2}\frac{\partial W_{r_2}}{\partial z} - \frac{W_{a_2}^2}{c_p \cos^2\lambda_2}\frac{\partial s_2}{\partial r_2} - 2\frac{W_{u_2}}{r_2}\frac{\partial(r_2 W_{u_2})}{\partial r_2} + 4\omega W_{u_2} - 2\frac{\partial H_E}{\partial r_2}$$

$$+ 2\omega^2 r_2 + \frac{1}{c_p}\left[2H_E - W_{u_2}^2\right]\frac{\partial s_2}{\partial r_2} = 0 \qquad (250)$$

To make this equation non-dimensional, it is multiplied by $(r_m/W_{a_m}^2)$, where the second subscript, m, denotes the mean streamline value. Then:

$$\frac{r_{2m}}{W_{a_{2m}}^2}\frac{\partial(W_{a_2}^2)}{\partial r_2} - 2\frac{W_{a_2}}{W_{a_{2m}}^2}\frac{W_{a_2}}{W_{a_2}} r_{2m}\frac{\partial(W_{r_2})}{\partial z} - \frac{W_{a_2}^2}{W_{a_{2m}}^2}\frac{r_{2m}}{c_p \cos^2\lambda_2}\frac{\partial s_2}{\partial r_2} + 2\frac{W_{u_2}W_{a_2} r_{2m}}{W_{a_{2m}} W_{a_2} r_2}\frac{\partial\left(\frac{r_2}{r_{2m}}\frac{W_{u_2}}{W_{a_{2m}}}\frac{W_{a_2}}{W_{a_2}}\right)}{\partial(r_2/r_{2m})}$$

$$+ 4\frac{\omega r_{2m} W_{u_2} W_{a_2}}{W_{a_{2m}}^2 W_{a_2}} - 2\frac{r_{2m}}{W_{a_{2m}}^2}\frac{\partial H_E}{\partial r_2} + \frac{2\omega^2 r_2 r_{2m}}{W_{a_{2m}}^2} + \frac{r_{2m}}{c_p}\left[\frac{2H_E}{W_{a_{2m}}^2} - \frac{W_{u_2}^2 W_{a_2}^2}{W_{a_{2m}}^2 W_{a_2}^2}\right]\frac{\partial s_2}{\partial r_2} \quad 0 \qquad (251)$$

Here, it will be observed, the subscripts, '2', can not be neglected unless the equation is to be applied to that station (rotor exit). Since the station of interest is station two, the subscript will be dropped. Let:

$$Y = \frac{W_a}{W_{a_m}} \qquad (252)$$

$$X = \frac{r}{r_m} \qquad (253)$$

and:

$$s^* = \frac{s}{c_p} \qquad (254)$$

Eq. (251) can now be written in terms of these non-dimensional quantities:

$$\frac{\partial(Y^2)}{\partial X} - 2\frac{Y^2}{W_a} r_m \frac{\partial W_r}{\partial z} - \frac{Y^2}{\cos^2\lambda}\frac{\partial s^*}{\partial X} + 2Y\frac{\tan\beta}{X}\frac{\partial(XY\tan\beta)}{\partial X} +$$

$$4\frac{U_m Y \tan\beta}{W_{a_m}} - \frac{2}{W_{a_m}^2}\frac{\partial H_E}{\partial X} + 2\frac{U_m U_2}{W_{a_m}^2} - \left[\frac{2H_E}{W_{a_m}^2} - Y^2\tan^2\beta\right]\frac{\partial s^*}{\partial X} = 0 \qquad (255)$$

But:

$$2Y\frac{\tan\beta}{X}\left[\frac{\partial}{\partial X}(XY\tan\beta)\right]=2Y\frac{\tan\beta}{X}\left[XY\frac{\partial\tan\beta}{\partial X}+X\tan\beta\frac{\partial Y}{\partial X}+Y\tan\beta\frac{\partial X}{\partial X}\right]$$

$$=2Y^2\tan\beta\frac{\partial\tan\beta}{\partial X}+2Y\tan^2\beta\frac{\partial Y}{\partial X}+\frac{2Y^2}{X}\tan^2\beta$$

Also, there is:

$$\frac{\partial\tan\beta}{\partial X}=\frac{1}{\cos^2\beta}\frac{\partial\beta}{\partial X}$$

and:

$$\tan^2\beta\frac{\partial Y}{\partial X}=\tan^2\beta\frac{\partial(Y^2)}{\partial X}$$

Eq. (255) then is:

$$\frac{\partial(Y^2)}{\partial X}(1+\tan^2\beta)-2\frac{Y^2}{W_a}r_m\frac{\partial W_r}{\partial z}-\frac{Y^2}{\cos^2\lambda}\frac{\partial s^*}{\partial X}+2Y^2\frac{\tan\beta}{\cos^2\beta}\frac{\partial\beta}{\partial X}+\frac{2Y^2}{X}\tan^2\beta$$

$$+\frac{4U_mY\tan\beta}{W_{am}}-\frac{2}{W_{am}^2}\frac{\partial H_\varepsilon}{\partial X}+2\frac{U_mU_2}{W_{am}^2}+\left[\frac{2H_\varepsilon}{W_{am}^2}-Y^2\tan^2\beta\right]\frac{\partial s^*}{\partial X}=0 \qquad (256)$$

Multiplying by $(\cos^2\beta/Y^2)$, and, since $(1+\tan^2\beta = 1/\cos^2\beta)$:

$$\frac{1}{Y^2}\frac{\partial(Y^2)}{\partial X}+\cos^2\beta\left(-\frac{2r_m}{W_a}\frac{\partial W_r}{\partial z}-\frac{1}{\cos^2\lambda}\frac{\partial s^*}{\partial X}\right)+2\tan\beta\frac{\partial\beta}{\partial X}+\frac{2}{X}\sin^2\beta+$$

$$\frac{4U_m\sin\beta\cos\beta}{W_{am}Y}+\frac{2U_mU_2\cos^2\beta}{W_{am}^2Y^2}-\frac{2\cos^2\beta}{W_{am}^2Y^2}\frac{\partial H_\varepsilon}{\partial X}+\left[\frac{2H_\varepsilon\cos^2\beta}{W_{am}^2Y^2}-\sin^2\beta\right]\frac{\partial s^*}{\partial X}=0 \qquad (257)$$

The second term of this equation accounts for the effects of streamline curvature, as represented by the $\cos^2\lambda$ and $(-\frac{2r_m}{W_a}\frac{\partial W_r}{\partial z})$. Fig. 15, p. 42, shows the sign convention for streamline curvature (i.e., positive for the radius of curvature in the positive coordinate direction). Fig. 15 defines also the streamline displacement, δr, and the length over which this displacement occurs, L. Streamline curvature can be approxi-

mated:[17]

$$-\frac{1}{W_a}\frac{\partial W_r}{\partial z} = \pm K\frac{\delta r}{L^2} \quad ; \quad K \cong 4 \text{ to } 6 \tag{258}$$

$$\cos^2\lambda = \frac{L^2}{L^2+(\delta r)^2} \tag{259}$$

It must be noted that (258) and (259) are defined here for curvature across the rotor only, because of the small blade heighth of the stator and because of the large flare area available across the rotor. In (258), k is positive for positive curvature. Putting (258) and (259) in (257):

$$\frac{d(\ln Y^2)}{dX} = -\cos^2\beta\left[-\left(\pm 2K r_m\frac{\delta r}{L^2}\right)-\left(\frac{L^2+(\delta r)^2}{L^2}\right)\frac{ds^*}{dX}\right]-2\tan\beta\frac{d\beta}{dX}-\frac{2}{X}\sin^2\beta-$$

$$\frac{4U_m\sin\beta\cos\beta}{W_{am}Y}-\frac{2U_mU_2\cos^2\beta}{W_{am}^2Y^2}+\frac{2\cos^2\beta}{W_{am}^2Y^2}\frac{dH_E}{dX}-\left[\frac{2H_E\cos^2\beta}{W_{am}^2Y^2}-\sin^2\beta\right]\frac{ds^*}{dX} \tag{260}$$

It is evident that (260) is non-dimensional, except for the terms containing equivalent enthalpy in BTU/lbm; let:

$$C_1 = 2gJ \qquad (\text{ft}^2\text{-lbm/BTU-sec}^2) \tag{261}$$

Then, (260) becomes completely non-dimensional as:

$$\frac{d(\ln Y^2)}{dX} = -\cos^2\beta\left[-\left(\pm K\frac{2(\delta r)r_m}{L^2}\right)-\left(\frac{L^2+(\delta r)^2}{L^2}\right)\frac{ds^*}{dX}\right]-2\tan\beta\frac{d\beta}{dX}-\frac{2}{X}\sin^2\beta-$$

$$\frac{4U_m\sin\beta\cos\beta}{W_{am}Y}-\frac{2U_mU_2\cos^2\beta}{W_{am}^2Y^2}+\frac{C_1\cos^2\beta}{W_{am}^2Y^2}\frac{dH_E}{dX}-\left[\frac{C_1H_E\cos^2\beta}{W_{am}^2Y^2}-\sin^2\beta\right]\frac{ds^*}{dX} \tag{262}$$

Eq. (262), the final result, is included in the basic paper as (26).

[17]Vavra, M. H. Aero Thermodynamics and Flow in Turbomachines (New York, London: John Wiley and Sons, Inc., 1960) p. 453.

B. Theoretical Basis for the Area Restriction Factor, ξ.[18]

Fig. 50 shows typical conditions at the exit of a blade row, with boundary layer on both sides of the flow channel. Outside the boundary layer the velocity is very nearly the theoretical velocity. Within the boundary layer, turbulent flow can be assumed, so that the velocity ratio can be taken as:

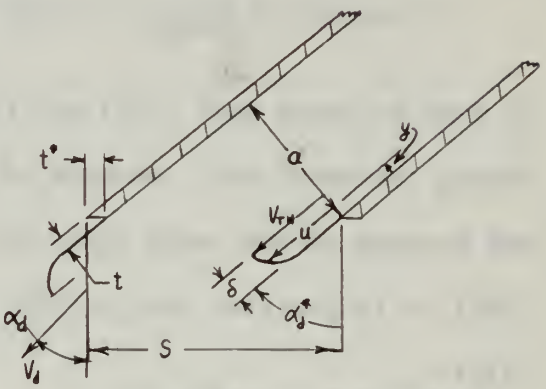

Illustration of Boundary Layer Effects at the Exit of a Blade Row

FIGURE 50

$$\frac{u}{V_{TH}} = \left(\frac{y}{\delta}\right)^{\frac{1}{n}} = \eta^m ; \quad m = \frac{1}{n} \qquad (263)$$

The mass flow rate leaving the blade row can be written:

$$\dot{m} = \rho_{TH} V_{TH} \cos\alpha_d \left(s - \frac{t}{\cos\alpha_d^*} - \frac{\xi\delta}{\cos\alpha_d}\right) + \sum \int_0^\delta u\rho \, dy \qquad (264)$$

Here, ρ_{TH} and V_{TH} are the values for isentropic expansion from inlet total pressure, p_{t_o}, to the pressure at the discharge, p_d, which is assumed constant across the spacing, s.

Fig. 51 depicts the thermodynamic process for the flow outside the boundary layer, and for a point inside the boundary layer. It is evident that the first term of (264) gives the flow rate outside the boundary layer, while the sum of integrals is the flow rate within the boun-

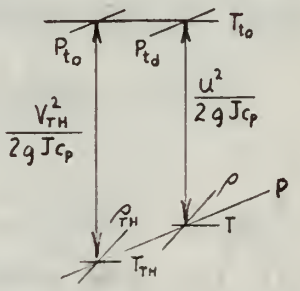

Thermodynamic Process through a Blade Row

FIGURE 51

[18] Vavra, M. H. Problems of Fluid Mechanics in Radial Turbomachines, Parts III and IV (Rhode-Saint-Genese, Belgium: Von Karman Institute for Fluid Dynamics, 1965) VKI Course Note 55b, pp. G46-50.

dary layers. The discharge angle is given by:

$$\alpha_d = \cos^{-1}\left(\frac{a}{s - t/\cos\alpha_d^*}\right) \tag{265}$$

With (265), (264) becomes;

$$\dot{m} = \rho_{TH} V_{TH} \frac{a\cos\alpha_d^*}{s\cos\alpha_d^* - t}\left[\frac{s\cos\alpha_d^* - t}{\cos\alpha_d^*} - \sum\delta\left(\frac{s\cos\alpha_d^* - t}{a\cos\alpha_d^*}\right)\right] + \sum\rho_{TH} V_{TH}\frac{a}{a}\delta\int_0^1 \frac{\rho}{\rho_{TH}}\frac{u}{V_{TH}}d\eta$$

Cancelling terms, there is:

$$\dot{m} = \rho_{TH} V_{TH}\, a\left\{1 - \sum\frac{\delta}{a}\left(1 - \int_0^1 \frac{\rho}{\rho_{TH}}\frac{u}{V_{TH}}d\eta\right)\right\} \tag{266}$$

For the constant pressure assumed at the discharge:

$$\frac{\rho}{\rho_{TH}} = \frac{T_{TH}}{T} = \frac{T_{t_o} - (T_{t_o} - T_{TH})}{T_{t_o} - (T_{t_o} - T_{TH})\left(\frac{u}{V_{TH}}\right)^2} = \frac{1 - X_e}{1 - X_e\left(\frac{u}{V_{TH}}\right)^2} \tag{267}$$

where:

$$X_e = 1 - \left(\frac{P_d}{P_{t_o}}\right)^{\frac{\gamma-1}{\gamma}} \tag{268}$$

Eq. (266) can then be written, with (263), as:

$$\dot{m} = \rho_{TH} V_{TH}\, a\left\{1 - \sum\frac{\delta}{a}\left[1 - (1 - X_e)\int_0^1 \frac{\eta^m}{1 - X_e\eta^{2m}}d\eta\right]\right\} \tag{269}$$

Defining the so-called displacement thickness:

$$\delta^* = \delta\left[1 - (1 - X_e)\int_0^1 \frac{\eta^m}{(1 - X_e\eta^{2m})}d\eta\right] \tag{270}$$

Eq. (269) becomes:

$$\dot{m} = \rho_{TH} V_{TH}\, a\left[1 - \frac{\sum\delta^*}{a}\right] \tag{271}$$

For V_d, the actual average discharge velocity, the loss coefficient of the blade row is:

$$\zeta = 1 - \left(\frac{V_d}{V_{TH}}\right)^2 \tag{272}$$

This loss coefficient can also be expressed in terms of the average loss of kinetic energy. Hence:

$$\zeta = \frac{\Delta E}{\dot{m}\frac{V_{TH}^2}{2}} = 1 - \frac{E}{\dot{m}\frac{V_{TH}^2}{2}} \tag{273}$$

where E is the actual kinetic energy of the flow:

$$E = \rho_{TH} V_{TH} \left(a - \Sigma\delta\right)\frac{V_{TH}^2}{2} + \Sigma\int_0^{\delta} \rho u \frac{u^2}{2} dy \tag{274}$$

Again, the first term represents the value for the extra-boundary layer flow and the second term the value for flow in the boundary layers. Eq. (274), transformed in the manner used to obtain (269), is:

$$E = \rho_{TH} \frac{V_{TH}^3}{2} a \left\{1 - \Sigma\frac{\delta}{a}\left[1 - (1-\chi_e)\int_0^1 \frac{\eta^{3m}}{(1-\chi_e\eta^{2m})} d\eta\right]\right\} \tag{275}$$

Then, the so-called energy thickness is:

$$\delta^{***} = \delta\left[1 - (1-\chi_e)\int_0^1 \frac{\eta^{3m}}{(1-\chi_e\eta^{2m})} d\eta\right] \tag{276}$$

The loss coefficient can now be expressed, using (271), (275), and (276), as:

$$\zeta = 1 - \frac{\rho_{TH}\frac{V_{TH}^3}{2} a\left[1 - \Sigma\frac{\delta^{***}}{a}\right]}{\rho_{TH}\frac{V_{TH}^3}{2} a\left[1 - \Sigma\frac{\delta^*}{a}\right]}$$

or:

$$\zeta = 1 - \frac{1 - \Sigma\frac{\delta^{***}}{a}}{1 - \Sigma\frac{\delta^*}{a}} \tag{277}$$

The area restriction factor, ξ, represents the fraction of the flow area which would be usable for uniform theoretical velocity. The definition of ξ is then:

$$\xi = 1 - \frac{\Sigma\delta^*}{a} \tag{278}$$

Also, the energy parameter is defined as:

$$H^{***} = \frac{\delta^{***}}{\delta^{*}} \tag{279}$$

Using (277) and (279):

$$\zeta \quad \frac{H^{***}-1}{H^{***}-1+\zeta} \tag{280}$$

Here, ζ is the profile loss coefficient.

C. Development of the Energy Parameter.

The integrands of (270) and (276) can be evaluated by expanding the denominator by means of the binomial theorem:

$$(1-X_e\eta^{2m})^{-1} = 1 + X_e\eta^{2m} + X_e^2\eta^{4m} + X_e^3\eta^{6m} + X_e^4\eta^{8m} + \ldots\ldots$$

The integral of (276) is then:

$$\int_0^1 [\eta^{3m} + X_e\eta^{5m} + X_e^2\eta^{7m} + X_e^3\eta^{9m} + X_e^4\eta^{11m} + \ldots.]\, d\eta$$

Integrating:

$$\int_0^1 \frac{\eta^{3m}}{1-X_e\eta^{2m}}\, d\eta = \frac{1}{3m+1} + \frac{X_e}{5m+1} + \frac{X_e^2}{7m+1} + \frac{X_e^3}{9m+1} + \frac{X_e^4}{11m+1} + \ldots.$$

Eq. (276) can now be expanded, giving:

$$\frac{\delta^{***}}{\delta} = 1 - \left(\frac{1}{3m+1} + \frac{X_e}{5m+1} + \frac{X_e^2}{7m+1} + \frac{X_e^3}{9m+1} + \frac{X_e^4}{11m+1}\right) + \frac{X_e}{3m+1} + \frac{X_e^2}{5m+1} + \frac{X_e^3}{7m+1} + \frac{X_e^4}{9m+1} + \frac{X_e^5}{11m+1}$$

or:

$$\frac{\delta^{***}}{\delta} = 1 - (X_e - 1)\left(\frac{1}{3m+1} + \frac{X_e}{5m+1} + \frac{X_e^2}{7m+1} + \frac{X_e^3}{9m+1} + \frac{X_e^4}{11m+1}\right)$$

Then:

$$\frac{\delta^{***}}{\delta} = (X_e - 1)\left(\frac{1}{X_e - 1} + \frac{1}{3m+1} + \frac{X_e}{5m+1} + \frac{X_e^2}{7m+1} + \frac{X_e^3}{9m+1} + \frac{X_e^4}{11m+1}\right) \tag{281}$$

By similar expansion and integration, there is for δ^*/δ :

$$\frac{\delta^*}{\delta} = (X_e - 1)\left(\frac{1}{X_e - 1} + \frac{1}{m+1} + \frac{X_e}{3m+1} + \frac{X_e^2}{5m+1} + \frac{X_e^3}{7m+1} + \frac{X_e^4}{9m+1}\right) \qquad (282)$$

Then, from (281) and (282), the energy parameter is:

$$H^{***} = \frac{\frac{1}{X_e - 1} + \frac{1}{3m+1} + \frac{X_e}{5m+1} + \frac{X_e^2}{7m+1} + \frac{X_e^3}{9m+1} + \frac{X_e^4}{11m+1}}{\frac{1}{X_e - 1} + \frac{1}{m+1} + \frac{X_e}{3m+1} + \frac{X_e^2}{5m+1} + \frac{X_e^3}{7m+1} + \frac{X_e^4}{9m+1}} \qquad (283)$$

Fig. 52 shows H^{***} as a function of pressure ratio for $\gamma = 1.4$ and $m = 0.15$.

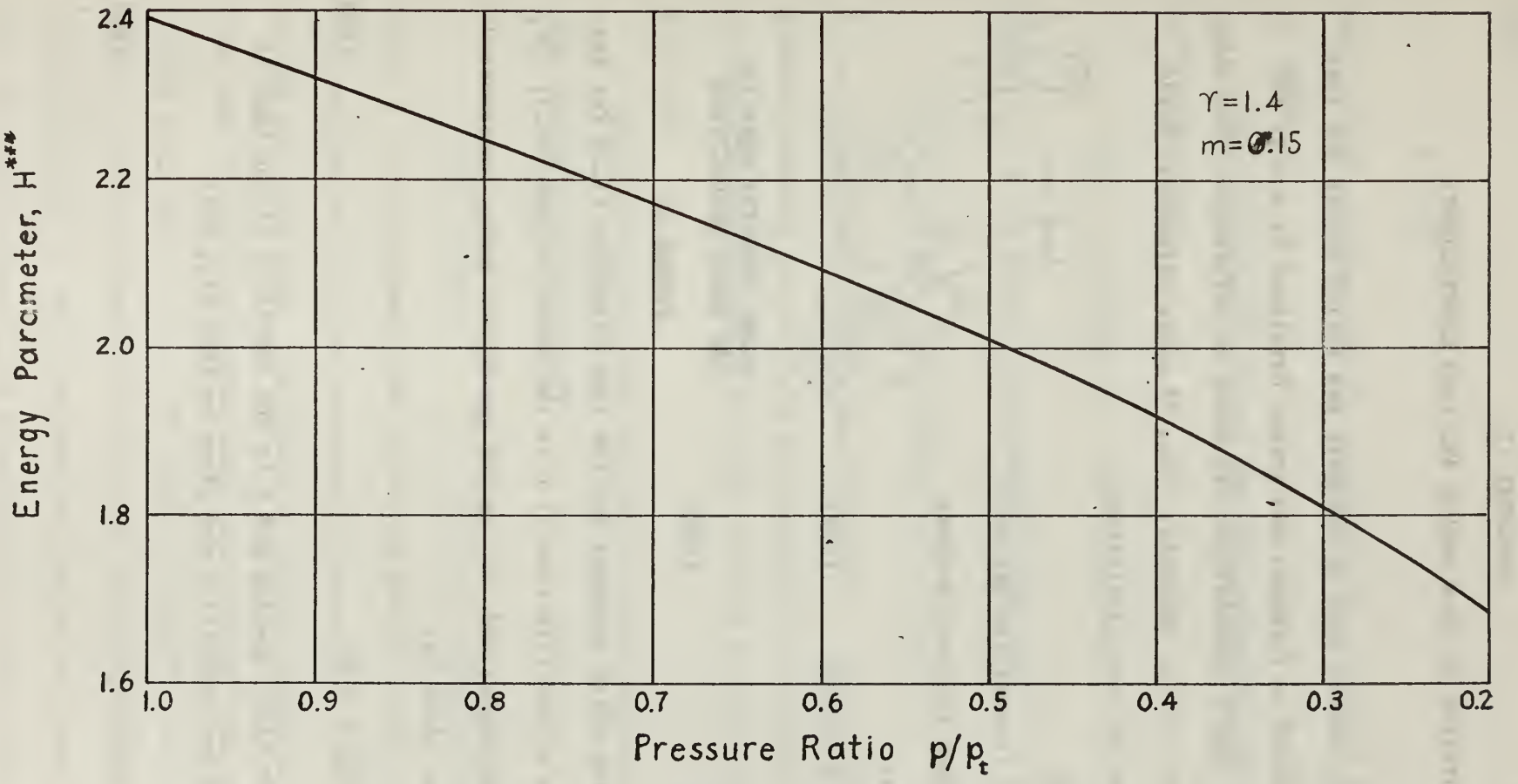

ENERGY PARAMETER H^{***}

AS A FUNCTION OF PRESSURE RATIO

FIGURE 52

APPENDIX II

COMPUTATION OF FLOW ANGLES AND LOSS COEFFICIENTS

A. General.

1. The basic method used to estimate gas outlet angles and loss coefficients is based on formulas and graphs developed by Ainley and Mathieson. [4,5] Where computations are based on information from other sources, footnotes will so indicate. Fig. 53 shows definitive blade geometry pertinent to the calculations.

B. Formulas Used.

The General formula for gas outlet angle prediction for Mach Numbers of 0.5 or less is:

$$\alpha_o = \tan^{-1}\left[(1-A)\tan\alpha_d' + A\tan\alpha_i'\right] \qquad (284)$$

Where:

$$A = F\,\frac{h}{h}\,\frac{\cos\alpha_i'}{\cos\alpha_d'} \qquad (285)$$

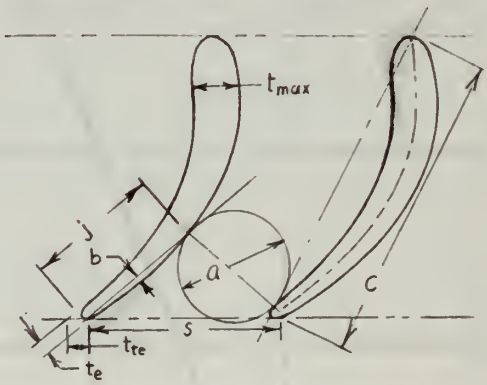

BLADE GEOMETRY USED IN GAS ANGLE PREDICTIONS

FIGURE 53

Here: F is a factor which accounts for the type clearance (1.35 for the unshrouded blades of the TTTR rotor); h is the blade heighth (in.); α_i' is the inlet blade angle; and α_d' is the gas outlet angle, uncorrected for tip clearance, given by:

$$\alpha_d' = \alpha_d^* + 4\,\frac{s}{e} \qquad (286)$$

In (286), s is the blade spacing and e is the curvature of the back of the blade. These two quantities are given by (see Fig. 53):

$$\alpha_d^* = \cos^{-1}\left(\frac{a}{s - t_{te}}\right) \qquad (287)$$

and:

$$e = \frac{j^2}{8b} \tag{288}$$

When a blade row has zero tip clearance the gas outlet angle is given by (286).

For a Mach Number of one, the mean streamline gas outlet angle is determined from:

$$(\alpha_d)_{M=1} = \cos^{-1}\left(\frac{A_{th}}{A_d}\right) \tag{289}$$

where A_{th} is the throat (exit opening) area and:

$$A_d = \frac{\pi}{4}\left(D_{T'}^2 - D_H^2\right) - t_{te} Z (r_T - r_H) \; ; \quad D_{T'} = D_T + 2K \tag{290}$$

It is evident that (289) is basically (287). Flow angles for other Mach Numbers (between 0.5 and 1.0) are estimated by drawing a smooth curve between the values for 0.5 and 1.0, but with an inflection point at M = 0.75.

The basic equation for the profile pressure loss coefficient for zero incidence, $(Y_p)_{i=0}$, is:

$$Y_{P(i=0)} = \left\{ Y_{P(\alpha_i=0)} + \left(\alpha_i/\alpha_{d'}\right)^2 \left[Y_{P(\alpha_i=-\alpha_d)} - Y_{P(\alpha_i=0)} \right] \right\} \left(\frac{t/c}{0.2}\right)^{-\alpha_i/\alpha_{d'}} \tag{291}$$

Here; t is the maximum blade thickness, and the ratio, t/c, is restricted to a maximum of 0.25; and the equality subscripts indicate which data curves are to be used. The values of profile pressure loss coefficient for other then zero incidence angle are obtained from curves of $Y_p/(Y_p)_{i=0}$ versus i/i_s, where i/i_s is the ratio of incidence angle to positive stalling incidence angle. This latter value is defined as the positive incidence angle at which the profile loss is two times its minimum value. For the calculations, i_s is determined from curves based on a solidity of

0.75, with corrections applied for the actual solidity.

Secondary and tip clearance losses are determined using:

$$Y_s + Y_k = \left[\lambda + B\ \frac{k}{h}\right]\left[\frac{C_L}{(s/c)}\right]^2\ \frac{\cos^2\alpha_d}{\cos^3\alpha_m} \tag{292}$$

where: α_m, the mean of the gas inlet and outlet angles, is a function of incidence angle; B is a type-clearance correction factor (0.5 for radial clearance); and:

$$\frac{C_L}{s/c} = 2(\tan\alpha_i + \tan\alpha_d)\cos\alpha_m = f(i) \tag{293}$$

$$\lambda = f\left[(A_d/A_i)^2/(1 + \text{I.D.}/\text{O.D.})\right] \tag{294}$$

Here:

$$A_{(\,)} = Z\, h_{(\,)}\, a_{(\,)} \tag{295}$$

The terms, I.D. and O.D., are the annulus inner and outer diameters in the exit plane, respectively. Values of λ are obtained from a curve based on the bracket quantity of (294).

Leaving losses are found from:[19]

$$\lambda_{MIX} \cong \cos^2\alpha_d\ \frac{(\delta/s)^2}{(1-\delta/s)^2} \tag{296}$$

where, see Fig. 50, p. 156:

$$\frac{\delta}{s} = \frac{\delta^* + t_e}{a + t_e} = \frac{\frac{\delta^*}{a} + \frac{t_e}{a}}{1 + \frac{t_e}{a}} \tag{297}$$

and:

$$\frac{\delta^*}{a} = \frac{\zeta_s + \zeta_p + \zeta_k}{H^{***} - 1 + (\zeta_s + \zeta_k + \zeta_p)} \tag{298}$$

[19]Vavra, M. H. Aero-Thermodynamics and Flow in Turbomachines (New York, London: John Wiley and Sons, Inc., 1960) p. 89.

The energy parameter, H^{***}, is obtained from Fig. 52, p. 161.

The pressure loss coefficients given by (291), (292) and (296) are defined as:

$$Y = \frac{\text{Loss in Total Pressure}}{\text{Outlet Total Pressure - Outlet Static Pressure}}$$

For use in the performance prediction program, values obtained must be converted to the loss coefficient, ζ. For incompressible flow, assumed for these calculations of loss coefficients, the required conversion is:

$$\zeta = \frac{Y}{1+Y} \tag{299}$$

This conversion should not be made, however, until the total pressure loss coefficient has been determined, since:

$$\Sigma\left(\frac{Y_i}{1+Y_i}\right) \neq \frac{\Sigma Y_i}{1+\Sigma Y_i} \tag{300}$$

Nevertheless, in these calculations, it was necessary to convert to ζ for the sum of profile and secondary and tip clearance values of Y in order to obtain the leaving losses. No appreciable error results due to the relatively small magnitude of such leaving losses.

C. Calculations.

Calculations for determining stator gas outlet angles are given in Table VIII, while stator loss coefficients are computed below. Table IX contains the computations for the rotor gas outlet angles and those for the rotor loss coefficients are tabulated in Table X.

Figs. 54 and 55 show the variations of predicted stator gas efflux angles with Mach Number and Radius, respectively; Figs. 56 and 57 show similar information for predicted rotor gas outlet angles. Fig. 58 shows rotor total loss and velocity coefficients versus incidence angle ratio, i/i_s.

Estimation of Stator Loss Coefficients

Losses will be taken as constant with radius and equal to those for the mean radius.

$Y_p = f(s/c, \alpha_i, \alpha_1)$:

$s/c = 0.603$; $\alpha_i = 0$; $\alpha_1 = 76.26^\circ$

$Y_p = 0.05$ (from curves)

$Y_s = \lambda (C_L/(s/c))^2 (\cos^2\alpha_1/\cos^3\alpha_m)$

$\alpha_m = \tan^{-1}(\tan\alpha_1/2) = 63.95^\circ$

$C_L/(s/c) = 2\tan\alpha_1 \cos\alpha_m = 2(4.09)(0.439) = 3.59$

$(C_L/(s/c))^2 = 12.9$

$= f((A_{th}/A_i)^2/(1+\text{I.D.}/\text{O.D.}))$

$A_{th} = aZh = (0.197)(31)(0.69) = 4.216 \text{in.}^2$

$A_i = (\pi/4)(9.17^2 - 7.79^2) = 18.38 \text{in.}^2$

$(A_{th}/A_i)^2/(1+\text{I.D.}/\text{O.D.}) = (4.216/18.38)^2(1+7.79/9.17) = 0.02855$

$= 0.0054$; $\cos\alpha_1 = 0.0567$; $\cos^3\alpha_m = 0.0848$

$Y_s = (0.0054)(12.9)(0.0567/0.0848) = 0.0467$

$Y_s + Y_p = 0.0967$

$\zeta_s + \zeta_p = (0.0967/1.0967) = 0.0883$

$\lambda_{mix} = \cos^2\alpha_1 (\delta/s)^2/(1 - \delta/s)^2$

$H^{***} = 2.28$ $(p/p_t = 0.843)$; $t_e = 0.024$

$\delta^*/a = (\zeta_s + \zeta_p)/(H^{***} - 1 + \zeta_s + \zeta_p) = (0.0883)/(1.28+0.0883) = 0.065$

$\delta/s = (\delta^*/a + t_e/a)/(1 + t_e/a) = (0.065+0.1218)/(1.1218) = 0.1663$

$\lambda_{mix} = (0.0563)(0.1663)^2/(0.8337)^2 = 0.00225$

$\zeta_{mix} = 0.002245$

$\zeta_{total} = 0.09054$

TABLE VIII

CALCULATION OF PREDICTED STATOR GAS OUTLET ANGLES

ITEM	HUB	MEAN	TIP
	$M \leq 0.5$		
radius (r) - in.	3.895	4.24	4.585
radius ratio, $X = r/r_m$	0.919	1.0	1.08
chord (c) - in.	----------	1.425	----------
spacing (s) - in.	0.7895	0.8594	0.9293
exit opening (a) - in.	0.177	0.197	0.223
blockage (t_{t_e}) - in.	----------	0.071	----------
$o = j^2/8b$; b=0.16; j=0.76	----------	4.52	----------
$s-t_{t_e}$	0.7185	0.7884	0.8583
$\cos^{-1}(\frac{a}{s-t_{t_e}})$ - deg.	75.73	75.50	74.93
$\alpha_1^* = f(\cos^{-1}(\frac{a}{s-t_{t_e}}))$	75.73	75.50	74.93
$4(s/o)$	0.698	0.76	0.822
$\alpha_1 = \alpha_1^* + 4(s/o)$	76.43	76.26	75.75
	$M = 1.0$		
$A_{th} = (31)(0.197)(0.69) = 4.216$ in.^{2}			
$A_1 = (\pi/4)(9.17^2 - 7.79^2) - (0.071)(31)(0.69) = 16.86$ in.^{2}			
$\alpha_1)_{M=1} = \cos^{-1}(A_{th}/A_1) = \cos^{-1}(4.216/16.86)$			
$\alpha_1)_{M=1}$		75.5	
$\Delta\alpha = (\alpha_1)_{M=1} - (\alpha_1)_{M\leq 0.5} = -0.76$			
$\alpha_1)_{M=1}$	75.67	75.5	74.99

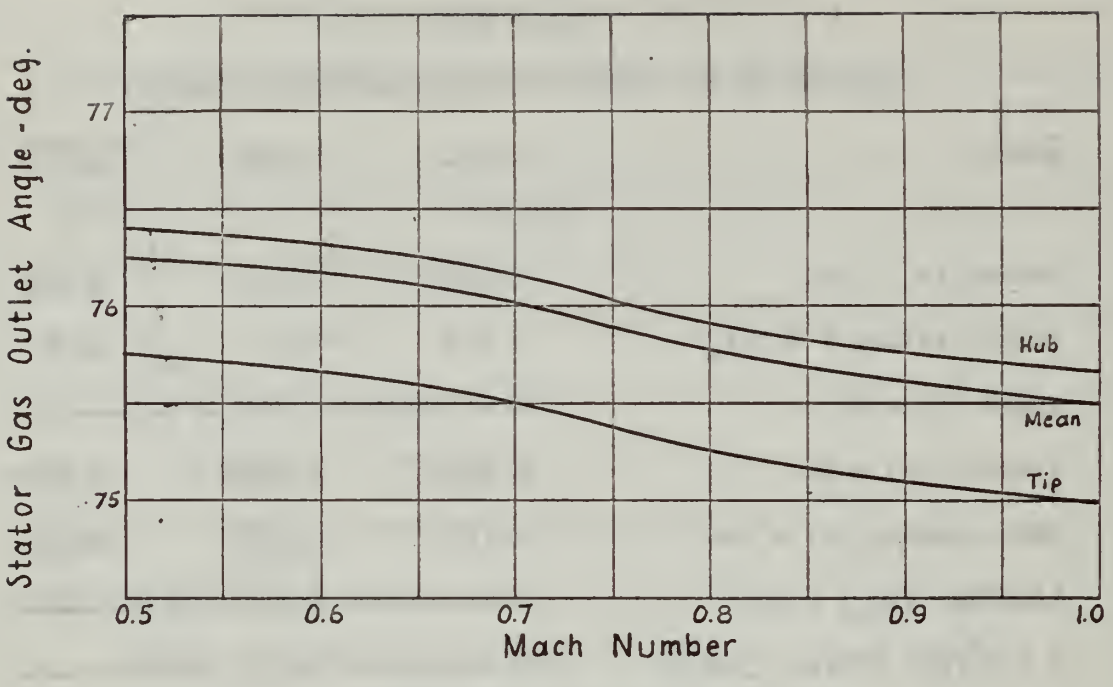

VARIATION OF PREDICTED STATOR
GAS OUTLET ANGLE WITH MACH NUMBER
FIGURE 54

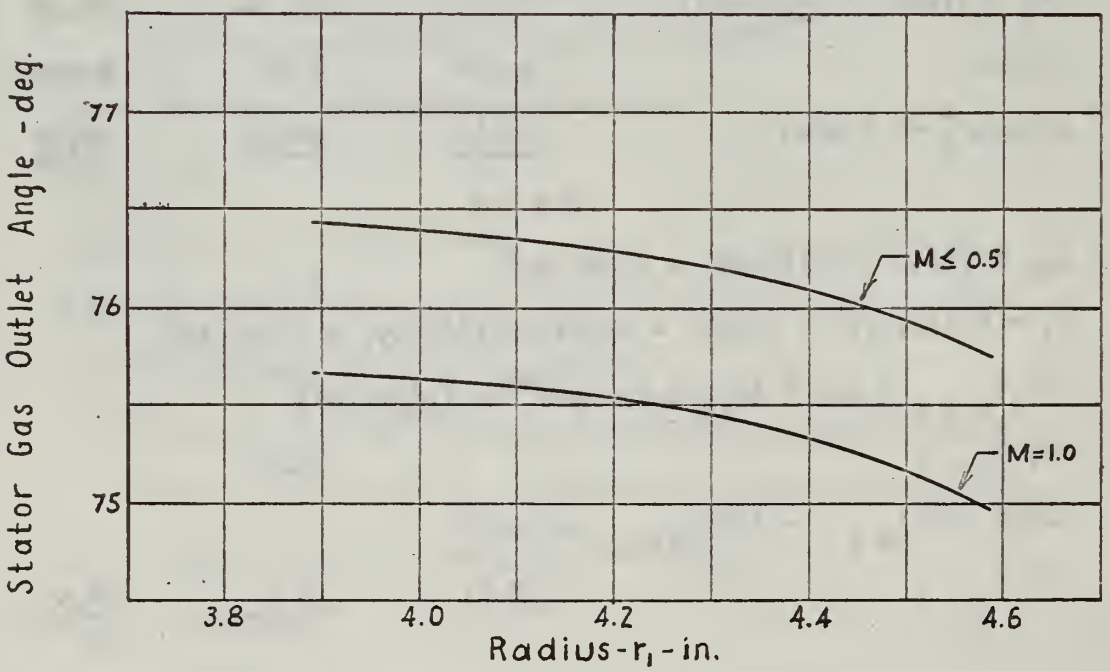

VARIATION OF PREDICTED STATOR
GAS OUTLET ANGLE WITH RADIUS

FIGURE 55

TABLE IX

CALCULATION OF PREDICTED ROTOR GAS OUTLET ANGLES

ITEM	HUB	MEAN	TIP
radius (r) - in.	3.825	4.35	4.875
radius ratio, $X = r/r_m$	0.88	1.0	1.12
chord (c) - in.	----------	0.751	----------
spacing (s) - in.	0.4006	0.4555	0.5224
exit opening (a) - in.	0.117	0.137	0.166
blockage (t_{t_e}) - in.	----------	0.0597	----------
$(s-t_{t_e})$	0.3409	0.3958	0.4627
$\cos^{-1}(\frac{a}{s-t_{t_e}})$ - deg.	-69.95	-69.7	-69.0
$\beta_2^* = f(\cos^{-1}(\frac{a}{s-t_{t_e}}))$ - deg.	-69.45	-69.2	-68.5
$\beta_2' = \beta_2^*$ (since $4s/e = 0$)	-69.45	-69.2	-68.5
tip clearance (k) - in.	----------	0.025	----------
blade heighth (h) - in.	----------	1.05	----------
k/h	----------	0.0238	----------
type-clearance factor (F)	----------	1.35	----------
$\cos\beta_1$ $(\beta_1 = 62^\circ)$	----------	0.469	----------
$\cos\beta_2'$	0.351	0.355	0.366
$\tan\beta_2'$	-2.67	-2.64	-2.54
$A = F(k/h)(\cos\beta_1/\cos\beta_2')$	0.043	0.0425	0.04125
(1-A)	0.957	0.9575	0.95875
$(1-A)\tan\beta_2'$	-2.555	-2.525	-2.435
$A(\tan\beta_1)$	0.0809	0.0799	0.0775
$C = ((1-A)\tan\beta_2' + A(\tan\beta_1))$	-2.474	-2.445	-2.358
$\beta_2 = \tan^{-1}(C)$	-68.0	-67.76	-67.0

TABLE IX (continued)

ITEM	HUB	MEAN	TIP

The foregoing calculations are for $M \leq 0.5$.

M_2=1, Mean Radius

$$A_t = A_t'(1-k/h) + D_T k$$

$$A_t' = aZh = (0.137)(60)(1.05) = 9.45$$

$$A_t = (9.45)(0.9762) + (9.75)(0.025) = 8.43+0.0766$$

$$A_t = 9.196 \text{ in.}^2$$

$$A_{n_2} = (\pi/4)((D_T+2k)^2 - D_H^2) - t_{t_e} Zh$$

$$= (\pi/4)((9.8)^2 - (7.65)^2) - (0.0579)(60)(1.05)$$

$$A_{n_2} = 29.2 - 3.645 = 25.655 \text{ in.}^2$$

$$\beta_2 = \cos^{-1}(A_{th}/A_{n_2}) = \cos^{-1}(9.196/25.655)$$

β_2 - deg.		-69.0	
$\Delta\beta_2 = (\beta_2)_{M=1} - (\beta_2)_{M \leq 0.5} = -1.24$ deg.			
β_2 - deg.	-69.24	-69.0	-68.24

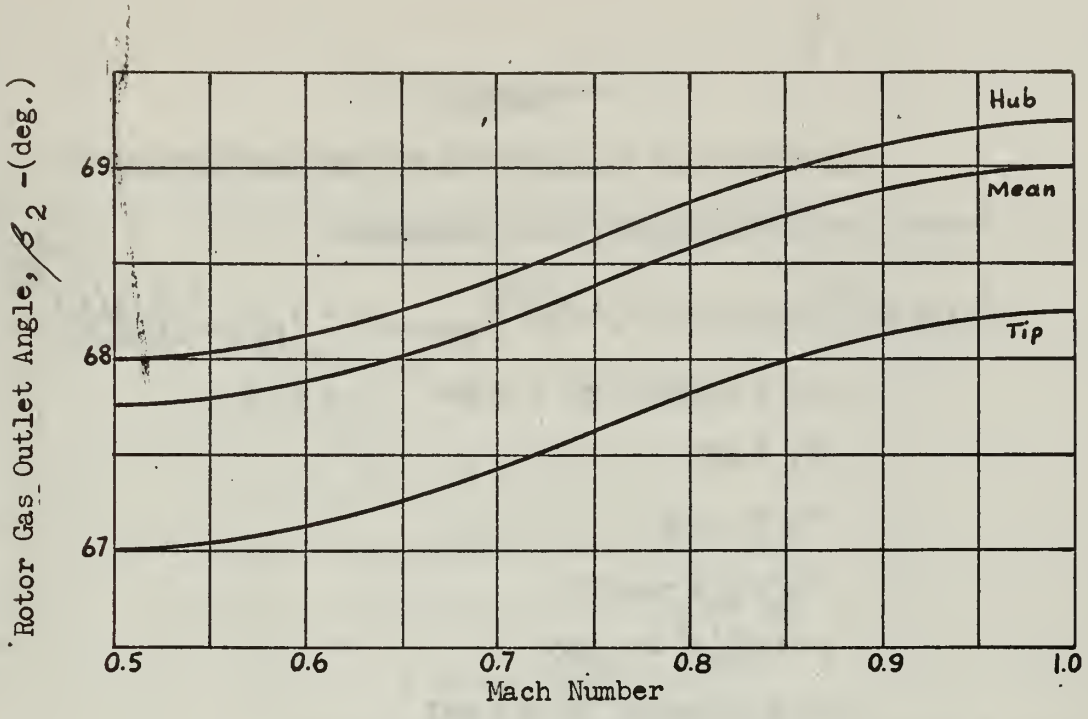

VARIATION OF PREDICTED ROTOR
GAS OUTLET ANGLE WITH MACH NUMBER

FIGURE 56

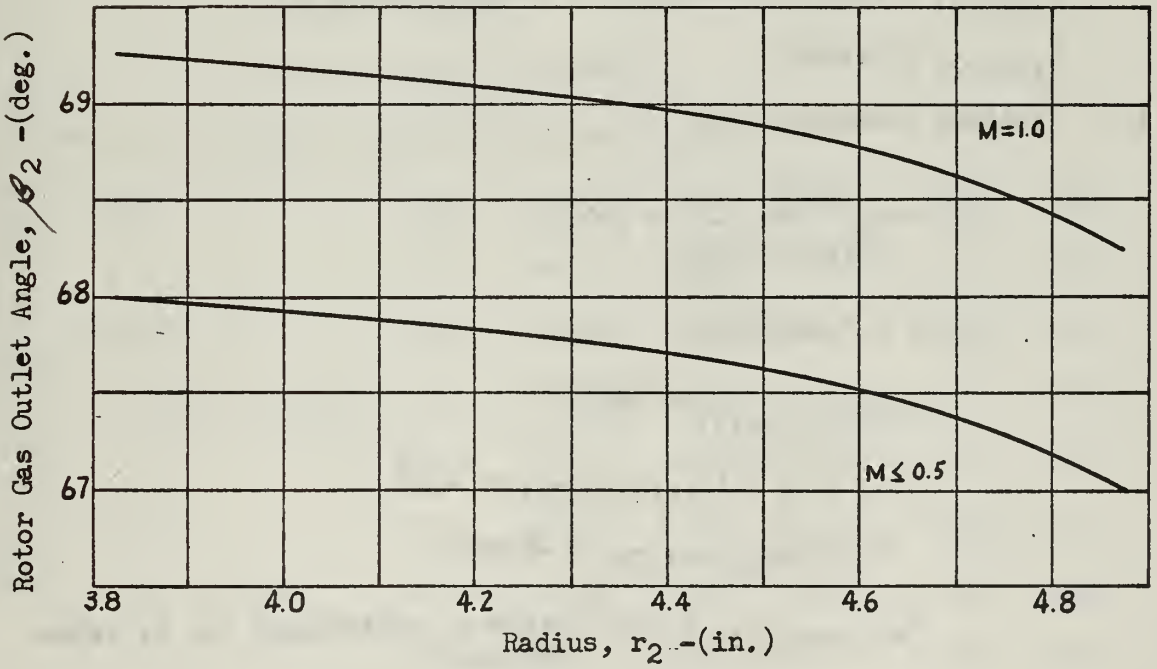

VARIATION OF PREDICTED ROTOR
GAS OUTLET ANGLE WITH RADIUS

FIGURE 57

TABLE X

CALCULATION OF PREDICTED ROTOR LOSS COEFFICIENTS

a. Profile Loss Coefficient, Zero Incidence.

$$Y_{p(i=0)} = \left\{Y_{p(\beta_1=0)} + (\beta_1/\beta_2')^2 \left[Y_{p(\beta_1=-\beta_2')} - Y_{p(\beta_1=0)}\right]\right\}\left(\frac{t/c}{0.2}\right)^{-\beta_1/\beta_2'}$$

$t/c = 0.296/0.751 = 0.394$ use 0.25

$\beta_1 = 62^\circ$

$\beta_2' = -69.2$

$\beta_1/\beta_2' = -0.897$

$(\beta_1/\beta_2')^2 = 0.803$

$s/c = 0.4555/0.751 = 0.607$

$Y_{p(\beta_1=0)} = 0.038$

$Y_{p(\beta_1=-\beta_2')} = 0.14$

$Y_{p(i=0)} = (0.038 + 0.803(0.14 - 0.038))(0.25/0.2)^{0.897}$

$Y_{p(i=0)} = 0.1464$

b. Stalling Incidence (i_s)

$$\frac{\beta_2}{\beta_{2(s/c=0.75)}} = 1.05$$

$\beta_2 = -67.76^\circ$

$\beta_{2(s/c=0.75)} = -64.5^\circ$

$\Delta i_s = i_s - i_{s(s/c=0.75)} = 4.4^\circ$

$\beta_1/\beta_{2(s/c=0.75)} = -0.962$

$i_{s(s/c=0.75)} = 9.0^\circ$ (value is conjectural due to extrapolation)

$i_s = 13.4^\circ$

TABLE X (continued)

c. Secondary and Tip Clearance Losses.

$Y_s + Y_k = [\lambda + B(k/h)]\,[C_L/(s/c)]^2\,(\cos^2\beta_2/\cos^3\beta_m)$

$B = 0.5$

$k/h = 0.0238$

$\cos^2\beta_2 = 0.1435$

$\lambda = f((A_2/A_1)^2/(1+I.D./O.D.))$

$A_2 = Zh_2a_2 = (60)(1.05)(0.137) = 8.63\ in^2$

$A_1 = Zh_1a_1 = (60)(1.05)(0.194) = 8.85\ in^2$

$(1+I.D./O.D.) = 1+7.65/9.80 = 1.765$

$((A_2/A_1)^2/(1+I.D./O.D.)) = (8.63/8.85)^2(1/1.765) = 0.538$

$\lambda = 0.03$ (extrapolated)

$Bk/h = 0.0119$

$\lambda + Bk/h = 0.0419$

$(\lambda + Bk/h)\cos^2\beta_2 = 0.00601$

$Y_s + Y_k = 0.00601\,(C_L/(s/c))^2(1/\cos^3\beta_m)$

i/i_s	-3.0	-1.5	-0.8	0.0	0.5	1.0
i	-40.2	-20.1	-10.72	0	6.7	13.4
$\tan\beta_1$	0.4	0.866	1.247	1.88	2.565	2.84
$(\tan\beta_1+\tan\beta_2)/2$	-1.022	-0.7875	-0.599	-0.2825	0.6	0.1975
β_m	-45.6	-38.3	-30.95	-15.8	3.45	11.2
$\cos\beta_m$	0.7	0.785	0.857	0.962	0.997	0.98
$\tan\beta_1 - \tan\beta_2$	2.845	3.311	3.692	4.325	5.010	5.285
$C_L/(s/c)$	3.98	5.20	6.32	8.33	10.0	10.34
$(C_L/(s/c))^2$	15.9	27.0	40.0	69.3	100.	107.5
$(1/\cos^3\beta_m)$	2.92	2.07	1.588	1.122	1.008	1.063
$Y_s + Y_k$	0.279	0.338	0.382	0.468	0.606	0.689

TABLE X (continued)

i/i_s	-3.0	-1.5	-0.8	0.0	0.5	1.0
$Y_s + Y_k$	0.279	0.338	0.382	0.468	0.606	0.689
d. Total Loss Coefficient.						
$Y_p/Y_{p(i=0)}$	4.28	2.1	1.42	1.0	1.22	2.08
Y_p	0.626	0.3075	0.208	0.1464	0.1787	0.3045
$Y_p + Y_s + Y_k$	0.905	0.6455	0.59	0.6144	0.7847	0.9935
$\zeta_p + \zeta_s + \zeta_k$	0.475	0.3925	0.371	0.38	0.439	0.498
$H^{***}-1$ $(M_2=0.5)$	1.28	1.28	1.28	1.28	1.28	1.28
$H^{***}-1+\zeta_p+\zeta_s+\zeta_k$	1.755	1.6725	1.651	1.66	1.719	1.778
δ^*/a	0.271	0.235	0.225	0.229	0.255	0.280
t_e/a	0.1824	-----same----------				
$\delta^*/a + t_e/a$	0.4534	0.4174	0.4074	0.4114	0.4374	0.4624
δ/s	0.3835	0.353	0.345	0.348	0.370	0.3915
$(1-\delta/s)$	0.6165	0.647	0.655	0.652	0.630	0.6085
$(\delta/s)^2$	0.147	0.1245	0.119	0.121	0.137	0.153
$(1-\delta/s)^2$	0.38	0.419	0.429	0.425	0.396	0.37
$(\delta/s)^2/(1-\delta/s)^2$	0.387	0.2975	0.278	0.285	0.346	0.414
λ_{mix}	0.0555	0.0426	0.0399	0.0409	0.0496	0.0594
ζ_{mix}	0.0526	0.0408	0.0384	0.0393	0.0473	0.056
ζ_{total}	0.5276	0.4333	0.4094	0.4193	0.4863	0.554
$\eta=1-\zeta_{tot}$	0.4724	0.5667	0.5906	0.5807	0.5137	0.446
$\psi=\sqrt{\eta}$	0.688	0.752	0.77	0.763	0.717	0.669
Take the profile loss coefficient as: $\zeta_p = (Y_p/(Y_p+Y_s+Y_k))\,\zeta_{total}$						
ζ_p	0.3295	0.187	0.1309	0.0906	0.10	0.1529

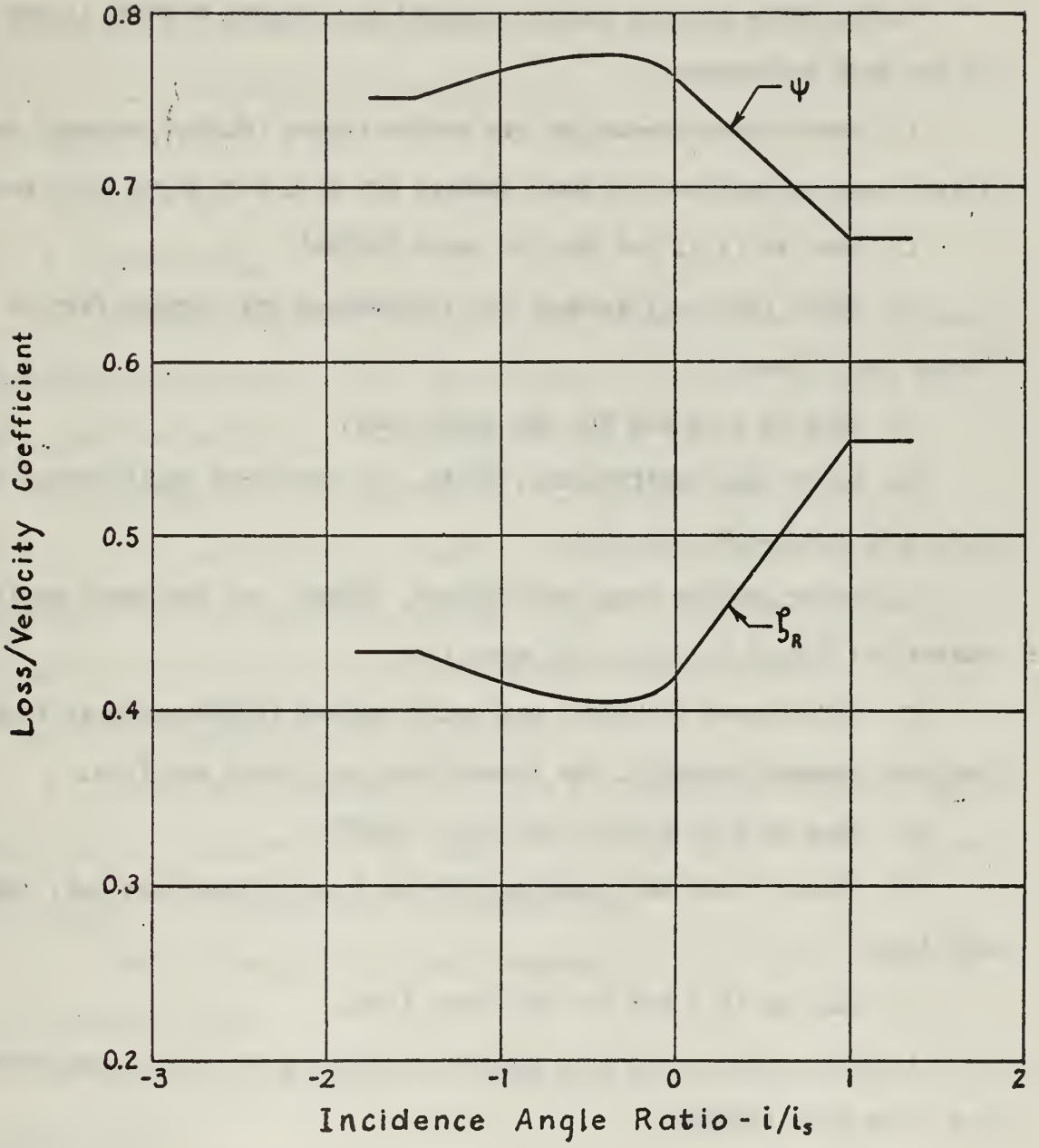

VARIATION OF ROTOR LOSS AND VELOCITY COEFFICIENTS
WITH THE RATIO OF
INCIDENCE ANGLE TO POSITIVE STALLING INCIDENCE ANGLE

FIGURE 58

APPENDIX III

COMPUTER PROGRAM FOR TURBINE PERFORMANCE PREDICTION

A. Inputs.

Listed below are the inputs required for Program PERFORM in the order of the READ statements.

1. Stator mean streamline gas outlet angles (ALFAM--radians) for stator mean streamline exit Mach Numbers of: 0.5, 0.7, 0.75, 0.8, and 1.

2. Same as (1.), but for the rotor (BETAM).

3. Radii (RS--in.) assumed for streamlines one through five at the stator exit plane.

4. Same as (3.) but for the rotor (RR).

5. Rotor loss coefficients, ZETAR, for incidence angle ratios of: 0.0, 0.5, 1.0, -0.8, and -1.5.

6. Rotor profile loss coefficients, ZETAPR, for incidence angle ratios of: 0.0, 0.5, 1.0, -0.8, and -1.5.

7. Differences in stator gas outlet angles (DALF--radians) from the mean streamline angle, for streamlines one, three and five.

8. Same as (7.) but for the rotor (DBET).

9. Stator blade exit opening (AS--in.) for streamlines one, three, and five.

10. Same as (9.) but for the rotor (AR).

11. The number of sets of assumed conditions for which computations are to be made (NSETS).

12. Assumed conditions for sets one through NSETS: stator mean streamline exit Mach Number (AMS); inlet total pressure (PTO--psia); inlet total temperature (TTO--$^{\circ}$R); rotor exit mean streamline Mach Number (AMR); wheel speed (RPM); and an indicator (NIND) which denotes whether assumed conditions except RPM are the same (NIND $\neq$ 0) or not (NIND = 0).

B. Outputs.

Sample output is included at the end of the program. Since symbols used to label output are generally those used in the analysis, printouts are self-explanatory for the most part. Printouts requiring clarification of meaning are given below in the order of the program output.

1. I-( ) denotes the integrand of ( ).

2. XI = ξ

3. PHI = Φ

4. ARAT = a/a_m

5. The SUMS 1-4, WSUM line gives the values of flow rate integrals between streamlines (in order) one and two, two and three, three and four, and four and five, followed by the sum of these values.

6. STREAMLINE FLOW FRACTIONS, M = . Here, M denotes the stator (M = 1) or the rotor (M = 2). Numbers printed are the value of $X = r/r_m$ followed by the flow fraction passing between the hub streamline and the streamline at X for streamlines two three and four in order.

7. W-FRAC denotes flow fraction.

8. The CONSTANT INTEGRAND 1-5 line of the ROTOR SOLUTION gives the values of the integrand for the angle part of Eq. (33) plus the entropy part ds_1^*/dX_2 for streamlines one through five.

9. INT2 is that part of the integrand of (33) for the remainder of the entropy term.

10. INT3 is that part of the integrand of (33) due to the equivalent enthalpy term.

11. INT4 is that part of the integrand of (33) due to coriolis acceleration and rotor peripheral velocity.

12. INT is the total integrand of (33) [illegible]

13. DSDX1-2 denotes ds_1^*/dX_2.

Units of printed values are: temperatures--°R; pressures--psia; angles--radians; velocities--ft/sec; radii--in.; and enthalpy terms--BTU/lbm.

```
..JOB0355F, ECKERT R H
      PROGRAM PERFORM
      DIMENSION ALFAM(10),BETAM(10),RS(10),RR(10),ZETAR(10),ZETAPR(10),
     1DALF(10),DBET(10),AS(10),AR(10),X1(10),X2(10),ALFA1(10),BETA2(10),
     2T1(10),P1(10),V1(10),VA1(10),SI1(10),SI2(10),YS(10),S1(10),
     3DSDX1(10),VU1(10),PRAT1(10),ZETAPS(10),WI1(10),VA2(10),WPER1(10),
     4U(10),BETA1(10),HE(10),TTE(10),PTE(10),W1(10),WU1(10),DHEDX(10),
     5DSDX2(10),WU2(10),W2(10),VU2(10),V2(10),YR(10),RI1(10),RI2(10),
     6RI3(10),RI4(10),RI(10),SR1(10),SR2(10),YOLD(10),AA(10),SR(10),
     7P2(10),T2(10),PRAT2(10),WPER2(10),DWDX(10),U2(10),T1IS(10),
     8 T2IS(10),PRAT3(10),SS(10),ALFA2(10)
      DIMENSION DELH(10),TT2(10),PT2(10),PT1(10),T2S(10),
     1ETAI(10),ETAS(10),PSIR(10),RSTAR(10),AKIS(10),ETAR(10)
      G=32.174
      CJ=778.16
      CP=0.24
      GAM=1.4
      EXP1=GAM/(GAM-1.)
      EXP2=1./EXP1
      READ 1,(ALFAM(I),I=1,5)
    1 FORMAT(5F8.4)
      READ 1,(BETAM(I),I=1,5)
      READ 1,(RS(I),I=1,5)
      READ 1,(RR(I),I=1,5)
      READ  1,(ZETAR(I),I=1,5)
      READ  1,(ZETAPR(I),I=1,5)
      READ 2,(DALF(I),I=1,5,2)
    2 FORMAT(3F8.4)
      READ 2,(DBET(I),I=1,5,2)
      READ 2,(AS(I),I=1,5,2)
      READ 2,(AR(I),I=1,5,2)
      CALL PARAB (ALFAM,1,2,3,AA1,BA1,CA1,0.5,0.7,0.75)
      CALL PARAB(ALFAM,3,4,5,AA2,BA2,CA2,0.75,0.8,1.0)
      CALL PARAB (BETAM,1,2,3,AB1,BB1,CB1,0.5,0.7,0.75)
      CALL PARAB (BETAM,3,4,5,AB2,BB2,CB2,0.75,0.8,1.0)
      DO 10 I=1,5
```

```
      X1(I)=RS(I)/RS(3)
   10 X2(I)=RR(I)/RR(3)
      ASF=AS(3)
      RSF=RS(3)
      ARF=AR(3)
      RRF=RR(3)
      AS(1)=AS(1)/AS(3)
      AS(5)=AS(5)/AS(3)
      AR(1)=AR(1)/AR(3)
      AR(5)=AR(5)/AR(3)
      AS(3)=1.
      AR(3)=1.0
      XS1=X1(1)
      XS3=X1(3)
      XS5=X1(5)
      XR1=X2(1)
      XR3=X2(3)
      XR5=X2(5)
      CALL PARAB (AS,1,3,5,AAS,BAS,CAS,XS1,XS3,XS5)
      CALL PARAB (AR,1,3,5,AAR,BAR,CAR,XR1,XR3,XR5)
      CALL PARAB(ZETAR,1,2,3,AZR1,BZR1,CZR1,0.,0.5,1.0)
      CALL PARAB(ZETAPR,1,2,3,AZPR1,BZPR1,CZPR1,0.,0.5,1.0)
      CALL PARAB(ZETAR,1,4,5,AZR2,BZR2,CZR2,0.,-0.8,-1.5)
      CALL PARAB(ZETAPR,1,4,5,AZPR2,BZPR2,CZPR2,0.,-0.8,-1.5)
      PRINT 999
      PRINT 35
  350FORMAT (/40H  PARABOLA CONSTANTS-IN FOLLOWING ORDER*,/22H ALFAM=F(
     1M,M=0.5-0.75), /22H ALFAM=F(M,M=0.75-1.0), /22H BETAM=F(M,M=0.5-0.
     275),/22H BETAM=F(M,M=0.75-1.0),/15H AS/AS(3)=F(X1),/15H AR/AR(3)=F
     3(X2),/ 26H ZETAR=F(I/IS,I/IS=0 TO 1),/27H ZETAPR=F(I/IS,I/IS=0 TO
     41),/29H ZETAR=F(I/IS,I/IS=0 TO -1.5),/30H ZETAPR=F(I/IS,I/IS=0 TO
     5-1.5),/32H ZETAR=F(I/IS,I/IS=-0.8 TO -3.0),/33H ZETAPR=F(I/IS,I/IS
     6=-0.8 TO -3.0),)
      PRINT 3,AA1,BA1,CA1
    3 FORMAT ( 23H                          A=,F10.5,3H B=,F10.5,3H C=,F10.5)
      PRINT 3,AA2,BA2,CA2
```

```
      PRINT 3,AB1,BB1,CB1
      PRINT 3,AB2,BB2,CB2
      PRINT 3,AAS,BAS,CAS
      PRINT 3,AAR,BAR,CAR
      PRINT 3,AZR1,BZR1,CZR1
      PRINT 3,AZPR1,BZPR1,CZPR1
      PRINT 3,AZR2,BZR2,CZR2
      PRINT 3,AZPR2,BZPR2,CZPR2
      PRINT 3,AZR3,BZR3,CZR3
      PRINT 3,AZPR3,BZPR3,CZPR3
      READ 4,NSETS
    4 FORMAT(I5)
      DO 400 J=1,NSETS
      READ 5,AMS,PTO,TTO,AMR,RPM,NIND
    5 FORMAT(5F8.4,I5)
      IF (NIND) 300,290,300
  290 IF(AMS-0.75) 30,40,50
   30 ALFA1(3)=AA1+BA1*AMS+CA1*AMS**2
      GO TO 60
   40 ALFA1(3)=ALFAM(3)
      GO TO 60
   50 IF (AMS-1.) 280,270,270
  270 ALFA1(3)=ALFAM(5)
      GO TO 60
  280 ALFA1(3)=AA2+BA2*AMS+CA2*AMS**2
   60 IF(AMR-0.75) 70,80,90
   70 BETA2(3)=AB1+BB1*AMR+CB1*AMR**2
      GO TO 100
   80 BETA2(3)=BETAM(3)
      GO TO 100
   90 BETA2(3)=AB2+BB2*AMR+CB2*AMR**2
  100 PRINT 999
  999 FORMAT (1H1)
      PRINT 9
      PRINT 7
    7 FORMAT (/45H SET NO.  PTO      TTO    M-STAT   M-ROTOR    RPM)
```

```
      PRINT 8,J,PTO,TTO,AMS,AMR,RPM
    8 FORMAT (I5,F9.2,F8.2,F7.2,F8.2,F10.0)
      DO 110 I=1,5,2
      ALFA1(I)=ALFA1(3)+DALF(I)
      BETA2(I)=BETA2(3)+DBET(I)
  110 CONTINUE
      CALL PARAB(ALFA1,1,3,5,AA3,BA3,CA3,XS1,XS3,XS5)
      CALL PARAB(BETA2,1,3,5,AB3,BB3,CB3,XR1,XR3,XR5)
      CALL STATOR(ALFA1,X1,1.,AA3,BA3,CA3,TTO,PTO,AMS,T1,P1,V1,VA1,
     1SI1,SI2,YS,S1,DSDX1,VU1,PRAT1,T1IS,SS)
      DO 120 I=1,5
      ZETAPS(I)=.0476
      PTE(I)=PTO
  120 TTE(I)=TTO
      CALL FLOWREF (PRAT1,ZETAPS,AAS,BAS,CAS,X1,WI1,PTE,PTO,TTE,TTO,ASF,
     131.,RSF,ASF,31.,RSF,1,WSTAT,VA2,WPER1,CODE,WLBM)
      VA2(3)=170.
      YR(1)=0.82
      YR(2)=0.92
      YR(3)=1.0
      YR(4)=1.075
      YR(5)=1.12
      FC1=1.
      FC2=FC1**2
  300 PRINT 999
      PRINT 9
    9 FORMAT (43H                                  STATOR SOLUTION)
      PRINT 7
      PRINT 8,J,PTO,TTO,AMS,AMR,RPM
      PRINT 11
   110FORMAT (/65H SLINE    R1       X1      S1      DSDX1 I-DSDX  I-ALFA  I
     1-TOTAL    Y)
      DO 140 I=1,5
   12 FORMAT (I4,2F8.3,6F8.5)
  140 PRINT 12,I,RS(I),X1(I),S1(I),DSDX1(I),SS(I),SI1(I),SI2(I),YS(I)
      CALL ROTOR1(VU1,VA1,RPM,U,BETA1,HE,TTE,PTE,X2,P1,T1,W1,WU1,X1,
```

```
     1RS,AZR1,BZR1,CZR1,AZR2,BZR2,CZR2,ZETAR,ZETAPR,AZPR1,BZPR1,CZPR1,
     2AZPR2,BZPR2,CZPR2,RR,DHEDX,DSDX1,S1,U2,OMEG,AZR3,BZR3,CZR3,
     3AZPR3,BZPR3,CZPR3)
      PRINT 13
  130FORMAT (/60H SLINE    T1       P1     ALFA1    BETA1     U1     W-FRAC
     1PTO/P1)
      DO 150 I=1,5
      PRAT1(I)=1./PRAT1(I)
   14 FORMAT (I4,F9.2,F7.2,2F8.4,F8.2,2F8.4)
  150 PRINT 14,I,T1(I),P1(I),ALFA1(I),BETA1(I),U(I),WPER1(I),PRAT1(I)
      PRINT 15
   15 FORMAT (/43H SLINE  VA1      VU1      V1       WU1       W1)
      DO 160 I=1,5
   16 FORMAT(I4,5F8.1)
  160 PRINT 16,I,VA1(I),VU1(I),V1(I),WU1(I),W1(I)
      CODE=1.
      PRINT 999
      PRINT 17
      PRINT 7
      PRINT 8,J,PTO,TTO,AMS,AMR,RPM
  201 DO 200 K=1,10
      CALL ROTOR2 (BETA2,HE,DHEDX,DSDX1,DSDX2,VA2,WU2,W2,VU2,V2,X2,U2,
     1FC1,FC2,AB3,BB3,CB3,YR,ZETAR,RI1,RI2,RI3,RI4,RI,SR1,SR2,YOLD,AA,
     2 SR,TTE,PTE,T2,P2,PRAT2,T2S,INDS)
      IF (INDS-1) 310,320,310
  320 PRINT 36,(AA(I),I=1,5)
   36 FORMAT (/35H ENTROPY INDETERMINATE,PRINT AA 1-5, 5F8.3)
      GO TO 400
 3100CALL FLOWREF (PRAT2,ZETAPR,AAR,BAR,CAR,X2,WI1,PTE,PTO,TTE,TTO,
     1 ASF,31.,RSF,ARF,60.,RRF,2,WSTAT,VA2,WPER2,CODE)
      IF (CODE-20.) 200,130,200
  200 CONTINUE
  130 CALL SLINE (RR,X2,DWDX,WPER2,WPER1,HE,U2,DHEDX,S1,DSDX1,
     1ARF,RRF,AAR,BAR,CAR,FC1,FC2,CODE)
      IF (CODE-40.) 201,220,201
  220 PRINT 999
```

```
      PRINT 17
   17 FORMAT (43H                                    ROTOR SOLUTION)
      PRINT 7
      PRINT 8,J,PTO,TTO,AMS,AMR,RPM
      PRINT 18
  180FORMAT (/68H SLINE    R2       X2     TTE       PTE    ZETAR    ZETAPR
     1DHEDX  DSDX1-2)
      DO 170 I=1,5
   19 FORMAT (I4,2F8.3,2F8.2,2F8.5,F8.3,F8.5)
 1700PRINT 19,I,RR(I),X2(I),TTE(I),PTE(I),ZETAR(I),ZETAPR(I),DHEDX(I),
     1DSDX1(I)
      PRINT 21
  210FORMAT (/66H SLINE    S2     DSDX2  I-BETA  I-OMEG I-DHEDX  I-DSDX
     1 I-TOT      Y)
      DO 180 I=1,5
   22 FORMAT (I4,F9.4,F7.5,6F8.4)
  180 PRINT 22,I,SR(I),DSDX2(I),RI1(I),RI2(I),RI3(I),RI4(I),RI(I),YR(I)
      PRINT 23
  230FORMAT (/60H SLINE    T2       P2    PTO/P2    ALFA2    BETA2     U2
     1W-FRAC)
      DO 190 I=1,5
      PRAT3(I)=PTO/P2(I)
      ALFA2(I)=ATANF(VU2(I)/VA2(I))
      V2(I)=VA2(I)/COSF(ALFA2(I))
   24 FORMAT (I4,F9.2,F7.2,3F8.3,F8.2,F8.5)
 1900PRINT 24,I,T2(I),P2(I),PRAT3(I),ALFA2(I),BETA2(I),U2(I),WPER2(I)
      PRINT 25
   25 FORMAT (/42H SLINE  VA2      VU2      V2       WU2      W2)
      DO 210 I=1,5
   26 FORMAT (I4,5F8.1)
  210 PRINT 26,I,VA2(I),VU2(I),V2(I),WU2(I),W2(I)
      DO 230 I=1,5
      DELH(I)=(U(I)*VU1(I)-U2(I)*VU2(I))/(G*CJ)
      TT2(I)=TTO-DELH(I)/CP
      PT2(I)=P2(I)*(TT2(I)/T2(I))**EXP1
      PT1(I)=P1(I)*(TTO/T1(I))**EXP1
```

```
      T2IS(I)=TTO*(P2(I)/PTO)**EXP2
      T2S(I)=TTE(I)*(P2(I)/PTE(I))**EXP2
      ETAI(I)=(TTO-TT2(I))/(TTO-T2IS(I))
      ETAS(I)=(TTO-T1(I))/(TTO-T1IS(I))
      ETAR(I)=(TTE(I)-T2(I))/(TTE(I)-T2S(I))
      RSTAR(I)=(T1IS(I)-T2IS(I))/(TTO-T2IS(I))
      AKIS(I)=2.*G*CJ*CP*(TTO-T2IS(I))/U(I)**2
  230 PSIR(I)=SQRTF(ETAR(I))
      DELH(10)=0.
      DO 240 I=1,4
      L=I+1
  240 DELH(10)=DELH(10)+.5*(WPER2(L)-WPER2(I))*(DELH(L)+DELH(I))
      HP=DELH(10)*CJ*WLBM/550.
      AMOM=HP*550./OMEG
      THETA=SQRTF(TTO/518.4)
      DELTA=PTO/14.7
      HP1=HP/(THETA*DELTA)
      AMOM1=AMOM/DELTA
      RPM1=RPM/THETA
      WLBM1=WLBM*THETA/DELTA
      PRINT 27
   27 FORMAT (/51H SLINE  DELH    PT1     TT2     PT2    T2IS     T2S)
      DO 250 I=1,5
   28 FORMAT(I4,6F8.2)
  250 PRINT 28,I,DELH(I),PT1(I),TT2(I),PT2(I),T2IS(I),T2S(I)
      PRINT 29
   29 FORMAT (/52H SLINE   ETAI   ETAS    ETAR    PSIR   RSTAR    AKIS)
      DO 260 I=1,5
   31 FORMAT (I4,F9.4,F7.4,2F8.4,F8.5,F8.3)
  260 PRINT 31,I,ETAI(I),ETAS(I),ETAR(I),PSIR(I),RSTAR(I),AKIS(I)
      PRINT 32
   32 FORMAT (/71H  HORSE   MOMENT   FLORATE  REF HORSE  REF MOMENT
     1      REF FLORATE)
      PRINT 34
  340FORMAT ( 69H  POWER   FT-LB    LBM/SEC    POWER      FT-LB     REF
     1 RPM    LBM/SEC)
```

```
      PRINT 33, HP,AMOM,WLBM,HP1,AMOM1,RPM1,WLBM1
   33 FORMAT (F7.1,F9.2,F9.3,F10.1,F12.3,F11.1,F10.3)
  400 CONTINUE
      END
      SUBROUTINE PARAB (V,I,J,K,A,B,C,VAR1,VAR2,VAR3)
      DIMENSION V(10)
      VAR12=VAR1**2
      VAR22=VAR2**2
      VAR32=VAR3**2
      D=VAR2*VAR32-VAR3*VAR22+VAR1*(VAR22-VAR32)+VAR12*(VAR3-VAR2)
      DA=V(I)*(VAR2*VAR32-VAR3*VAR22)+VAR1*(VAR22*V(K)-VAR32*V(J))
     1 + VAR12*(V(J)*VAR3-V(K)*VAR2)
      DB=V(J)*VAR32-V(K)*VAR22+V(I)*(VAR22-VAR32)+VAR12*(V(K)-V(J))
      DC= VAR2*V(K)-VAR3*V(J)+VAR1*(V(J)-V(K))+V(I)*(VAR3-VAR2)
      A=DA/D
      B=DB/D
      C=DC/D
      RETURN
      END
      SUBROUTINE STATOR (ALFA1,X,R,A,B,C,TTO,PTO,AM,T,P,V1,VA1,SI1,SI2,
     1 Y,S,DSDX,VU1,PRAT,T1IS,SS)
      DIMENSION ALFA1(10),X(10),T(10),P(10),V1(10),VA1(10),SI1(10),
     1SI2(10),Y(10),S(10),DSDX(10),VU1(10),PRAT(10),T1IS(10),SS(10)
      T(3)=TTO/(1.+.2*AM**2)
      V1(3)=49.01*SQRTF(T(3))*AM
      VA1(3)=V1(3)*COSF(ALFA1(3))
      C1=2.*32.174*778.16*.24
      C2=VA1(3)**2/(C1*TTO)
      ZETA=.09054
      ETA=1.-ZETA
      ZETAP=.0476
      DO 10 I=1,5
      XSQ=X(I)**2
      ALFA1(I)=A+B*X(I)+C*X(I)**2
      DALFDX=B+2.*C*X(I)
      TAN=-2.*TANF(ALFA1(I))
```

```
      PROD=TAN*DALFDX
      SINSQ=-2.*SINF(ALFA1(I))**2/X(I)
   10 SI1(I)=PROD+SINSQ
      DO 90 J=1,5
      IF(J-1)70,70,80
   70 DO 100 I=1,5
      SS(I)=0.
  100 SI2(I)=SI1(I)
      GO TO 40
   80 DO 20 I=1,5
      AA=C2*Y(I)**2/COSF(ALFA1(I))**2
      AB=(1.-AA)/(1.-AA/ETA)
   20 S(I)=LOGF(AB)
      DSDX(1)=(S(2)-S(1))/(X(2)-X(1))
      DSDX(2)=0.5*(DSDX(1)+(S(3)-S(2))/(X(3)-X(2)))
      DSDX(3)=0.5*((S(4)-S(3))/(X(4)-X(3))+(S(3)-S(2))/(X(3)-X(2)))
      DSDX(4)=0.5*((S(5)-S(4))/(X(5)-X(4))+(S(4)-S(3))/(X(4)-X(3)))
      DSDX(5)=(S(5)-S(4))/(X(5)-X(4))
      DO 30 I=1,5
      SS(I) =(1.-COSF(ALFA1(I))**2/(C2*Y(I)**2))*DSDX(I)
   30 SI2(I)= SS(I)+SI1(I)
   40 SUM1=(SI2(1)+SI2(2))*(X(2)-X(1))/4.
      SUM2=(SI2(2)+SI2(3))*(X(3)-X(2))/4.
      SUM3=(SI2(3)+SI2(4))*(X(4)-X(3))/4.
      SUM4=(SI2(4)+SI2(5))*(X(5)-X(4))/4.
      EN2=-SUM2
      EN1=-SUM2-SUM1
      EN3=SUM3
      EN4=SUM3+SUM4
      Y(1)=1.+EN1+EN1**2/2.+EN1**3/6.
      Y(2)=1.+EN2+EN2**2/2.+EN2**3/6.
      Y(3)=1.
      Y(4)=1.+EN3+EN3**2/2.+EN3**3/6.
      Y(5)=1.+EN4+EN4**2/2.+EN4**3/6.
      IF(J-1)110,110,120
  120 IF(J-3)130,110,130
```

```
130 IF(J-5)90,110,90
110 PRINT 2
  2 FORMAT (/49H SLINE  ITERATION  I-ALFA  I-DSDX1  I-TOTAL      Y)
    DO 140 I=1,5
  3 FORMAT (I4,I9,F12.4,F9.5,F9.4,F8.4)
140 PRINT 3,I,J,SI1(I),SS(I),SI2(I),Y(I)
 90 CONTINUE
    DO 60 I=1,5
    VA1(I)=VA1(3)*Y(I)
    VU1(I)=VA1(I)*TANF(ALFA1(I))
    V1(I)=VA1(I)/COSF(ALFA1(I))
    T(I)=TTO-V1(I)**2/C1
    T1IS(I)=TTO-(TTO-T(I))/ETA
    P(I)=PTO*(T1IS(I)/TTO)**3.5
 60 PRAT(I)=P(I)/PTO
    RETURN
    END
    SUBROUTINE FLOWREF (PRAT,ZETAP,AA,BA,CA,X,WI,PTE,PTO,TTE,TTO,AS,
   1 ZS,RS,AR,ZR,RR,M,WSTAT,VA2,WPER,CODE,WLBM)
    DIMENSION PRAT(10),ZETAP(10),X(10),WI(10),PTE(10),TTE(10),
   1 VA2(10),WPER(10)
    GAM=1.4
    G=32.174
    C=0.15
    F1=1./(C+1.)
    F2=1./(3.*C+1.)
    F3=1./(5.*C+1.)
    F4=1./(7.*C+1.)
    F5=1./(9.*C+1.)
    F6=1./(11.*C+1.)
    PRATCR=(2./(GAM+1.))**(GAM/(GAM-1.))
    PHICR=(2./(GAM+1.))**(1./(GAM-1.))*SQRTF(2.*GAM/(GAM+1.))
    DO 10 I=1,5
    XE=1.-PRAT(I)**((GAM-1.)/GAM)
    XE2=XE**2
    XE3=XE**3
```

```
      XE4=XE**4
      XEINV=1./(XE-1.)
      HNUM=XEINV+F2+XE*F3+XE2*F4+XE3*F5+XE4*F6
      HDEN=XEINV+F1+XE*F2+XE2*F3+XE3*F4+XE4*F5
      HSTAR=HNUM/HDEN
      XI=(HSTAR-1.)/(HSTAR-1.+ZETAP(I))
      IF (PRATCR-PRAT(I)) 20,30,30
  200 PHI=SQRTF(2.*GAM/(GAM-1.)*(PRAT(I)**(2./GAM)-PRAT(I)**
     1 ((GAM+1.)/GAM)))
      GO TO 40
   30 PHI=PHICR
   40 ARAT=AA+BA*X(I)+CA*X(I)**2
      IF (M-2) 130,120,130
  120 IF (I-5) 130,140,130
  140 ARAT=ARAT+2.*3.1416*4.875*.025/(ZR*AR*RR*(X(5)-X(4)))
  130 PRINT 14,XI,PHI,ARAT
   14 FORMAT (/5H  XI=, F6.4, 6H  PHI=, F7.5, 7H  ARAT=,F6.4)
   10 WI(I)=(PTE(I)/PTO)/SQRTF(TTE(I)/TTO)*ARAT*XI*PHI
      PRINT 15,(WI(I),I=1,5)
   15 FORMAT (/20H  FLOW INTEGRAND 1-5, 5F10.5)
      SUM1=(WI(1)+WI(2))*(X(2)-X(1))/2.
      SUM2=(WI(2)+WI(3))*(X(3)-X(2))/2.
      SUM3=(WI(3)+WI(4))*(X(4)-X(3))/2.
      SUM4=(WI(4)+WI(5))*(X(5)-X(4))/2.
      WSUM=SUM1+SUM2+SUM3+SUM4
      PRINT 13, SUM1,SUM2,SUM3,SUM4,WSUM
   13 FORMAT (/15H SUMS 1-4, WSUM, 5F10.5)
      IF(M-1) 50,60,50
   60 WSTAT=AS*ZS*RS*WSUM
      WLBM=PTO*SQRTF(G/(53.345*TTO))*WSTAT
      GO TO 70
   50 WREQ=WSTAT/(AR*ZR*RR)
      DIFF=ABSF(WREQ-WSUM)
      IF(DIFF-.0005) 80,80,90
   80 VA2(3)=VA2(3)
      CODE=20.
```

```
      PRINT 1,WSUM,WREQ,VA2(3)
      GO TO 70
   90 IF(WSUM-WREQ) 100,80,110
  100 VA2(3)=VA2(3)+DIFF/.00035
      PRINT 1,WSUM,WREQ,VA2(3)
      GO TO 70
  110 VA2(3)=VA2(3)-DIFF/.00035
      PRINT 1,WSUM,WREQ,VA2(3)
    1 FORMAT(35H REF FLOWS,COMPUTED-REQUIRED,AX VEL,2F10.4,F10.2)
   70 WPER(1)=0.
      WPER(2)=SUM1/WSUM
      WPER(3)=(SUM1+SUM2)/WSUM
      WPER(4)=(SUM1+SUM2+SUM3)/WSUM
      WPER(5)=1.
      PRINT 2,WSTAT,WLBM
   20FORMAT (/35H REF FLOW RATE-STATOR-SQUARE INCHES,F8.5,18H FLOW RATE
     1-LBM/SEC,F8.5)
      PRINT 11,M
   11 FORMAT (/30H STREAMLINE FLOW FRACTIONS, M=,I2)
      PRINT 12,X(2),WPER(2),X(3),WPER(3),X(4),WPER(4)
   12 FORMAT(6F10.4)
      RETURN
      END
      SUBROUTINE ROTOR1(VU1,VA1,RPM,U,BETA1,HE,TTE,PTE,X2,P1,T1,W1,WU1,
     1X1,RS,AZ1,BZ1,CZ1,AZ2,BZ2,CZ2,ZETAR,ZETAPR,AZP1,BZP1,CZP1,AZP2,
     2BZP2,CZP2,RR,DHEDX,DSDX,S,U2,OMEG,AZ3,BZ3,CZ3,AZP3,BZP3,CZP3)
      DIMENSION VU1(10),VA1(10),U(10),BETA1(10),HE(10),TTE(10),PTE(10),
     1X2(10),P1(10),T1(10),W1(10),WU1(10),X1(10),RS(10),ZETAR(10),
     2ZETAPR(10),RR(10),DHEDX(10),DSDX(10),S(10),U2(10)
      C=2.*32.174*778.16*.24
      OMEG=RPM*3.1416/30.
      DO 10 I=1,5
      U(I)=OMEG*RS(I)/12.
      U2(I)=U(I)*RR(I)/RS(I)
      WU1(I)=VU1(I)-U(I)
      BETA1(I)=ATANF(WU1(I)/VA1(I))
```

```
      W1(I)=VA1(I)/COSF(BETA1(I))
      TTE(I)=T1(I)+W1(I)**2/C+(U2(I)**2-U(I)**2)/C
      PTE(I)=P1(I)*(TTE(I)/T1(I))**3.5
      HE(I)=TTE(I)*.24
      BINC=BETA1(I)-62./57.3
      RINC=BINC/(13.4/57.3)
      RINC2=RINC**2
      IF (RINC) 30,20,80
   80 IF (RINC-1.) 20,20,70
   70 RINC=1.
      RINC2=1.
      PRINT 1,RINC
    10FORMAT (/58H RATIO OF INCIDENCE TO STALL INCIDENCE EXCEEDED, USE I
     1/IS=, F5.1)
   20 ZETAR(I)=AZ1+BZ1*RINC+CZ1*RINC2
      ZETAPR(I)=AZP1+BZP1*RINC+CZP1*RINC2
      GO TO 10
   30 IF (ABSF(RINC)-1.5) 40,40,50
   50 RINC=-1.5
      RINC2=RINC**2
      PRINT 1,RINC
   40 ZETAR(I)=AZ2+BZ2*RINC+CZ2*RINC2
      ZETAPR(I)=AZP2+BZP2*RINC+CZP2*RINC2
   10 CONTINUE
      DSDX(1)=(S(2)-S(1))/(X2(2)-X2(1))
      DSDX(2)=0.5*(DSDX(1)+(S(3)-S(2))/(X2(3)-X2(2)))
      DSDX(3)=0.5*((S(4)-S(3))/(X2(4)-X2(3))+(S(3)-S(2))/(X2(3)-X2(2)))
      DSDX(5)=(S(5)-S(4))/(X2(5)-X2(4))
      DSDX(4)=0.5*(DSDX(5)+(S(4)-S(3))/(X2(4)-X2(3)))
      DHEDX(1)=(HE(2)-HE(1))/(X2(2)-X2(1))
      DHEDX(2)=0.5*(DHEDX(1)+(HE(3)-HE(2))/(X2(3)-X2(2)))
      DHEDX(3)=0.5*((HE(3)-HE(2))/(X2(3)-X2(2))+(HE(4)-HE(3))/
     1 (X2(4)-X2(3)))
      DHEDX(5)=(HE(5)-HE(4))/(X2(5)-X2(4))
      DHEDX(4)=0.5*(DHEDX(5)+(HE(4)-HE(3))/(X2(4)-X2(3)))
   60 CONTINUE
```

```
      RETURN
      END
      SUBROUTINE ROTOR2 (BETA2,HE,DHEDX,DSDX1,DSDX2,VA2,WU2,W2,VU2,V2,
     1X2,U,FC1,FC2,AXB,BXB,CXB,YR,ZETAR,RI1,RI2,RI3,RI4,RI,SR1,SR2,YOLD,
     2AA,SR,TTE,PTE,T2,P2,PRAT2,T2S,INDS)
      DIMENSION BETA2(10),HE(10),DHEDX(10),DSDX1(10),DSDX2(10),VA2(10),
     1WU2(10),W2(10),VU2(10),V2(10),X2(10),U(10),YR(10),ZETAR(10),
     2RI1(10),RI2(10),RI3(10),RI4(10),RI(10),SR1(10),SR2(10),YOLD(10),
     3AA(10),SR(10),TTE(10),PTE(10),T2(10),P2(10),PRAT2(10),T2S(10)
      INDS=0
      C=2.*32.174*778.16
      GAM=1.4
      C1=C/VA2(3)**2
      DO 10 I=1,5
      BETA2(I)=AXB+FC1*BXB*X2(I)+FC2*CXB*X2(I)**2
      DBETDX=BXB*FC1+2.*CXB*X2(I)*FC2
      TAN=-2.*TANF(BETA2(I))
      PROD=TAN*DBETDX
      SIN=-2.*SINF(BETA2(I))**2/X2(I)
      RI1(I)=PROD+SIN+DSDX1(I)
      SR1(I)=-4.*U(3)    *COSF(BETA2(I))*SINF(BETA2(I))/(VA2(3)*YR(I))
      SR2(I)=2.*U(3)*U(I)*COSF(BETA2(I))**2/(VA2(3)**2*YR(I)**2)
      YOLD(I)=YR(I)
      AA(I)=(VA2(3)*YR(I)/COSF(BETA2(I)))**2/(C*HE(I))
   10 RI3(I)=C*COSF(BETA2(I))**2/(VA2(3)*YR(I))**2*DHEDX(I)
      PRINT 121,(RI1(I),I=1,5)
  121 FORMAT(/23H CONSTANT INTEGRAND 1-5, 5F8.5)
      PRINT 122
  122 FORMAT(/53H SLINE  GRAD-S    INT2    INT3      INT4     INT     Y-VAL)
      DO 20 J=1,13
      DO 30 I=1,5
      AA(I)=AA(I)*(YR(I)/YOLD(I))**2
      ANUM=1.-AA(I)
      ADEN=1.-AA(I)/(1.-ZETAR(I))
      AB=ANUM/ADEN
      IF (AB) 130,130,30
```

```
130 INDS=1
    GO TO 150
 30 SR(I)=LOGF(ANUM/ADEN)
    DSDX2(1)=(SR(2)-SR(1))/(X2(2)-X2(1))
    DSDX2(2)=0.5*(DSDX2(1)+(SR(3)-SR(2))/(X2(3)-X2(2)))
    DSDX2(3)=0.5*((SR(3)-SR(2))/(X2(3)-X2(2))+(SR(4)-SR(3))/
   1 (X2(4)-X2(3)))
    DSDX2(5)=(SR(5)-SR(4))/(X2(5)-X2(4))
    DSDX2(4)=0.5*(DSDX2(5)+(SR(4)-SR(3))/(X2(4)-X2(3)))
    DO 40 I=1,5
    SR1(I)=SR1(I)*YOLD(I)/YR(I)
    SR2(I)=SR2(I)*(YOLD(I)/YR(I))**2
    RI2(I)=SR1(I)-SR2(I)
    RI3(I)=RI3(I)*(YOLD(I)/YR(I))**2
    RI4(I)=DSDX2(I)-(DSDX1(I)+DSDX2(I))*C1*HE(I)
   1 *(COSF(BETA2(I))/YR(I))**2
 40 RI(I)=RI1(I)+RI2(I)+RI3(I)+RI4(I)
    SUM1=(RI(1)+RI(2))*(X2(2)-X2(1))/4.
    SUM2=(RI(2)+RI(3))*(X2(3)-X2(2))/4.
    SUM3=(RI(3)+RI(4))*(X2(4)-X2(3))/4.
    SUM4=(RI(4)+RI(5))*(X2(5)-X2(4))/4.
    EN1=-(SUM2+SUM1)
    EN2=-SUM2
    EN4=SUM3
    EN5=SUM3+SUM4
    DO 50 I=1,5
 50 YOLD(I)=YR(I)
    YR(1)=1.+EN1+EN1**2/2.+EN1**3/6.+EN1**4/24.+EN1**5/120.
    YR(2)=1.+EN2+EN2**2/2.+EN2**3/6.+EN2**4/24.+EN2**5/120.
    YR(3)=1.0
    YR(4)=1.+EN4+EN4**2/2.+EN4**3/6.+EN4**4/24.+EN4**5/120.
    YR(5)=1.+EN5+EN5**2/2.+EN5**3/6.+EN5**4/24.+EN5**5/120.
    NCOUNT=0
    DO 110 I=1,5
    TEST=ABSF(YOLD(I)-YR(I))
    IF (TEST-.005) 110,110,120
```

```
110 NCOUNT=NCOUNT+1
    IF (NCOUNT-5) 120,140,120
120 IF (J-3) 80,100,80
 80 IF (J-6) 90,100,90
 90 IF (J-9) 160,100,160
160 IF (J-12) 20,100,20
100 DO 60 I=1,5
123 FORMAT (I4,F10.5,5F8.4)
 60 PRINT 123,I,DSDX2(I),RI2(I),RI3(I),RI4(I),RI(I),YR(I)
 20 CONTINUE
140 DO 70 I=1,5
    VA2(I)=YR(I)*VA2(3)
    WU2(I)=VA2(I)*TANF(BETA2(I))
    W2(I)=VA2(I)/COSF(BETA2(I))
    VU2(I)=WU2(I)+U(I)
    T2(I)=TTE(I)-W2(I)**2/(0.24*C)
    T2S(I)=TTE(I)-(TTE(I)-T2(I))/(1.-ZETAR(I))
    P2(I)=PTE(I)*(T2S(I)/TTE(I))**(GAM/(GAM-1.))
 70 PRAT2(I)=P2(I)/PTE(I)
150 RETURN
    END
    SUBROUTINE SLINE (RR,X,DWDX,WPER2,WPER1,HE,U,DHEDX,S,DSDX1,
   1ARF,RRF,AAR,BAR,CAR,FC1,FC2,CODE)
    DIMENSION RR(10),X(10),DWDX(10),WI(10),WPER2(10),WPER1(10),HE(10),
   1DHEDX(10),S(10),DSDX1(10),U(10)
    SAVE=RR(3)
    SAVE1=X(3)
    DO 10 I=1,4
    J=I+1
 10 DWDX(I)=(WPER2(J)-WPER2(I))/(X(J)-X(I))
    N=0
    DO 20 I=2,4
    K=I+1
    J=I-1
    IF (ABSF(WPER2(I)-WPER1(I))-.005) 30,30,40
 40 IF (WPER2(I)-WPER1(I)) 50,30,60
```

```
 50 XN=X(I)+(WPER1(I)-WPER2(I))/DWDX(J)
    SL=(HE(K)-HE(I))/(X(K)-X(I))
    DEL=2.*(SL-DHEDX(I))/(X(K)-X(I))
    DHEDX(I)=DHEDX(I)+DEL*(XN-X(I))
    HE(I)=HE(I)+DHEDX(I)*(XN-X(I))
    SL=(S(K)-S(I))/(X(K)-X(I))
    DEL=2.*(SL-DSDX1(I))/(X(K)-X(I))
    DSDX1(I)=DSDX1(I)+DEL*(XN-X(I))
    S(I)=S(I)+DSDX1(I)*(XN-X(I))
    GO TO 70
 60 XN=X(I)-(WPER2(I)-WPER1(I))/DWDX(I)
    SL=(HE(I)-HE(J))/(X(I)-X(J))
    DEL=2.*(SL-DHEDX(I))/(X(I)-X(J))
    DHEDX(I)=DHEDX(I)+DEL*(XN-X(I))
    HE(I)=HE(I)+DHEDX(I)*(XN-X(I))
    SL=(S(I)-S(J))/(X(I)-X(J))
    DEL=2.*(SL-DSDX1(I))/(X(I)-X(J))
    DSDX1(I)=DSDX1(I)+DEL*(XN-X(I))
    S(I)=S(I)+DSDX1(I)*(XN-X(I))
 70 RR(I)=XN*SAVE
    IF (I-3) 20,90,20
 90 ARN=AAR+BAR*XN+CAR*XN**2
    ARF=ARN*ARF
    GO TO 100
 30 N=N+1
    IF (N-3) 20,400,20
100 U(I)=U(I)*XN/X(I)
 20 CONTINUE
    DO 80 I=1,5
 80 X(I)=RR(I)/RR(3)
    FC1=RR(3)/SAVE
    FC2=FC1**2
    BAR=BAR*FC1
    CAR=CAR*FC2
    RRF=RR(3)
    PRINT 501
```

```
501 FORMAT (/47H SLINE  XNEW   HENEW    DHEDX      S-NEW   DSDX1)
    DO 110 I=1,5
502 FORMAT (I4,F9.4,F9.2,F9.4,F9.6,F9.5)
110 PRINT 502,I,X(I),HE(I),DHEDX(I),S(I),DSDX1(I)
    GO TO 401
400 CODE=40.
401 RETURN
    END
    END
```

STATOR SOLUTION

SET NO.	PTO	TTO	M-STAT	M-ROTOR	RPM
1	30.10	602.00	1.00	.50	14000.

SLINE	ITERATION	I-ALFA	I-DSDX1	I-TOTAL	Y
1	1	-2.0256	.00000	-2.0256	1.0732
2	1	-1.6318	.00000	-1.6318	1.0305
3	1	-1.2772	.00000	-1.2772	1.0000
4	1	-.9554	.00000	-.9554	.9784
5	1	-.6667	.00000	-.6667	.9638

SLINE	ITERATION	I-ALFA	I-DSDX1	I-TOTAL	Y
1	3	-2.0256	.21039	-1.8152	1.0635
2	3	-1.6318	.21473	-1.4170	1.0261
3	3	-1.2772	.20168	-1.0755	1.0000
4	3	-.9554	.19103	-.7643	.9821
5	3	-.6667	.19166	-.4750	.9709

SLINE	ITERATION	I-ALFA	I-DSDX1	I-TOTAL	Y
1	5	-2.0256	.21342	-1.8121	1.0634
2	5	-1.6318	.21805	-1.4137	1.0260
3	5	-1.2772	.20477	-1.0724	1.0000
4	5	-.9554	.19389	-.7615	.9822
5	5	-.6667	.19463	-.4720	.9710

XI= .9519 PHI= .68473 ARAT= .8921

XI= .9533 PHI= .68473 ARAT= .9438

XI= .9544 PHI= .68473 ARAT=1.0000

XI= .9553 PHI= .68473 ARAT=1.0604

XI= .9560 PHI= .68457 ARAT=1.1240

FLOW INTEGRAND 1-5 .58148 .61608 .65349 .69364 .73563

SUMS 1-4, WSUM .02657 .02623 .02641 .02651 .10570

REF FLOW RATE-STATOR-SQUARE INCHES 2.76946 FLOW RATE-LBM/SEC 2.63857

STREAMLINE FLOW FRACTIONS, M= 1

.9587 .2513 1.0000 .4994 1.0392 .7492

STATOR SOLUTION

SET NO.	PTO	TTO	M-STAT	M-ROTOR	RPM
4	30.10	602.00	1.00	.50	11000.

SLINE	R1	X1	S1	DSDX1	I-DSDX	I-ALFA	I-TOTAL	Y
1	3.895	.914	.02417	-.02933	.21342	-2.02557	-1.81215	1.06339
2	4.084	.959	.02190	-.02878	.21305	-1.63176	-1.41371	1.02601
3	4.260	1.000	.02010	-.02771	.20477	-1.27722	-1.07245	1.00000
4	4.427	1.039	.01860	-.02948	.19389	-.95537	-.76148	.98219
5	4.585	1.076	.01735	-.03176	.19463	-.66666	-.47203	.97102

SLINE	T1	P1	ALFA1	BETA1	U1	W-FRAC	PTO/P1
1	485.52	13.03	1.3210	1.2088	373.89	.0000	.4329
2	494.41	14.00	1.3200	1.1922	392.04	.2513	.4650
3	501.73	14.83	1.3175	1.1725	408.93	.4994	.4926
4	507.97	15.56	1.3138	1.1496	424.96	.7492	.5171
5	513.30	16.21	1.3091	1.1237	440.13	1.0000	.5387

SLINE	VA1	VU1	V1	WU1	W1
1	292.5	1146.4	1183.1	772.5	826.0
2	282.2	1101.5	1137.1	709.5	763.5
3	275.1	1062.7	1097.7	653.8	709.3
4	270.2	1028.1	1063.0	603.1	660.9
5	267.1	997.3	1032.4	557.2	617.9

ROTOR SOLUTION

SET NO.	PTO	TTO	M-STAT	M-ROTOR	RPM
4	30.10	602.00	1.00	.50	11000.

CONSTANT INTEGRAND 1-5-1.90029-1.57019-1.31869-1.11998 -.98713

SLINE	GRAD-S	INT2	INT3	INT4	INT	Y-VAL
1	.03078	1.9155	2.2997	-.0574	2.2575	.8555
2	.02988	1.7514	2.0217	-.0266	2.1763	.9322
3	.02865	1.6343	1.9137	-.0136	2.2157	1.0000
4	.02426	1.5474	1.7544	.2312	2.4131	1.0657
5	.02019	1.4923	1.5942	.4387	2.5381	1.1188
1	.02811	1.9316	2.2243	.1001	2.3556	.8442
2	.02572	1.7599	1.9845	.1797	2.3539	.9247
3	.02130	1.6343	1.9137	.3086	2.5379	1.0000
4	.01411	1.5385	1.7935	.6372	2.8492	1.0769
5	.00896	1.4770	1.6598	.8676	3.0173	1.1407
1	.02904	1.9230	2.2652	.0463	2.3343	.8508
2	.02807	1.7543	2.0091	.0642	2.2575	.9299
3	.02698	1.6343	1.9137	.0597	2.2891	1.0000
4	.02303	1.5461	1.7606	.2798	2.4665	1.0676
5	.01919	1.4905	1.6023	.4761	2.5817	1.1218

XI= .9269 PHI= .44113 ARAT= .8257

XI= .9293 PHI= .46755 ARAT= .9088

XI= .9316 PHI= .48787 ARAT=1.0000

XI= .9335 PHI= .50565 ARAT=1.0947

XI= .9344 PHI= .51771 ARAT=1.6862

FLOW INTEGRAND 1-5 .22625 .26910 .31416 .36165 .57639

SUMS 1-4, WSUM	.01918	.01866	.01858	.01842	.07484
REF FLOWS, COMPUTED-REQUIRED, AX VEL			.0748	.0731	140.66

REF FLOW RATE-STATOR-SQUARE INCHES 2.76946 FLOW RATE-LBM/SEC 2.63857

STREAMLINE FLOW FRACTIONS, M= 2

.9360	.2563	1.0000	.5055	1.0550	.7538

CONSTANT INTEGRAND 1-5-1.90029-1.57019-1.31869-1.11998 -.98713

SLINE	GRAD-S	INT2	INT3	INT4	INT	Y-VAL

XI= .9272 PHI= .42575 ARAT= .8257

XI= .9296 PHI= .45403 ARAT= .9088

XI= .9320 PHI= .47481 ARAT=1.0000

XI= .9338 PHI= .49183 ARAT=1.0947

XI= .9348 PHI= .50275 ARAT=1.6862

FLOW INTEGRAND 1-5 .21844 .26140 .30586 .35189 .55997

SUMS 1-4, WSUM .01858 .01814 .01809 .01791 .07272
REF FLOWS,COMPUTED-REQUIRED,AX VEL .0727 .0731 140.66

REF FLOW RATE-STATOR-SQUARE INCHES 2.76946 FLOW RATE-LBM/SEC 2.63857

5 STREAMLINE FLOW FRACTIONS, M= 2
.9360 .2555 1.0000 .5050 1.0550 .7537

SLINE	XNEW	HENEW	DHEDX	S-NEW	DSDX1
1	.8596	130.05	4.9096	.024173	-.02933
2	.9372	130.43	5.1341	.021901	-.02878
3	1.0000	130.77	5.5917	.020130	-.02769
4	1.0563	131.09	5.7975	.018601	-.02948
5	1.0956	131.32	5.7875	.017353	-.03176

CONSTANT INTEGRAND 1-5-1.89799-1.56829-1.32172-1.11863 -.98596

2 SLINE GRAD-S INT2 INT3 INT4 INT Y-VAL

XI= .9272 PHI= .42669 ARAT= .8257

XI= .9296 PHI= .45473 ARAT= .9088
XI= .9320 PHI= .47491 ARAT= .9981

XI= .9338 PHI= .49230 ARAT=1.0947

XI= .9347 PHI= .50318 ARAT=1.6872

FLOW INTEGRAND 1-5 .21892 .26180 .30533 .35223 .56077

SUMS 1-4, WSUM .01864 .01781 .01851 .01795 .07291
REF FLOWS,COMPUTED-REQUIRED,AX VEL .0729 .0734 140.66

REF FLOW RATE-STATOR-SQUARE INCHES 2.76946 FLOW RATE-LBM/SEC 2.63857

STREAMLINE FLOW FRACTIONS, M= 2
.9372 .2556 1.0000 .4999 1.0563 .7538

SET NO.	PTO	TTO	M-STAT	M-ROTOR	RPM
4	30.10	602.00	1.00	.50	11000.

SLINE	R2	X2	TTE	PTE	ZETAR	ZETAPR	DHEDX	DSDX1-2
1	3.825	.860	541.88	19.14	.49199	.10278	4.910	-.02933
2	4.170	.937	543.47	19.49	.48239	.09827	5.134	-.02878
3	4.450	1.000	544.90	19.79	.47109	.09407	5.592	-.02769
4	4.700	1.056	546.23	20.07	.45796	.09073	5.797	-.02948
5	4.875	1.096	547.17	20.28	.44313	.08896	5.787	-.03176

SLINE	S2	DSDX2	I-BETA	I-OMEG	I-DHEDX	I-DSDX	I-TOT	Y
1	.0153	.02843	-1.8980	1.8799	2.4395	.0867	2.5081	.8413
2	.0175	.02687	-1.5683	1.7176	2.1487	.1307	2.4288	.9258
3	.0191	.02512	-1.3217	1.6025	2.0523	.1484	2.4815	1.0000
4	.0205	.02072	-1.1186	1.5145	1.8823	.3935	2.6716	1.0752
5	.0212	.01651	-.9860	1.4606	1.7169	.6104	2.8019	1.1347

SLINE	T2	P2	PTO/P2	ALFA2	BETA2	U2	W-FRAC
1	533.53	17.18	1.752	.554	-1.188	367.17	.00000
2	533.52	17.18	1.752	.551	-1.185	400.29	.25560
3	533.54	17.20	1.750	.547	-1.180	427.12	.49991
4	533.44	17.20	1.750	.535	-1.175	451.17	.75376
5	533.25	17.22	1.748	.520	-1.170	467.97	1.00000

SLINE	VA2	VU2	V2	WU2	W2
1	118.3	73.3	139.2	-293.9	316.8
2	130.2	80.0	152.8	-320.3	345.8
3	140.7	85.6	164.7	-341.5	369.4
4	151.2	89.6	175.8	-361.6	391.9
5	159.6	91.3	183.9	-376.7	409.1

SLINE	DELH	PT1	TT2	PT2	T2IS	T2S
1	16.05	27.66	535.14	17.36	512.89	525.44
2	15.97	27.88	535.46	17.40	512.89	524.25
3	15.90	28.06	535.76	17.45	513.02	523.43
4	15.84	28.20	536.02	17.49	513.01	522.64
5	15.83	28.33	536.06	17.54	513.18	522.17

SLINE	ETAI	ETAS	ETAR	PSIR	RSTAR	AKIS
1	.7503	.9095	.5080	.7128	-.43734	7.660
2	.7467	.9095	.5176	.7194	-.32756	6.968
3	.7444	.9095	.5289	.7273	-.23903	6.395
4	.7415	.9095	.5420	.7362	-.16187	5.922
5	.7424	.9095	.5569	.7462	-.09809	5.510

HORSE POWER	MOMENT FT-LB	FLORATE LBM/SEC	REF HORSE POWER	REF MOMENT FT-LB	REF RPM	REF FLORATE LBM/SEC
59.4	28.36	2.639	26.9	13.850	10207.7	1.389

APPENDIX IV

COMPUTER PROGRAM FOR EXHAUSTER ANALYSIS

A. Inputs.

Listed below are the inputs required for Program EJECTOR in the order of the READ statements.

1. The several values of polytropic efficiency assumed for the flow: through the turbine--ETAT; through the stator--ETAA; from the turbine hood to the ejector nozzle exit plane--ETAD; to the ejector nozzle throat--ETAN; from the ejector nozzle throat to the nozzle exit plane--ETAI; in the diverging portion (subsonic)--ETAC--and (supersonic) --ETAU; after a shock in the diverging portion--ETAL. NSETS is the number of inlet conditions for which the analysis is to be done.

2. Inlet conditions one through NSETS; total pressure (PTO--psia); and total temperature (TTO--$^{\circ}$R).

B. Outputs.

Sample output is included at the end of the program. Labels for the printouts are the symbols from the equations for the analysis. Units are: temperatures--$^{\circ}$R; pressures--psia; velocities--ft/sec; and flow rates--lbm/sec.

```
..JOB0355F, ECKERT, R H
      PROGRAM EJECTOR
C     THIS PROGRAM FINDS POSSIBLE OPERATING CONDITIONS FOR THE TRAN-
C     SONIC TURBINE TEST RIG, USNPGS PROPULSION LAB, WITH EXHAUSTER
C     INSTALLED.
      READ 1, ETAT,ETAA,ETAD,ETAN,ETAI,ETAC,ETAU,ETAL,NSETS
    1 FORMAT (8F6.4,I5)
      AM1=4.216
      AM2=2.971
      DLL=6.4
      DELL=.0075
      ALFAL=.86
      GL=1.5
      Z=10.
      DLS=1.2
      DELS=.005
      ALFAS=.89
      GS=1.25
      PI=3.1416/4.
      AN=PI*3.65**2
      AI=PI*4.74**2
      A2=PI*7.5**2
      A1T=A2-PI*4.76**2
      A3=PI*14.**2
      BL12=86.
      BL23=41.
      GAM=1.4
      R=53.345
      CJ=778.16
      CP=.24
      G=32.174
      C1=2.*G*CJ*CP
      C2=2.*GAM/(GAM-1.)
      ENT=GAM/(GAM-ETAT*(GAM-1.))
      ENA=GAM/(GAM-ETAA*(GAM-1.))
      ENDD=GAM/(GAM-ETAD*(GAM-1.))
```

```
      ENN=GAM/(GAM-ETAN*(GAM-1.))
      ENI=GAM/(GAM-ETAI*(GAM-1.))
      ENC=GAM*ETAC/(1.-GAM*(1.-ETAC))
      ENU=GAM/(GAM-ETAU*(GAM-1.))
      ENL=GAM*ETAL/(1.-GAM*(1.-ETAL))
      PRINT 110
 1100FORMAT (/63H     ENT       ENA      ENDD       ENN       ENI       ENC       EN
     1U      ENL)
      PRINT 104,ENT,ENA,ENDD,ENN,ENI,ENC,ENU,ENL
  104 FORMAT(8F8.4)
      ZETAT=1.-ETAT
      ZETAA=1.-ETAA
      ZETAD=1.-ETAD
      ZETAN=1.-ETAN
      ZETAI=1.-ETAI
      ZETAC=1.-ETAC
      ZETAU=1.-ETAU
      ZETAL=1.-ETAL
      PHIM =(2./(ENA+1.))**(1./(ENA-1.))*SQRTF(C2*(ENA-1.)/(ENA+1.))
      PHIN=(2./(ENN+1.))**(1./(ENN-1.))*SQRTF(C2*(ENN-1.)/(ENN+1.))
      PRINT 111
  111 FORMAT (/40H           PHI-BLADES           PHI-NOZZLE)
      PRINT 105,PHIM,PHIN
  105 FORMAT(2F20.10)
      DO 400 J=1,NSETS
      READ 2,PTO,TTO
    2 FORMAT(2F8.4)
   30FORMAT (/21H  TOTAL PRESSURE,PTO=,F8.4,24H  TOTAL TEMPERATURE,TTO=
     1,F8.4)
      PRINT 998
  998 FORMAT (1H1)
      PRINT 3,PTO,TTO
      CALL NOZZLE (PHIN,AN,AI,ENI,PTO,TTO,P1N,T1N,WN,C1,C2,V1N,ETAI)
      PA=14.7
      DO 10 I=1,2
      P1=6.
```

```
      IF(I-1)11,11,12
   11 APHIM=AM1*PHIM
      GO TO 13
   12 APHIM=AM2*PHIM
  130 CALL TURBINE (APHIM,PTD,PTO,P1,ENT,ENDD,A1T,DLL,DELL,ALFAL,GL,Z,
     1 DLS,DELS,ALFAS,GS,C2,V1T,T1T,TTD,ETAD,WT,TTO,C1,PA)
      CALL MMENTUM (WN,WT,P1,V1N,V1T,TTO,TTD,P21,PT21,V21,TT2,T21,I1T,
     1 A2,W,C1,BL12,1.)
      CALL SUBCOMP (W,TT2,T21,P21,P3,ENC,A3,C2)
      DIFF=PA-P3
      IF(ABSF(DIFF)-.0001) 40,40,20
   20 P1=P1+DIFF*(2./1.65)
      GO TO 13
   40 T3=T21*(P3/P21)**((ENC-1.)/ENC)
      V3=SQRTF(C1*(TT2-T3))
      IND=10
  999 FORMAT (/29H  SQRTF CHECK INDICATOR, IND=, I4)
      PT3=P3*(TT2/T3)**(1.4/(1.4-1.))
      IF (I-1) 30,30,50
   30 PRINT 100
  100 FORMAT (/42H  SUBSONIC SOLUTION CONVERGING GUIDE VANES)
      GO TO 60
   50 PRINT 101
 1060 FORMAT(/70H         PTD         TTD           PIT         TIT          V
     1IT            WT)
      PRINT 102,PTD,TTD,P1,T1T,V1T,WT
  102 FORMAT (6F12.5)
      PRINT 107
  107 FORMAT(/45H         PIN         TIN           WN         VIN)
      PRINT 103,P1N,T1N,WN,V1N
  103 FORMAT ( 4F12.5)
      PRINT 108
 1080 FORMAT(/69H        PT2         TT2           P2          T2
     1 W          V2 )
      PRINT 102,PT21,TT2,P21,T21,W,V21
      PRINT 109
```

```
109 FORMAT(/44H       PT3         P3            T3          V3)
    PRINT 103,PT3,P3,T3,V3
    CALL MMENTUM (WN,WT,P1,V1N,V1T,TTO,TTD,P22,PT22,V22,TT2,T22,T1T,
101 FORMAT (/48H  SUBSONIC SOLUTION CONVERGE-DIVERGE GUIDE VANES)
 60 PRINT 106
   1 A2,W,C1,BL12,-1.)
    IF(I-1) 200,200,300
200 PRINT 131
1310FORMAT (//71H  SUPERSONIC SOLUTION MOMENTUM EQUATION - DUCT - CONV
   1ERGING GUIDE VANES)
    GO TO 130
300 PRINT 132
1320FORMAT (//76H  SUPERSONIC SOLUTION MOMENTUM EQUATION - DUCT - CONV
   1ERG-DIVERGE GUIDE VANES)
130 PRINT 108
    PRINT 102,PT22,TT2,P22,T22,W,V22
    CALL SHOCK (TT2,T22,PT22,P22,V22,AMX,TY,PTY,PY,VY,AMY,GAM,G,R,1.)
    CALL SUBCOMP (W,TT2,TY,PY,P3,ENC,A3,C2)
    IF(ABSF(P3-PA)-.0001) 22,22,24
 24 IF (P3-PA) 21,22,23
 21 PRINT 112,P3
1120FORMAT (// 68H  SHOCK AT DIFFUSER ENTRANCE FOR MOMENTUM SOLUTION V
   1ELOCITY DOES NOT/65H  PROVIDE ADEQUATE COMPRESSION TO ADJUST FLOW
   2TO AMBIENT PRESSURE/38H SUPERSONIC SOLUTION NON-EXISTENT, P3=,
   3 F8.3)
    GO TO 10
 230CALL SUPEXP (W,TT2,T22,P22,ENU,BL23,R,G,C2,C1,BL23,T3,PT3,P3,V3,
   11.)
    IF(ABSF(P3-PA)-.0001) 37,37,38
 38 IF(P3-PA) 33,37,39
 33 CALL SHOCK (TT2,T3,PT3,P3,V3,AM3,TY3,PTY3,PY3,VY3,AMY3,GAM,G,R,2.)
    IF(ABSF(PY3-PA)-.0001) 32,32,34
 34 IF(PY3-PA) 31,32,32
 31 PRINT 113
113 FORMAT (//45H  SHOCK AT EXIT. CHECK SHOWS SHOCK IN DIFFUSER)
    GO TO 35
```

```
 35 XL=0
    DIFF1=1.
    YY=1.
 36 XL=XL+10.*YY
    CALL SUPEXP (W,TT2,T22,P22,ENU,XL,R,G,C2,C1,BL23,TU,PTU,PU,VU,2.)
    CALL SHOCK (TT2,TU,PTU,PU,VU,AMU,TL,PTL,PL,VL,AML,GAM,G,R,4.)
    CALL SUBCOMP (W,TT2,TL,PL,P3,ENC,A3,C2)
    DIFF=P3-PA
    IF(ABSF(P3-PA)-.0001)71,71,72
 72 IF(DIFF) 61,61,62
 61 IF(DIFF1) 63,63,64
 62 IF(DIFF1) 64,63,63
 63 DIFF1=DIFF
    GO TO 36
 64 DIFF1=DIFF
    YY=-.1*YY
    GO TO 36
 22 T3=TY*(P3/PY)**((ENC-1.)/ENC)
    V3=SQRTF(C1*(TT2-T3))
    PT3=P3*(TT2/T3)**(GAM/(GAM-1.))
 68 IF(I-1) 65,65,66
 65 PRINT 118
118 FORMAT (//44H  SUPERSONIC SOLUTION CONVERGING GUIDE VANES)
    GO TO 67
 66 PRINT 119
119 FORMAT (// 50H  SUPERSONIC SOLUTION CONVERGE-DIVERGE GUIDE VANES)
 67 PRINT 109
    PRINT 103,PT3,P3,T3,V3
    GO TO 10
 37 PRINT 120
120 FORMAT (// 42H  SHOCK AT EXIT CHECK SHOWS FULL EXPANSION)
    GO TO 68
 39 PRINT 121
1210FORMAT (// 73H  SHOCK AT EXIT CHECK SHOWS UNDER-EXPANSION - PRINT
   1EXIT PLANE CONDITIONS)
    GO TO 68
```

```
 32 PRINT 122
1220FORMAT (// 71H  SHOCK AT EXIT CHECK - OBLIQUE SHOCK EXIT PLANE-PRI
   1NT COND PRIOR SHOCK)
    GO TO 68
 71 PRINT 125
1250FORMAT (/ 73H   TU-DEGR  PTU-PSIA  PU-PSIA  MACH-U  TL-DEGR  PTL-P
   1SIA  PL-PSIA  MACH-L)
    PRINT 126,TU,PTU,PU,AMU,TL,PTL,PL,AML
126 FORMAT (F10.2,F9.3,F10.3,F8.3,F9.2,F9.3,F10.3,F8.3)
    TY=TL
    PY=PL
    GO TO 22
 10 CONTINUE
400 CONTINUE
    END
    SUBROUTINE TURBINE (APHIM,PTD,PTO,P1,ENT,ENDD,A1T,DLL,DELL,ALFAL,
   1 GL,Z,DLS,DELS,ALFAS,GS,C2,V1T,T1T,TTD,ETAD,WT,     TTO,C1,PA)
    EXP1=2./ENDD
    EXP2=(ENT+1.)/ENT
    EXP3=(ENDD+1.)/ENDD
    EXP4=(ENT+1.)/(2.*ENT)
    EXP5=(ENT-1.)/ENT
    EXP6=(ENDD-1.)/ENDD
    AL=3.1416*DLL*DELL
    AS=3.1416*DLS*DELS
    R1=1.1
  1 PTD=R1*P1
    X1=SQRTF(C2*R1**EXP2*((1./R1)**EXP1-(1./R1)**EXP3))
    IND=1
999 FORMAT (/29H  SQRTF CHECK INDICATOR, IND=, I4)
    PHIL=(1.-PTD/PTO)/4.0791
    PHIL=SQRTF(PHIL)
    IND=2
    APHIL=AL*PHIL
    PHIS=(1.-(PTD/PA)**2)/(Z +2./1.4*LOGF(PA/PTD))
    PHIS=SQRTF(PHIS) *0.874
```

```
      IND=3
      APHIS=AS*PHIS
      APHIS=APHIS* PA/PTO*SQRTF(TTO/520.)
      F1=(APHIM + APHIL+APHIS)*(PTO/P1)**EXP4/A1T
      DIFF=F1-X1
      IF(ABSF(DIFF)-.0001)10,10,11
   11 R1=R1+DIFF*(.222/.35)
      GO TO 1
   10 TTD=TTO*(PTD/PTO)**EXP5
      T1T=TTD*(1./R1)**EXP6
      IND=4
      V1T=SQRTF(C1*(TTD-T1T))
      WT=PTO*SQRTF(32.174/(TTO*53.345))*(APHIM+APHIL+APHIS)
      RETURN
      END
      SUBROUTINE NOZZLE (PHIN,AN,AI,ENI,PTO,TTO,P1N,T1N,WN,C1,C2,V1N,
     1 ETAI)
      PHII=PHIN * AN/AI
      EXP1=2./ENI
      EXP2=(ENI+1.)/ENI
      EXP3=(ENI-1.)/ENI
      R=.52
   20 F=SQRTF(C2*(R**EXP1-R**EXP2))
      DIFF=F-PHII
      IF(ABSF(DIFF)-.0001)40,40,10
   10 R=R-DIFF
      GO TO 20
   40 T1N=TTO*R**EXP3
      V1N=SQRTF(C1*(TTO-T1N))
      P1N=R*PTO
      WN=PHIN*PTO*AN*SQRTF(32.174/(53.345*TTO))
      RETURN
      END
      SUBROUTINE MMENTUM(WN,WT,P1,V1N,V1T,TTO,TTD,P21,PT21,V21,TT2,T21,
     1 T1T,A2,W,C1,BL12,XX)
C     SOLVE MOMENTUM EQUATION FOR FRICTION FORCE = ZERO
```

```
      W=WN+WT
      B1=W/32.174*(1.-53.345/(2.*778.16*.24))
      B2=(WN*V1N+WT*V1T)/32.174 +P1*A2
      TT2=(WN*TTO+WT*TTD)/W
      B3=W*53.345*TT2
      B=B2/B1
      C=B3/B1
      ROOT=SQRTF((B/2.)**2-C)
      IND=5
  999 FORMAT (/29H  SQRTF CHECK INDICATOR, IND=, I4)
      V21=B/2.-ROOT *XX
      P21=B3 /(A2*V21)-W*53.345*V21/(A2*C1)
      T21=TT2-V21**2/C1
C     FRICTION FACTOR .017 APPLIED FOR AVERAGE CONDITIONS STATIONS 1T-2
      PAV1=(P1+P21)/2.
      TAV1=(T1T+T21)/2.
      RHO1= PAV1*144./(32.174*53.345*TAV1)
      VAV1=(V1T+V21)/2.
      DELP1=.017*BL12*RHO1*VAV1**2/(15.*144.)
      PST1=P1-DELP1
      B21=(WN*V1N+WT*V1T)/32.174 + PST1*A2
      BN1=B21/B1
      V21=BN1/2.-SQRTF((BN1/2.)**2 - C)*XX
      IND=6
      P21=B3/(A2*V21)-W*53.345*V21/(A2*C1)
      T21=TT2-V21**2/C1
      PT21=P21*(TT2/T21)**(1.4/(1.4-1.))
      RETURN
      END
      SUBROUTINE SUBCOMP(W,TT2,T21,P21,P3,ENC,A3,C2)
      Y=(W*SQRTF(T21*53.345/32.174)/(A3*P21))**2/C2
      IND=7
  999 FORMAT (/29H  SQRTF CHECK INDICATOR, IND=, I4)
      EXP1=2./ENC
      EXP2=(ENC+1.)/ENC
      R1=TT2/T21
```

```
      R2=1.
   10 F=R1*R2**EXP1-R2**EXP2
      DIFF=F-Y
      IF(ABSF(DIFF)-.0001) 40,40,20
   20 R2=R2+DIFF*.15/.059
      GO TO 10
   40 P3=P21*R2
      RETURN
      END
      SUBROUTINE SHOCK (TT,TX,PTX,PX,VX,AMX,TY,PTY,PY,VY,AMY,GAM,G,R,
     1CODE)
      VC=SQRTF(GAM*G*R*TX)
      AMX=VX/VC
      AMX2=AMX**2
      D1=2./(GAM-1.)
      D2=2.*GAM/(GAM-1.)
      D1I=1./D1
      D3=2./(GAM+1.)
      D3I=1./D3
      D4=(GAM-1.)/(GAM+1.)
      D4I=1./D4
      D5=2.*GAM/(GAM+1.)
      EXP1=1./(GAM-1.)
      EXP2=GAM/(GAM-1.)
      AMY2=(AMX2+D1)/(D2*AMX2-1.)
      TYX=(1.+D1I*AMX2)*(D2*AMX2-1.)/(D3I*D4I*AMX2)
      PYX=D5*AMX2-D4
      RHOYX=PYX/TYX
      F1=(D3I*AMX2)**EXP2
      F2=(1.+D1I*AMX2)**EXP2
      F3=(D5*AMX2-D4)**EXP1
      PTYX=F1/(F2*F3)
      PTYPX=F1/F3
      TY=TYX*TX
      PTY=PTYX*PTX
      PY=PYX*PX
```

```
      AMY=SQRTF(AMY2)
      PRINT 1,CODE
    1 FORMAT (//30H CONDITIONS ACROSS SHOCK,CODE=,F5.1)
      PRINT 2
   20FORMAT (/60H   MACHX   MACHY   PTY/PTX   PY/PX    TY/TX    PTY       PY
     1     TY)
      PRINT 3,AMX,AMY,PTYX,PYX,TYX,PTY,PY,TY
    3 FORMAT(2F7.3,F9.4,F7.4,F8.4,2F8.3,F8.2)
      VCY=SQRTF(GAM*G*R*TY)
      VY=AMY*VCY
      RETURN
      END
      SUBROUTINE SUPEXP (W,TT,T1,P1,EN,X,R,G,C2,C1,BL23,T2,PT2,P2,V2,
     1 CODE)
      EXP1=1./(EN-1.)
      EXP2=2./EN
      EXP3=(EN+1.)/EN
      EXP4=EN/(EN-1.)
      EXP5=(EN-1.)/EN
      PTO=P1*(TT/T1)**EXP4
      PHIST=(2./(EN+1.))**EXP1*SQRTF(C2*(EN-1.)/(EN+1.))
      AST=W*SQRTF(TT*R/G)/(PHIST*PTO)
      RU=3.75+(7.-3.75)*X/BL23
      AX=3.1416*RU**2
      PHI2=PHIST*AST/AX
      X1=1.
      PR=P1/PTO
      SAVE=PHIST
    5 PR=PR-.1*X1
      F=SQRTF(C2*(PR**EXP2-PR**EXP3))
      DIFF=PHI2-F
      IF(ABSF(DIFF)-.0001)100,100,10
   10 DIFF1=PHI2-SAVE
      IF(DIFF) 20,100,30
   20 IF(DIFF1)40,60,50
   40 SAVE=F
```

```
      GO TO 5
   50 SAVE=F
      X1=-.1*X1
      GO TO 5
   30 IF(DIFF1) 50,60,40
   60 PR=PR+.1*X1
  100 P2=PR*PTO
      T2=TT*PR**EXP5
      V2=SQRTF(C1*(TT-T2))
      PT2=P2*(TT/T2)**(1.4/.4)
      PRINT 1,CODE
    1 FORMAT(//42H CONDITIONS FOR SUPERSONIC EXPANSION,CODE=,F5.2)
      PRINT 2
    2 FORMAT (/53H                INLET                              OUTLET)
      PRINT 3
   30FORMAT (/66H  PTOTAL  PSTATIC  TTOTAL  TSTATIC  PTOTAL  PSTATIC  T
     1TOTAL  TSTATIC)
      PRINT 4
    4 FORMAT (F8.3,F9.3,F8.2,F9.2,F8.3,F9.3,F8.2,F9.2)
      RETURN
      END
      END
```

TOTAL PRESSURE,PTC= 44.0000 TOTAL TEMPERATURE,TTC=660.0000

SUBSONIC SOLUTION CONVERGING GUIDE VANES

PTC	TTC	PIT	TIT	VIT	WT
7.85558	456.24633	6.52130	434.34373	513.04497	3.80911

PIN	TIN	WN	VIN
6.53868	404.23992	9.37759	1753.16979

PT2	TT2	P2	T2	W	V2
16.07014	601.14371	12.42089	558.49115	13.18671	715.94580

PT3	P3	T3	V3
14.95073	14.70008	598.24684	186.58279

SUPERSONIC SOLUTION MOMENTUM EQUATION - DUCT - CONVERGING GUIDE VANES

PT2	TT2	P2	T2	W	V2
17.17212	601.14371	4.05714	398.06012	13.18671	1562.23013

CONDITIONS ACROSS SHOCK,CODE= 1.0

MACHX	MACHY	PTY/PTX	PY/PX	TY/TX	PTY	PY	TY
1.597	.669	.8962	2.8102	1.3862	15.389	11.401	551.77

SHOCK AT DIFFUSER ENTRANCE FOR MOMENTUM SOLUTION VELOCITY DOES NOT PROVIDE ADEQUATE COMPRESSION TO ADJUST FLOW TO AMBIENT PRESSURE
SUPERSONIC SOLUTION NON-EXISTENT, P3= 13.879

SUBSONIC SOLUTION CONVERGE-DIVERGE GUIDE VANES

PTC	TTC	PIT	TIT	VIT	WT
7.06254	445.95982	6.39500	434.40972	372.56360	2.71252

PIN	TIN	WN	VIN
6.53868	404.23992	9.37759	1753.16979

PT2	TT2	P2	T2	W	V2
15.82209	611.97829	12.80547	576.08686	12.09011	656.75437

PT3	P3	T3	V3
14.91364	14.69994	609.45988	173.96841

SUPERSONIC SOLUTION MOMENTUM EQUATION - DUCT - CONVERG-DIVERGE GUIDE VANES

PT2	TT2	P2	T2	W	V2
19.14293	611.97829	3.05071	362.11646	12.09011	1732.83636

CONDITIONS ACROSS SHOCK, CODE= 1.0

MACHX	MACHY	PTY/PTX	PY/PX	TY/TX	PTY	PY	TY
1.858	.604	.7867	3.8595	1.5752	15.061	11.774	570.41

SHOCK AT DIFFUSER ENTRANCE FOR MOMENTUM SOLUTION VELOCITY DOES NOT PROVIDE ADEQUATE COMPRESSION TO ADJUST FLOW TO AMBIENT PRESSURE
SUPERSONIC SOLUTION NON-EXISTENT, P3= 13.829

APPENDIX V

COMPUTER PROGRAMS PERTINENT TO FLOW RATE MEASUREMENTS

A. Program ORIFICE.

Inputs for this program are: the upstream pipe diameter (D1--in.); the orifice diameter (D2--in.); the discharge coefficient, K_∞, for the flange taps (AKF); the discharge coefficient, K^*, for vena contracta taps (AKV); and the Reynolds Number for which the value of K^* applies (REV).

Outputs from the program are (see Table III, p. 102): the diameter ratio (BETA); the constant in the expression, $X = C_x\dot{w}/z$, ($XC = C_x$); the constant in the expression for Y_1 ($YC = C_y$); the value of A for the flange taps (AF) and for the vena contracta taps (AVC); and the constant C for the flange taps (CFL) and for the vena contracta taps (CVC).

B. Program FLOCAL.

Inputs for this program, in the order of the READ statements are:

1. The number of data points (N); atmospheric pressure (PA--in.Hg); reference manometer reading (TARE); and the base supply total pressure for the test (PUS--psia).

2. For data points one through N: temperature (TN) and pressure (PN) upstream of the flow nozzle; differential pressure across the nozzle (HWN); temperature upstream of the orifice (TOR); pressures upstream of the orifice for flange taps (PFL) and for vena-contracta taps (PVC); and the differential pressures across the flange taps (HWFL) and the vena-contracta taps (HWVC). Temperatures are in $^\circ$F, pressures are manometer readings (in.Hg) and differential pressures are in.H_2O.

Sample output is included at the end of the program. Column headings are self-explanatory.

C. Program FLOCAL2.

Inputs for this program in the order of the READ statements are:

1. The total number of values of nozzle discharge coefficient to be read (N); the number of values of discharge coefficient to be read for test number one (K1) and for test two (K2).

2. Values of discharge coefficient one through N for flange taps (AK) and for vena-contracta taps (AK2).

Sample output is included at the end of the program. The BEGIN and END values in the output specify which of the N values of discharge coefficient were used in the computations for the DATA GROUP. The column labeled POINT gives the number of the program's calculation subsequent to initial passage of the minimum error value of discharge coefficient. The desired value of discharge coefficient is obtained from the calculation which shows minimum error.

D. Program LABRINT.

No inputs are required for this program. Outputs are values of overall seal pressure ratio (BETA) and the corresponding values of the flow function (PHI = φ).

E. Program LABLEAK.

Inputs for this program are:

1. The number of data points (N); ambient pressure (PA--in.Hg); and the number of throttlings of the labyrinth seal (Z).

2. Test data for points one through N: reference manometer reading (TARE); temperature upstream of the square-edged orifice (T); pressures upstream of the orifice for flange taps (PFL) and the vena contracta taps (PVC); differential pressures across the orifice for flange taps (HWFL) and vena-contracta taps (HWVC); turbine plenum temperature (TP); and turbine plenum total pressure (PPT). Temperatures are in $^{\circ}$F,

pressures are manometer readings (in.Hg) and differential pressures are in in.H_2O.

Sample output is included at the end of the program. Column headings are self-explanatory.

F. Program MINSQ2.

Inputs for this program are:

1. The number of sets of values of pressure and flow function to be read (N); and initial assumed values for the constants A and B.

2. Values of pressure ratio (R) and flow function (W) for sets one through N.

Sample output is included at the end of the program. Values of B and associated errors during final iterations are included in the output. Values of the flow function (W) as computed using the constant B, along with the experimental values, are printed for each test pressure ratio (R). In addition, values of the flow function computed from the parabolic equation are given for pressure ratios from 0.15 to 0.95.

```
..0355F, ECKERT  R H
      PROGRAM ORIFICE
      N=1
      DO 10 I=1,N
      READ 1,D1,D2,AKF,AKV,REV
    1 FORMAT (2F10.4,2F10.6,F20.10)
      BETA=D2/D1
      C=359.1*D2**2/3600.*SQRTF(.4912*144./53.345)
      CFL=AKF*C
      BF=530./SQRTF(D1)
      BETA2=BETA**2
      BETA3=BETA**3
      BETA4=BETA**4
      AF=D2*(830.-5000.*BETA+9000.*BETA2-4200.*BETA3+BF)
      BV=BF-100.
      AV=D2*(830.-5000.*BETA+9000.*BETA2-4200.*BETA3+BV)
      YC=(.41+.35*BETA4)/(1.4*13.59)
      XC=6.316*100.*3600.*1.E-6/D2
      ZETA=1.+AV/REV
      AKV=AKV/ZETA
      CVC=AKV*C
      PRINT 2
   20FORMAT (//66H                                    FLANGE TAPS
     1    VENA TAPS)
      PRINT 3
   30FORMAT (68H    BETA       XC       YC            AF        CFL
     1 AV        CVC)
      PRINT 4,BETA,XC,YC,AF,CFL,AV,CVC
    4 FORMAT (F8.4,F9.4,F8.4,F13.2,F11.5,F12.3,F9.6)
   10 CONTINUE
      END
      END
```

```
..JOB0355F,ECKERT
      PROGRAM FLOCAL
C     THIS PROGRAM COMPUTES FROM EXPERIMENTAL DATA VALUES OF NOZZLE
C     DISCHARGE COEFFICIENT VERSUS WEIGHT RATE OF FLOW (LBM/SEC) FOR
C     THE FLOW NOZZLE OF THE TRANSONIC TURBINE TEST RIG, USNPGS.
      DIMENSION TN(150), TTN (150),PN (150), HWN (150), AKN (150),
     1 REN(150),TOR(150),TTOR(150),PFL(150),HWFL(150),WFL(150),
     2PVC(150), HWVC(150),WVC(150), RENV(150),AKNV(150)
      K=3
   80 READ 2,N,PA,TARE,PUS
    2 FORMAT (I3,3F8.2)
      K=K+1
      DO 1 I=1,N
      READ 1,TN(I),PN(I),HWN(I),TOR(I),PFL(I),HWFL(I),PVC(I),HWVC(I)
    1 FORMAT (8F8.2)
      DO 10 I=1,N
      TTN(I) =TN(I)+459.7
      TTOR(I)=TOR(I)+459.7
      PN(I)=TARE-PN(I)+PA
      PFL(I)=TARE-PFL(I)+PA
      PVC(I)=TARE-PVC(I)+PA
   10 CONTINUE
      CFL=1.4257
      CVC=1.4405
      AFL=.002180
      AVC=.001756
      CALL ORIFICE (N,CFL,TOR,PFL,HWFL,AFL,TTOR,WFL)
      CALL ORIFICE (N,CVC,TOR,PVC,HWVC,AVC,TTOR,WVC)
      CALL NOZZLE (N,TN,PN,HWN,WFL,TTN,AKN,REN)
      CALL NOZZLE (N,TN,PN,HWN ,WVC ,TTN,AKNV,RENV)
      PA=.4912*PA
      PRINT 400
  400 FORMAT (//47H                          TEST SERIES   BASE PRESSURE)
      PRINT 401,K,PUS
  401 FORMAT (I26,F16.0)
      PRINT 6
```

```
  6 FORMAT (/35H  AMB PRESS   DATA SETS   GAMMA=1.4)
    PRINT 7,PA,N
  7 FORMAT (F11.4, I9)
    PRINT 8
 80FORMAT (76H                  BASED ON FLANGE TAPS            BASED O
  1N VENA CONTRACTA TAPS)
    PRINT 9
 90FORMAT (78H POINT    LBM/SEC    DISCH COEFF  REYNOLDS    LBM/SEC
  1  DISCH COEFF  REYNOLDS)
    DO 15 J=1,N
    PRINT 12,J,WFL(J), AKN (J), REN (J), WVC (J), AKNV (J), RENV (J)
 12 FORMAT (I5,1PE13.3,1PE14.4,1PE10.2,1PE12.3,1PE14.4,1PE10.2)
 15 CONTINUE
    IF(K-6) 60,70,70
 60 GO TO 80
 70 PRINT 300
300 FORMAT (/ 20 H  END PROGRAM FLOCAL )
    END
    SUBROUTINE ORIFICE (N,C,TO,P,HW,A,TTO,W)
    DIMENSION TO(150), P(150), HW(150),TTO(150), W(150)
    DO 50 I=1,N
    ALFA = 1.0+.00193*(TO(I)-68.)/100.
    Y=1.-.026*HW(I)/P(I)
    W(I)=C*ALFA*Y*SQRTF(P(I)*HW(I)/TTO(I))
    Z=1.9+.24*(TO(I)/100.-1.)
    X=.5359*W(I)/Z
    ZETA=1.0+A/X
    W(I)=ZETA*W(I)
 50 CONTINUE
    RETURN
    END
    SUBROUTINE NOZZLE (N,T,P,HW,W,TT,AK,RE)
    DIMENSION T(150), P(150), HW(150), W(150),TT(150), AK(150),
   1RE(150)
    DO 60 I=1,N
    ALFA=1.0+.00252*(T(I)-68.)/100.
```

```
      Z=1.9+.24*(T(I)/100.-1.)
      D=3600.*SQRTF(53.345/(.491*144.))/(359.1*4.25**2)
      Y=1.0-(.41+.35*((4.25/6.065)**4))/(1.4*13.59)*HW(I)/P(I)
      AK(I) = D*W(I)*SQRTF(TT(I)/(P(I)*HW(I)))/(ALFA*Y)
      RE(I)=6.316*100.*3600.*W(I)/(4.25*Z)
   60 CONTINUE
      RETURN
      END
      END
```

13	2.293E+00	1.0099E+00	6.55E+05	2.283E+00	1.0058E+00	6.52E+05
14	1.801E+00	1.0037E+00	5.14E+05	1.791E+00	9.9836E-01	5.11E+05

TEST SERIES 6 BASE PRESSURE 45.

AMB PRESS 14.6771 DATA SETS 13 GAMMA=1.4

	BASED ON FLANGE TAPS			BASED ON VENA CONTRACTA TAPS		
POINT	LBM/SEC	DISCH COEFF	REYNOLDS	LBM/SEC	DISCH COEFF	REYNOLDS
1	1.825E+00	9.8630E-01	5.19E+05	1.833E+00	9.9028E-01	5.21E+05
2	2.592E+00	9.9940E-01	7.36E+05	2.591E+00	9.9894E-01	7.36E+05
3	3.124E+00	1.0007E+00	8.86E+05	3.133E+00	1.0035E+00	8.89E+05
4	3.581E+00	1.0011E+00	1.01E+06	3.579E+00	1.0006E+00	1.01E+06
5	3.938E+00	1.0012E+00	1.11E+06	3.934E+00	1.0003E+00	1.11E+06
6	4.308E+00	1.0004E+00	1.22E+06	4.303E+00	9.9924E-01	1.22E+06
7	4.555E+00	1.0011E+00	1.29E+06	4.555E+00	1.0010E+00	1.29E+06
8	4.455E+00	9.9859E-01	1.26E+06	4.453E+00	9.9829E-01	1.26E+06
9	4.176E+00	1.0007E+00	1.18E+06	4.173E+00	9.9996E-01	1.18E+06
10	3.773E+00	1.0004E+00	1.06E+06	3.767E+00	9.9882E-01	1.06E+06
11	3.329E+00	1.0042E+00	9.40E+05	3.313E+00	9.9940E-01	9.35E+05
12	2.806E+00	1.0027E+00	7.91E+05	2.790E+00	9.9681E-01	7.86E+05
13	2.250E+00	9.9940E-01	6.35E+05	2.235E+00	9.9269E-01	6.31E+05

END PROGRAM FLOCAL
TIME, 0 MINUTES AND 28 SECONDS

```
..JOB0355F, ECKERT, R.H.
      PROGRAM FLOCAL2
C     THIS PROGRAM COMPUTES BY LEAST SQUARES THE ERRORS FOR VARIOUS
C     ASSUMED VALUES FOR THE NOZZLE DISCHARGE COEFFICIENT = CONSTANT
C     AND VALUES OF THE COEFFICIENT DETERMINED BY PROGRAM FLOCAL.
      DIMENSION AK(100), ERR(30,30), AKF(30,30), AK2(100),
     1 ERR2(30,30),AKF2(30,30)
      READ 1,N, K1,K2
    1 FORMAT (3I3)
      DO 2 I=1,N
      READ 3,AK(I),AK2(I)
    3 FORMAT (2F8.4)
    2 CONTINUE
      DO 100 J=1,5
      IF (J-1) 60,60,70
   70 IF (J-2) 61,61,71
   71 IF (J-3) 62,62,72
   72 IF (J-4) 63,63,73
   73 IF (J-5) 64,64,64
   60 K4=1
      K5=K1
      GO TO 80
   61 K4=K1+1
      K5=K2
      GO TO 80
   62 K4=1
      K5=K2
      GO TO 80
   63 K4=1
      K5=N
      GO TO 80
   64 K4=K2+1
      K5=N
   80 CALL MINSQ (K4,K5,AK,AKF,ERR,J)
      CALL MINSQ (K4,K5,AK2,AKF2,ERR2,J)
      PRINT 11
```

```
 11 FORMAT (/38H             DATA GROUP    BEGIN    END)
    PRINT 12,J,K4,K5
 12 FORMAT (I18,I11,I9)
    PRINT 202
202 FORMAT (/51H                FLANGE TAPS        VENA CONTRACTA TAPS)
    PRINT 200
200 FORMAT (51H  POINT   ERROR  NOZZLE COEFF   ERROR  NOZZLE COEFF)
    DO 100 I=1,20
    PRINT 201,I,ERR(J,I),AKF(J,I),ERR2(J,I),AKF2(J,I)
201 FORMAT (I6,F9.5,F10.4,F12.5,F12.4)
100 CONTINUE
    END
    SUBROUTINE MINSQ (K4,K5,AK,AKF,ERR,J)
    DIMENSION AK(100),AKF(30,30),ERR(30,30)
    SAVE=1.
    DO 10 I=1,100
    AI=I
    A=.989+.001*AI
    D=0.
    DO 20 K=K4,K5
 20 D=D+(A-AK(K))**2
    D=SQRTF(D)
    IF (SAVE-D) 30,30,10
 10 SAVE=D
 30 SAVE=D
    DO 40 L=1,20
    AL=L
    AKF(J,L)=A-.0001*AL
    ERR(J,L)=0.
    DO 50 K=K4,K5
 50 ERR(J,L)=ERR(J,L)+(AKF(J,L)-AK(K))**2
 40 ERR(J,L)=SQRTF(ERR(J,L))
    RETURN
    END
    END
```

DATA GROUP	BEGIN	END
4	1	33

	FLANGE TAPS		VENA CONTRACTA TAPS	
POINT	ERROR	NOZZLE COEFF	ERROR	NOZZLE COEFF
1	.01677	1.0019	.01688	1.0019
2	.01663	1.0018	.01674	1.0018
3	.01650	1.0017	.01662	1.0017
4	.01639	1.0016	.01652	1.0016
5	.01630	1.0015	.01644	1.0015
6	.01623	1.0014	.01638	1.0014
7	.01618	1.0013	.01635	1.0013
8	.01615	1.0012	.01633	1.0012
9	.01614	1.0011	.01633	1.0011
10	.01615	1.0010	.01635	1.0010
11	.01618	1.0009	.01639	1.0009
12	.01623	1.0008	.01645	1.0008
13	.01630	1.0007	.01653	1.0007
14	.01639	1.0006	.01663	1.0006
15	.01650	1.0005	.01675	1.0005
16	.01663	1.0004	.01689	1.0004
17	.01678	1.0003	.01704	1.0003
18	.01695	1.0002	.01722	1.0002
19	.01713	1.0001	.01741	1.0001
20	.01734	1.0000	.01762	1.0000

```
..0355F, ECKERT R H
      PROGRAM LABRINT
      Z=10.
      PRINT 1
    1 FORMAT (/17H    BETA       PHI)
      DO 10 I=1,40
      AI=I
      BETA = .025*AI
      PHI=SQRTF((1.-BETA**2)/(Z+2./1.4*LOGF(1./BETA)))
      PRINT 2,BETA,PHI
    2 FORMAT (2F10.8)
   10 CONTINUE
      END
      END
```

```
..JOB0355F, ECKERT, R.H.
      PROGRAM LABLEAK
C     THIS PROGRAM COMPUTES AIR WT RATE OF FLOW THROUGH LABYRINTHS OF
C     THE PLENUM OF THE TRANSONIC TURBINE TEST RIG, USNPGS.  BASIS IS
C     FLOW MEASURED BY STANDARD ORIFICE INSTALLATION (.825IN DIA/2IN
C     DIA  PIPE) UPSTREAM OF THE PLENUM.  ALL OTHER OUTLETS CAPPED.
      DIMENSION TARE(100), T(100), PFL(100), HWFL(100),PVC(100),TR(100),
     1 HWVC (100), WFL(100), REFL(100), WVC(100), TT(100), REVC (100) ,
     2TP(100),PPT(100),CFL(100),PHIFL(100),CVC(100),PHIVC(100),BETA(100)
      DO 40 J=1,3
      READ 1,N,PA,Z
    1 FORMAT (I3,2F8.2)
      DO 2 I=1,N
      READ 3, TARE(I), T(I), PFL(I), HWFL(I), PVC(I), HWVC(I),
     1 TP(I),PPT(I)
    3 FORMAT (8F8.3)
      TT(I) = T(I) + 459.7
      PFL(I) = TARE (I) -PFL(I) +PA
      PVC(I) = TARE(I) -  PVC(I) + PA
      TP(I)=TP(I)+459.7
      PPT(I)=.4912*(TARE(I)-PPT(I)+PA)
      TR(I)=SQRTF(TP(I)/TT(I))
    2 CONTINUE
      CFL=.0476
      CVC=.04761
      AFL=.0003049
      AVC=.0002249
      R=53.345
      D=6.4
      DEL=.0075
      A=3.1416*D*DEL
      CALL ORIFICE (N, CFL, T, PFL, HWFL, AFL, TT, WFL, REFL)
      CALL ORIFICE(N,CVC,T,PVC,HWVC,AVC,TT,WVC,REVC)
      PA=.4912*PA
      DO 20 I=1,N
      PFL(I)=.4912*PFL(I)
```

```
      PVC(I)=.4912*PVC(I)
   20 BETA(I)=PA/PPT(I)
      PRINT 6
    6 FORMAT (/34H  DATA GROUP  AMB PRESS  GAMMA=1.4)
      PRINT 7,J,PA
    7 FORMAT (I8,F14.4)
      PRINT 4
    4 FORMAT (//46H                    PRINT STANDARD ORIFICE DATA)
      PRINT  8
   80FORMAT (//66H           UPSTREAM OF ORIFICE                    FLOW
     1 RATE-LBM/SEC)
      PRINT 9
   90FORMAT (66H  POINT  PRESS-PSIA  TEMP-DEG R  REYNOLDS NO    FLANGE
     1  VENA CONT)
      DO 10 I=1,N
      PRINT 11, I, PFL(I),TT(I), REFL(I), WFL(I), WVC(I)
   11 FORMAT(I6,2F12.3,1PE13.4,1PE13.4,1PE11.4)
   10 CONTINUE
      CALL COEFF (WFL,TP,PPT,R,A,CFL,PHIFL,BETA,N,Z)
      CALL COEFF (WVC,TP,PPT,R,A,CVC,PHIVC,BETA,N,Z)
      PRINT 98
   98 FORMAT (/46H                     PRINT LABYRINTH LEAK DATA)
      PRINT 100
 1000FORMAT (/85H          PLENUM CONDITIONS                      DISCH
     1 COEFF-BASIS      REF FLOW RATE)
      PRINT 99
   99 FORMAT (45H          TEMP-  PRESS  PRESS             TEMP)
      PRINT 101
 1010FORMAT (87H  POINT  DEG-R  -PSIA  RATIO    PHI     RATIO    FLANGE
     1   VENA CONT  FLANGE   VENA CONT)
      DO 30 I=1,N
      PRINT 102,I,TP(I),PPT(I),BETA(I),PHIFL(I),   TR(I),CFL(I),CVC(I)
     1WFL(I),WVC(I)
  102 FORMAT (I6,F8.1,F7.3,F7.4,F8.5,F10.5,F9.5,F11.5,F9.5,F11.5)
   30 CONTINUE
   40 CONTINUE
```

```
      END
      SUBROUTINE ORIFICE (N,C,TO,P,HW,A,TTO,W,RE)
      DIMENSION TO(100), P(100), HW(100), TTO(100), W(100), RE(100)
      DO 50 I=1,N
      ALFA = 1.0+.00193*(TO(I)-68.)/100.
      Y=1.-.022  *HW(I)/P(I)
      W(I)=C*ALFA*Y*SQRTF(P(I)*HW(I)/TTO(I))
      Z=1.9+.24*(TO(I)/100.-1.)
      X=2.7561*W(I)/Z
      ZETA=1.0+A/X
      W(I)=ZETA*W(I)
      RE(I) = 6.316*100.*3600.*W(I)/(.875*Z)
   50 CONTINUE
      RETURN
      END
      SUBROUTINE COEFF(W,T,P,R,A,C,PHI,BETA,N,Z)
      DIMENSION W(100),T(100),P(100),C(100),PHI(100),BETA(100)
      DO 10 I=1,N
      W(I)=SQRTF(T(I)*R/32.174)*W(I)/(2.*P(I)*A)
      PHI(I)=SQRTF((1.-BETA(I)**2)/(Z+2./1.4*LOGF(1./BETA(I))))
      C(I)=W(I)/PHI(I)
   10 W(I)=2.*W(I)
      RETURN
      END
      END
```

DATA GROUP 3 AMB PRESS 14.8195 GAMMA=1.4 PRINT STANDARD ORIFICE DATA

POINT	UPSTREAM OF ORIFICE PRESS-PSIA	TEMP-DEG R	REYNOLDS NO	FLOW RATE-LBM/SEC FLANGE	VENA CONT
1	30.047	545.200	7.4188E+04	5.3250E-02	5.2937E-02
2	32.601	549.200	8.2503E+04	5.9524E-02	5.9167E-02
3	35.249	553.200	9.0474E+04	6.5609E-02	6.5255E-02
4	37.415	557.200	9.7576E+04	7.1119E-02	7.0653E-02
5	40.116	559.200	1.0647E+05	7.7796E-02	7.7107E-02
6	42.671	561.200	1.1397E+05	8.3490E-02	8.3535E-02
7	44.341	564.200	1.1884E+05	8.7384E-02	8.7014E-02
8	43.172	560.200	1.1624E+05	8.5047E-02	8.4797E-02
9	41.054	556.200	1.1049E+05	8.0427E-02	8.0026E-02
10	38.824	559.200	1.0302E+05	7.5279E-02	7.5129E-02
11	35.676	556.200	9.3669E+04	6.8185E-02	6.7620E-02
12	33.623	551.200	8.7438E+04	6.3245E-02	6.2738E-02
13	31.422	549.200	7.9745E+04	5.7534E-02	5.7294E-02

PRINT LABYRINTH LEAK DATA

POINT	PLENUM CONDITIONS TEMP-DEG-R	PRESS -PSIA	PRESS RATIO	PHI	TEMP RATIO	DISCH COEFF-BASIS FLANGE	VENA CONT	REF FLOW RATE FLANGE	VENA CONT
1	529.7	29.703	.4989	.26138	.98568	.67396	.66999	.35232	.35025
2	531.7	32.105	.4616	.26621	.98394	.68565	.68155	.36505	.36287
3	533.2	34.728	.4267	.27003	.98176	.68973	.68601	.37250	.37050
4	534.7	36.840	.4023	.27234	.97960	.69982	.69522	.38118	.37868
5	535.7	39.483	.3753	.27452	.97876	.70927	.70298	.38942	.38597
6	537.2	41.948	.3533	.27603	.97838	.71350	.71390	.39390	.39412
7	538.2	43.599	.3399	.27683	.97669	.71712	.71409	.39704	.39536
8	538.2	42.464	.3490	.27630	.98017	.71797	.71586	.39674	.39558
9	537.7	40.386	.3669	.27513	.98323	.71660	.71303	.39431	.39234
10	537.2	38.201	.3879	.27355	.98013	.71287	.71145	.39001	.38923
11	536.7	35.116	.4220	.27050	.98231	.70998	.70411	.38411	.38093
12	535.7	33.092	.4478	.26780	.98584	.70523	.69957	.37772	.37469
13	535.2	31.068	.4770	.26431	.98717	.69202	.68914	.36582	.36429

```
..JOB0355F, ECKERT  R H
      PROGRAM MINSQ2
C     THIS PROGRAM FITS A PARABOLA OF FORM R=A-B*W**2 TO EXPERIMENTAL
C     DATA, USING LEAST SQUARES WITH W VALUES AT R VALUES
      DIMENSION R(100), W(100), WF(100), RF(100)
      READ 1,N,A,B
    1 FORMAT (I5,2F10.5)
      DO 10 I=1,N
      READ 2, R(I),W(I)
    2 FORMAT (2F10.7)
   10 CONTINUE
      SAVE=1.
      X=1.
      DEL1=1.
   30 B=B+.01*X
      SUM = 0.
      DO 20 I=1,N
      WF(I)=SQRTF((A-R(I))/B)
      DIFF=ABSF(WF(I)-W(I))
   20 SUM=SUM+DIFF**2
      SUM = SQRTF(SUM)
      IF (SUM-.01) 40,40,50
   50 DEL2=SAVE-SUM
      IF (DEL1) 60,100,70
   60 IF (DEL2) 80,40,90
   70 IF (DEL2) 90,40,80
   90 X=-.1*X
      PRINT 11, B,SUM
```

```
 80 SAVE=SUM
    DEL1=DEL2
    GO TO 30
100 B=B-.1*X
    SUM =SAVE
 40 DO 110 I=1,N
    RF(I)=R(I)
110 WF(I)=SQRTF ((A-RF(I))/B)
    L=N+1
    M=L+16
    DO 120 I=L,M
    J=I-N
    AI=J
    RF(I)=1.0-.05*AI
120 WF(I)=SQRTF((A-RF(I))/B)
    PRINT 11,B,SUM
 11 FORMAT (3H B= F15.12,7H ERROR= F10.8)
    PRINT 21
 21 FORMAT (//46H  POINT  PRESS RATIO  W-COMPUTED  W-EXPERIMENT)
    DO 130 I=1,N
130 PRINT 31,I,R(I),WF(I),W(I)
 31 FORMAT (I5,F13.4,F12.5,F14.5)
    DO 140 I=L,M
140 PRINT 41,I,RF(I),WF(I)
 41 FORMAT (I5,F13.5,F12.5)
    END
    END
```

```
B= 4.080000000307 ERROR= .02080026
B= 4.079000000260 ERROR= .02078588
B= 4.079100000206 ERROR= .02078722
B= 4.079090000247 ERROR= .02078708
B= 4.079091000254 ERROR= .02078710
B= 4.079090900254 ERROR= .02078710
B= 4.079090910265 ERROR= .02078710
B= 4.079090909217 ERROR= .02078710
B= 4.079090909334 ERROR= .02078710
```

POINT	PRESS RATIO	W-COMPUTED	W-EXPERIMENT
1	.6098	.30929	.31852
2	.5459	.33365	.34119
3	.5053	.34825	.35426
4	.4659	.36185	.36605
5	.4342	.37243	.37219
6	.4050	.38192	.38136
7	.3794	.39005	.38798
8	.3568	.39709	.39419
9	.3376	.40298	.39884
10	.4989	.35049	.34994
11	.4616	.36330	.36223
12	.4267	.37489	.36985
13	.4023	.38279	.37934
14	.3753	.39134	.38732
15	.3533	.39817	.39515
16	.3399	.40228	.39708
17	.3490	.39949	.39696
18	.3669	.39396	.39303
19	.3879	.38737	.38957
20	.4220	.37643	.38160
21	.4478	.36793	.37436
22	.4770	.35807	.36397

23	.95000	.11071
24	.90000	.15657
25	.85000	.19176
26	.80000	.22143
27	.75000	.24756
28	.70000	.27119
29	.65000	.29292
30	.60000	.31315
31	.55000	.33214
32	.50000	.35011
33	.45000	.36720
34	.40000	.38353
35	.35000	.39919
36	.30000	.41425
37	.25000	.42879
38	.20000	.44286
39	.15000	.45649

APPENDIX VI

COMPUTER PROGRAM FOR TURBINE TEST DATA REDUCTION

A. Inputs.

Listed below are the inputs for Program TTTRPGS in the order of the READ statements.

1. The number of data sets (NSETS).

2. For each data set, the number of data points (NPTS), the run number (NRUN), the date of the run (NMOM) and (NDAY), ambient pressure (PA--in. Hg abs.), and ambient temperature (TA--$^{\circ}$R).

3. For each data point, one to NPTS, values of: the reference manometer reading (PTARE); the pressure upstream of the flow nozzle (PN); plenum pressure (PP); turbine inlet total pressure (PTO) and static pressure (PO); the stator exit plane pressures at the tip (P1T), the hub (P1H), and in the vicinity of the cover plate (P1I); and the turbine discharge pressure (P2). These pressures are manometer readings (in. Hg). If P1I has not been measured, the value of P1H is used for P1I also.

4. For each data point, one to NPTS, values of: flow nozzle differential pressure (HW--in.H_2O); the temperatures upstream of the flow nozzle (TN) and in the plenum (TP); the inlet total temperature (TTO); the axial tare force (AXTARE--lb); the axial force reading (AX) and the stator moment reading (AMOMS), both in kc.; rotor moment (AMOMR--in.lb.); and wheel speed (REV) in RPM. Temperatures are in $^{\circ}$F.

B. Outputs.

Sample output from TTTRPGS is included at the end of the program. Column headings are the standard symbols for the turbine stations and are self explanatory. Temperatures are in $^{\circ}$R, pressures are in psia.; angles are in degrees, and velocities are in ft/sec. The column labeled SPEED gives rotor mean streamline peripheral velocity, U_1.

```
      PROGRAM TTTRPGS
     0DIMENSION PTARE(50),PN(50),PP(50),PTO(50),PO(50),P1T(50),P1H(50),
     1P1I(50),P2(50),HW(50),TN(50),TP(50),TTO(50),AXTARE(50),AX(50),
     2AMOMS(50),AMOMR(50),WN(50),WL(50),WB(50),PHIVS(50),VU1(50),
     3PHIAS(50),T1(50),VA1(50),ALFA1(50),V1(50),T1IS(50),PHI(50),
     4ETAS(50),REV(50),OMEG(50),TT2(50),P1(50),DH(50),DHIS(50),VA2(50),
     5VU2(50),V2(50),ALFA2(50),BETA1(50),BETA2(50),WU2(50),W2(50),
     6PSI(50),PT1(50),PT2(50),T2IS(50),PRAT(50),T2(50),WU1(50),W1(50),
     7AKIS(50),RSTAR(50),ETA(50),U(50),U2(50),ETAR(50),PTOP1(50)
      GAM=1.399
      CP=.2403
      R=53.342
      CJ=778.16
      G=32.174
      C1=2.*G*CJ*CP
      C2=SQRTF(GAM*G*R)
      READ 1,NSETS
    1 FORMAT (I5)
      DO 400 J=1,NSETS
      READ 11,NPTS,NRUN,NMON,NDAY,PA,TA,TYPE
   11 FORMAT (4I5,3F10.5)
      DO 10 I=1,NPTS
     0READ 21,PTARE(I),PN(I),PP(I),PTO(I),PO(I),P1T(I),P1H(I),P1I(I),
     1P2(I)
   21 FORMAT(9F8.4)
     0READ 21,HW(I),TN(I),TP(I),TTO(I),AXTARE(I),AX(I),AMOMS(I),AMOMR(I)
     1,REV(I)
      PSUM=PTARE(I)+PA
      PN(I)=PSUM-PN(I)
      PP(I)=.4912*(PSUM-PP(I))
      PTO(I)=.4912*(PSUM-PTO(I))
      PO(I)=.4912*(PSUM-PO(I))
      P1T(I)=.4912*(PSUM-P1T(I))
      P1H(I)=.4912*(PSUM-P1H(I))
      P1I(I)=.4912*(PSUM-P1I(I))
      P2(I)=.4912*(PSUM-P2(I))
      TP(I)=TP(I)+459.7
      TTO(I)=TTO(I)+459.7
      AX(I)=.025*(AX(I)-10000.)-AXTARE(I)
      OMEG(I)=3.1416/30.*REV(I)
   10 AMOMS(I)=.3*(AMOMS(I)-10000.)
      PA=.4912*PA
      TA=TA+459.7
      CALL FLORATE(NPTS,PN,TN,HW,PP,TP,P2,PA,TA,WN,WB,WL,WS)
      PRINT 131
      PRINT 51
      PRINT 61
      PRINT 62,NRUN,NMON,NDAY,TYPE
```

```
      OCALL STATOR(NPTS,G,C1,GAM,R,P1H,P1T,P11,AX,AMOMS,WB,PHIVS,PA,
     1VU1,PHIAS,TTO,T1,VA1,ALFA1,V1,T1IS,PHI,ETAS,P1,PT1,PTO,OMEG,TYPE,
     2 PTOP1)
        IF (TYPE) 100,90,100
   90 GO TO 300
  100 M=NPTS
      CALL ROTOR(M,G,C1,GAM,CP,CJ,R,C2,TTO,TT2,VU1,VA1,WB,AMOMR,
     1OMEG,T1,P1,P2,DH,DHIS,VA2,VU2,V2,ALFA2,BETA1,BETA2,WU2,W2,T2,PSI,
     2U,ETA,PRAT,W1,PTO,WU1,PT2,T2IS,U2)
  300 PRINT 131
  131 FORMAT (1H1)
      PRINT 51
   51 FORMAT (//43H        IDENTIFICATION AND NON REFERRED DATA)
      PRINT 61
   61 FORMAT (//41H                    RUN    MONTH    DAY    TYPE)
      PRINT 62,NRUN,NMON,NDAY,TYPE
   62 FORMAT (I16,I8,I7,F8.1)
      PRINT 71
5  71 FORMAT (//45H                                    PRESSURES  PSIA)
      PRINT 72
  720 FORMAT ( 65H POINT  PTO/P1     PTO       PO       PT1       P1
     1PT2       P2)
4     DO 20 I=1,NPTS
   20 PRINT 73,I,PTOP1(I),PTO(I),PO(I),PT1(I),P1(I),PT2(I),P2(I)
   73 FORMAT (I4,7F9.3)
      PRINT 74
3  74 FORMAT (//45H                                TEMPERATURES DEG.R)
      PRINT 75
  750 FORMAT (  65H POINT  TTO       TT1       T1IS      T1        TT2
     1T2IS       T2)
2     DO 30 I=1,NPTS
   30 PRINT 76,I,TTO(I),TTO(I),T1IS(I),T1(I),TT2(I),T2IS(I),T2(I)
   76 FORMAT (I4,7F9.2)
      PRINT 131
      PRINT 51
      PRINT 61
      PRINT 62,NRUN,NMON,NDAY,TYPE
      PRINT 81
  810 FORMAT (//55H                                VELOCITIES-FPS---ANGLES-D
     1EG)
      PRINT 82
  820 FORMAT (/ 71H POINT  ALFA1      VU1        VA1        V1       BETA1
     1      WU1        W1)
      DO 40 I=1,NPTS
   40 PRINT 77,I,ALFA1(I),VU1(I),VA1(I),V1(I),BETA1(I),WU1(I),W1(I)
   77 FORMAT (I4,F10.3,3F10.2,F10.3,2F10.2)
      IF (TYPE) 120,110,120
  110 DO 160 I=1,NPTS
```

```
  160 PRAT(I)=PTO(I)/P1(I)
      GO TO 130
  120 PRINT 84
  840FORMAT (/ 71H POINT  ALFA2       VU2        VA2        V2       BETA2
     1       WU2        W2)
      DO 50 I=1,NPTS
   50 PRINT 77,I,ALFA2(I),VU2(I),VA2(I),V2(I),BETA2(I),WU2(I),W2(I)
      PRINT 131
      PRINT 51
      PRINT 61
      PRINT 62,NRUN,NMON,NDAY,TYPE
  130 PRINT 93
   93 FORMAT (//51H                                          TURBINE   LEAKAGE)
      PRINT 94
  940FORMAT (66H          PRESS    SPEED    FLOW   FLORATE   FLORATE   H
     1ORSE  SPEED)
      PRINT 96
  960FORMAT (65H POINT  RATIO   REV/MIN  FUNCTION LBM/SEC   LBM/SEC   P
     1OWER   FPS)
      DO 60 I=1,NPTS
C     PTARE ARRAY USED FOR HORSEPOWER
      PTARE(I)=AMOMR(I)*OMEG(I)/(12.*550.)
   60 PRINT 95,I,PRAT(I),REV(I),PHI(I),WB(I),WL(I),PTARE(I),U(I)
   95 FORMAT (I4,F9.3,F10.1,F9.5,F9.3,F10.5,F8.2,F8.2)
      IF (TYPE) 150,140,150
  140 DO 170 I=1,NPTS
  170 WB(I)=WB(I)*SQRTF(TTO(I)/518.4)/(PTO(I)/14.7)
      GO TO 180
 1500CALL REFERD (NPTS,DHIS,T1IS,U,TTO,PTO,T1,T2,AMOMR,REV,AKIS,
     1RSTAR,CP,T2IS,WB,G,CJ,PTARE)
  180 PRINT 101
  101 FORMAT (//45H                          REFERRED DATA-EFFICIENCIES)
      PRINT 61
      PRINT 62,NRUN,NMON,NDAY,TYPE
      PRINT 102
 1020FORMAT (/64H          PRESS    SPEED   MOMENT  FLOTURB  KISEN-    DEGR
     1EE    HORSE)
      PRINT 103
 1030FORMAT ( 64H POINT   RATIO   REV/MIN    FTLB    LBM/SEC  TROPIC   REACT
     1ION   POWER)
      DO 70 I=1,NPTS
   70 PRINT 104,I,PRAT(I),REV(I),AMOMR(I),WB(I),AKIS(I),RSTAR(I)
     1,PTARE(I)
  104 FORMAT (I4,F9.2,F9.1,F8.2,F8.3,F9.4,F9.4,F8.2)
      PRINT 111
 1110FORMAT(//63H          **** EFFICIENCIES *****  ******** COEFFICIENTS
     1 ********)
      PRINT 112
```

```
1120FORMAT (63H POINT  INTERN   STATOR   ROTOR  VEL-STAT  AREA-STAT  V
   1EL-ROTOR)
      DO 80 I=1,NPTS
      ETAR(I)=PSI(I)**2
   80 PRINT 113,I,ETA(I),ETAS(I),ETAR(I),PHIVS(I),PHIAS(I),PSI(I)
  113 FORMAT (I4,F10.4,F9.4,F8.4,F9.4,F10.4,F11.4)
  400 CONTINJE
      END
      SUBROUTINE FLORATE (M,PN,TN,HW,PP,TP,P2,PA,TA,WN,WB,WL,WS)
     0DIMENSION PN(50),TN(50),HW(50),PP(50),TP(50),P2(50),WN(50),WB(50)
5    1,WL(50),WS(50)
      AK=.9992
      BETA=4.25/7.975
      D2SQ=4.25**2
4     AL=3.1416*6.4*.0075
      AS=3.1416*1.2*.005
      C=AK*359.1*SQRTF(.4912*144./53.342)*D2SQ/3600.
      DO 10 I=1,M
3     ALFA=1.+.00252*(TN(I)-68.)/100.
      Y=1.-(.41+.35*BETA**4)/(1.399*13.59)*HW(I)/PN(I)
      WN(I)=ALFA*C*Y*SQRTF(PN(I)*HW(I)/(TN(I)+459.7))
      WL(I)=SQRTF((1.-P2(I)/PP(I))/4.0791)
2     WL(I)=WL(I)*AL*PP(I)*SQRTF(32.174/(53.342*TP(I)))
   10 WB(I)=WN(I)-WL(I)
      RETURN
      END
     0SUBROUTINE STATOR (M,G,C1,GAM,R,P1H,P1T,P1I,AX,AMOMS,WB,PHIVS,PA,
     1VU1,PHIAS,TTO,T1,VA1,ALFA1,V1,T1IS,PHI,ETAS,P1,PT1,PTO,OMEG,TYPE,
     2 PTOP1)
     0DIMENSION P1H(50),P1T(50),P1I(50),AX(50),AMOMS(50),WB(50),
     1PHIVS(50),VU1(50),PHIAS(50),TTO(50),T1(50),VA1(50),PTO(50),
     2ALFA1(50),V1(50),T1IS(50),PHI(50),ETAS(50),P1(50),PT1(50)
     3,OMEG(50), PTOP1(50)
      AHUB=3.1416*7.79**2/4.
      ATIP=3.1416*9.17**2/4.
      ACASE=3.1416*9.8**2/4.
      ABLOCK=31.*.071*.69
      ASTAT=ATIP-AHUB
      ASTAT1=ASTAT-ABLOCK
      ACAT=ACASE-ATIP
      RMEAN = 4.26
      ASTAR=4.216
      RATCR=      ((GAM+1.)/2.)**(GAM/(GAM-1.))
      PHITH=(2./(GAM+1.))**(1./(GAM-1.))*SQRTF(2.*GAM/(GAM+1.))
      F=0.5
      C3=2.378/2.07*1.E-7*(7.79/2.)**2/4.
      DO 10 I=1,M
      P1(I)=(P1T(I)+P1H(I))/2.
```

```
      IF (TYPE) 110,100,110
  100 FOR = P1I(I)*AHUB
      GO TO 120
  110 FOR=AHUB*(P1H(I)-C3*(F*OMEG(I))**2)
  120 VA1(I)=G/WB(I)*(AX(I)-P1(I)*ASTAT+PA*ACASE-FOR-P1T(I)*ACAT)
      VU1(I)=AMOMS(I)*G/(WB(I)*RMEAN)
      ALFA1(I)=ATANF(VA1(I)/VU1(I))
      V1(I)=VU1(I)/COSF(ALFA1(I))
      T1(I)=TTO(I)-V1(I)**2/C1
      T1IS(I)=TTO(I)*(P1(I)/PTO(I))**((GAM-1.)/GAM)
      V1IS=SQRTF(C1*(TTO(I)-T1IS(I)))
      PHIVS(I)=V1(I)/V1IS
      ETAS(I)=(TTO(I)-T1(I))/(TTO(I)-T1IS(I))
      PHI(I)=WB(I)*SQRTF(TTO(I)*R/G)/(ASTAR*PTO(I))
      ALFA1(I)=90.-ALFA1(I)*57.3
      AEFF=WB(I)*T1(I)*R/(P1(I)*VA1(I))
      PRINT 883
  883 FORMAT (//45H                          MOMENTUM EQUATION SOLUTION)
     0PRINT 884,I,VA1(I),V1(I),VU1(I),ALFA1(I),T1(I),PHIVS(I),ETAS(I),
     1 PHI(I)
 8840FORMAT (/ 6H POINT I4,/ 5H VA1= F20.3,/ 4H V1= F21.3,/ 5H VU1=
     1 F20.3,/ 7H ALFA1= F18.3,/ 4H T1= F21.3,/ 9H VEL PHI=F17.4,
     2 /10H STAT EFF= F17.5,/10H FLOW PHI= F17.5)
      PRINT 885,AEFF
  885 FORMAT (10H EFF AREA=, F17.5)
      PTOP1(I)=PTO(I)/P1(I)
      IF (PTOP1(I)-RATCR) 40,30,30
   40 PRINT 882,I
      PHIRAT=1.
  882 FORMAT (//27H FLOW NOT CHOKED - POINT NO,I4)
      GO TO 20
   30 PHIRAT=PHI(I)/PHITH
      PRINT 881,I,PHIRAT
  881 FORMAT (/23H  FLOW CHOKED-POINT NO. I3,12H  REST FACT= F9.5)
   20 X=1.
      TOL=1.
      DIFF1=1.
      DEL=1.
      Y=1.
      V1IS=SQRTF(C1*(TTO(I)-T1IS(I)))
      T1(I)=T1IS(I)
  140 T1(I)=T1(I)+X*DEL*Y
      V1(I)=SQRTF(C1*(TTO(I)-T1(I)))
      ENP=(V1(I)/V1IS)**2
      IF(VU1(I)-V1(I)) 130,401,401
  130 ALFA1(I)=ASINF(VU1(I)/V1(I))
      RHO=WB(I)*144./(ASTAT1*COSF(ALFA1(I))*V1(I))
      TEST=P1(I)*144./(RHO*R)
```

```
      DIFF2=TEST-T1(I)
      IF (ABSF(DIFF2)-TOL) 400,400,50
   50 IF (DIFF1 ) 60,60,70
   60 IF (DIFF2) 90,90,80
   70 IF (DIFF2) 80,80,90
   90 DIFF1=DIFF2
      Y=Y+1.
      GO TO 140
   80 DIFF1=DIFF2
      X=-.1*X
      Y=1.
      GO TO 140
  401 PRINT 891,I
 8910 FORMAT (/52H NO MATCH CONTINUITY STATOR-USE ALFA1=76DEG-POINT NO,
     1I4)
      ALFA1(I)=76./57.3
      V1(I)=VU1(I)/SINF(ALFA1(I))
      T1(I)=TTO(I)-V1(I)**2/C1
      ENP=(V1(I)/V1IS)**2
  400 VA1(I)=V1(I)*COSF(ALFA1(I))
      ETAS(I)=(TTO(I)-T1(I))/(TTO(I)-T1IS(I))
      PHIVS(I)=SQRTF(ENP)
      PHIAS(I)=PHIRAT
      ALFA1(I)=ALFA1(I)*57.3
   10 PT1(I)=P1(I)*(TTO(I)/T1(I))**(GAM/(GAM-1.))
      RETURN
      END
      SUBROUTINE ROTOR (M,G,C1,GAM,CP,CJ,R,C2,TTO,TT2,VU1,VA1,WB,AMOMR,
     1OMEG,T1,P1,P2,DH,DHIS,VA2,VU2,V2,ALFA2,BETA1,BETA2,WU2,W2,T2,PSI,
     2U,ETA,PRAT,W1,PTO,WU1,PT2,T2IS,U2)
     DIMENSION TTO(50),TT2(50),VU1(50),VA1(50),WB(50),AMOMR(50),
     1 OMEG(50),T1(50),P1(50),P2(50),DH(50),DHIS(50),VA2(50),VU2(50),
     2V2(50),ALFA2(50),BETA1(50),BETA2(50),WU2(50),W2(50),T2(50),
     3PSI(50),PT2(50),T2IS(50),ETA(50),PRAT(50),PTO(50),
     4U(50),WU1(50),W1(50),U2(50)
      AROT2=3.1416/4.*(9.8 **2-7.65**2)-60.*.0597*1.05
      RMEAN = 4.26
      RMEAN2=4.45
      DO 10 I=1,M
      DH(I)=(AMOMR(I)*OMEG(I))/(12.*WB(I)*CJ)
      T2IS(I)=TTO(I)*(P2(I)/PTO(I))**((GAM-1.)/GAM)
      DHIS(I)=CP*(TTO(I)-T2IS(I))
      ETA(I)=DH(I)/DHIS(I)
      PRAT(I)=PTO(I)/P2(I)
```

```
      U(I)=RMEAN*OMEG(I)/12.
      U2(I)=RMEAN2*OMEG(I)/12.
      VU2(I)=VU1(I)*U(I)/U2(I)-G*CJ*DH(I)/U2(I)
      WU2(I)=VU2(I)-U2(I)
      WU1(I)=VU1(I)-U(I)
      TT2(I)=TTO(I)-DH(I)/CP
      BETA1(I)=ATANF (WU1(I)/VA1(I))
      W1(I)=ABSF(WU1(I))/SINF(BETA1(I))
      HEQ=CP*(T1(I)+W1(I)**2/C1+(U2(I)**2-U(I)**2)/C1)
      TTE=HEQ/CP
      T2S=T1(I)*(P2(I)/P1(I))**((GAM-1.)/GAM)
      T2(I)=T2S
      W2TH=SQRTF(C1*(HEQ/CP-T2S))
      X=1.
      TOL=1.
      DIFF1=1.
      DEL=1.
      Y=1.
  100 T2(I)=T2(I)+X*DEL*Y
      W2(I)=SQRTF(C1*(TTE-T2(I)))
      CHECK=ABSF(WU2(I))
      IF (CHECK-W2(I)) 30,20,20
   30 BETA2(I)=ASINF(WU2(I)/W2(I))
      PSI(I)=W2(I)/W2TH
      RHO=WB(I)*144./(AROT2*COSF(BETA2(I))*W2(I))
      TEST=P2(I)*144./(RHO*R)
      DIFF2=TEST-T2(I)
      IF (ABSF(DIFF2)-TOL) 400,400,50
   50 IF (DIFF1 ) 60,60,70
   60 IF (DIFF2) 90,90,80
   70 IF (DIFF2) 80,80,90
   90 DIFF1=DIFF2
      Y=Y+1.
      GO TO 100
   80 DIFF1=DIFF2
      X=-.1*X
      Y=1.
      GO TO 100
   20 PRINT 51,I
  510 FORMAT (/51H NO MATCH CONTINUITY ROTOR-USE BETA2=70DEG-POINT NO,
     1 I4)
      BETA2(I)=-70./57.3
      W2(I)=WU2(I)/SINF(BETA2(I))
      T2(I)=TTE-W2(I)**2/C1
      PSI(I)=W2(I)/W2TH
  400 VA2(I)=W2(I)*COSF(BETA2(I))
      ALFA2(I)=ATANF(VU2(I)/VA2(I))
      V2(I)=VU2(I)/SINF(ALFA2(I))
```

```
      BETA2(I)=BETA2(I)*57.3
      ALFA2(I)=ALFA2(I)*57.3
      BETA1(I)=BETA1(I)*57.3
   10 PT2(I)=P2(I)*(TT2(I)/T2(I))**(GAM/(GAM-1.))
      RETURN
      END
     0SUBROUTINE REFERD (M,DHIS,T1IS,U,TTO,PTO,T1,T2,AMOMR,REV,AKIS,
     1RSTAR,CP,T2IS,WB,G,CJ,PTARE)
     0DIMENSION DHIS(50),T1IS(50),U(50),TTO(50),PTO(50),T1(50),T2(50),
     1AMOMR(50),REV(50),AKIS(50),RSTAR(50),WB(50),T2IS(50),PTARE(50)
      TSTD=518.4
      PSTD=14.7
      DO 10 I=1,M
      DHIS12=CP*(T1IS(I)-T2IS(I))
      RSTAR(I)=DHIS12/DHIS(I)
      AKIS(I)=DHIS(I)*2./U(I)**2*G*CJ
      THETA=SQRTF(TTO(I)/TSTD)
      DELTA=PTO(I)/PSTD
      WB(I)=WB(I)*THETA/DELTA
      AMOMR(I)=AMOMR(I)/(12.*DELTA)
      PTARE(I)=PTARE(I)/(THETA*DELTA)
   10 REV(I)=REV(I)/THETA
      RETURN
      END
      END
```

MOMENTUM EQUATION SOLUTION

3

```
      POINT    5
      VA1=                251.652
      V1=                1206.730
2     VU1=               1180.198
      ALFA1=               77.962
      T1=                 508.679
      VEL PHI=               .9705
      STAT EFF=              .94178
      FLOW PHI=              .65448
      EFF AREA=            20.49830

       FLOW CHOKED-POINT NO.   5  REST FACT=    .95605
```

IDENTIFICATION AND NON REFERRED DATA

RUN	MONTH	DAY	TYPE
4	1	25	10.0

PRESSURES PSIA

POINT	PTO/P1	PTO	PO	PT1	P1	PT2	P2
1	2.343	34.905	34.684	35.154	14.901	15.278	14.790
2	2.327	34.905	34.684	34.614	14.999	15.179	14.790
3	2.317	35.298	35.077	34.360	15.237	15.356	14.790
4	2.295	35.494	35.273	35.104	15.465	15.474	14.790
5	2.226	35.003	34.978	33.799	15.723	15.565	14.790
6	2.187	35.273	35.052	33.932	16.129	15.678	14.790

TEMPERATURES DEG.R

POINT	TTO	TT1	T1IS	T1	TT2	T2IS	T2
1	629.70	629.70	493.97	492.97	521.94	492.92	517.12
2	629.70	629.70	494.90	496.08	520.13	492.92	516.30
3	642.70	642.70	505.77	509.67	531.30	501.49	525.64
4	641.70	641.70	506.33	507.93	528.63	499.92	521.85
5	629.70	629.70	501.20	506.23	519.75	492.53	512.23
6	630.70	630.70	504.54	510.15	522.76	492.23	514.14

VELOCITIES-FPS---ANGLES-DEG

POINT	ALFA1	VU1	VA1	V1	BETA1	WU1	W1
1	76.024	1244.67	309.90	1282.66	65.230	671.46	739.52
2	75.829	1229.39	310.56	1268.01	64.066	638.48	710.01
3	75.596	1225.38	314.84	1265.18	62.466	603.81	680.96
4	75.856	1230.21	310.14	1268.71	61.652	574.73	653.07
5	75.530	1180.20	304.68	1218.89	58.195	491.22	578.04
6	75.611	1166.56	299.41	1204.37	55.493	435.46	528.46

POINT	ALFA2	VU2	VA2	V2	BETA2	WU2	W2
1	26.867	108.76	214.71	240.69	-66.343	-490.01	534.99
2	30.498	108.99	185.05	214.76	-70.000	-508.28	540.91
3	32.667	140.86	219.71	260.99	-66.634	-508.43	553.88
4	40.181	184.17	218.10	285.46	-66.461	-500.55	546.00
5	44.464	210.67	214.68	300.78	-67.138	-509.03	552.45
6	55.810	266.45	181.04	322.13	-70.000	-497.26	529.19

IDENTIFICATION AND NON REFERRED DATA

RUN	MONTH	DAY	TYPE
4	1	25	10.0

POINT	PRESS RATIO	SPEED REV/MIN	FLOW FUNCTION	TURBINE FLORATE LBM/SEC	LEAKAGE FLORATE LBM/SEC	HORSE POWER	SPEED FPS
1	2.360	15419.0	.64950	2.958	.06270	108.38	573.21
2	2.360	15895.0	.65110	2.965	.06270	110.46	590.91
3	2.387	16720.0	.65300	2.977	.06329	112.75	621.58
4	2.400	17632.0	.65034	2.984	.06335	114.70	655.48
5	2.367	18533.0	.65448	2.989	.06335	111.74	688.98
6	2.385	19666.0	.65082	2.993	.06348	109.84	731.10

REFERRED DATA-EFFICIENCIES

RUN	MONTH	DAY	TYPE
4	1	25	10.0

POINT	PRESS RATIO	SPEED REV/MIN	MOMENT FTLB	FLOTURB LBM/SEC	KISEN-TROPIC	DEGREE REACTION	HORSE POWER
1	2.36	13990.1	15.55	1.373	5.0090	.0077	41.41
2	2.36	14422.0	15.37	1.376	4.7135	.0144	42.21
3	2.39	15016.4	14.75	1.380	4.3977	.0303	42.17
4	2.40	15847.8	14.15	1.375	3.9706	.0452	42.70
5	2.37	16815.6	13.30	1.384	3.4771	.0632	42.58
6	2.38	17829.4	12.22	1.376	3.1173	.0889	41.50

	**** EFFICIENCIES *****			******** COEFFICIENTS ********		
POINT	INTERN	STATOR	ROTOR	VEL-STAT	AREA-STAT	VEL-ROTOR
1	.7879	1.0074	.4856	1.0037	.9488	.6968
2	.8010	.9912	.5227	.9956	.9511	.7230
3	.7889	.9715	.5570	.9857	.9539	.7463
4	.7975	.9882	.5490	.9941	.9500	.7409
5	.8016	.9609	.6321	.9802	.9561	.7951
6	.7795	.9555	.5861	.9775	.9507	.7655

INITIAL DISTRIBUTION LIST

		No. Copies
1.	Defense Documentation Center Cameron Station Alexandria, Virginia 22314	20
2.	Library U.S. Naval Postgraduate School Monterey, California 93940	2
3.	Commander, Naval Air Systems Command Navy Department Washington, D.C. 20360	1
4.	Commander Naval Air Systems Command (BUWEPS/RAPP 14) Navy Department Washington, D.C. 20360	1
5.	Office of Naval Research (Power Branch) Department of the Navy Washington, D.C. 20360 (Attn: Mr. J. R. Patton, Jr.)	1
6.	Chairman, Department of Aeronautics U.S. Naval Postgraduate School Monterey, California 93940	2
7.	Professor M. H. Vavra Department of Aeronautics U.S. Naval Postgraduate School Monterey, California 93940	2
8.	Mr. L. T. Clark Department of Aeronautics U.S. Naval Postgraduate School Monterey, California 93940	1
9.	CDR Richard H. Eckert Patrol Squadron THIRTY-ONE U.S. Naval Air Station North Island San Diego, California	3

Security Classification

DOCUMENT CONTROL DATA - R&D

(Security classification of title, body of abstract and indexing annotation must be entered when the overall report is classified)

1. ORIGINATING ACTIVITY *(Corporate author)*
U. S. Naval Postgraduate School
Monterey, California

2a. REPORT SECURITY CLASSIFICATION

2b. GROUP

3. REPORT TITLE
PERFORMANCE ANALYSIS AND INITIAL TESTS OF A TRANSONIC TURBINE TEST RIG

4. DESCRIPTIVE NOTES *(Type of report and inclusive dates)*
Thesis

5. AUTHOR(S) *(Last name, first name, initial)*
ECKERT, Richard H., CDR, USN

6. REPORT DATE	7a. TOTAL NO. OF PAGES	7b. NO. OF REFS
May 1966	245	11

8a. CONTRACT OR GRANT NO.

b. PROJECT NO.

c.

d. Unlimited distribution

9a. ORIGINATOR'S REPORT NUMBER(S)

9b. OTHER REPORT NO(S) *(Any other numbers that may be assigned this report)*

10. AVAILABILITY/LIMITATION NOTICES
Qualified requesters may obtain copies of this report from DDC.

11. SUPPLEMENTARY NOTES

12. SPONSORING MILITARY ACTIVITY
Naval Air Systems Command
Navy Department
Washington, D.C. 20360

13. ABSTRACT

The primary purpose of the Transonic Turbine Test Rig of the United States Naval Postgraduate School, Monterey, California, is to permit investigation of turbine performance and flow conditions for transonic rotor inlet velocities. This turbine also has provisions for investigation of the effects on performance of widely varied axial and tip clearances. High turbine total-to-total pressure ratios are achievable, since an ejector-type exhauster assembly can maintain a partial vacuum in an airtight turbine discharge hood. This study is concerned primarily with intial turbine performance tests--of the nature of suitability tests--both with and without the rotor installed. The installation is described, and results of flow rate calibration and labyrinth seal leakage tests are included, along with turbine performance test results. Also presented are a simplified three dimensional turbine performance prediction and a one-dimensional analysis of exhauster performance. The turbine performance prediction method uses the so-called equivalent enthalpy (and corresponding equivalent total thermodynamic properties) to permit analysis of the relative flow through the rotor in a manner analogous to that used for absolute flows.

DD FORM 1 JAN 64 1473

Security Classification

14. KEY WORDS	LINK A		LINK B		LINK C	
	ROLE	WT	ROLE	WT	ROLE	WT
Transonic Turbine, USNPGS Monterey, California						

INSTRUCTIONS

1. ORIGINATING ACTIVITY: Enter the name and address of the contractor, subcontractor, grantee, Department of Defense activity or other organization *(corporate author)* issuing the report.

2*a*. REPORT SECURITY CLASSIFICATION: Enter the overall security classification of the report. Indicate whether "Restricted Data" is included. Marking is to be in accordance with appropriate security regulations.

2*b*. GROUP: Automatic downgrading is specified in DoD Directive 5200.10 and Armed Forces Industrial Manual. Enter the group number. Also, when applicable, show that optional markings have been used for Group 3 and Group 4 as authorized.

3. REPORT TITLE: Enter the complete report title in all capital letters. Titles in all cases should be unclassified. If a meaningful title cannot be selected without classification, show title classification in all capitals in parenthesis immediately following the title.

4. DESCRIPTIVE NOTES: If appropriate, enter the type of report, e.g., interim, progress, summary, annual, or final. Give the inclusive dates when a specific reporting period is covered.

5. AUTHOR(S): Enter the name(s) of author(s) as shown on or in the report. Enter last name, first name, middle initial. If military, show rank and branch of service. The name of the principal author is an absolute minimum requirement.

6. REPORT DATE: Enter the date of the report as day, month, year, or month, year. If more than one date appears on the report, use date of publication.

7*a*. TOTAL NUMBER OF PAGES: The total page count should follow normal pagination procedures, i.e., enter the number of pages containing information.

7*b*. NUMBER OF REFERENCES: Enter the total number of references cited in the report.

8*a*. CONTRACT OR GRANT NUMBER: If appropriate, enter the applicable number of the contract or grant under which the report was written.

8*b*, 8*c*, & 8*d*. PROJECT NUMBER: Enter the appropriate military department identification, such as project number, subproject number, system numbers, task number, etc.

9*a*. ORIGINATOR'S REPORT NUMBER(S): Enter the official report number by which the document will be identified and controlled by the originating activity. This number must be unique to this report.

9*b*. OTHER REPORT NUMBER(S): If the report has been assigned any other report numbers *(either by the originator or by the sponsor)*, also enter this number(s).

10. AVAILABILITY/LIMITATION NOTICES: Enter any limitations on further dissemination of the report, other than those imposed by security classification, using standard statements such as:

(1) "Qualified requesters may obtain copies of this report from DDC."

(2) "Foreign announcement and dissemination of this report by DDC is not authorized."

(3) "U. S. Government agencies may obtain copies of this report directly from DDC. Other qualified DDC users shall request through _____."

(4) "U. S. military agencies may obtain copies of this report directly from DDC. Other qualified users shall request through _____."

(5) "All distribution of this report is controlled. Qualified DDC users shall request through _____."

If the report has been furnished to the Office of Technical Services, Department of Commerce, for sale to the public, indicate this fact and enter the price, if known.

11. SUPPLEMENTARY NOTES: Use for additional explanatory notes.

12. SPONSORING MILITARY ACTIVITY: Enter the name of the departmental project office or laboratory sponsoring *(paying for)* the research and development. Include address.

13. ABSTRACT: Enter an abstract giving a brief and factual summary of the document indicative of the report, even though it may also appear elsewhere in the body of the technical report. If additional space is required, a continuation sheet shall be attached.

It is highly desirable that the abstract of classified reports be unclassified. Each paragraph of the abstract shall end with an indication of the military security classification of the information in the paragraph, represented as *(TS), (S), (C), or (U)*.

There is no limitation on the length of the abstract. However, the suggested length is from 150 to 225 words.

14. KEY WORDS: Key words are technically meaningful terms or short phrases that characterize a report and may be used as index entries for cataloging the report. Key words must be selected so that no security classification is required. Identifiers, such as equipment model designation, trade name, military project code name, geographic location, may be used as key words but will be followed by an indication of technical context. The assignment of links, roles, and weights is optional.

DD FORM 1 JAN 64 1473 (BACK)